Cosmological Inflation with Multiple Fields and the Theory of Density Fluctuations

ISBN 90-393-3091-3

Cover illustration: The upper figure gives an artist's impression of a scalar field (consisting of two components) slowly rolling under the influence of a quadratic potential on a spherical field manifold. This inflation model is treated in section 6.5. The lower figure is a map of the temperature fluctuations in the cosmic microwave background radiation as observed by the COBE satellite, see figure 1.4 for details (the COBE datasets were developed by the NASA Goddard Space Flight Center under the guidance of the COBE Science Working Group and were provided by the NSSDC). Together they indicate the important relation between observations of the CMBR and inflation models: inflation explains the existence of the tiny fluctuations, and observations can constrain inflationary parameters.

Cosmological Inflation with Multiple Fields and the Theory of Density Fluctuations

Kosmologische Inflatie met Meerdere Velden en de Theorie van de Dichtheidsfluctuaties

(met een samenvatting in het Nederlands)

PROEFSCHRIFT

ter verkrijging van de graad van doctor aan de Universiteit Utrecht op gezag van de Rector Magnificus, Prof. dr. W.H. Gispen, ingevolge het besluit van het College voor Promoties in het openbaar te verdedigen op maandag 9 september 2002 des middags te 12.45 uur

door

Barend Jan Willem van Tent

geboren op 27 maart 1974 te Amersfoort

PROMOTOR: Prof. dr. G. 't Hooft

Spinoza Instituut en
Instituut voor Theoretische Fysica,
Universiteit Utrecht

Aan mijn ouders

Much human ingenuity has gone into finding the ultimate Before.
The current state of knowledge can be summarized thus:

In the beginning there was nothing, which exploded.

— Terry Pratchett, *Lords and Ladies.*

Contents

1 Introduction **7**
- 1.1 The Big Bang theory . . . 7
- 1.2 Inflation . . . 14
- 1.3 The cosmic microwave background radiation . . . 18
- 1.4 Outline of this thesis . . . 21

2 Background theory **23**
- 2.1 Friedmann-Robertson-Walker universes . . . 23
- 2.2 Single-field inflation . . . 29
- 2.3 Slow roll . . . 31
- 2.4 Example: ϕ^n potentials . . . 34
- 2.5 Historical overview . . . 38

3 Multiple-field inflation **43**
- 3.1 Motivation and geometrical concepts . . . 43
- 3.2 Equations of motion . . . 46
- 3.3 Multiple-field slow roll . . . 49
- 3.4 Example: quartic potential . . . 52

4 Perturbations during multiple-field inflation **55**
- 4.1 Introduction . . . 55
- 4.2 Scalar perturbations . . . 58
- 4.3 Quantization of the scalar perturbations . . . 62
- 4.4 Solution of the scalar perturbation equations to first order . . . 66
  - 4.4.1 Setup . . . 66
  - 4.4.2 Slow roll for the perturbations . . . 68
  - 4.4.3 Calculation . . . 70
- 4.5 Vector and tensor perturbations . . . 73
- 4.6 Summary and conclusion . . . 77

5 Perturbations after inflation and the link with observations **79**
- 5.1 Temperature fluctuations in the CMBR . . . 80
  - 5.1.1 Temperature anisotropies . . . 80
  - 5.1.2 The CMBR power spectrum . . . 82
  - 5.1.3 Sources of the anisotropies . . . 85
- 5.2 Perturbations after inflation . . . 88

5.2.1 Gravitational potential 88
5.2.2 Entropy perturbations 91
5.3 Spectral amplitudes and indices from inflation 94
5.4 Linking inflation and the CMBR 99
5.4.1 The Sachs-Wolfe effect 100
5.4.2 Observational values 104
5.5 Summary and conclusion 105

6 Inflation models with a quadratic potential **107**
6.1 Flat field manifold and equal masses 107
6.2 Flat field manifold and general mass matrix 109
6.2.1 Analytical expressions for the background 109
6.2.2 Analytical expressions for the perturbations 112
6.2.3 Numerical example 115
6.3 Curved field manifold: general remarks 119
6.4 Spherical field manifold and equal masses 122
6.5 Curved field manifold and general mass matrix 126
6.6 Summary and conclusion 131

7 Conclusion and outlook **133**

A Conventions and definitions **137**

B Explicit expressions for the metric quantities **141**

Bibliography **145**

Samenvatting **151**

Dankwoord **155**

Curriculum vitae **157**

Chapter 1

Introduction

This thesis deals with a theory of the very early universe, called inflation theory. It focuses especially on how inflation can produce the seeds for the large-scale structures (galaxies and clusters of galaxies) that we see in our present universe. The first three sections of this chapter provide a general introduction to cosmology. The first section discusses the Big Bang theory, which describes the evolution of the universe. The second discusses the problems in this standard Big Bang theory and introduces a period of inflation as a possible solution to some of them. The third section gives an introduction on the cosmic microwave background radiation, observations of which are very important as they provide information about the early universe and inflation. Section 1.4 gives a detailed outline of the further contents of this thesis. This first chapter is meant for a broader audience and does not contain any formulae. More information on the general cosmology discussed here can be found in a number of textbooks, among others [176, 100, 149, 32, 151].

1.1 The Big Bang theory

For a long time people have been looking up at the sky and trying to observe all the fascinating objects and phenomena that exist away from our own planet. With the progress of technology it has become possible to make more and more accurate observations, increasing our knowledge and understanding of the universe, but also creating new puzzles. Presently our picture of the universe looks as follows. At the smallest scales we find our solar system, with the sun, the nine planets and many moons, asteroids and comets. Our solar system is part of the Milky Way galaxy, which consists of hundreds of billions (10^{11}) of stars. The Milky Way is part of the Local Group of galaxies, which contains about 30 galaxies, among them the Andromeda galaxy (M31) and the Large and Small Magellanic Clouds. This is an example of a (rather small) cluster of galaxies. This cluster, in its turn, is part of the Virgo supercluster, which is centered around the Virgo cluster and contains thousands of galaxies. The whole visible universe contains very many superclusters, which seem to be organized in a filamentary structure (like the Great Wall), with large voids in between.

To give some indication of the sizes and distances involved, let us give some numbers. The unit of distance used in astronomy is the parsec.[1] It is approximately the distance

[1] 1 pc = $3.086 \cdot 10^{16}$ m = 3.26 lightyear (a lightyear is the distance light travels in one year).

from the Sun to its nearest neighbour stars, which is about a hundred thousand times larger than the distance from the Earth to the Sun. The distance to the centre of the Milky Way is of the order of ten thousand parsec, while the distance to the Andromeda galaxy is approximately one million parsec (1 Mpc). The centre of the Virgo supercluster is at a distance of about 20 Mpc, and structures like the Great Wall have sizes of the order of a hundred megaparsec. Finally the size of the whole observable universe is of the order of ten thousand Mpc (10 Gpc).

Although this means that there is a lot of structure at different scales, at the very largest scales observations show the universe to be very isotropic, i.e. the spatial distribution of matter is on average the same in all directions. Unfortunately we can only make observations from our one planet in the universe. To be able to draw more general conclusions from these observations, there is a common assumption called the cosmological principle, which states that our spatial position in the universe is in no way exceptional. Then one can draw the conclusion that the universe must be isotropic as seen from any point in space. Or, in other words, the universe considered at one time must be homogeneous at large scales. Universe models that are spatially homogeneous and isotropic are called Friedmann-Robertson-Walker universes and they are described in section 2.1.

One of the essential characteristics of cosmological observations is that because of the finite speed of light one automatically looks back in time when looking out into space. If we assume that the universe evolves in time, this means that our observations become influenced by evolutionary effects. And indeed these effects are observed, for example at the largest distances we find more quasars (an abbreviation of quasi-stellar object, originally quasi-stellar radio source), which are probably galaxies in the process of formation. The fact that we observe evolutionary effects is a point in favour of the Big Bang theory, whose main characteristic is that the universe evolves.

The principal observational ingredient of the Big Bang theory is the discovery by E. Hubble in 1929 [80] that all galaxies recede from our galaxy according to a simple law. This law, known as Hubble's law, states that the recession velocity of a galaxy is proportional to its distance, the constant of proportionality being Hubble's constant H_0 with a value of approximately 70 km/s Mpc^{-1} (a more exact value can be found in table 1.1).[2] Combining Hubble's law with the cosmological principle leads to the important conclusion that the universe is expanding. A well-known analogue is the raisin pudding: a pudding with raisins randomly scattered through it, which swells steadily. The raisins represent clusters of galaxies, which do not expand themselves because of the gravitational attraction. As seen from one raisin all other raisins recede, and the raisin recession velocity increases with distance. Because of the expansion light from other galaxies is redshifted to lower frequencies, so that a certain distance corresponds with a certain redshift.

If we extrapolate this expansion back in time, we find that the universe becomes smaller and smaller and the density and temperature become progressively higher. If the extrapolation is valid, one finally arrives at a singularity: the universe is just a point and the density and temperature are infinite. This singularity is called the Big Bang and this extrapolated time is chosen as the zero point of the time scale, $t = 0$. The standard Big Bang theory is a theory which takes the Big Bang as a starting point and gives a model for the further evolution of the universe based on the physics at high energies as we know it.

[2] Superimposed upon this Hubble velocity the galaxies have their own velocities of the order of 100 km/s caused by gravitational attraction within clusters and superclusters. This only changes the Hubble velocity appreciably for nearby galaxies, but it is the reason that the Andromeda galaxy does not recede from our galaxy but approaches it.

Cosmological quantity	Symbol	Value
Hubble constant	H_0	72 ± 8 km/s Mpc^{-1} ($= 2.3 \cdot 10^{-18}$ s^{-1})
Temperature of CMBR	T_0	2.725 ± 0.001 K
Age of universe	t_0	13.4 ± 1.6 Gyr ($= 4.23 \cdot 10^{17}$ s)
Radiation density parameter	Ω_r	$4.8^{+1.3}_{-0.9} \cdot 10^{-5}$
Baryonic matter	Ω_b	0.04 ± 0.01
Total matter	Ω_m	0.3 ± 0.1
Dark energy	Ω_Λ	0.7 ± 0.1
Total density parameter	$\Omega_{\rm tot}$	1.00 ± 0.06

Table 1.1: Present values of a number of cosmological parameters, according to [123].

This means that at energies per particle exceeding 100 GeV the standard Big Bang theory in essence only extrapolates known physics, since we cannot yet make measurements at such high energies. An example of a potential 'new' physical process at higher energies, which is not included in the standard Big Bang theory, is inflation, see section 1.2.

Although the history of the universe according to the standard Big Bang theory is described below, we now single out two aspects that played a crucial role in observationally confirming the Big Bang theory. These are the cosmic microwave background radiation (CMBR) and nucleosynthesis. According to the Big Bang scenario the universe was very hot at early times, so that many photons with a high temperature were produced. These photons should still be around, although with a much lower temperature because the expansion of the universe increases their wavelengths to larger values, which corresponds with a lower frequency or energy (this is called redshift). And indeed this CMBR with a temperature of about 3 K was first measured in 1965. The CMBR is discussed more thoroughly in section 1.3. Another consequence of a hot early universe is that nuclear reactions should have caused the formation of some light elements besides hydrogen, in particular deuterium and helium. This is called nucleosynthesis, and indeed observations of deuterium and helium abundances agree with predictions from Big Bang nucleosynthesis. (The homogeneous distribution of helium points to a cosmological origin anyway, as opposed to formation in stars, while deuterium is only destroyed by stars.)

Regarding the matter (and more exotic forms of energy) content of the universe, observations have led to the picture given in table 1.1. The energy densities of the various components are given relative to the critical density of the universe, in the form of the so-called density parameters Ω_i (in other words, $\Omega_i = \rho_i/\rho_c$, where ρ_i is the energy density of component i and ρ_c is the critical density of the universe; see section 2.1 for more information). For a spatially flat universe the total energy density by definition equals the critical density, so that $\Omega_{\rm tot} = 1$. An equivalent statement is that the curvature density parameter $\Omega_K = \Omega_{\rm tot} - 1$ is zero. Present observations strongly favour a flat universe, which is an argument in favour of inflation, as will be explained in section 1.2.

The components contributing to the total energy density are the following. First there is radiation: the photons flying around through the universe, most of which are CMBR photons. Even though there are very many of them (about 400 per cm^3), they contribute only a tiny fraction to the total energy density of the universe, since their energies have been redshifted to very low values by the expansion of the universe.

Next there is the contribution of matter. One way to determine the total matter contribution is from its gravitational influence on the rotation of galaxies and clusters. It turns

out to be much larger than the mass density we see directly in stars and other luminous objects, and even larger than the total amount of baryonic matter that is predicted by Big Bang nucleosynthesis. This is strong evidence for the presence of non-baryonic dark matter, that consists of particles not part of the Standard Model of particle physics, for example supersymmetric partner particles. Of course the fact that the total baryonic mass density is larger than the luminous mass density points to the existence of baryonic dark matter as well, for example heavy planets, dark gas clouds and stellar remnants. (The luminous density parameter is about 0.005, although it depends rather strongly on the exact definition of luminous matter.) Dark matter is generally divided into cold dark matter (consisting of massive particles and abbreviated as CDM) and hot dark matter (consisting of light particles, which still move at relativistic speeds, abbreviated as HDM). Despite the evidence for and ideas about dark matter, non-baryonic dark matter has never been observed directly, and its constitution is still one of the unsolved puzzles of cosmology.

The final component contributing to the total energy density is called dark energy or quintessence. It is an even more exotic and mysterious form of energy than dark matter, since it has a negative pressure. Recent observations of distant supernovae combined with CMBR data seem to lead to the conclusion that the largest part of the total energy density is of this form. A possible candidate for the dark energy is a cosmological constant. It is important to note that the values in table 1.1 are the present values of the density parameters Ω_i. Since the energy densities of the various components depend on time in different ways, their relative contributions will vary in time. (To be more explicit: if a is the expansion factor of the universe, the radiation and HDM energy densities behave as a^{-4}, baryon and CDM energy densities as a^{-3}, the energy density associated with curvature effects of the universe as a^{-2}, and the energy density of the cosmological constant is constant. See section 2.1 for more details.)

We continue with a chronological summary of the standard Big Bang theory, see figure 1.1. The times at which the different events are thought to have happened are model dependent, in particular they depend on the curvature of the universe. However, as mentioned above, current observations indicate that the universe is flat, so that the times given here are calculated using first a flat radiation-dominated Friedmann-Robertson-Walker universe and for later times a flat matter-dominated FRW universe (see section 2.1).

The first item to figure on a chronological list is the Planck time, 10^{-43} s. Before this time quantum fluctuations were so large (compared to the size of the universe itself, or at least of the causally connected part of the universe, see the discussion about the horizon in sections 1.2 and 2.1) that they completely distorted the universe. In other words, it is theoretically impossible to say anything definite about the universe before this time, at least until a theory of quantum gravity has been developed. A possible candidate for this theory might be string theory, although a lot of research still has to be done. In string theory the fundamental objects are no longer point particles, but tiny one-dimensional strings. The various particles then correspond with different vibration modes of the strings. In this description gravity is automatically included, which makes string theory a candidate for the theory of total unification (unification of the four fundamental interactions in nature: gravity and the strong, weak, and electromagnetic forces).

Neither do we have any certain theories about what happened between 10^{-43} and 10^{-10} s (between 10^{19} and 100 GeV). After the supposed total unification of the four fundamental forces during the Planck era, a symmetry breaking is assumed to have taken place at the Planck time, in which gravity separated from the other three forces. At an energy of the order of 10^{16} GeV the remaining grand unification (GUT = grand uni-

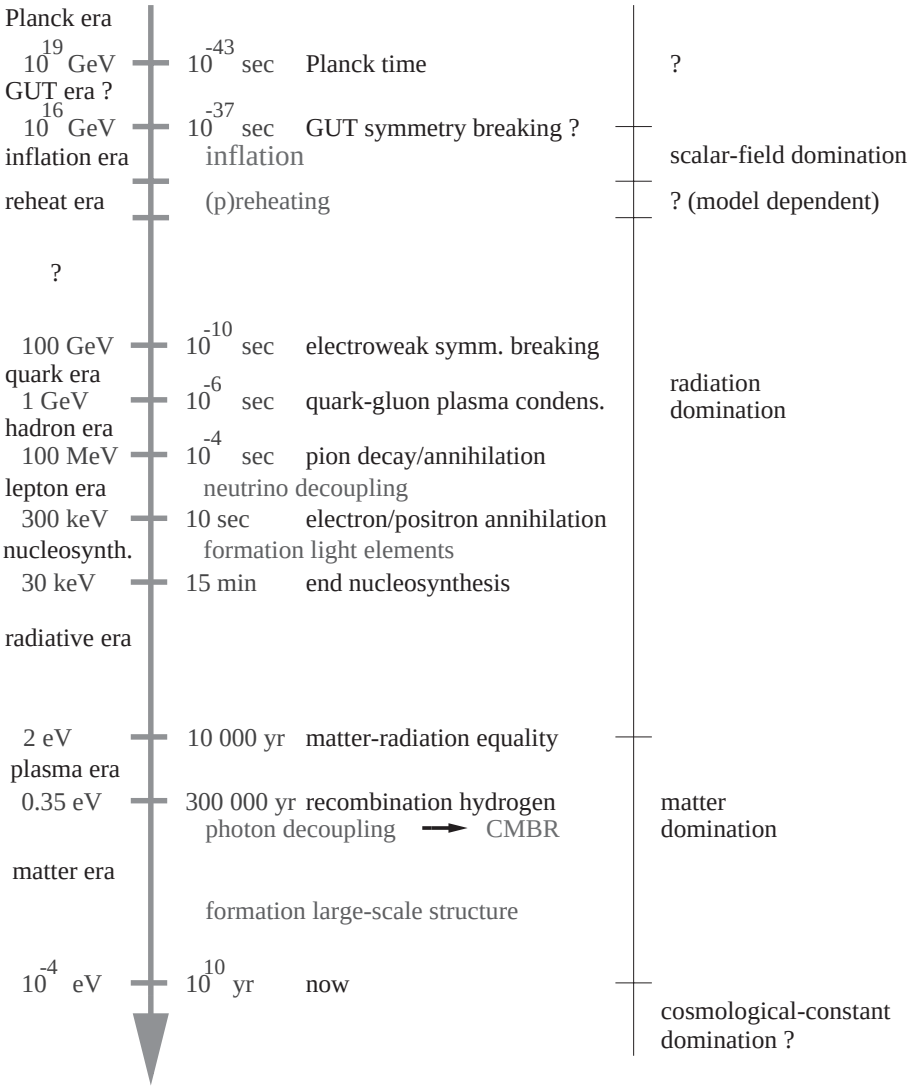

Figure 1.1: The chronology of the standard Big Bang theory. Included here is the inflation era, which is not part of the standard Big Bang theory, but an extension of it that solves a number of problems as discussed in section 1.2. We have taken a characteristic model of inflation starting at the GUT scale, but there are many other models where inflation started at higher or even at lower energies. Given are the names of the various eras, the energies and times when there was a transition from one era to another, the processes that caused these transitions, and some important events that took place in the eras. The form of energy dominating during each period is indicated in the figure on the right-hand side.

fied theory) was broken when the strong force (presumably) split off from the combined electromagnetic-weak force. Finally at 100 GeV the electro-weak symmetry was broken and the universe became as we know it, with four fundamental forces with quite different characteristics. (Some references to papers and books on high-energy theories can be found in section 3.1.)

For times later than about 10^{-10} s the standard Big Bang scenario gives a quite explicit model, as summarized in figure 1.1. The first era after this moment is called the quark era. During this era the universe was filled with a gas consisting of elementary particles, i.e. quarks, leptons and gauge bosons, called a quark-gluon plasma (gluons are the gauge bosons of the stronge force). The massive gauge bosons disappeared as a result of annihilation and decay processes, as did other heavy particles. When the average energy per particle had dropped to about 1 GeV it became possible for quarks and gluons to remain bound in composite particles called hadrons, and the hadron era began. (There are two types of hadrons: baryons consisting of three quarks and mesons consisting of a quark and an anti-quark.) However, there were far fewer hadrons than leptons and photons. This is because by this time the energy had dropped to such a low value that even the lightest baryons (protons and neutrons) could no longer be created in large numbers, unlike the lighter (or even massless) leptons and photons. This means that most of the baryons disappeared as a result of annihilation (and decay). The hadron era ended when the lightest mesons (pions) had also disappeared.

At that moment, at an energy of the order of 100 MeV, the lepton era began. The muons vanished because of annihilation and decay processes (the tau leptons had already gone by this time). So after the start of the lepton era the universe consisted primarily of photons, neutrinos and electrons/positrons. In addition there was a much smaller quantity of protons and neutrons. We draw attention to the following three events during the lepton era. In the first place, when the universe was about 0.01 s old the characteristic time interval between collisions of neutrinos and electrons became larger than the age of the universe. This means that neutrinos became essentially free: they no longer had any interactions with the other particles in the universe. This is called the decoupling of the neutrinos. The neutrinos were the first particle species belonging to the Standard Model that were no longer in thermal equilibrium with the rest of the universe. Secondly, during the lepton era the mean particle energy became of the order of the mass difference between protons and neutrons (neutrons are heavier). According to the Boltzmann distribution (which is valid in the case of thermal equilibrium) this means that the number of neutrons decreased somewhat compared with the number of protons. Moreover, unbound neutrons are unstable with a half-life value of about 900 s, an effect which made itself felt at the end of the lepton era (when the universe was about 10 s old) and led to an additional decrease of neutrons. Finally the lepton era ended when the energy had dropped below the value for electron-positron pair creation and the electrons had mostly disappeared as a result of annihilation.

It was at this point that the nucleosynthesis epoch began. The universe then consisted of lots of photons and decoupled neutrinos and relatively few protons, neutrons and electrons. When the universe was about 3 minutes old, the photon energy had dropped to a value low enough for deuterium to form from a proton and a neutron. Deuterium is rather susceptible to photodissociation, so that at higher energies all deuterium that formed was immediately destroyed by photons. Once deuterium had formed, helium could be produced. However, apart from a little lithium and beryllium, no heavier elements were formed because of the fact that there are no stable isotopes with a mass of 5 or 8 atomic

masses. To overcome this hurdle a high density and temperature are needed for a far longer time than a few minutes, a situation which was realized only much later in the cores of stars. The observed homogeneous distribution of helium and deuterium in the universe also points to a cosmological origin of these elements (production of helium in stars could not have led to such a homogeneous distribution, while deuterium cannot be produced in stars). The fact that the Big Bang theory gives a quantitative explanation for the observed abundances is a strong point in its favour.

After all neutrons had either been bound in (mainly) helium or decayed, the nucleosynthesis era ended. It was followed by the radiative era, during which nothing much happened. The radiative era ended after about 10 000 years, when the dominant form of energy was no longer radiation (i.e. relativistic particles) but matter (i.e. non-relativistic particles). Although there are many more photons and neutrinos than non-relativistic particles, the energy density of radiation drops more rapidly in an expanding universe than that of matter. This is caused by the expansion of the wavelength of radiation in addition to the effects of increasing volume that affect matter and radiation equally. Hence matter eventually started to dominate.

The following era is called the plasma era, because the universe then consisted of a plasma of photons and ionized matter. During this epoch photons were still in thermal equilibrium with matter by means of scattering by electrons. However, as temperature dropped further it became possible for the protons and electrons to combine into neutral hydrogen atoms. This process is called recombination, although in this context the prefix 're' is a little strange. Most helium was by this time already in the form of neutral atoms because of its higher ionization energy, but the recombination of hydrogen was more important as there was more of it (six times more electrons ended up in hydrogen atoms than in helium atoms). Exact calculations using the Saha formula (see [100, 32]) show that the largest amount of recombination happened at a temperature of about 3500 K. (Note that this is a much lower temperature than the 160 000 K that would be expected solely on the basis of the ionization energy of hydrogen, 13.6 eV. This is caused mainly by the small baryon to photon ratio.) At this moment, some 300 000 years after the Big Bang, the photons decoupled and the universe became transparent, since there were no longer free electrons to collide with. In other words, the mean free path of the photons became much larger than the size of the universe and generically they no longer had any interactions with the rest of the universe and only cooled because of the expansion. This means that all these photons should still be present nowadays, cooled to a temperature of about 3 K. The observation of this cosmic microwave background radiation of 2.73 K was the most decisive observation in favour of the Big Bang theory.[3] The observed high degree of isotropy in the background radiation again indicates a universe that at early times was very homogeneous. In section 1.3 the CMBR is discussed more extensively.

After recombination the matter era began. It is during this era that all matter structures like (super)clusters, galaxies, stars and planets were formed. The (large-scale) structure of the universe during the matter era, and especially the way it came into being, is still the subject of cosmology, but the study of individual objects of these kinds is where

[3]There should also be a neutrino background. Because of the fact that the neutrinos had already decoupled before the electrons and positrons annihilated (which led to a little increase in temperature for coupled particle species), the neutrino background temperature should now be about 1.9 K. However, because of the fact that neutrinos have very little interaction with other particles (and the low-energy neutrinos of the cosmic background have even less interaction than high-energy neutrinos from, for example, the sun) this neutrino background has not yet been observed.

one moves from cosmology to other branches of astronomy. Interestingly, if the recent observations indicating a sizable dark energy component are correct, we are on the brink of entering a new era in the evolution of the universe. If this dark energy is a cosmological constant, then we will enter a new era of inflation, but one that will never stop. However, if it has a different source, then this new period of inflation might well stop again after some time, or even never really start. Even though the present observational values exclude a recollapse of the universe, our ideas might change if the dark energy component turns out to be some evolving quantity. As long as we do not know more about it, it will be impossible to predict the future of our universe.

1.2 Inflation

Even though the standard Big Bang model discussed in the previous section is very successful in explaining many aspects of the universe we observe, there are some issues that are not resolved. The main motivation for proposing a period of inflation was to solve a number of these problems. They are [119]:

The horizon (causality) problem As is derived in section 2.1, in a radiation or matter-dominated universe, as described by the standard Big Bang theory, the horizon grows faster than space itself (the horizon bounds that part of space within which causal contact (information exchange) is possible). In other words, if we go back in time the horizon shrinks faster than a volume of space does. This means that, if we take the part of our universe that we can now observe (i.e. a volume that is now exactly equal to the horizon volume) and consider it at an earlier time, we find that, although it was smaller than it is now, it was larger than the horizon at that time. Hence according to the standard Big Bang theory the early universe consisted of many different 'cells' without the possibility of any causal contact with each other. Yet all these different cells started expanding at the same time, in the same way, to constitute together the homogeneous and isotropic universe that we observe. If we look at two opposite parts of the universe that even now are not in causal contact, we observe that the background radiation from the two places has the same temperature. Also we know from observations of cosmological abundances that the process of nucleosynthesis took place in approximately the same way everywhere in our part of the universe. According to the standard Big Bang theory, our presently observable universe consisted of about a million causally disconnected regions at the time of recombination, when the CMBR was formed, and of about 10^{24} at the time of nucleosynthesis. These strange phenomena constitute the horizon problem.

The flatness problem As discussed in section 1.1, present observations indicate that the universe is very flat, or in other words that the density parameter Ω_K associated with the curvature is almost zero. Since the associated energy density decreases less rapidly with time than that of matter and radiation (see section 2.1), this means that at earlier times Ω_K was even smaller. So the flatness problem is the following: why did the universe start out with Ω_K practically (within factors of 10^{-60} according to the standard Big Bang theory) equal to zero, when in principle it could have taken any value?

The monopole (topological defect) problem In grand unified theories topological defects are generally produced during symmetry-breaking phase transitions at high

temperatures, e.g. domain walls (boundaries between regions of different phases) and magnetic monopoles. The problem is that these objects are not observed, while the theories generally predict that they would by now dominate the energy density in the universe [161, 23].

The large-scale homogeneity problem At the largest scales, i.e. the earliest times, the universe is very homogeneous and isotropic. In particular we see from the background radiation that at the time of recombination there were only fluctuations at the level of 10^{-5}. In the context of the standard Big Bang theory this can only be solved by imposing extremely homogeneous and isotropic initial conditions, but it seems much more likely that they were chaotic and uncorrelated. (It is not so that these evolve naturally towards more homogeneity. For example, in [33] it was proved that it is extremely unlikely for a homogeneous anisotropic universe to evolve to an isotropic one.) So why is our universe so homogeneous and isotropic on the largest scales?

The small-scale inhomogeneity (density perturbations) problem This is the reverse side of the previous problem. Given that the universe was homogeneous and isotropic at the earliest times, what caused the formation of inhomogeneities like clusters and galaxies at later times? It is thought that these large-scale structures were made by gravitational collapse seeded by the tiny density perturbations that we observe in the CMBR. The theory of large-scale structure formation is a subject by itself, which will not be treated in this thesis. It crucially involves assumptions about the energy content of the universe, in particular about dark matter. Information on this subject can be found in e.g. [149, 32, 37]. However, the main point of the density perturbation problem is the question of what caused the small fluctuations that acted as seeds in an otherwise homogeneous universe.

For completeness' sake let us say that there are some more problems with the standard Big Bang model: the singularity problem (was there a beginning of the universe?), the cosmological constant problem (what is the origin of dark energy, why is its density so small compared with 'natural' (e.g. Planck) densities and why is it of the same order as the matter density exactly now?), the dark matter problem (what is the origin of dark matter?) and the baryon asymmetry problem (why is there more matter than antimatter?). However, as inflation is not a necessary ingredient for solutions to these problems[4] (as far as solutions have been found at all), we do not discuss them any further.

So what is inflation? Inflation [61, 119] is a very rapid expansion of the universe. It is believed to have happened in our (part of the) universe at a very early time, in most scenarios starting somewhere between the Planck and the GUT time (10^{-43} to 10^{-35} s after the Big Bang). The expansion is extremely fast, inflating the universe by a factor minimally of the order of about 10^{26} (but in some scenarios no less than 10^{10^7}!) in a time span of about 10^{-30} seconds or even less. (The fact that the expansion speed is much larger than the speed of light is not in contradiction with the theory of relativity, because this is the expansion speed of spacetime itself, not the velocity of something moving against the background of spacetime.) This rapid expansion can be caused by a scalar field, often called the inflaton, with an (almost) constant potential energy that acts

[4] Linde introduced the concept of eternal inflation as a possible solution to the singularity problem [117, 118, 119], but we will not discuss it in this thesis.

as an effective cosmological constant. Because of the enormous expansion, the universe becomes extremely cold and empty. Hence a period of reheating after the inflationary period is necessary to convert this potential energy to energy of other fields and thus 'refill' the universe with matter and radiation.

The models we will be considering are called slow-roll inflation models (for an historical overview with references see section 2.5). In the next chapters this is worked out in much more detail, but the main idea is as follows. The inflaton scalar field has a very flat potential with a minimum, along which it rolls down slowly. During the slow-roll phase the potential energy is quasi-constant, leading to rapid expansion. Inflation ends when the inflaton gets close to the minimum and starts rolling faster. Finally it oscillates around this minimum and coupling to other fields then causes a transfer of energy from the inflaton to matter and radiation fields: reheating. There is also the possibility of an initial period of resonances during these oscillations, leading to explosive particle production, which is called preheating [97, 98].

Instead of the simple single-field model we sketched here, more complicated inflation models with multiple scalar fields are nowadays considered more viable. There are two main reasons to consider multiple fields. The first is that there is more freedom and it is easier to construct models that satisfy all observational constraints without very unnatural parameter values. The other reason is that in general high-energy theories, like grand unification, supersymmetry or effective supergravity from string theory, there are many scalar fields, and it seems highly unlikely that only one of them would play a role during inflation. See section 3.1 for a more thorough discussion of the motivation for looking at multiple-field inflation.

It is the main characteristic of inflation, the rapid expansion, that provides the solution to the horizon, flatness, monopole and homogeneity problems. During this expansion the curvature energy density drops very rapidly (compared with the dominant scalar-field energy density) and the corresponding density parameter Ω_K goes to zero, so that the universe becomes effectively flat, even if it started out with non-zero curvature. An analogy for the universe after inflation is the Earth, which we observe as relatively flat, while in fact it is a sphere. However, one should realize that this a lower-dimensional analogy: the surface of the Earth is two-dimensional, while space is three-dimensional. The relation $\Omega_K = 0$ (to extremely high accuracy) can be seen as a rather generic prediction from inflation, even though there are some more contrived models that lead to an open or closed universe [122, 55, 48]. At the same time the enormous expansion dilutes any existing topological defects or inhomogeneities, thus solving the monopole and homogeneity problems. Of course one should take care that they are not reintroduced after inflation, for example by the process of reheating, which puts some constraints on the reheating temperature, see e.g. [5, 135] and references therein.

The horizon problem is also solved by the rapid expansion, basically by making the horizon distance much larger than it would be in the standard Big Bang theory. This is illustrated in figure 1.2. Figure 1.2(a) shows the situation in the standard Big Bang scenario without inflation. Drawn as a function of time are the horizon distance and the radius of that part of the universe that at our present time enters the horizon. As can be seen from the figure, this radius has never before been inside the horizon, giving rise to the horizon problem. To solve it, one would want the horizon curve to somehow lie much higher, so that the radius curve would lie completely beneath it. This can be accomplished by inflation, see figure 1.2(b). Inflation changes the horizon from the curve marked 'horizon(standBB)' to the curve marked 'horizon(inflation)' and it also changes

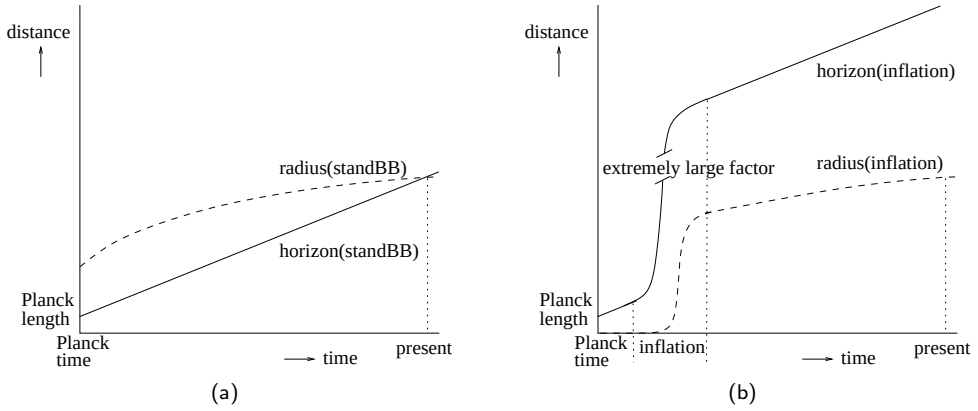

Figure 1.2: Two figures to clarify the horizon problem and its inflationary solution. Represented are the (particle) horizon distance and the radius of our presently observable part of the universe as a function of time, (a) for the standard Big Bang theory (without inflation) and (b) for the theory with inflation. Without inflation the radius is larger than the horizon (horizon problem), with inflation it lies completely within the horizon. (Standard Big Bang: horizon $\propto t$, radius $\propto t^{1/2}, t^{2/3}$; during inflation: horizon, radius $\propto \exp(Ht)$, see section 2.1.)

the behaviour of the radius with time. Now the radius is inside the horizon everywhere, so there are no longer causally unconnected regions in our observable part of the universe and the horizon problem is resolved.

The other problem, regarding the density perturbations, is also solved by inflation, but in a different way. Here it is not just the (classical) effect of the expansion, but also quantum effects that play a role. Basically the idea is that tiny quantum fluctuations, which are always present, are inflated to macroscopic density perturbations because of the rapid expansion during inflation. As soon as the wavelengths of these fluctuations are stretched beyond the Hubble length (or event horizon), they lose their quantum character and become effectively classical. This subject of density perturbations from inflation is the central issue of this thesis and is worked out in great detail in the next chapters.

Because no alternative has yet been proposed that can, with such relative ease, solve so many problems at the same time, inflation is now quite generally accepted as part of the evolution of the early universe. However, the existence of inflation has not been proved, and is actually very difficult to prove, because inflation models can accommodate such a wide range of values for observational parameters [106]. Indications for the correctness of inflation have come mostly from the absence or exclusion of alternatives, rather than from direct evidence for inflation itself. The most robust predictions of inflation are a flat universe, a scalar density perturbation spectrum with multiple peaks, gravitational wave perturbations and no vector perturbations (see sections 4.1 and 5.1 for an explanation of these concepts). The first two are in agreement with present observations, while the last two cannot yet be measured with sufficient accuracy. As mentioned above, however, some specific inflation models have been constructed that predict an open or closed universe. Hence, even if the universe turns out not to be flat after all, inflation cannot be ruled out completely. Furthermore, there is no proof that inflation models can never produce vector perturbations, so even a future observation of these need not rule out inflation, although this might change with further study. While gravitational wave perturbations are always

produced, their amplitude can be undetectably small. Hence it is difficult to really prove or disprove inflation. In this thesis we will assume the existence of inflation, and consider observations to see what kind of constraints they can set on the various models.

1.3 The cosmic microwave background radiation

In this section we give an introduction to the cosmic microwave background radiation (abbreviated as CMBR). The CMBR can be considered as the 'afterglow' of the Big Bang. Because of the recombination of hydrogen, 300 000 years after the Big Bang the universe became transparent for the photons produced in the earlier phases of the evolution of the universe. This moment (or, more correctly, period) is called decoupling and took place during matter domination. Since decoupling the photons have been moving freely about the universe, without interactions. Of course this is not completely true, as there were some photons that ended up in a star or even in one of our detectors, but the mean free path of the photons after decoupling has been so large that in a first approximation they can be considered to have moved without interactions. On small scales corrections to this approximation can become important, see the secondary sources of anisotropies below.

Because of the tight coupling between matter and radiation before the moment of decoupling, the photons were distributed according to a Planck distribution, which means that the energy density spectrum was a black-body spectrum characterized by one temperature. The collection of points where the photons of the CMBR that are now arriving at Earth had their last scattering before the universe became transparent is called the last-scattering surface. Note that because of this definition the coordinate distance to the last-scattering surface increases with time, simply because the photons are able to travel larger distances in more time. In reality the recombination of all hydrogen in the universe was not an instantaneous event. Hence the last-scattering surface is not a smooth, infinitely thin surface, but has a certain finite thickness. Even without interactions the energy of the photons changed: the photons shifted to longer wavelengths because of the expansion of the universe. A black-body spectrum remains a black-body spectrum during expansion, so that the photons continued to be distributed according to the Planck distribution and remained characterized by one temperature, which, however, became progressively lower.

After the introduction of the concept of a hot Big Bang in the 1940s by G. Gamow (see e.g. [47]) it was realized that the existence of a background temperature is a logical consequence of the physics described by this model. The first accurate calculation of this temperature was performed by R.A. Alpher and R.C. Herman in 1948 [6]. They predicted a temperature of 5 K, not far off the actual value. However, because the Big Bang theory was not really accepted at that time, these predictions were forgotten for nearly twenty years. It was only in 1965 that the background radiation was finally measured by A.A. Penzias and R.W. Wilson [152] and that the link with the Big Bang theory was established [38]. For an excellent description of the early CMBR studies and all the 'missed opportunities', see chapter 2 of [150].

After 1965 the CMBR has been studied extensively. Probably the most important measurements so far, from the point of view of inflation, have been made by NASA's COBE (COsmic Background Explorer) satellite. This satellite, launched in 1989, carried three instruments. FIRAS (Far InfraRed Absolute Spectrometer) measured the spectrum of the CMBR very accurately in the wavelength range where the maximum of the spectrum is located (0.1 mm $\leq \lambda \leq$ 1 cm). It operated for more than a year before the

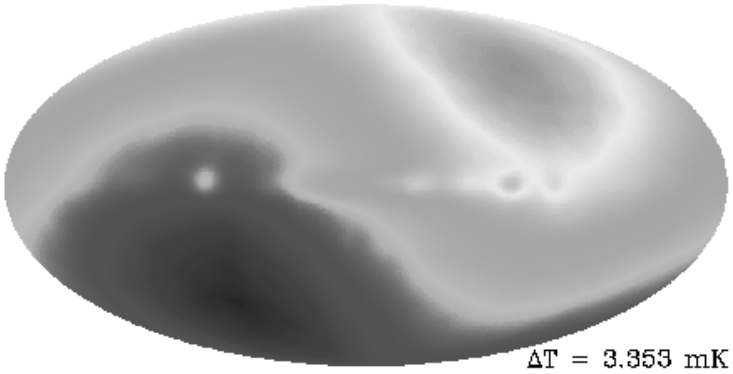

Figure 1.3: Full-sky projection of the four-year COBE DMR map, including the dipole anisotropy. Figure taken from [30].

cryogens ran out, and showed that the CMBR spectrum is a black-body spectrum with a temperature of 2.725 K (see table 1.1). The second instrument was DIRBE (Diffuse InfraRed Background Experiment). Its primary objective was to map the sky in the range of 1 μm $\leq \lambda \leq$ 0.3 mm and thus look for the emission from primeval galaxies and other luminous early objects, whose radiation lies mainly in this wavelength range because of the cosmic redshift and reprocessing by dust. Secondary objectives included studies of foreground astrophysical sources, e.g. thermal emission from interstellar dust and galactic starlight. The DIRBE instrument operated for a year at cryogenic temperatures and for another three years at reduced sensitivity after the cryogens were finished. The third instrument, the most important one from our point of view, was the DMR (Differential Microwave Radiometer). It searched for anisotropies in the CMBR by making differential measurements of the sky brightness in all directions at three wavelengths: 3.3, 5.7, and 9.5 mm (frequencies 90, 53, and 31 GHz, chosen because of minimal galactic emission at these wavelengths). After four years of data collection the DMR experiment was concluded in 1994. The results of the analyses of the first year of DMR data were published in 1992, those of two years in 1994 and finally those of the full four years of DMR data in 1996 [15]. More information on COBE and the DMR instrument can be found in [177, 19] and on the website [30].

From the DMR measurements we know that there is a large dipole anisotropy, caused by our motion with respect to the last-scattering surface, which is the result of gravitational attraction (the Earth moving around the sun, the sun moving around the centre of the galaxy, our galaxy moving within the Local Group, etc.), see [15] and figure 1.3. However, there are other, much smaller fluctuations, see figure 1.4. Before going on we first have to explain what is meant exactly by temperature fluctuations in the CMBR. Two different kinds of distortion are possible. The spectrum may not be Planckian with a single temperature in a given direction, and the spectrum may be Planckian in a given direction, but with different temperatures in different directions. The first possibility has been excluded to high accuracy by FIRAS. It is the second kind of distortion, measured by the DMR, which is generally meant by the term temperature fluctuations. Before discussing the importance of these anisotropies, we first mention some other measurements.

The COBE satellite had an angular resolution of about 7 degrees, and could therefore only look at anisotropies on rather large scales. The next generation of satellites should

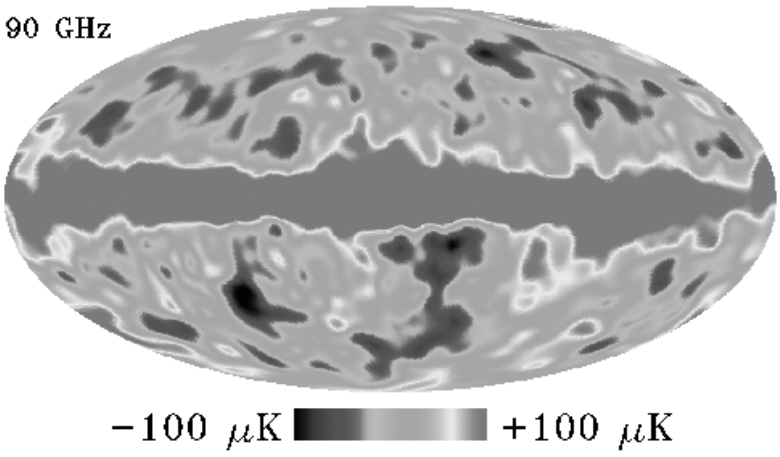

Figure 1.4: Full-sky projection of the 90 GHz four-year COBE DMR map. The dipole has been removed and the result has been smoothed to 10° effective resolution. The central band of the map is dominated by the bright emission from our galaxy. Figure taken from [30].

substantially increase the angular resolution of the observations as well as improve them in other respects, like sensitivity. The first of the new satellites is NASA's MAP (Microwave Anisotropy Probe), which was launched on June 30, 2001 and should chart the CMBR for two years with an angular resolution of 0.3 degrees. The first scientific results are expected at the end of 2002. The next one is ESA's Planck satellite, which is scheduled to be launched in 2007 and is expected to obtain an angular resolution of better than 10 arcminutes, as well as a sensitivity ten times higher than MAP. More information on these satellite missions can be found at their websites [130, 155]. In the mean time observations have been made by other means, of which the most important are the balloon-based experiments BOOMERanG (Balloon Observations Of Millimetric Extragalactic Radiation and Geophysics) and MAXIMA (Millimeter Anisotropy eXperiment IMaging Array). Although balloon experiments are much cheaper than satellites, the disadvantage is that they have a much shorter duration and only a small part of the sky is covered. This means that they cannot observe the temperature fluctuations on the largest scales, which are the most important from the point of view of inflation, see below. Even though their observation of the first and second acoustic peaks in the spectrum (see section 5.1) was very important, the COBE data are still the most accurate for constraining inflationary parameters, until the MAP data arrive. More information on BOOMERanG and MAXIMA can be found at their websites [22, 134].

The anisotropies observed by these experiments can be explained by a number of physical processes. They can be divided into three classes, conventionally called primary, secondary and tertiary sources of anisotropies (see e.g. [192]). Primary sources are those that were of importance during decoupling, for example density fluctuations at the surface of last scattering (regions of higher density are hotter). Secondary sources are those effects that played a role when the photons were travelling from the last-scattering surface towards our detectors, for example their interaction with hot clouds of gas. Finally, tertiary sources are foregrounds and noise, just contamination of the data. The difference between secondary and tertiary sources is that the secondary ones reprocess the CMBR photons,

while the tertiary ones simply remove them and/or add other photons. A more detailed discussion of the temperature anisotropies and their sources is given in section 5.1.

From a fundamental point of view the primary sources of anisotropies are the most important: they indicate the existence of small inhomogeneities at the time of recombination. These small inhomogeneities were the gravitational seeds for the large inhomogeneities that exist now: galaxies, clusters and superclusters. As indicated in section 1.2, inflation offers an explanation both for the large degree of homogeneity in the universe and for the small inhomogeneities. But this also works the other way round: to obtain a universe of the observed degree of homogeneity we can put a lower limit on the total amount of inflation. Moreover, the observed spectrum of anisotropies in the background radiation puts constraints on parameters in the inflation models. Observations of anisotropies at the largest scales are the most important for this, for the following reason. Inflation produced a spectrum of fluctuations at all scales. As long as the wavelength of a perturbation mode remained larger than the Hubble length (event horizon), this perturbation was more or less frozen. However, after inflation the Hubble length grew faster than the universe (and hence the wavelengths), so that one by one the perturbation modes reentered the horizon. After that happened, the primordial fluctuations on these scales were changed by local physical processes. So for observations of the primordial inflationary spectrum we need to look at the largest scales that were still outside the horizon at decoupling, that is scales larger than about one degree. In this way observations of the CMBR give us constraints on theoretical high-energy models far beyond the range of present or future particle accelerator experiments on Earth.

1.4 Outline of this thesis

The main objective of the work presented in this thesis is to develop a general analytical formalism for the treatment of density perturbations from slow-roll inflation. The word 'general' here refers to general models of slow-roll inflation, with an arbitrary number of scalar fields, which may live in a non-trivial field space. We emphasize the use of an analytical treatment (as opposed to a numerical one), as it provides more insight into the underlying physics: we can immediately see the dependences on the various variables and parameters in the results. Chapter 4, which treats the perturbations during inflation, is the central chapter of this thesis. However, chapter 3, which sets up the background theory of multiple-field slow-roll inflation, and chapter 5, which discusses what happens with the perturbations after inflation and how they enter into the CMBR, where they are observed, are of equal importance. The other chapters are the introductory chapter 2, introducing general cosmological concepts and single-field inflation, chapter 6, with detailed examples illustrating the general theory of chapters 3 to 5, and chapter 7 with the conclusions and outlook.

In more detail the contents of this thesis are the following (see also the table of contents on page 4). Chapter 2 starts with a discussion of many general cosmological concepts for the class of Friedmann-Robertson-Walker universes. Next the concept of inflation with a single scalar field is introduced, as well as the concept of slow roll and its consequences for inflation theory. An example to illustrate these concepts is provided. An historical overview of inflation models concludes this chapter.

Chapter 3 starts with a discussion of the motivation for trying to extend the standard single-field inflation theory to the case of multiple fields with a non-trivial field manifold.

Some geometrical concepts necessary for the multiple-field treatment are also introduced here. Next we generalize the inflationary equations of motion to the multiple-field case in a way that is covariant with respect to the field manifold and valid for a general choice of time variable. A basis on the field space that is induced by the background dynamics and that plays an important role in the rest of the thesis is defined. Furthermore, the concept of slow roll is generalized to the case of multiple fields as well. The multiple-field concepts and the differences with single-field inflation are illustrated by means of an example.

In chapter 4 the concepts of scalar, vector and tensor perturbations are defined and the relevant quantities and equations for the scalar perturbations are derived. Next we deal with the quantization and initial conditions of the scalar perturbations. The equations are then solved, leading to explicit expressions for the scalar perturbation quantities at the end of multiple-field inflation, valid to first order in slow roll and given in terms of background quantities only. Several issues play a role here, most important a correct treatment of the transition that occurs when the perturbation modes are inflated to super-horizon scales. The (much simpler) results for vector and tensor perturbations are also derived. A summary and discussion of the results of chapters 3 and 4 concludes this chapter.

Chapter 5 starts with a detailed description of the CMBR. Observational quantities are defined and observational features are described and explained qualitatively. Next we treat the perturbations after inflation during the radiative and matter eras until the time of recombination. Adiabatic and isocurvature perturbations are defined and treated separately. With these results the correlators of the perturbation quantities, which have their origin during inflation, are calculated at the time of recombination. The analytical, quantitative link between these correlators and the observations of the CMBR is described as well. The results of this chapter are summarized and the various aspects of perturbations after inflation that still have to be studied are pointed out.

Chapter 6 treats the example of inflation with a quadratic potential in various settings. First the simplest case of equal masses is discussed, followed by the case of a general mass matrix, both in a flat field space. Then we give some general results regarding the generalization to curved field spaces (not restricted to the case of a quadratic potential). Next two different cases of a quadratic potential with equal masses on a spherical field space are treated. The generalization to the situation of a general mass matrix on a curved field manifold is the subject of the next section. Finally there are some concluding remarks.

The conclusions of this work, as well as an outlook on further research that still needs to be done in this field, are given in chapter 7. Finally there are two appendices. Appendix A gives the more standard conventions and definitions that are used throughout this thesis (readers familiar with general relativity and field theory probably need not consult it). Appendix B gives expressions for various metric quantities in a Friedmann-Robertson-Walker universe with perturbations, which are used mainly in chapter 4.

This thesis is based on the following papers of mine. The general treatment of multiple-field slow-roll inflation in chapter 3 (in particular the basis in field space and the generalized treatment of slow roll) was first presented in [59] and worked out further in [60]. The treatment of the scalar perturbations during inflation in chapter 4 is based completely on [60]. Parts of chapter 5 (mainly of section 5.3) were presented in [60] and [195], but the other results are part of a paper that is still in preparation [194]. Finally the examples discussed in chapter 6 are based on examples treated in [59] and [60].

Chapter 2

Background theory

In this chapter the theory of the background during single-field inflation is treated. It can be viewed as another, more technical introduction. In section 2.1 the general theory of Friedmann-Robertson-Walker universes is discussed and the basic cosmological equations and definitions needed in this thesis are introduced. This is material that can be found in most textbooks on cosmology, e.g. [100, 149, 151]. In section 2.2 we concentrate on the case of a universe dominated by a single scalar field to introduce the basic concepts of inflation. Section 2.3 introduces the slow-roll approximation, which plays a very important role in this thesis. An explicit example with a potential of the form ϕ^n is worked out in section 2.4 to illustrate these concepts. Finally a brief historical overview of the various inflation scenarios is given in section 2.5. The generalization of the background theory to multiple fields follows in chapter 3, while the theory of the small perturbations on top of this background is the subject of chapter 4. Some information on the conventions and standard definitions used throughout this thesis can be found in appendix A.

2.1 Friedmann-Robertson-Walker universes

The standard metric used in cosmology is the Robertson-Walker metric [165, 198]. It is the most general metric for a spacetime that is spatially homogeneous. It can be written both in spherical and cartesian coordinates:

$$\mathrm{d}s^2 = -\mathrm{d}t^2 + a^2(t)\left(\frac{\mathrm{d}r^2}{1-Kr^2} + r^2(\mathrm{d}\theta^2 + \sin^2\theta\,\mathrm{d}\varphi^2)\right). \tag{2.1}$$

$$= -\mathrm{d}t^2 + a^2(t)\,\mathrm{d}\mathbf{x}^T\left(\mathbb{1} + \frac{K\mathbf{x}\,\mathbf{x}^T}{1-K\mathbf{x}^T\mathbf{x}}\right)\mathrm{d}\mathbf{x}. \tag{2.2}$$

With the superscript T we denote the transpose and $a(t)$ is the scale factor of the universe which has the dimension of length (the spatial coordinate r or $\mathbf{x}$ is dimensionless). The constant K is discussed below. The first form is probably the most familiar; the second form is obtained from the first by adding and subtracting an $a^2\mathrm{d}r^2$ and using $r^2 = \mathbf{x}^T\mathbf{x}$, so that $r\mathrm{d}r = \mathbf{x}^T\mathrm{d}\mathbf{x}$.

The quantity K is related to the curvature scalar of the 3-dimensional spatial part as $R^{(3)} = 6K/a^2$ (for a formal definition of quantities like the scalar curvature see ap-

pendix A), but by a suitable coordinate rescaling we can always make K take only one of the three values $+1, 0, -1$:

- $K = +1$: closed universe (positive spatial curvature);
- $K = 0$: flat universe (zero spatial curvature), in this case the spatial part is just Euclidean three-dimensional space;
- $K = -1$: open universe (negative spatial curvature).

As indicated in section 1.1, observations seem to point to a flat universe. As this is also predicted by inflation, we will only consider a spatially flat ($K = 0$) universe in this thesis. The only exception is this section, where we will keep the expressions more general and derive results for general curvature. In the flat case the metric simplifies to the expected $\mathrm{d}s^2 = -\mathrm{d}t^2 + a^2(t)\mathrm{d}\mathbf{x}^T\mathrm{d}\mathbf{x}$.

The choice for the Robertson-Walker metric is based on cosmological observations: the universe is very isotropic at large scales. Of course we can only make observations from our single position in space. To say something about the homogeneity of the whole of space we need to make an assumption: our spatial position in the universe is in no way exceptional. This is called the cosmological principle. More mathematically the cosmological principle can be formulated as the following two assumptions [203]:

1. The hypersurfaces with constant comoving time coordinate are maximally symmetric subspaces of the whole of spacetime.
2. Not only the metric $g_{\mu\nu}$, but all cosmic tensors, such as the energy-momentum-stress tensor $T_{\mu\nu}$, are form-invariant with respect to the isometries of these subspaces.

Some terminology needs to be explained, and this is done first. Then we will try to make clear why this formal definition says the same as the text above it. In the following three paragraphs we follow [203], chapters 13 and 14, where rigorous proofs can be found.

Consider a general infinitesimal coordinate transformation:

$$x^\mu \to \tilde{x}^\mu = x^\mu + \xi^\mu(x). \tag{2.3}$$

This causes a change to the metric given by

$$\delta g_{\mu\nu} = -(D_\mu \xi_\nu + D_\nu \xi_\mu). \tag{2.4}$$

(Covariant derivatives and other basic notation and conventions are defined in appendix A, see also appendix B.) Hence, if the vector ξ^μ satisfies the relation

$$D_\mu \xi_\nu + D_\nu \xi_\mu = 0, \tag{2.5}$$

the metric is unchanged by the coordinate transformation. In that case the coordinate transformation is called an isometry, and the corresponding vector ξ^μ is called a Killing vector. A space that admits the maximum number of Killing vectors (that is $d(d+1)/2$ in d dimensions) is called a maximally symmetric space. A homogeneous space that is isotropic about some point is maximally symmetric. The converse of this last statement also holds.

A tensor is called form-invariant with respect to a coordinate transformation if its form is unchanged by the transformation (i.e. if the transformed tensor is the same function

of $\tilde{x}^\mu$ as the original tensor was of x^μ). The metric tensor is form-invariant under an isometry. A tensor is called maximally form-invariant if it is form-invariant with respect to all isometries of a maximally symmetric space. The only maximally form-invariant scalar is a constant, the only maximally form-invariant vector (in more than 1 dimension) is the zero-vector, and the only maximally form-invariant second rank tensor (in more than 2 dimensions) is the metric tensor multiplied by a possible constant.

Now we can easily see what the mathematical definition of the cosmological principle means in non-mathematical language. The first part says that the universe is spatially homogeneous and isotropic. The second part more or less means that our spatial position is in no way exceptional since cosmic observables are invariant under isometries like translations. As is proved in [203], under the assumption that we have a 4-dimensional spacetime with a metric with 1 negative (time) and 3 positive (space) eigenvalues, the first part of the cosmological principle is sufficient to derive the Robertson-Walker metric.

The Robertson-Walker metric still contains the a priori undetermined function $a(t)$. It is determined by taking into account the matter content of the universe as well and solving the equation of motion for $a(t)$ that follows from the Einstein equation. The latter equation is derived by applying the action principle to the action

$$S = \int \mathrm{d}^4x \left(\kappa^{-2}\sqrt{-g}\left(\frac{1}{2}R - \Lambda\right) + \mathcal{L}_m \right), \tag{2.6}$$

where g is the determinant of the metric tensor, R the Ricci scalar curvature, Λ the cosmological constant and $\mathcal{L}_m$ the matter Lagrangean (density). The quantity κ is the inverse reduced Planck mass defined by

$$\kappa^2 \equiv 8\pi G = \frac{8\pi}{M_P^2}, \tag{2.7}$$

see appendix A. The resulting Einstein equation [40] is

$$G_{\mu\nu} + \Lambda g_{\mu\nu} = \kappa^2 T_{\mu\nu}, \qquad T_{\mu\nu} \equiv -\frac{2}{\sqrt{-g}}\frac{\delta S_m}{\delta g^{\mu\nu}}, \tag{2.8}$$

with $G_{\mu\nu}$ the Einstein tensor defined in appendix A, $T_{\mu\nu}$ the energy-momentum-stress-tensor and $S_m = \int \mathrm{d}^4x\, \mathcal{L}_m$.

The second part of the cosmological principle states that all cosmic tensors are maximally form-invariant with respect to the spatial coordinates, which has some very constraining consequences for the energy-momentum-stress tensor $T_{\mu\nu}$. Using the remarks made on maximally form-invariant tensors above we see that the most general form for $T_{\mu\nu}$ is:

$$T_{00} = \rho(t), \qquad T_{0i} = 0, \qquad T_{ij} = p(t)g_{ij}, \tag{2.9}$$

where $\rho(t)$ and $p(t)$ are arbitrary functions of time only. Defining a vector u^μ with components $u^0 = 1$, $u^i = 0$ (which is just the four-velocity $\mathrm{d}x^\mu/\mathrm{d}t$ of a comoving observer/particle in the universe), we can also write this as

$$T^\mu_{\ \nu} = (\rho(t) + p(t))\, u^\mu u_\nu + p(t)\delta^\mu_\nu. \tag{2.10}$$

This is the same form as for a perfect fluid with energy density ρ, pressure p and four-velocity u^μ. So assuming only the cosmological principle the $T_{\mu\nu}$ of the universe is necessarily restricted to that of a perfect fluid. Universe models thus obtained are referred to as Friedmann models [46] or Friedmann-Robertson-Walker (FRW) universes.

The time coordinate t used in the Robertson-Walker metric (2.1) is called comoving time. Derivatives with respect to this time coordinate are denoted by a dot, and the corresponding Hubble parameter is defined as $H \equiv \dot{a}/a$. One can also define a conformal time coordinate η by the relation $\mathrm{d}t = a\mathrm{d}\eta$. With this time coordinate the scale factor is an overall factor in front of the total metric, so that this metric is conformal to one for a static universe. Derivatives with respect to conformal time are denoted by a prime and the corresponding Hubble parameter is $\mathcal{H} \equiv a'/a = aH$. Another quantity that, although not exactly a time coordinate, is sometimes used as one is the number of e-folds N. It is defined as $a = a_0 \exp(N)$, which leads to the relations $\mathrm{d}N = H\mathrm{d}t = \mathcal{H}\mathrm{d}\eta$. The derivative with respect to N is denoted by the subscript $_{,N}$. Since $a_{,N}/a = 1$ there is no need for an additional Hubble parameter. For easier access we summarize these definitions:

$$\mathrm{d}t = a\,\mathrm{d}\eta, \qquad H = \frac{\dot{a}}{a}, \qquad \mathcal{H} = \frac{a'}{a} = aH, \qquad \mathrm{d}N = H\mathrm{d}t = \mathcal{H}\mathrm{d}\eta. \tag{2.11}$$

Just like a, the comoving time t has the dimension of length (or inverse mass), while H has the dimension of mass. On the other hand η, $\mathcal{H}$ and N are all dimensionless. Of course it is possible to use a more general time variable τ with $\mathrm{d}t = b\,\mathrm{d}\tau$, where b is an a priori unspecified function of time. By making specific choices for b the three special cases above are recovered. We return to this general time variable in section 3.2.

Working out the Einstein equation (2.8) for a FRW universe we find from the (00) component (see appendix B) the so-called Friedmann equation:

$$H^2 = \frac{\kappa^2}{3}\,\rho + \frac{1}{3}\Lambda - \frac{K}{a^2}. \tag{2.12}$$

Combining this equation with the (ij) component of the Einstein equation we find an equation that can be written in the following two ways:

$$\frac{\ddot{a}}{a} = -\frac{\kappa^2}{6}\,(\rho + 3p) + \frac{1}{3}\Lambda \qquad \Leftrightarrow \qquad \dot{H} = -\frac{\kappa^2}{2}\,(\rho + p) + \frac{K}{a^2}. \tag{2.13}$$

From the energy-momentum conservation condition $D_\mu T^\mu_0 = 0$ we obtain

$$\dot{\rho} + 3H(\rho + p) = 0. \tag{2.14}$$

This equation is not independent of the other two, as the conservation condition that $D_\mu T^\mu_\nu = 0$ is included in the Einstein equation, since $D_\mu G^\mu_\nu = 0$ by construction (Bianchi identity). Dividing the Friedmann equation by H^2 and bringing the curvature term to the left-hand side we get the following relation:

$$1 + \Omega_K = \Omega + \Omega_\Lambda \equiv \Omega_{\mathrm{tot}}, \tag{2.15}$$

$$\Omega \equiv \frac{\rho}{\rho_c}, \quad \Omega_\Lambda \equiv \frac{\rho_\Lambda}{\rho_c}, \quad \Omega_K \equiv \frac{\rho_K}{\rho_c}, \quad \rho_\Lambda \equiv \frac{\Lambda}{\kappa^2}, \quad \rho_K \equiv \frac{3K}{\kappa^2 a^2}, \quad \rho_c \equiv \frac{3H^2}{\kappa^2}.$$

Here we defined the density parameters Ω_i. The density parameter Ω can be split into radiation, luminous matter and cold and hot dark matter components. The critical density ρ_c is the value of the total energy density that is necessary for a flat universe ($K = 0$). A higher density means a closed universe, a lower density an open one. Although the total sum $\Omega_{\mathrm{tot}} - \Omega_K = 1$ is time independent, the individual density parameters have different

dependences on the scale factor, and hence the contributions of the individual components to the total will vary in time.

We can immediately draw the conclusion from the first form of (2.13) that if $\Lambda = 0$ the expansion is accelerating for $p < -\rho/3$, and decelerating for $p > -\rho/3$. We now concentrate on the case of a universe where ρ is dominated by matter with $p = 0$, i.e. $\Omega = \Omega_m$. According to (2.14) this means that $\rho \propto a^{-3}$. From (2.12) we see that, if $\Lambda = 0$ and $K = +1$, there is a time when $\dot{a} = 0$, after which the universe will start to shrink and finally disappear in a singularity, called the Big Crunch. If $K = 0$ or $K = -1$, the universe will expand forever (still taking $\Lambda = 0$). Note that for $\Lambda = 0$ the values $K = +1, 0, -1$ correspond with $\Omega_m > 1, = 1, < 1$, respectively. Instead of considering the case $\Lambda = 0$, $\rho \neq 0$ we can also look at the situation for $\rho = 0$, $\Lambda \neq 0$. In that case the expansion of the universe is accelerating for $\Lambda > 0$ and decelerating for $\Lambda < 0$. If $K = +1$ in this situation, there is also a time when $\dot{a} = 0$. However, in this case the expansion of the universe is accelerating, so that this value of a corresponds with a minumum rather than a maximum. In other words, the case $K = +1$, $\rho = 0$ has no Big Bang. For $\rho = 0$ the values $K = +1, 0, -1$ correspond with $\Omega_\Lambda > 1, = 1, < 1$, respectively.

In the previous paragraph we have discussed the behaviour on the axes of an Ω_Λ versus Ω_m plot (under the assumption that $p = 0$). The complete plot is given in figure 2.1. By definition (2.15) $\Omega_\Lambda + \Omega_m = 1 + \Omega_K$, so that the line $\Omega_\Lambda + \Omega_m = 1$ corresponds with a flat universe. From (2.13) we find that the condition $\ddot{a} = 0$, which separates a universe with accelerating expansion from a decelerating one, is given by the line $\Omega_\Lambda = \Omega_m/2$. To determine the curve that bounds the region of no Big Bang (i.e. the boundary between regions where $a = 0$ in the past is or is not allowed) and the curve that bounds the region of recollapse (i.e. the boundary between regions where $a = 0$ in the future is or is not allowed) a more complicated calculation is necessary, but the intersection of these curves with the axes is clear from the discussion in the previous paragraph. Especially the region of recollapse is intuitively clear: in principle a positive cosmological constant will make the universe expand forever, except when the matter density is large enough to make it recollapse before the cosmological constant can start to dominate. A detailed analysis is given in [42], with the results

$$\Omega_\Lambda = 4\Omega_m \left[\cos\left(\frac{1}{3}\arccos(\Omega_m^{-1} - 1) + \frac{4}{3}\pi\right)\right]^3 \tag{2.16}$$

(with $\Omega_m \geq 1$) for the recollapse boundary, and

$$\Omega_\Lambda = 4\Omega_m \left[\mathrm{coss}\left(\frac{1}{3}\mathrm{arccoss}(\Omega_m^{-1} - 1)\right)\right]^3 \tag{2.17}$$

for the no Big Bang boundary, with coss = cosh for $\Omega_m \leq \frac{1}{2}$ and coss = cos for $\Omega_m \geq \frac{1}{2}$.

If we assume an equation of state of the form $p = w\rho$, with w a constant, then we can solve (2.14) explicitly to find

$$\rho \propto a^{-3(1+w)}, \qquad w = \frac{p}{\rho}. \tag{2.18}$$

Note that equation (2.14) deals with the total energy density and pressure. For the individual components i one has

$$\dot{\rho}_i + 3H(\rho_i + p_i) = X_i, \qquad \sum_i X_i = 0, \tag{2.19}$$

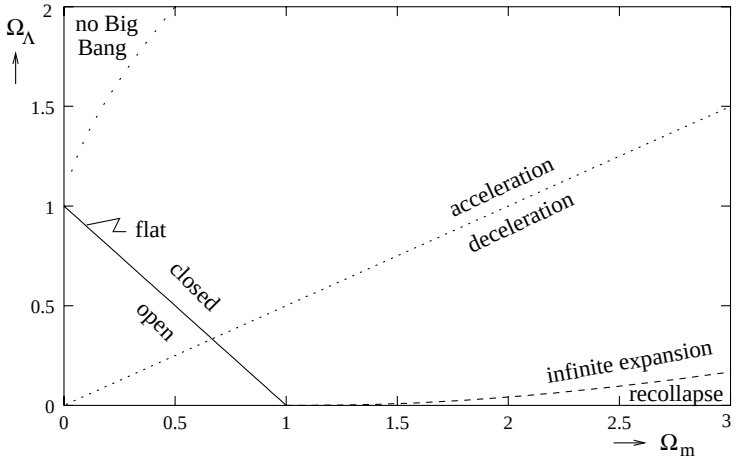

Figure 2.1: A figure showing the expansion behaviour of the universe for different combinations of cosmological constant and matter densities in an Ω_Λ versus Ω_m plot. Matter with $p = 0$ is assumed to dominate other sources, like radiation. The curvature density parameter Ω_K is given by the relation $\Omega_K = \Omega_m + \Omega_\Lambda - 1$. For a further discussion see the main text.

with X_i a measure of the interactions between the different components. Only if the interaction term X_i is zero can we use the solution (2.18) also for the individual components in the case that more than one of these are important at the same time. Three special cases are of particular interest: radiation, matter and vacuum domination.

	Equation of state	Energy density	Scale factor ($K = 0$)
Radiation dom.	$w = \frac{1}{3}$	$\rho \propto a^{-4}$	$a \propto t^{1/2}$
Matter dom.	$w = 0$	$\rho \propto a^{-3}$	$a \propto t^{2/3}$
Vacuum dom.	$w = -1$	$\rho =$ constant	$a \propto \exp(\kappa\sqrt{\frac{\rho}{3}}\, t) = \exp(Ht)$

In all these cases we have also taken $\Lambda = 0$. However, the case of vacuum energy domination with $p = -\rho$ is completely equivalent to a cosmological constant in an otherwise empty universe, as can be seen from (2.10) and (2.8). The time dependence of the scale factor follows from the Friedmann equation (2.12), which can easily be solved for $K = 0$. (Solutions for a non-flat universe are more complicated and are not needed in this thesis. They can be found in e.g. [87].) In the case of radiation domination, or when interaction between the photons and other components can be neglected, we find from the thermodynamical result $\rho_{\rm rad} \propto T^4$ that the (radiation) temperature $T \propto a^{-1}$. The results $\rho \propto a^{-3}$ for matter and $\rho \propto a^{-4}$ for radiation have a simple physical explanation. The energy density of matter is inversely proportional to the volume and hence decreases proportionally to a^{-3}. For radiation there is an additional decrease caused by the redshift of the wavelengths with a factor a.

We conclude this section by defining some distance and related concepts, like horizons. The geometrical distance d between two points (at the same time t) separated by a

coordinate (or comoving) distance r_0 is defined by

$$d(t) = a(t) \int_0^{r_0} \frac{\mathrm{d}r}{\sqrt{1 - Kr^2}}, \tag{2.20}$$

where we used the spatial part of (2.1). For the case of a flat universe this simplifies to the expected $d(t) = a(t)r_0$.

Next we proceed with a discussion of the horizon. Actually there are two relevant horizons: the particle horizon and the event horizon. Our particle horizon is the boundary of that region in space from the past of which we, living at time t, can in principle obtain information. The geometrical distance at time t to this boundary is often called the particle horizon as well. In other words, the particle horizon bounds that region of space with which causal contact has been possible in the past. Because of the spatial homogeneity the particle horizons of all points in space are the same. Since our particle horizon is by definition connected with us by a null geodesic, we obtain from (2.1), using $\mathrm{d}s^2 = 0$, that

$$\int_0^t \frac{\mathrm{d}t'}{a(t')} = \int_0^{r_0} \frac{\mathrm{d}r}{\sqrt{1 - Kr^2}}. \tag{2.21}$$

Combining this with (2.20) we find for the particle horizon:

$$d_H(t) = a(t) \int_0^t \frac{\mathrm{d}t'}{a(t')}. \tag{2.22}$$

Using $a(t) \propto t^{1/2}$ for a flat radiation-dominated FRW universe and $a(t) \propto t^{2/3}$ for a flat matter-dominated FRW universe we get $d_H(t) = 2t = 1/H(t)$ for radiation domination and $d_H(t) = 3t = 2/H(t)$ for matter domination. Expressions for closed and open FRW universes can be found in e.g. [87]. In the situation of vacuum domination one obtains the result $d_H(t) = (\exp(Ht) - 1)/H$.

The other horizon, our event horizon, is defined as the boundary of that region in space from which it will be possible for us, between our time t and a certain later time $t_{\max}$, to obtain information. In other words, the event horizon bounds that region of space with which causal contact will be possible in the future. Completely analogously to equation (2.22) we obtain for the geometrical event horizon distance

$$d_E(t) = a(t) \int_t^{t_{\max}} \frac{\mathrm{d}t'}{a(t')}. \tag{2.23}$$

One usually takes $t_{\max} = \infty$, at least for those universes that do not recollapse. For the matter and radiation-dominated FRW universes this gives $d_E = \infty$, but for vacuum domination we find the finite value $d_E = 1/H$.

2.2 Single-field inflation

In this section we concentrate on the case of a specific kind of matter: scalar fields. Here we only take a single real scalar field, but in the next chapter we extend this to the case of multiple fields, which is the main subject of this thesis. When discussing inflation we only consider flat backgrounds without a cosmological constant: $K = 0 = \Lambda$. This is

motivated by observations: as indicated in the introduction the universe seems to be flat, which is also a prediction from inflation (one of the reasons for introducing inflation in the first place). And although there seems to be a dark energy component, which might be a cosmological constant, it is only becoming important at the present time. This means that it was negligible at much earlier times, as it does not scale with the scale factor of the universe. Two remarks are in order here. In the first place $K = +1, 0, -1$ is determined by the topology of space, which does not change by inflation. However, the physical quantity that enters the equations is the spatial curvature, which is proportional to K/a^2, and it is this quantity that is reduced to zero by inflation. Effectively the result is the same as setting $K = 0$. Secondly, any transitory effects at the start of inflation, when the universe had not yet been inflated to effective flatness, are neglected. In section 4.3 there is a discussion related to this subject, showing that for a large class of initial states the exact initial conditions are irrelevant, provided that there is a sufficiently large amount of inflation. As our subject is the theory of perturbations from inflation, we take the presence of sufficient inflation as a starting point.

Considering the general action (2.6) we now have the following matter Lagrangean:

$$\mathcal{L}_m = \sqrt{-g}\left(-\frac{1}{2}g^{\mu\nu}\partial_\mu\phi\partial_\nu\phi - V(\phi)\right), \tag{2.24}$$

with ϕ a real scalar field with potential V. From this we derive the energy-momentum tensor and the field equation:

$$T^\mu_{\ \nu} = \partial^\mu\phi\,\partial_\nu\phi - \delta^\mu_\nu\left(\frac{1}{2}\partial^\lambda\phi\,\partial_\lambda\phi + V(\phi)\right), \qquad D^\mu\partial_\mu\phi - \frac{\partial V}{\partial\phi} = 0. \tag{2.25}$$

As explained in the introduction, we consider the background to be homogeneous. As we are only considering the background in this (and the next) chapter, this means that the (background) field ϕ depends only on time and not on spatial coordinates. In that case the energy-momentum tensor and field equation simplify to

$$T^\mu_{\ \nu} = -\delta^{\mu 0}\delta_{\nu 0}\dot\phi^2 + \delta^\mu_\nu\left(\frac{1}{2}\dot\phi^2 - V(\phi)\right), \qquad \ddot\phi + 3H\dot\phi + \frac{\partial V}{\partial\phi} = 0. \tag{2.26}$$

(See appendix B for expressions for the metric connection used to work out the covariant derivative in the field equation.) Comparing this with (2.10) we can determine the energy density and pressure of the scalar field:

$$\rho = \frac{1}{2}\dot\phi^2 + V(\phi), \qquad p = \frac{1}{2}\dot\phi^2 - V(\phi). \tag{2.27}$$

The Friedmann equations (2.12) and (2.13) then read as

$$H^2 = \frac{\kappa^2}{3}\left(\frac{1}{2}\dot\phi^2 + V(\phi)\right), \qquad \dot H = -\frac{1}{2}\kappa^2\dot\phi^2. \tag{2.28}$$

Note that the conservation equation (2.14) also gives the field equation (2.26); of the three equations in (2.26) and (2.28) only two are independent. To solve these equations analytically we need the concept of slow roll, which is discussed in the next section.

We conclude this section with an estimate of the amount of inflation that is necessary to solve the horizon and flatness problems. As discussed in section 1.2, inflation solves

the horizon problem by causing the present horizon to be much larger than it seems to be. To solve the horizon problem we demand that the region we can presently see (and which would be our present horizon if there was no inflation) was within the horizon at the beginning of inflation. Ignoring numerical factors of order one this means that (see the text below (2.22))

$$\frac{1}{H_0} < \frac{a_0}{a_{\rm begin}} \frac{1}{H_{\rm begin}}. \tag{2.29}$$

The minimal amount of inflation can then be written as

$$\frac{a_{\rm end}}{a_{\rm begin}} = \frac{a_{\rm end}}{a_0} \frac{H_{\rm begin}}{H_0}. \tag{2.30}$$

We use the relation $T \propto a^{-1}$ discussed in the text below (2.19) and make the further approximation that all energy in the scalar field is used for reheating, so that the energy scale at the end of reheating is equal to the one at the beginning of inflation, which we denote by M (i.e. $T_{\rm end} \sim M$ and $\rho_{\rm begin} \sim M^4$). Then we obtain the following rough order of magnitude estimate:

$$\frac{a_{\rm end}}{a_{\rm begin}} = \frac{T_0}{M} \frac{\kappa M^2}{H_0} = 10^{29} \kappa M \sim e^{60}, \tag{2.31}$$

where we used the values of T_0 and H_0 from table 1.1 and estimated $\kappa M \sim 10^{-3}$. This number of 60 e-folds is a rather rough estimate, but it gives an indication of how much inflation is needed to solve the horizon problem, and it is the number that is conventionally quoted in the literature. A more detailed derivation, also taking into account incomplete reheating, can be found in [108], equation [5.16]. If the reheating temperature is lower, the number of e-folds is smaller, but the dependence on the various energy scales is only logarithmical.

To solve the flatness problem we demand that Ω_K at the beginning of inflation can be of the same order of magnitude as Ω_K is now, instead of the many orders of magnitude smaller it has to be in the standard Big Bang theory. From (2.15) we see that $\Omega_K = K/(a^2H^2)$. Therefore the condition that $(\Omega_K)_0 = (\Omega_K)_{\rm begin}$ gives exactly the same relation (2.29) as the solution of the horizon problem. Hence both the horizon and flatness problems are solved if there are at least about 60 e-folds of inflation.

2.3 Slow roll

The equations of the previous section are too difficult to solve analytically in general. Fortunately, the concept of inflation itself as well as observations indicate that a certain simplifying approximation is well-motivated: the so-called slow-roll approximation [185, 108, 111]. Basically this approximation assumes that the potential is sufficiently flat, so that the scalar field varies only slowly. This means that second-order time derivatives can be neglected with respect to first-order time derivatives, and kinetic energy can be neglected compared with potential energy.

The first motivation for slow-roll inflation is simply the amount of inflation that is needed to solve the horizon and other problems. As discussed at the end of the previous section, this means that during the very short period of inflation the universe must expand

by at least the same factor as during all the time after inflation up till now. This naturally leads to the idea of exponential expansion. As shown in section 2.1 that is the kind of expansion you get with vacuum domination: a cosmological constant or, equivalently, a kind of matter with $p = -\rho =$ constant. Looking at the pressure and energy density of a scalar field in (2.27) we see that this is precisely the situation we have if there is no roll at all: the kinetic terms are zero and the potential is constant. This automatically means that ϕ must be in a (local) minimum of its potential, i.e. a vacuum, hence the name vacuum domination.

Of course no roll at all would mean that inflation never ends. In the literature there have been two main ways of solving this so-called graceful exit problem: bubble formation and slow roll (references can be found in section 2.5). The first method works in the case where the field ϕ is really trapped in a local minimum of the potential, which is not the global minimum. After some time the field will tunnel through the potential barrier to the global minimum, leading to the production of bubbles of the new phase inside the old inflating phase. In practice there are often problems with this procedure. This is the reason that the other method, slow roll, is generally preferred. In this thesis we will not discuss bubbles and only treat slow-roll inflation.

The idea with slow roll, as mentioned above, is that we have a very flat potential, along which the field slowly rolls down. This means that the kinetic terms are not exactly zero, but small, and the potential is only quasi-constant, leading to very rapid, so-called quasi-exponential inflation. Inflation ends when the field starts rolling more rapidly in the neighbourhood of the global minimum. Reheating occurs during the oscillations around this minimum by coupling to other fields. In this way it is rather easy to construct models that lead to sufficient inflation before a graceful exit and sufficient reheating. As will be explained in later chapters, slow-roll inflation also naturally leads to an almost scale-invariant spectrum of density perturbations, which agrees with observations. This is the other main motivation for considering slow-roll inflation.

We now make this concept of slow roll more precise. We define the following two slow-roll functions [34]:

$$\tilde{\epsilon} \equiv -\frac{\dot{H}}{H^2} = \frac{\frac{1}{2}\kappa^2\dot{\phi}^2}{H^2}, \qquad \tilde{\eta} \equiv \frac{\ddot{\phi}}{H\dot{\phi}}. \tag{2.32}$$

Although $\tilde{\epsilon}$ is defined in terms of $\dot{H}$, it is also given in terms of $\dot{\phi}$ using (2.28), which is a form that is equally useful. From this last form, using (2.28) for H^2, we see that for a positive potential V the function $\tilde{\epsilon} < 3$. For slow roll to be a valid approximation these functions must be (much) smaller than one, which is the reason they are called slow-roll functions. The function $\tilde{\epsilon}$ shows the size of the kinetic term compared with the potential, while $\tilde{\eta}$ measures the size of the second-order time derivative of the field with respect to the first-order time derivative term in the field equation. Using these definitions as shorthand notation, we can rewrite the Friedmann equation (2.28) and the field equation (2.26). Using the second expression for $\tilde{\epsilon}$ the former is easy:

$$H = \frac{\kappa}{\sqrt{3}}\sqrt{V}\left(1 - \frac{1}{3}\tilde{\epsilon}\right)^{-\frac{1}{2}}. \tag{2.33}$$

Rewriting the field equation is a bit more complicated, but writing it first in the form $\partial V/\partial\phi = \ldots$, where the right-hand side is rewritten in terms of slow-roll functions, and

then adding $\dot{\phi}$ to the left-hand side, and the equivalent $H\sqrt{2\tilde{\epsilon}}/\kappa$ to the right-hand side, we find

$$\dot{\phi} + \frac{1}{\kappa\sqrt{3}}\frac{1}{\sqrt{V}}\frac{\partial V}{\partial \phi} = -\sqrt{\frac{2}{3}}\sqrt{V}\frac{\sqrt{\tilde{\epsilon}}}{1-\frac{1}{3}\tilde{\epsilon}}\left(\frac{1}{3}\tilde{\eta} + \frac{\frac{1}{3}\tilde{\epsilon}}{1+\sqrt{1-\frac{1}{3}\tilde{\epsilon}}}\right). \tag{2.34}$$

These two equations are still exact. From them we can define more precisely what is meant by slow roll. Slow roll is valid if $\tilde{\epsilon}$ and $\sqrt{\tilde{\epsilon}}\,\tilde{\eta}$ are (much) smaller than unity. If slow roll is valid, we can use expansions in powers of these slow-roll functions to estimate the relevance of various terms in a given expression. For example, to first order the Friedmann equation (2.33) is approximated by replacing $(1-\tilde{\epsilon}/3)^{-1/2}$ by $(1+\tilde{\epsilon}/6)$. The background field equation up to and including first order is given by (2.34) with the right-hand side set to zero, as all those terms are order 3/2 or higher. Sometimes it is also useful to have an expression for the field equation in terms of the number of e-folds N:

$$\phi_{,N} + \frac{1}{\kappa^2}\frac{\partial V/\partial\phi}{V} = -\frac{\sqrt{2}}{3\kappa}\frac{(\tilde{\epsilon}+\tilde{\eta})\sqrt{\tilde{\epsilon}}}{1-\frac{1}{3}\tilde{\epsilon}}, \tag{2.35}$$

from which we can derive the same conclusions regarding orders in slow roll.

At the level of the solutions of these equations we make the following definition. An approximate solution of an equation of motion is said to be accurate to first order in slow roll, if the relative difference between this solution and the exact one is of a smaller numerical order than the slow-roll functions. In general this relative error depends on the size of the integration interval. Let us explain this with the following example. From its definition we can easily derive that the time derivative of $\tilde{\epsilon}$ is one order higher in slow roll:

$$\dot{\tilde{\epsilon}} = 2H\tilde{\epsilon}(\tilde{\epsilon}+\tilde{\eta}). \tag{2.36}$$

Hence we can make the assumption that to first order the slow-roll functions are constant. Switching to the number of e-folds N, we can integrate (2.36) to find the variation of $\tilde{\epsilon}$ over an interval $[N_1, N_2]$:

$$\Delta\tilde{\epsilon} = \int_{N_1}^{N_2} \mathrm{d}N\, 2\tilde{\epsilon}(\tilde{\epsilon}+\tilde{\eta}) = 2\tilde{\epsilon}_0(\tilde{\epsilon}_0+\tilde{\eta}_0)(N_2-N_1). \tag{2.37}$$

Here the subscript $_0$ denotes some reference time in this interval when the slow-roll functions are evaluated. Hence we see that if the interval (N_2-N_1) becomes larger than $1/(2(\tilde{\epsilon}_0+\tilde{\eta}_0))$, $\Delta\tilde{\epsilon}$ becomes larger than $\tilde{\epsilon}_0$ and the assumption of taking $\tilde{\epsilon}$ constant to first order over this interval is certainly not valid anymore. Neither are any results obtained using this approximation expected to be valid to first order during longer intervals. Of course this is a very rough estimate of the interval of validity of first-order results. It is not really meant as an expression to be used in calculations, but more as an illustration of the issue of integration intervals in slow-roll solutions that should be kept in mind when treating specific cases. In the literature these effects are usually ignored and the solution of an equation of motion valid to first order is (implicitly) assumed to be accurate to first order as well. However, with that assumption the numerical error between slow-roll and exact solution may become very large depending on the size of the interval of integration, which is the reason for our more careful definition.

The slow-roll functions (2.32) are defined as functions of derivatives of the field ϕ and the Hubble parameter H. If the leading-order slow-roll approximation works well — that is if the right-hand side of (2.34) can be neglected, as well as the $\tilde{\epsilon}$ in (2.33) — then we can use these two equations to eliminate $\dot{\phi}$ and H in favour of the potential V. This is the way the original single-field slow-roll parameters were defined [108]. However, this original definition has the disadvantage that the slow-roll conditions become consistency checks. While we can expand the exact equations in powers of the slow-roll functions, that is impossible by construction in the case of the original slow-roll parameters [111]. For completeness' sake we compare the slow-roll functions defined in (2.32) with the original ones defined in terms of the potential, ϵ and η:

$$\epsilon = \frac{1}{2\kappa^2}\frac{(\partial V/\partial\phi)^2}{V^2} = \tilde{\epsilon}, \qquad \eta = \frac{1}{\kappa^2}\frac{\partial^2 V/\partial\phi^2}{V} = -\tilde{\eta} + \tilde{\epsilon}, \tag{2.38}$$

where the last equalities in both equations are only valid to leading order in the slow-roll approximation. To distinguish the newer slow-roll functions from the original slow-roll parameters we added the tilde in the notation. Another reason was to avoid confusion with the conformal time η.

2.4 Example: ϕ^n potentials

In this section we work out the example of a ϕ^n potential, both analytically and numerically. This is to illustrate the inflationary concepts that were introduced in this chapter, as well as to be able to make comparisons when treating the multiple-field case. We take the following monomial potential:

$$V(\phi) = \frac{1}{n}\,\kappa^{-4} g\,(\kappa\phi)^n \tag{2.39}$$

with the coupling constant g dimensionless. The first-order slow-roll field equation (2.34) and Friedmann equation (2.33) read as

$$\dot{\phi} = -\frac{1}{\kappa^2}\sqrt{\frac{ng}{3}}\,(\kappa\phi)^{\frac{n}{2}-1}, \qquad H = \frac{1}{\kappa}\sqrt{\frac{g}{3n}}\,(\kappa\phi)^{\frac{n}{2}}\left(1+\frac{1}{6}\tilde{\epsilon}\right). \tag{2.40}$$

Taking as initial condition $\phi(0) = \phi_0$ and solving this field equation we find

$$\phi(t) = \begin{cases} \phi_0\left(1-\frac{t}{t_\infty}\right)^{\frac{2}{4-n}} & \text{for } n \neq 4, \\ \phi_0\,\exp\left(-\frac{2}{\kappa}\sqrt{\frac{g}{3}}\,t\right) & \text{for } n = 4, \end{cases} \qquad t_\infty \equiv \frac{2}{4-n}\,(\kappa\phi_0)^{\frac{4-n}{2}}\kappa\sqrt{\frac{3}{ng}}. \tag{2.41}$$

In the special case of a quadratic potential ($n = 2$) this simplifies to

$$\phi(t) = \phi_0\left(1-\frac{t}{t_\infty}\right), \qquad t_\infty = \sqrt{\frac{3}{2}}\frac{\kappa^2\phi_0}{m}, \tag{2.42}$$

with $g = m^2$ (dimensionless).

Instead of the comoving time t, it is often more convenient to use the number of e-folds N as a time variable during inflation. Equation (2.35) gives to leading order

$$\phi_{,N} = -\frac{n}{\kappa^2}\frac{1}{\phi} \qquad \Rightarrow \qquad \phi(N) = \sqrt{\frac{2n}{\kappa^2}\,(N_\infty - N)}, \qquad N_\infty \equiv \frac{\kappa^2\phi_0^2}{2n}. \tag{2.43}$$

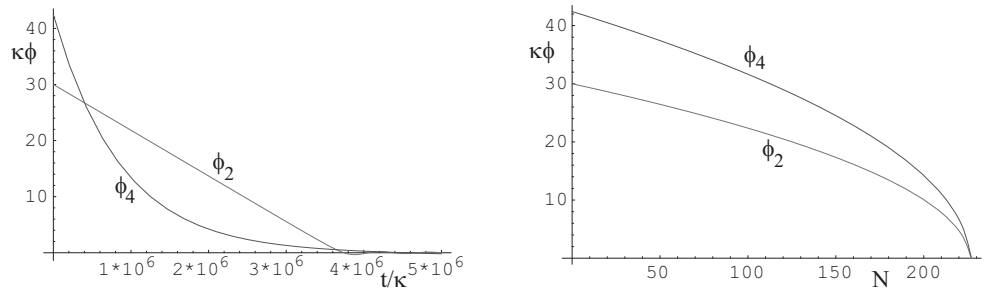

Figure 2.2: The exact numerical solutions for the field $\kappa\phi$ for a quadratic and a quartic potential, with $m = 10^{-5}$ and $\lambda = 10^{-12}$ respectively. The initial condition for the quadratic potential is $\kappa\phi_0 = 30$ and for the quartic potential $\kappa\phi_0 = 30\sqrt{2}$. In (a) The field is given as a function of comoving time, in (b) as a function of the number of e-folds. Everything is expressed in terms of Planck units κ as indicated.

Here there is no need to treat the case $n = 4$ separately. The solution for $\phi(N)$ can be inverted to give an expression for $N(t)$:

$$N(t) = N_\infty \left(1 - \frac{\phi(t)^2}{\phi_0^2}\right). \tag{2.44}$$

As in these potentials ϕ eventually rolls down to zero, N_∞ gives the leading-order estimate for the total amount of inflation. Note that it only depends on the initial condition ϕ_0 and the exponent n of the potential, not on the coupling constant g. The slow-roll functions $\tilde{\epsilon}$ and $\tilde{\eta}$ can be determined using the expressions in terms of N:

$$\begin{aligned} \tilde{\epsilon} &= -\frac{H_{,N}}{H} = \frac{n^2}{2\kappa^2}\frac{1}{\phi^2} = \frac{n}{4}\frac{1}{N_\infty - N}, \\ \tilde{\eta} &= \frac{\phi_{,NN}}{\phi_{,N}} - \tilde{\epsilon} = \frac{n(2-n)}{2\kappa^2}\frac{1}{\phi^2} = \frac{2-n}{4}\frac{1}{N_\infty - N}. \end{aligned} \tag{2.45}$$

As we are working to leading order in slow roll, it is not surprising that these expressions are identical to the ones obtained by using the old definition in terms of the potential (2.38). It is clear that they are not valid anymore at the end of inflation, when $N \to N_\infty$.

Next we consider two specific cases to illustrate the results. These are a quadratic potential ($n = 2$) with $m = 10^{-5}$ and initial condition $\kappa\phi_0 = 30$, and a quartic potential ($n = 4$) with $\lambda = 10^{-12}$ and initial condition $\kappa\phi_0 = 30\sqrt{2}$. The values for m and λ have been chosen to give the right order of magnitude for the density perturbations, as will be discussed in later chapters. The initial conditions have been chosen to ensure sufficient inflation, and moreover to give the same total amount of inflation for both potentials, $N_\infty = 225$. Numerically we find $N = 226.3$ before the oscillations start for the quadratic potential and $N = 226.4$ for the quartic potential. In the following we denote by the exact numerical solution the numerical solution of the exact equation of motion (2.26), while the analytical slow-roll solution is the one given in (2.41), or alternatively in (2.43). Since the exact equation of motion is a second-order equation, we also need to specify the initial condition for the field velocity in that case. For this we take the value given by the analytical slow-roll solution.

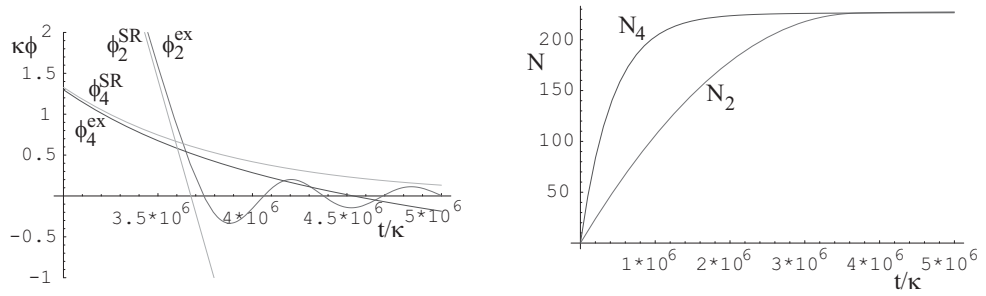

(a) (b)

Figure 2.3: (a) A comparison between the exact numerical solution (i.e. the numerical solution of the exact equation of motion (2.26)) and the analytical slow-roll solution (2.41) for the field $\kappa\phi$ as a function of comoving time near the end of inflation in the same two situations as in figure 2.2. (b) The number of e-folds N as a function of comoving time.

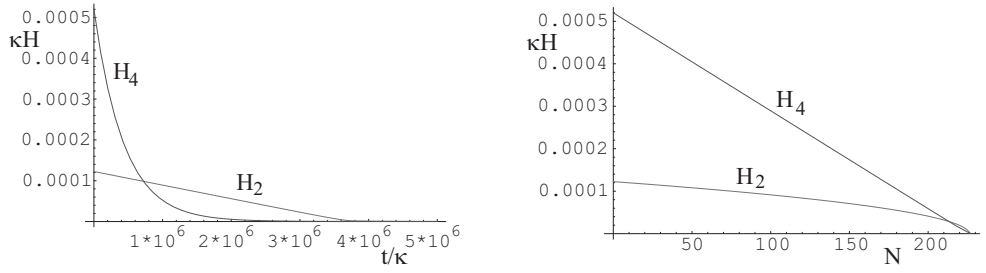

(a) (b)

Figure 2.4: The exact numerical solutions for the Hubble parameter H for the same quadratic and quartic potentials as in figure 2.2, as a function of (a) comoving time and (b) number of e-folds.

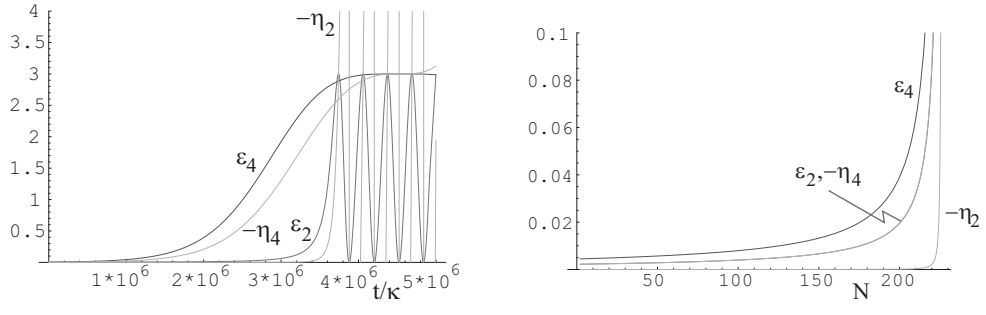

(a) (b)

Figure 2.5: The exact numerical solutions for the slow-roll functions $\tilde{\epsilon}$ and $\tilde{\eta}$ for the same quadratic and quartic potentials as in figure 2.2, as a function of (a) comoving time and (b) number of e-folds. The graphs of $\tilde{\epsilon}$ for the quadratic potential and of $-\tilde{\eta}$ for the quartic potential as a function of N lie on top of each other. Note the different vertical axes in the two figures.

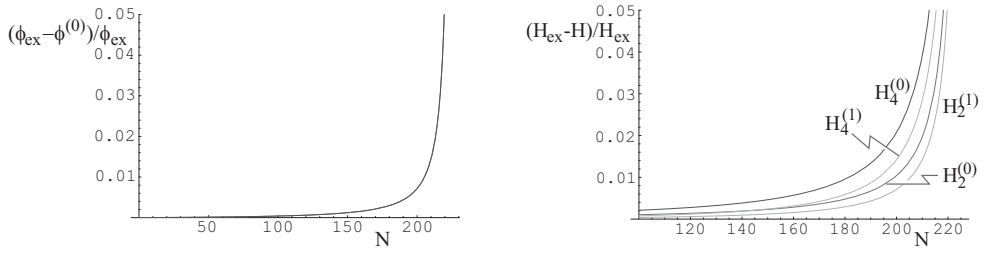

(a) (b)

Figure 2.6: (a) The relative error in the analytical slow-roll solution for the field compared to the exact numerical solution as a function of the number of e-folds in the same two situations as in figure 2.2. The curves for the quadratic and quartic potential lie on top of each other. (b) The relative error in the analytical slow-roll solution for the Hubble parameter compared to the exact numerical solution as a function of the number of e-folds. Shown are the errors of both the zeroth and the first-order slow-roll solution ((2.40) without and with the $\tilde{\epsilon}/6$ term).

In figure 2.2 the field ϕ is plotted, both as a function of comoving time t and as a function of the number of e-folds N. The scaling with $\sqrt{n}$ (see (2.43)) can be recognized in figure 2.2(b), as well as the linear and exponential behaviour in figure 2.2(a) (see (2.42) and (2.41)). Figure 2.3(b) shows the relation between the number of e-folds and comoving time. Since N grows more rapidly with time for the quartic potential than for the quadratic potential, we always find that $\phi_4 > \phi_2$ as a function of N, while as a function of t ϕ_4 becomes smaller than ϕ_2 very quickly, see figure 2.2. Figure 2.3(a) is the same as figure 2.2(a), but zoomed in on the end of inflation. The slow-roll solutions have been added to the plot and we see that the slow-roll approximation becomes bad at the end of inflation, completely missing the oscillatory behaviour of the exact solution, as expected. However, until the very end of inflation the slow-roll solution is a very good approximation, as can be seen from figure 2.6(a), where the relative error in the field is plotted.

In figure 2.4 the Hubble parameter H is plotted as a function of t and of N. For the quartic potential the linear behaviour that follows from (2.43) and (2.40) can be seen in figure 2.4(b). On the other hand, in terms of comoving time the relation is linear for the quadratic potential, see figure 2.4(a) and (2.42) and (2.40). The relative error in the zeroth and first-order slow-roll approximations for H (i.e. (2.40) without and with the term $\tilde{\epsilon}/6$) is shown in figure 2.6(b). As expected the slow-roll approximation is very good during most of the inflationary period (in terms of N) and only becomes bad at the end of inflation. The first-order approximation is somewhat better than the zeroth-order one.

The slow-roll functions $\tilde{\epsilon}$ and $\tilde{\eta}$ are plotted in figure 2.5 as a function of t and of N. The scaling of $\tilde{\epsilon}$ with n (see (2.45)) can be recognized in figure 2.5(b). The fact that in that figure the curves of $\tilde{\epsilon}$ for the quadratic potential and of $-\tilde{\eta}$ for the quartic potential lie practically on top of each other also agrees with the slow-roll results in (2.45). According to the slow-roll solution $\tilde{\eta} = 0$ for a quadratic potential, in agreement with the fact that only at the very end of inflation the exact numerical expression starts to deviate from zero. In figure 2.5(a) the behaviour of the slow-roll functions after slow-roll inflation has ended can also be seen. We observe that $\tilde{\epsilon} \leq 3$, as it should be according to its definition.

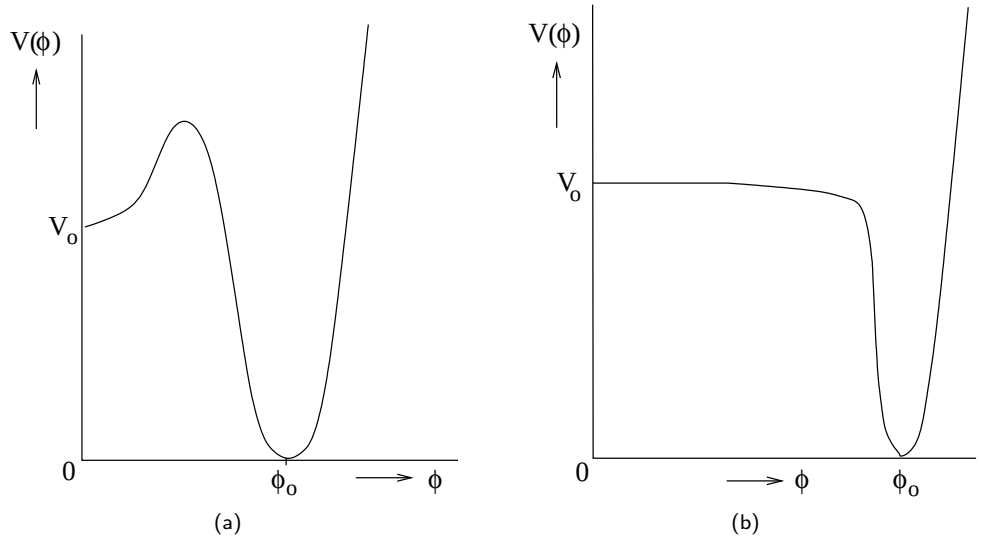

Figure 2.7: (a) The potential of old inflation [61] with bubble nucleation as exit mechanism. (b) The potential of new inflation [114] introducing the concept of slow roll.

2.5 Historical overview

In this section we give a brief overview of inflation scenarios that played an important role in the establishment of the inflationary paradigm. Some of these have been ruled out by observations, while others are still viable. Most of them play no further role in this thesis, since, although it would be interesting to apply the theory of the next chapters to all of them, that is beyond the scope of this work.

Old inflation The term inflation was invented by A. Guth when he proposed his original model in 1981 [61]. It is based on the idea of a phase transition in the early universe: a potential with a global minimum at $\phi = 0$ changes after a phase transition to the form shown in figure 2.7(a), and the scalar field ϕ is trapped in what is now a local minimum at zero, behind a potential barrier. Its potential energy becomes the dominant energy density in the universe and acts as an effective cosmological constant, leading to exponential expansion. Inflation ends when the field reaches the global minimum by means of quantum tunneling through the barrier. This leads to the production of bubbles of the new phase inside the old inflating phase. The idea was that these bubbles would grow and collide, and by colliding reheat the universe (before the collisions the original energy of the scalar field is trapped in the bubble walls). However, it was found [64] that, if there is sufficient inflation in this model to solve the horizon problem, the bubbles are too far apart to collide and there is insufficient reheating. Hence this model was never viable, but it introduced the concept of inflation into the general cosmological community.

Starobinsky model Before Guth's model, A. Starobinsky had already proposed an inflationary model [178], without using this name. However, for several reasons his idea was not picked up by the cosmological community as Guth's was. One of the reasons was that Starobinsky's model is rather complicated, based on one-loop quan-

tum corrections to the Einstein equations, where Guth's model is very simple, clearly showing the basic concepts. Actually Starobinsky's model was the first example of the so-called higher derivative gravity (or higher curvature) inflation models. These models were later shown to be equivalent to standard Einstein gravity plus a scalar field, see [141] and references therein.

New inflation The problems with the old inflation model led A. Linde to propose a new model, called new inflation [114]. A bit later this same model was also proposed in [4]. Again the existence of a phase transition in the early universe is assumed, after which the potential has the form indicated in figure 2.7(b), with the field ϕ starting off near zero and slowly rolling towards the absolute minimum at ϕ_0. Actually a very specific potential was used in this model: the SU(5) Coleman-Weinberg potential [51, 31]. In this model reheating occurs during the oscillations around the minimum of the potential at the end of inflation by means of the weak coupling of the inflaton to other fields. However, it turns out that the parameter values in this potential are not compatible with the observational constraints from the fluctuations in the CMBR [63], so that in the end the original new inflation model is not viable either, though for different reasons than old inflation. Very importantly, however, new inflation introduced the concept of slow-roll inflation. More information about later, changed versions of the original new inflation model can be found in [119].

Chaotic inflation In 1983 Linde realized that slow-roll inflation could take place with much simpler potentials, like a quadratic or quartic potential. He called these models chaotic inflation [115], because chaotic initial conditions are used to explain the large initial field values needed in these models. Nowadays the name chaotic inflation is generally used for all single-field models with a potential satisfying the slow-roll conditions in some region and having a minimum with zero potential in which inflation ends and reheating occurs. To have sufficient inflation, initial conditions high up the potential are needed. Many of these models have been proposed, some with generic simple potentials, some with specific potentials motivated by particular high-energy theories. References can be found in [119, 125]. We discussed the class of ϕ^n chaotic inflation models in section 2.4. The examples we will discuss in section 3.4 and chapter 6 can be classified as multiple-field chaotic inflation models.

Power-law inflation Later on it was realized that exponential potentials lead to power-law inflation instead of exponential inflation [124, 105], as can be seen from (2.35) and (2.33). An interesting aspect of power-law inflation is that the slow-roll functions are constant, so that many calculations are simplified and can be done analytically. However, in its simplest form this model lacks a way to end inflation, which is of course unacceptable. A multiple-field version of power-law inflation was proposed in [110] under the name of **assisted inflation**. This name was chosen because inflation is possible in this model if there are enough fields, even though their individual potentials may be too steep to support inflation separately.

Extended inflation Extended inflation (1989) [102] is based on old inflation, but it assumes Brans-Dicke gravity [25] instead of standard Einstein gravity. By means of a conformal transformation this can be rewritten as standard Einstein gravity plus a scalar field with an exponential potential [62] (plus the old inflation scalar field). Compared to old inflation, there is now power-law inflation caused by the Brans-Dicke field while the old inflation field is trapped behind the barrier, and it turns

out that in this model sufficient inflation and reheating by bubble percolation can both be realized at the same time. Compared to power-law inflation, there is now a motivation for the exponential potential as well as a mechanism to end inflation. However, observations of the fluctuations in the CMBR combined with tests of Einstein gravity rule out extended inflation: with the Brans-Dicke parameter in the range allowed by tests of deviations from Einstein gravity the bubbles would cause density fluctuations in the CMBR that are much too large [107]. Extensions have been proposed that avoid these problems by using more complicated alternative gravity theories [184, 11, 36, 112] and go under the name of **hyperextended inflation**. However, the point remains that for inflation models ending by means of bubble nucleation it is generally more difficult to satisfy the observational constraints from density perturbations in the CMBR than for slow-roll inflation models. This is the reason that slow-roll inflation is by far the most popular variant.

Natural inflation Natural inflation, first introduced in 1990 [45], is based on a pseudo-Nambu-Goldstone-boson potential:

$$V(\phi) = \Lambda^4 \left(1 + \cos\frac{\phi}{f}\right), \tag{2.46}$$

where a global spontaneous symmetry breaking at a scale f has been assumed and an additional soft explicit symmetry breaking at a lower scale Λ. The name 'natural inflation' was chosen because a potential like this can arise naturally from particle physics models. In [45, 1] it was found that a working model can be constructed if $f \sim M_P$ and $\Lambda \sim M_{\rm GUT}$. However, f cannot be much smaller than M_P, or else there is insufficient inflation to solve the horizon problem. The fact that a mass scale at or above the Planck value is needed can be considered an objection against this model. There is also a supersymmetric two-field version of this scenario, called **supernatural inflation** [163]. The authors claim that in this model the necessary small parameters and flat potentials appear naturally from the underlying theory.

Hybrid inflation The term hybrid inflation was properly introduced in 1994 [121], although the corresponding model was first proposed in [120]. It is now used as a collective term for inflation scenarios with two scalar fields, one field being responsible for the mechanism of graceful exit, while the other field provides the main drive for inflation. It combines elements from single-field inflation scenarios. In fact, the extended inflation scenario discussed above may well be considered as a hybrid model of power-law inflation and old inflation after performing the conformal transformation.

The hybrid inflation model of [121] is a combination (hybrid) of chaotic inflation and a kind of spontaneous symmetry breaking inflation, but without the tunneling (and bubble) part of old inflation. This model has the following potential:

$$V(\sigma,\phi) = \frac{1}{4\lambda}(M^2 - \lambda\sigma^2)^2 + \frac{1}{2}m^2\phi^2 + \frac{1}{2}g^2\phi^2\sigma^2, \tag{2.47}$$

which is shown in figure 2.8. The parameters and initial conditions are chosen in such a way that initially the curvature of the potential in the σ direction is much greater than in the ϕ direction and $\sigma = 0$ at the start of inflation. Inflation is then first driven by the field ϕ in the way of chaotic inflation with a potential $\frac{1}{2}m^2\phi^2$. Because

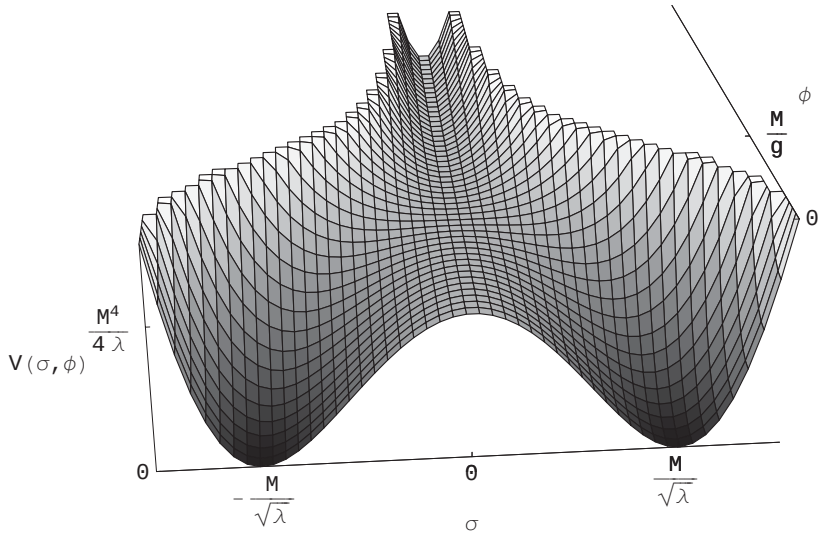

Figure 2.8: The potential of the original hybrid inflation model [121]. One starts with $\sigma = 0$ and ϕ large. As soon as ϕ becomes smaller than M/g, σ can move away from zero to the absolute minimum of the potential and inflation ends.

ϕ decreases this term will become smaller than the vacuum energy $M^4/(4\lambda)$ after some time, which then takes over as the driving force for inflation, while ϕ continues to roll down to zero. Meanwhile the field σ is still at zero, which is at first a stable minimum (the curvature $\partial^2 V/\partial\sigma^2$ is $g^2\phi^2 - M^2 > 0$). However, after $g^2\phi^2$ has become smaller than M^2, $\sigma = 0$ is an unstable maximum and the field σ makes a second-order phase transition to the new minimum at $\sigma = \pm M/\sqrt{\lambda}$, $\phi = 0$, thus breaking the symmetry. Inflation ends when this absolute minimum of the potential is reached, and the universe is reheated during the oscillations of the fields around this minimum.

One of the good things of hybrid inflation (or more generally of multiple-field models) is that one can often obtain sufficient inflation, a graceful exit and the correct density perturbation spectrum without very small values of the coupling constants and very large initial conditions [121, 137]. There are by now many hybrid inflation models; a review with references is given in [125].

Thermal inflation Thermal inflation [126, 127] is different from other models of inflation in the sense that it takes place at much lower energies (between about 10^7 and 10^3 GeV). Also the total amount of inflation is only about 10 e-folds. Hence it is not meant as a stand-alone scenario of inflation, but as an addition to a 'standard' model of inflation at high energies, with the purpose of removing any unwanted relics that may have been produced after the first stage of inflation. In particular thermal inflation was introduced to remove modulus fields produced in high-energy models based on string theory (see also [7]). Thermal inflation is basically just a variation of the old inflation model, with a field trapped behind a potential barrier. Only here the barrier is caused by finite temperature effects and disappears below a certain critical temperature, so that quantum tunneling does not play a role. As

thermal inflation leads only to about 10 e-folds of inflation, it does not disturb the inflationary perturbations from the first stage on observationally relevant scales.

Warm inflation The model of warm inflation [16] is based on the idea of having inflation and reheating at the same time. In this model the inflaton is in thermal equilibrium with other fields during the whole period of inflation, and releases sufficient vacuum energy into the heat bath to compensate for the dilution due to inflationary expansion. Simultaneously it is the backreaction of the heat bath on the inflaton that slows its roll down the potential, so that sufficient inflation can be achieved. It is unclear, however, if this concept can produce a working model of inflation [207, 17]. An extension of the warm inflation concept, called extended warm inflation, was discussed in [128].

Chapter 3

Multiple-field inflation

In this chapter the theory of the background is generalized to the case of multiple-field inflation. It is based on my papers [59, 60]. In section 3.1 we give the motivation for looking at this more complicated situation with multiple scalar fields and a non-trivial field metric. Some geometrical concepts that are necessary to treat this case are also introduced. In section 3.2 the equations of motion for multiple-field inflation are derived. This is done in a very general setting, using a general time variable. A basis for the field manifold that is induced by the dynamics of the system is defined. Section 3.3 generalizes the concept of slow roll to multiple-field inflation, introducing the multiple-field slow-roll functions. Finally an example of a quartic potential is worked out in section 3.4 to illustrate the various concepts introduced in this chapter. A summary of the results in this chapter, together with those of chapter 4, will be given in section 4.6.

3.1 Motivation and geometrical concepts

As discussed in section 1.2, inflation provides a solution for a number of problems in the standard Big Bang theory and is now quite generally accepted as part of the evolution of the early universe. As shown in the previous chapter we can use scalar fields and a potential satisfying certain conditions to produce inflation. In fact one really needs fields that behave as scalars under spacetime transformations, since inflation models are based on a field moving away from or towards zero, either in the context of slow roll or of a phase transition. A non-zero global (space-independent) background spinor or vector field would break Lorentz invariance, so that inflation is only possible with an (effective) scalar field. Moreover, a massless spinor or vector field is conformally invariant (i.e. its equation of motion is invariant under conformal transformations of the metric). In particular this means that it does not 'see' the expansion of the universe, as with conformal time this is just a conformal transformation of Minkowski spacetime. Another way of looking at it is that classical conformal fields have $\mathrm{tr}\, T^{\mu}_{\nu} = 0$, so that they never satisfy the $p < -\rho/3$ condition for inflation.

Although inflation-model builders often simply assume a potential with certain desired features, the fields and potential should actually be given by high-energy models. In the end we would like to have a consistent high-energy theory that describes physics at the very high energies that existed in the early universe, and which should incorporate the

concept of inflation. In other words, it makes much more sense to work with the fields and potentials predicted by present high-energy models, even though a consensus on these has not been reached, than simply assume whatever we like. This is our main motivation to consider multiple-field inflation with non-minimal kinetic terms, since that is the kind of configuration one typically gets from (string-inspired) high-energy models, as we will now briefly discuss.

The theory describing fundamental particles and interactions up to energies of about 100 GeV is the Standard Model of particle physics [53, 202, 168, 71, 72] (for a review see e.g. [154, 69]). It has been tested extensively and is very successful in describing nature. However, there are various indications that the Standard Model is probably not the whole picture, that there must be some extensions that become important at higher energies (for a discussion see e.g. [153]). One of these possible extensions is the concept of a grand unified theory (GUT) [51, 166]. The idea here is that the whole Standard Model with all its different couplings, masses and symmetries is generated dynamically from a unified theory with a single symmetry group. This process involves the mechanism of (spontaneous) symmetry breaking, the same mechanism that (at much lower energies) breaks the electroweak symmetry in the Standard Model, leaving us at present with electromagnetism (the massless photon) and three massive vector bosons mediating the weak force. The way in which mass is generated during spontaneous symmetry breaking is called the Higgs mechanism [70], and it involves one or more scalar particles, called Higgs bosons. Although the single Higgs boson of the Standard Model is unsuitable for inflation, GUTs generally contain many more of them, which are candidates for the scalar fields needed in inflation. The energy scale associated with this unification, determined from the behaviour of the Standard Model coupling constants, is about 10^{15} GeV.

One of the problems in the Standard Model is that the quantum corrections to the Higgs mass are quadratically divergent, and should hence be very large if new particles exist at the GUT scale, which is so much higher than the electroweak scale (100 GeV). This is not observed, which can only be explained within the Standard Model by extreme finetuning. This is called the gauge hierarchy problem [52, 189]. The fact that it provides a solution for this problem was the main motivation for another possible extension of the Standard Model, called supersymmetry (SUSY) [205, 148, 204, 29]. SUSY is an additional symmetry between bosons and fermions. Then each fermion has an associated boson (named by putting an 's' in front of the name of the fermion, like selectron) and each boson has an associated fermion (named by changing the end of the name of the boson to 'ino', like photino). These associated particles have the same mass but different spin, and cancel the quadratically divergent quantum corrections to the Higgs mass. SUSY effectively doubles the amount of particles, and in particular leads to a lot of additional scalars, which is important from the point of view of inflation. We do not observe supersymmetry in the present world, so that it must be a broken symmetry at the observable energy scales. One of the consequences of supersymmetry is that the behaviour of the coupling constants seems to point even more strongly towards a unification at a high energy, in this case at 10^{16} GeV, than in the case of the Standard Model without SUSY [174]. Hence the concepts of grand unified theories and supersymmetry can very well be combined.

Above we described the effects of global supersymmetry. If, in addition, it is gauged (i.e. made local), then we find it automatically includes gravity as well [44, 147, 204]. This is the reason why local supersymmetry is called supergravity (SUGRA). SUGRA does not provide a theory of quantum gravity, so it should be seen as an effective theory, i.e. a theory that gives a good description below a certain energy scale, but is known to be

only a limit of the complete theory, corrections becoming important above this scale. This complete theory could for example be string theory, of which supergravity is indeed an effective description at lower energies [56, 160].

Apart from providing us with the necessary scalar fields, these theories also constrain their properties. When there is more than a single scalar field, it becomes useful to view them as a vector. Just as a vector in space gives the coordinates of a certain point in space with respect to the origin, the scalar fields can also be seen as the coordinates of a field space, which takes the form of a certain manifold. We call the geometry of the field manifold non-trivial if it is curved and trivial if it is flat. Supersymmetry requires the manifold of the complex scalar fields z^α associated with the spin-$\frac{1}{2}$ fermions to be of a special type, called a Kähler manifold [209]. A Kähler manifold is a complex manifold with the additional property that all its local geometrical properties are encoded in one real scalar function, the Kähler potential $K(z,\bar{z})$, with $\bar{z}^{\underline{\alpha}}$ the complex conjugate of the field z^α. In particular the complex Hermitean metric $\mathbf{G}$ of the Kähler manifold can locally be expressed as the second mixed derivative of the Kähler potential: $G_{\underline{\alpha}\delta} = K_{,\underline{\alpha}\delta}$, with $G_{\alpha\delta} = G_{\underline{\alpha}\underline{\delta}} = 0$. More information on various types of manifolds can be found in [143].

In the case of $N = 1$ supergravity (only one supercharge) in four dimensions with only scalar multiplets the Lagrangean for the complex scalar fields z is of the general form [35, 148, 58]:

$$\mathcal{L}_m = \sqrt{-g}\left(-g^{\mu\nu}G_{\underline{\alpha}\alpha}\partial_\mu\bar{z}^{\underline{\alpha}}\partial_\nu z^\alpha - V(z,\bar{z})\right), \quad V(z,\bar{z}) = \kappa^{-2}e^{\kappa^2\mathcal{K}}\left(G^{\alpha\underline{\alpha}}\mathcal{K}_{,\alpha}\mathcal{K}_{,\underline{\alpha}} - 3\kappa^{-2}\right), \tag{3.1}$$

where $\mathcal{K}(z,\bar{z})$ is defined as $\mathcal{K}(z,\bar{z}) = K(z,\bar{z}) + \kappa^{-2}\ln|\mathcal{W}(z)|^2$ with $\mathcal{W}(z)$ the holomorphic superpotential. For non-trivial field manifolds the Kähler metric will in general make this theory non-renormalizable, but as supergravity is an effective theory the limit of infinite cut-off does not make sense anyway. In the above Lagrangean the Kähler potential $\mathcal{K}$ is still undetermined and depends on the specific model. If the four-dimensional supergravity Lagrangean (3.1) comes for example from a (heterotic) string theory by compactification, this string theory and the way of compactification determine the Kähler metric [206, 162, 160]. (As supersymmetric string theories live in ten dimensions, one must somehow remove six dimensions from the effective theory to describe the present four-dimensional world. One way is to compactify these dimensions, and the moduli, roughly the radii of the compactification manifold, then act as scalar fields in the resulting four-dimensional description.)

The previous discussion gives our motivation for studying inflation in the very general context of multiple scalar fields with a non-trivial field metric. Since a complex field can always be written in terms of two real fields, it is sufficient only to consider the case of real scalar fields. In fact, the case of real scalar fields with an arbitrary field metric is even more general, as the additional information provided by the complex Kähler structure is not taken into account. In this thesis we will only consider this general case, so no assumption about the origin of the scalar fields and their metric is made. An interesting subject for future study would be to investigate the possible simplifications to the theory if a supersymmetric (Kähler) origin of the field metric is assumed. In the remainder of this section we introduce the geometrical concepts that will be needed throughout this thesis. More details can be found in appendix A.

The real scalar fields ϕ^a are labeled with Roman indices $a, b, c, \ldots$. We combine them into a vector $\boldsymbol{\phi} = (\phi^a)$. They can be interpreted as the coordinates of a real manifold on

which a metric $\mathbf{G}$ is defined. This metric is assumed to be positive definite (otherwise the corresponding matter Hamiltonian is not bounded from below). The definition of the manifold is coordinate independent, therefore its description should be invariant under non-singular local coordinate transformations

$$\phi^a \to \tilde{\phi}^a = X^a(\phi). \tag{3.2}$$

A scalar is a quantity that is invariant under this transformation. (The word 'scalar' in scalar field is related to its invariance under spacetime transformations, not transformations on the field manifold.) Vectors $\mathbf{A} = (A^a)$ are not invariant, but transform as

$$A^a \to \tilde{A}^a = X^a_b(\phi)A^b, \qquad X^a_b(\phi) = X^a_{,b}(\phi), \tag{3.3}$$

where the comma denotes differentiation with respect to local coordinates. Examples of (tangent) vectors are the spacetime derivative of the background field $\partial_\mu\boldsymbol{\phi}$ and the field perturbation $\boldsymbol{\delta\phi}$ treated in chapter 4. In general the field $\boldsymbol{\phi}$ itself does not transform as a vector, as its components are the coordinates of the manifold (consider for example a translation). Next to the tangent vectors we can also define cotangent vectors that transform with X^{-1}. They can be constructed from the tangent vector $\mathbf{A}$ using the metric G_{ab}: $(\mathbf{A}^\dagger)_a \equiv A^b G_{ba}$. Using index-free notation this reads as $\mathbf{A}^\dagger = \mathbf{A}^T\mathbf{G}$. An example of a cotangent vector is the covariant derivative $\boldsymbol{\nabla}$. Using the metric $\mathbf{G}$ we introduce an inner product of two vectors $\mathbf{A}$ and $\mathbf{B}$ and the corresponding norm:

$$\mathbf{A}\cdot\mathbf{B} \equiv \mathbf{A}^\dagger\mathbf{B} = \mathbf{A}^T\mathbf{G}\mathbf{B} = A^a G_{ab} B^b, \qquad |\mathbf{A}| \equiv \sqrt{\mathbf{A}\cdot\mathbf{A}}, \tag{3.4}$$

which are by construction invariant under the coordinate transformation (3.2).

In appendix A various derivatives are defined that play an important role in this thesis. The covariant derivative on the field manifold with respect to the fields (A.19) is denoted by $\boldsymbol{\nabla}$ and the one with respect to spacetime coordinates (A.20) by $\mathcal{D}_\mu$. Our treatment of multiple-field inflation and perturbations is manifestly covariant with respect to the coordinate transformations (3.2) of the field manifold. Hence scalar results are guaranteedly invariant under this kind of transformations, like rotations of the coordinates.

3.2 Equations of motion

In this section we generalize the background equations for single-field inflation to the case of multiple fields. As explained in section 3.1 we allow for the possibility of non-minimal kinetic terms. Moreover, we also generalize the equations to the case of a general time variable. The main reason for this is that we need those general equations in our discussion of slow roll on the perturbations in §4.4.2. In addition, different equations are best solved using different time variables: comoving time, for example, is more convenient for background equations, while conformal time is necessary to solve some perturbation equations analytically, see §4.4.3. Hence it is convenient to set up the formalism for a general time variable, to avoid repetitions of almost identical equations. Moreover, with this approach various definitions and conclusions are manifestly independent of the choice of time coordinate, in particular those related to the slow-roll approximation.

For the background of the universe we have a flat Robertson-Walker metric in terms of a general time variable τ:

$$\mathrm{d}s^2 = -b^2\mathrm{d}\tau^2 + a^2\mathrm{d}\mathbf{x}^2. \tag{3.5}$$

Next to the spatial scale factor $a(\tau)$ we have introduced the temporal scale factor $b(\tau)$, which is defined by the specific choice of time variable. A derivative with respect to the general time variable τ is denoted by $' \equiv \partial_\tau$. Hubble parameters $H_a \equiv \partial_\tau a/a$ and $H_b \equiv \partial_\tau b/b$ are associated with the scale factors a and b. For the specific time coordinates introduced in section 2.1 the relations are as follows:

	Comoving t	Conformal η	e-folds N
$b =$	1	a	$1/H$
$H_a =$	H	$\mathcal{H}$	1
$H_b =$	0	$\mathcal{H}$	$-H_{,N}/H$

For the matter part of the universe we consider real scalar fields $\boldsymbol{\phi} = (\phi^a)$ that are the coordinates on a possibly non-trivial field manifold with metric $\mathbf{G}$. For the scalar field theory with a potential V on this manifold the matter Lagrangean that is quadratic in the derivatives can be written as

$$\mathcal{L}_m = \sqrt{-g}\left(-\frac{1}{2}\partial^\mu\boldsymbol{\phi}\cdot\partial_\mu\boldsymbol{\phi} - V(\boldsymbol{\phi})\right) = \sqrt{-g}\left(-\frac{1}{2}g^{\mu\nu}\partial_\mu\boldsymbol{\phi}^T\mathbf{G}\partial_\nu\boldsymbol{\phi} - V(\boldsymbol{\phi})\right). \tag{3.6}$$

Note that the kinetic term contains both the inverse spacetime metric $g^{\mu\nu}$ and the field metric $\mathbf{G}$. Various geometrical definitions can be found in section 3.1 and in appendix A.

The equation of motion for the scalars is given by

$$g^{\mu\nu}\left(\mathcal{D}_\mu\delta^\lambda_\nu - \Gamma^\lambda_{\mu\nu}\right)\partial_\lambda\boldsymbol{\phi} - \mathbf{G}^{-1}\boldsymbol{\nabla}^T V = 0, \tag{3.7}$$

and the Einstein equation reads as

$$\frac{1}{\kappa^2}G^\mu_{\ \nu} = T^\mu_{\ \nu} = \partial^\mu\boldsymbol{\phi}\cdot\partial_\nu\boldsymbol{\phi} - \delta^\mu_\nu\left(\frac{1}{2}\partial^\lambda\boldsymbol{\phi}\cdot\partial_\lambda\boldsymbol{\phi} + V\right). \tag{3.8}$$

Using the results of appendix B we obtain from (3.7) and (3.8) the background equation of motion for the scalar fields $\boldsymbol{\phi}$,

$$\mathcal{D}\boldsymbol{\phi}' + 3H_a\boldsymbol{\phi}' + b^2\,\mathbf{G}^{-1}\boldsymbol{\nabla}^T V = 0, \tag{3.9}$$

and the Friedmann equations

$$H_a^2 = \frac{1}{3}\kappa^2\left(\frac{1}{2}|\boldsymbol{\phi}'|^2 + b^2V\right), \qquad \mathcal{D}H_a = -\frac{1}{2}\kappa^2|\boldsymbol{\phi}'|^2. \tag{3.10}$$

Here we have introduced the slow-roll derivative $\mathcal{D}$. It is basically a covariant time derivative defined in such a way that it is easy to switch to another time coordinate: the transformation rules for such a coordinate change are included in its definition. If A is a quantity that is invariant under a change of time coordinate, for example the scalar field $\boldsymbol{\phi}$, the slow-roll derivative is defined by

$$\mathcal{D}(b^n A) = (\mathcal{D}_\tau - nH_b)(b^n A). \tag{3.11}$$

In particular this means that $\mathcal{D}\boldsymbol{\phi}' = (\mathcal{D}_\tau - H_b)\boldsymbol{\phi}'$, $\mathcal{D}^2\boldsymbol{\phi}' = (\mathcal{D}_\tau - 2H_b)(\mathcal{D}_\tau - H_b)\boldsymbol{\phi}'$, and $\mathcal{D}H_a = (\partial_\tau - H_b)H_a$. Note that the slow-roll derivative equals the comoving time derivative $\mathcal{D}_t$ if comoving time is used ($b = 1$), while with conformal time it reads as $\mathcal{D} = \mathcal{D}_\eta - n\mathcal{H}$. The slow-roll derivative is a necessary ingredient to be able to write

the equations in terms of a general time variable. From the single equation (3.9) we can immediately determine the field equation in terms of specific time coordinates, e.g.:

$$\mathcal{D}_t\dot{\boldsymbol{\phi}} + 3H\dot{\boldsymbol{\phi}} + \mathbf{G}^{-1}\boldsymbol{\nabla}^T V = 0, \qquad \mathcal{D}_\eta\boldsymbol{\phi}' + 2\mathcal{H}\boldsymbol{\phi}' + a^2\mathbf{G}^{-1}\boldsymbol{\nabla}^T V = 0,$$
$$\mathcal{D}_N\boldsymbol{\phi}_{,N} + \left(3 + \frac{H_{,N}}{H}\right)\boldsymbol{\phi}_{,N} + \frac{1}{H^2}\,\mathbf{G}^{-1}\boldsymbol{\nabla}^T V = 0. \tag{3.12}$$

The slow-roll derivative has the important property that when it is applied to quantities like field velocities or Hubble parameters, only terms of one order higher in the slow-roll approximation are obtained, as we will show in the next section. This is the reason for its name.

We conclude this section by introducing a basis $\{\mathbf{e}_n\}$ on the field manifold that is induced by the dynamics of the system. This general basis was first introduced in our paper [59] in terms of comoving time. (The treatment with the angle of [54] is a special case of this basis in the limit of only two fields.) This basis does not only help to simplify the equations, but it is also an important ingredient of the quantization scheme for the perturbations discussed in section 4.3. Moreover, it makes it possible to distinguish between effectively single-field ($\mathbf{e}_1$) and truly multiple-field effects.

We define the first unit vector $\mathbf{e}_1$ as the direction of the field velocity $\boldsymbol{\phi}'$. The second unit vector $\mathbf{e}_2$ points in the direction of that part of the field acceleration $\mathcal{D}\boldsymbol{\phi}'$ that is perpendicular to the first unit vector $\mathbf{e}_1$. This Gram-Schmidt orthogonalization process can be extended to any n. Using the notation

$$\boldsymbol{\phi}^{(1)} \equiv \boldsymbol{\phi}' \qquad \text{and} \qquad \boldsymbol{\phi}^{(n)} \equiv \mathcal{D}^{(n-1)}\boldsymbol{\phi}' \quad \text{for} \quad n \geq 2 \tag{3.13}$$

we define the unit vector $\mathbf{e}_n$ as pointing in the direction of that part of $\boldsymbol{\phi}^{(n)}$ that is perpendicular to the first $n-1$ unit vectors $\mathbf{e}_1, \ldots, \mathbf{e}_{n-1}$. Of course, if there are N scalar fields, there can never be more than N basis vectors: higher derivatives simply cannot point in new directions. Using the projection operators $\mathbf{P}_n$, which project on the $\mathbf{e}_n$, and $\mathbf{P}_n^\perp$, which project on the subspace that is perpendicular to $\mathbf{e}_1, \ldots, \mathbf{e}_n$, the definitions of the unit vectors are given by

$$\mathbf{e}_n = \frac{\mathbf{P}_{n-1}^\perp \boldsymbol{\phi}^{(n)}}{|\mathbf{P}_{n-1}^\perp \boldsymbol{\phi}^{(n)}|}, \qquad \mathbf{P}_n = \mathbf{e}_n\mathbf{e}_n^\dagger, \qquad \mathbf{P}_n^\perp = \mathbb{1} - \sum_{q=1}^{n}\mathbf{P}_q, \tag{3.14}$$

for all $n = 1, 2, \ldots$ and with the definition $\mathbf{P}_0^\perp \equiv \mathbb{1}$. Of course $|\mathbf{P}_{n-1}^\perp \boldsymbol{\phi}^{(n)}|$ is assumed to be non-zero in this definition; if it is zero the corresponding basis vector simply does not exist. Note that the unit vectors $\mathbf{e}_n$ will in general depend on time. However, because the slow-roll derivative $\mathcal{D}$ was used in the definition of this basis, the definition does not depend on a specific choice of time variable.

As mentioned before, if there are N scalar fields, there are no more than N basis vectors. On the other hand, there might be less if none of the derivatives have a component in a certain direction in field space. If this is true for all time, it means that the system can simply be reduced to a lower-dimensional one. However, as its definition depends on time, it is possible that one of the $\mathbf{e}_n$ vanishes only at a certain time, and one might wonder if this limit is well-defined. It turns out that all physical quantities occur in combinations that are well-behaved under this limit (see e.g. (4.76) and (5.37)).

By construction the vector $\boldsymbol{\phi}^{(n)}$ can be expanded in these unit vectors as

$$\boldsymbol{\phi}^{(n)} = (\mathbf{P}_1 + \ldots + \mathbf{P}_n)\,\boldsymbol{\phi}^{(n)} = \sum_{p=1}^{n} \phi_p^{(n)} \mathbf{e}_p, \qquad \phi_p^{(n)} = \mathbf{e}_p \cdot \boldsymbol{\phi}^{(n)}. \tag{3.15}$$

In particular, $\phi_n^{(n)} = \mathbf{e}_n \cdot \boldsymbol{\phi}^{(n)} = |\mathbf{P}_{n-1}^{\perp} \boldsymbol{\phi}^{(n)}|$. As the projection operators $\mathbf{P}_1$ and $\mathbf{P}_1^{\perp}$ turn out to be the most important in our discussions, we introduce the short-hand notation

$$\mathbf{P}^{\parallel} \equiv \mathbf{P}_1 = \mathbf{e}_1 \mathbf{e}_1^{\dagger} = \frac{\dot{\boldsymbol{\phi}} \dot{\boldsymbol{\phi}}^{\dagger}}{|\dot{\boldsymbol{\phi}}|^2} = \frac{\boldsymbol{\phi}'(\boldsymbol{\phi}')^{\dagger}}{|\boldsymbol{\phi}'|^2}, \qquad \mathbf{P}^{\perp} \equiv \mathbf{P}_1^{\perp} = \mathbb{1} - \mathbf{P}^{\parallel}. \tag{3.16}$$

In terms of these two operators one can write a general vector and matrix as $\mathbf{A} = \mathbf{A}^{\parallel} + \mathbf{A}^{\perp}$ and $\mathbf{M} = \mathbf{M}^{\parallel\parallel} + \mathbf{M}^{\parallel\perp} + \mathbf{M}^{\perp\parallel} + \mathbf{M}^{\perp\perp}$, with $\mathbf{A}^{\parallel} \equiv \mathbf{P}^{\parallel}\mathbf{A}$ and $\mathbf{M}^{\parallel\,\parallel} \equiv \mathbf{P}^{\parallel}\mathbf{M}\mathbf{P}^{\parallel}$, etc.

3.3 Multiple-field slow roll

We discussed the notion of slow roll in section 2.3 in the context of single-field inflation. Slow-roll inflation is driven by a scalar field potential that is very flat and therefore acts as an effective cosmological constant. This concept can be generalized to multiple scalar fields in a geometrical way using the unit vectors introduced in the previous section. Basically, the system consisting of (3.9) and (3.10) is said to be in the slow-roll regime if the comoving time derivatives satisfy $|\mathcal{D}_t \dot{\boldsymbol{\phi}}| \ll |3H\dot{\boldsymbol{\phi}}|$ and $\frac{1}{2}|\dot{\boldsymbol{\phi}}|^2 \ll V$, analogous to the single-field case. However, because of the vector nature some additional subtleties arise.

We introduce the following functions for an arbitrary time variable τ (in this form first defined in our paper [60], in terms of comoving time given in our earlier paper [59]):

$$\tilde{\epsilon}(\boldsymbol{\phi}) \equiv -\frac{\mathcal{D}H_a}{H_a^2}, \qquad \tilde{\boldsymbol{\eta}}^{(n)}(\boldsymbol{\phi}) \equiv \frac{\mathcal{D}^{n-1}\boldsymbol{\phi}^{\cdot}}{(H_a)^{n-1}|\boldsymbol{\phi}^{\cdot}|}. \tag{3.17}$$

Just as in the single-field case we see from (3.10) that $\tilde{\epsilon} < 3$ for a positive potential V. Note that $\tilde{\boldsymbol{\eta}}^{(1)}$ is simply equal to $\mathbf{e}_1$. We will use the short-hand notation $\tilde{\boldsymbol{\eta}} \equiv \tilde{\boldsymbol{\eta}}^{(2)}$ and $\tilde{\boldsymbol{\xi}} \equiv \tilde{\boldsymbol{\eta}}^{(3)}$. Both these vectors can be decomposed in components parallel $(\tilde{\eta}^{\parallel}, \tilde{\xi}^{\parallel})$ and perpendicular $(\tilde{\eta}^{\perp}, \tilde{\boldsymbol{\xi}}^{\perp})$ to the field velocity $\boldsymbol{\phi}^{\cdot}$:

$$\tilde{\boldsymbol{\eta}} = \frac{\mathcal{D}\boldsymbol{\phi}^{\cdot}}{H_a|\boldsymbol{\phi}^{\cdot}|}, \qquad \tilde{\eta}^{\parallel} = \mathbf{e}_1 \cdot \tilde{\boldsymbol{\eta}} = \frac{\mathcal{D}\boldsymbol{\phi}^{\cdot} \cdot \boldsymbol{\phi}^{\cdot}}{H_a|\boldsymbol{\phi}^{\cdot}|^2}, \qquad \tilde{\eta}^{\perp} = \mathbf{e}_2 \cdot \tilde{\boldsymbol{\eta}} = \frac{|(\mathcal{D}\boldsymbol{\phi}^{\cdot})^{\perp}|}{H_a|\boldsymbol{\phi}^{\cdot}|}, \tag{3.18}$$

$$\tilde{\boldsymbol{\xi}} = \frac{\mathcal{D}^2\boldsymbol{\phi}^{\cdot}}{H_a^2|\boldsymbol{\phi}^{\cdot}|}, \quad \tilde{\xi}^{\parallel} = \mathbf{e}_1 \cdot \tilde{\boldsymbol{\xi}} = \frac{\mathcal{D}^2\boldsymbol{\phi}^{\cdot} \cdot \boldsymbol{\phi}^{\cdot}}{H_a^2|\boldsymbol{\phi}^{\cdot}|^2}, \quad \tilde{\xi}_2 = \mathbf{e}_2 \cdot \tilde{\boldsymbol{\xi}}, \quad \tilde{\xi}_3 = \mathbf{e}_3 \cdot \tilde{\boldsymbol{\xi}} = \frac{|\mathbf{P}_2^{\perp}(\mathcal{D}^2\boldsymbol{\phi}^{\cdot})|}{H_a^2|\boldsymbol{\phi}^{\cdot}|}.$$

Note that, while $\tilde{\boldsymbol{\eta}}^{\perp}$ has only one non-zero component in our basis (which is the reason why we define a scalar $\tilde{\eta}^{\perp}$), $\tilde{\boldsymbol{\xi}}$ in general has two directions perpendicular to $\mathbf{e}_1$.

In terms of the functions $\tilde{\epsilon}, \tilde{\boldsymbol{\eta}}$ the Friedmann equation (3.10) and the background field equation (3.9) read as

$$H_a = \frac{\kappa}{\sqrt{3}}\, b\, \sqrt{V} \left(1 - \frac{1}{3}\tilde{\epsilon}\right)^{-1/2}, \tag{3.19}$$

$$\boldsymbol{\phi}^{\cdot} + \frac{2}{\sqrt{3}}\,\frac{1}{\kappa}\, b\, \mathbf{G}^{-1}\boldsymbol{\nabla}^T\sqrt{V} = -\sqrt{\frac{2}{3}}\, b\, \sqrt{V}\, \frac{\sqrt{\tilde{\epsilon}}}{1 - \frac{1}{3}\tilde{\epsilon}} \left(\frac{1}{3}\tilde{\boldsymbol{\eta}} + \frac{\frac{1}{3}\tilde{\epsilon}\,\mathbf{e}_1}{1 + \sqrt{1 - \frac{1}{3}\tilde{\epsilon}}}\right). \tag{3.20}$$

As in the single-field case we can now define precisely what is meant by slow roll, since these two background equations are still exact. Slow roll is valid if $\tilde{\epsilon}$, $\sqrt{\tilde{\epsilon}}\,\tilde{\eta}^{\parallel}$ and $\sqrt{\tilde{\epsilon}}\,\tilde{\eta}^{\perp}$ are (much) smaller than one. For this reason $\tilde{\epsilon}$, $\tilde{\eta}^{\parallel}$ and $\tilde{\eta}^{\perp}$ are called slow-roll functions. The function $\tilde{\boldsymbol{\xi}}$ is called a second-order slow-roll function because it involves two slow-roll derivatives, and it is assumed to be of an order comparable to $\tilde{\epsilon}^2$, $\tilde{\epsilon}\tilde{\eta}^{\parallel}$, etc. Let us anticipate at this point the importance of the slow-roll function $\tilde{\eta}^{\perp}$ with regard to multiple-field effects. The slow-roll function $\tilde{\eta}^{\parallel}$ is the one that reduces to $\tilde{\eta}$ in the single-field case, $\tilde{\eta}^{\perp}$ is zero by construction then, as there is simply no perpendicular direction in the single-field case. When discussing the perturbations we will find that $\tilde{\eta}^{\perp}$ is indeed crucial to determine whether multiple-field effects are important.

As in the single-field case we can use expansions in powers of the slow-roll functions to estimate the relevance of various terms in a given expression, provided slow roll is valid. At the same time one has to be careful about the slow-roll order of the solutions of these equations: the relative difference between the exact solution and the solution of a first-order slow-roll equation can easily become larger than first order if the interval of integration is too large, see the discussion around equation (2.37). Note that it is not necessary to assume that $\tilde{\epsilon}$, $\tilde{\eta}^{\parallel}$, etc. are of the same order. Although in many models this is true, one can also construct models where for example $\tilde{\eta}^{\parallel}$ is much smaller than $\tilde{\epsilon}$. In that case one can simplify the above expansions accordingly. As those cases are then just limits of the expressions where all slow-roll functions are of the same order, it is sufficiently general to consider only the latter situation.

In our vector notation all these equations look very much like the single-field case. For example, taking the number of e-folds as specific time coordinate we find from (3.20)

$$\boldsymbol{\phi}_{,N} + \frac{1}{\kappa^2}\frac{\mathbf{G}^{-1}\boldsymbol{\nabla}^T V}{V} = -\frac{\sqrt{2}}{3\kappa}\frac{\sqrt{\tilde{\epsilon}}(\tilde{\boldsymbol{\eta}} + \tilde{\epsilon}\,\mathbf{e}_1)}{1-\frac{1}{3}\tilde{\epsilon}}, \tag{3.21}$$

which looks very much like (2.35). However, even when taking a field metric equal to the identity and forgetting about the slow-roll corrections on the right-hand side, equation (3.20) (or (3.21)) in general describes a coupled system of differential equations. When looking at the a component of this vector equation, $\partial^a V/V$ in general depends on all fields, not just on ϕ^a. This makes the multiple-field case intrinsically much harder to solve.

The slow-roll functions (3.17) are all defined as functions of covariant derivatives of the velocity $\boldsymbol{\phi}^{\mathrm{i}}$ and the Hubble parameter H_a. As in the single-field case we can rewrite these definitions in terms of the potential and its derivatives only, if the leading-order slow-roll approximation works well. That is if the right-hand side of (3.20) can be neglected, as well as the $\tilde{\epsilon}$ in (3.19). As discussed in section 2.3, the slow-roll conditions then become consistency checks and one cannot expand the exact equations in powers of the slow-roll functions. However, it may be useful to have these expressions if one is only interested in the leading-order slow-roll results. To leading order in slow roll we find

$$\tilde{\epsilon} = \frac{1}{2\kappa^2}\frac{|\boldsymbol{\nabla}V|^2}{V^2}, \qquad \tilde{\eta}^{\parallel} - \tilde{\epsilon} = -\frac{1}{\kappa^2}\frac{\boldsymbol{\nabla}V\,\mathbf{M}^2\mathbf{G}^{-1}\boldsymbol{\nabla}^T V}{V|\boldsymbol{\nabla}V|^2} = -\frac{1}{\kappa^2}\frac{\mathrm{tr}\left[\left(\mathbf{M}^2\right)^{\parallel\parallel}\right]}{V},$$
$$\tilde{\eta}^{\perp} = \frac{1}{\kappa^2}\frac{|\mathbf{P}^{\perp}\mathbf{M}^2\mathbf{G}^{-1}\boldsymbol{\nabla}^T V|}{V\,|\boldsymbol{\nabla}V|} = \frac{1}{\kappa^2}\frac{\sqrt{\mathrm{tr}\left[\left(\mathbf{M}^2\right)^{\parallel\perp}\left(\mathbf{M}^2\right)^{\perp\parallel}\right]}}{V}. \tag{3.22}$$

The mass matrix $\mathbf{M}^2$ is defined as $\mathbf{M}^2 \equiv \mathbf{G}^{-1}\boldsymbol{\nabla}^T\boldsymbol{\nabla}V$ and $\mathbf{P}^{\parallel}$ projects along the direction

determined by $\boldsymbol{\nabla} V$, which, to lowest order, is identical to the direction of $\boldsymbol{\phi}^{;}$. One can compare this with the single-field slow-roll parameters in (2.38).

We conclude this section by deriving a number of results for derivatives. The derivatives of the slow-roll functions can be computed from their definitions and are given by:

$$\mathcal{D}\tilde{\epsilon} = \tilde{\epsilon}^{;} = 2H_a\tilde{\epsilon}(\tilde{\epsilon} + \tilde{\eta}^{\parallel}), \qquad \mathcal{D}\tilde{\boldsymbol{\eta}}^{(n)} = \mathcal{D}_\tau\tilde{\boldsymbol{\eta}}^{(n)} = H_a[\tilde{\boldsymbol{\eta}}^{(n+1)} + ((n-1)\tilde{\epsilon} - \tilde{\eta}^{\parallel})\tilde{\boldsymbol{\eta}}^{(n)}], \tag{3.23}$$

$$\mathcal{D}\tilde{\eta}^{\parallel} = (\tilde{\eta}^{\parallel})^{;} = H_a[\tilde{\xi}^{\parallel} + (\tilde{\eta}^{\perp})^2 + (\tilde{\epsilon} - \tilde{\eta}^{\parallel})\tilde{\eta}^{\parallel}], \qquad \mathcal{D}\tilde{\eta}^{\perp} = (\tilde{\eta}^{\perp})^{;} = H_a[\tilde{\xi}_2 + (\tilde{\epsilon} - 2\tilde{\eta}^{\parallel})\tilde{\eta}^{\perp}].$$

We can draw the important conclusion that the time derivative of a slow-roll function is one order higher in slow roll. This was to be expected, as the time derivative is equal to the slow-roll derivative since the slow-roll functions do not depend on b (i.e. are invariant under a change of time coordinate).

In an analogous way we can derive an expression for the time derivatives of the basis vectors defined in (3.14):

$$\mathcal{D}\mathbf{e}_i = \mathcal{D}_\tau\mathbf{e}_i = H_a\left(\frac{\tilde{\eta}^{(i+1)}_{i+1}}{\tilde{\eta}^{(i)}_{i}}\,\mathbf{e}_{i+1} - \frac{\tilde{\eta}^{(i)}_{i}}{\tilde{\eta}^{(i-1)}_{i-1}}\,\mathbf{e}_{i-1}\right). \tag{3.24}$$

As defined before, $\tilde{\eta}^{(i)}_{i} \equiv \mathbf{e}_i \cdot \tilde{\boldsymbol{\eta}}^{(i)}$. The derivative of $\mathbf{e}_i$ has components only in the $\mathbf{e}_{i+1}$ and the $\mathbf{e}_{i-1}$ directions. For $i = 1$ the second term is absent. The explicit results for $i = 1, 2$ are:

$$\mathcal{D}\mathbf{e}_1 = H_a\tilde{\eta}^{\perp}\mathbf{e}_2, \qquad \mathcal{D}\mathbf{e}_2 = H_a\frac{\tilde{\xi}_3}{\tilde{\eta}^{\perp}}\,\mathbf{e}_3 - H_a\tilde{\eta}^{\perp}\mathbf{e}_1. \tag{3.25}$$

We see that the time derivative of a basis vector gives a first-order slow-roll result, which shows a nice interplay between the basis vectors and the notion of slow roll. For later use we define a matrix Z by

$$(Z)_{mn} = -(Z^T)_{mn} = \frac{1}{H_a}\,\mathbf{e}_m \cdot \mathcal{D}\mathbf{e}_n. \tag{3.26}$$

This matrix is invariant under coordinate transformations of the field manifold. The anti-symmetry of Z follows because $(\mathbf{e}_m \cdot \mathbf{e}_n)^{;} = 0$. To determine its components we use (3.24) and find that the only non-zero components of Z read as

$$Z_{n\,n+1} = -Z_{n+1\,n} = -\frac{\tilde{\eta}^{(n+1)}_{n+1}}{\tilde{\eta}^{(n)}_{n}}, \tag{3.27}$$

which is first order in slow roll. Hence Z is anti-symmetric, first order in slow roll and only non-zero just above and below the diagonal. In matrix form it is given by

$$Z = \begin{pmatrix} 0 & -\tilde{\eta}^{\perp} & & \emptyset \\ \tilde{\eta}^{\perp} & 0 & -\frac{\tilde{\xi}_3}{\tilde{\eta}^{\perp}} & \\ & \frac{\tilde{\xi}_3}{\tilde{\eta}^{\perp}} & 0 & \ddots \\ \emptyset & & \ddots & \ddots \end{pmatrix}. \tag{3.28}$$

3.4 Example: quartic potential

In this section we work out the example of a special quartic multiple-field potential, to illustrate the concepts introduced in this chapter. We take a flat field manifold; for examples with a non-trivial field manifold see chapter 6. The potential is given by

$$V(\boldsymbol{\phi}) = \frac{1}{4}\left(\boldsymbol{\phi}^T \mathbf{m}^2 \boldsymbol{\phi}\right)^2, \tag{3.29}$$

with $\mathbf{m}^2$ a symmetric, dimensionless and positive-definite matrix. This special potential is chosen because then the first-order slow-roll field equation (see (3.20)) can be solved analytically in terms of comoving time:

$$\dot{\boldsymbol{\phi}} = -\frac{2}{\kappa\sqrt{3}}\,\mathbf{m}^2\boldsymbol{\phi} \qquad \Rightarrow \qquad \boldsymbol{\phi}(t) = e^{-2\mathbf{m}^2 t/(\kappa\sqrt{3})}\boldsymbol{\phi}_0, \tag{3.30}$$

using the initial condition $\boldsymbol{\phi}(0) = \boldsymbol{\phi}_0$. Hence we expect the fields corresponding with the largest eigenvalues to go to zero quicker than those with smaller eigenvalues. The first-order result for the Hubble parameter follows from (3.19):

$$H = \frac{\kappa}{2\sqrt{3}}\,\boldsymbol{\phi}^T\mathbf{m}^2\boldsymbol{\phi}\left(1+\frac{\tilde{\epsilon}}{6}\right) = \frac{\kappa\boldsymbol{\phi}_0^T\boldsymbol{\phi}_0}{2\sqrt{3}}\,F_1(t), \tag{3.31}$$

where the last expression is only valid to leading order in slow roll, as the $\tilde{\epsilon}/6$ has been neglected. We have defined the short-hand notation

$$F_n(t) \equiv \frac{\boldsymbol{\phi}_0^T\mathbf{m}^{2n}e^{-4\mathbf{m}^2 t/(\kappa\sqrt{3})}\boldsymbol{\phi}_0}{\boldsymbol{\phi}_0^T\boldsymbol{\phi}_0}. \tag{3.32}$$

For the number of e-folds we find

$$N(t) = \int_0^t H\mathrm{d}t = N_\infty\left(1-F_0(t)\right), \qquad N_\infty = \frac{1}{8}\kappa^2\boldsymbol{\phi}_0^T\boldsymbol{\phi}_0. \tag{3.33}$$

Here N_∞ is the slow-roll estimate of the total amount of inflation. In the single-field limit (and the notation of section 2.4 with $\lambda = m^4$) the functions F_n reduce to $(\sqrt{\lambda})^n\phi(t)^2/\phi_0^2$, and all results agree with the corresponding ones in section 2.4.

The first two unit vectors of the basis (3.14) are given by

$$\begin{aligned}\mathbf{e}_1 &= \frac{\dot{\boldsymbol{\phi}}}{|\dot{\boldsymbol{\phi}}|} = -F_2^{-1/2}\,\mathbf{m}^2 e^{-2\mathbf{m}^2 t/(\kappa\sqrt{3})}\hat{\boldsymbol{\phi}}_0 \\ \mathbf{e}_2 &= \frac{\ddot{\boldsymbol{\phi}} - (\mathbf{e}_1^T\ddot{\boldsymbol{\phi}})\mathbf{e}_1}{|\ddot{\boldsymbol{\phi}} - (\mathbf{e}_1^T\ddot{\boldsymbol{\phi}})\mathbf{e}_1|} = \frac{F_2\mathbf{m}^4 - F_3\mathbf{m}^2}{\sqrt{F_4F_2^2 - F_3^2F_2}}\,e^{-2\mathbf{m}^2 t/(\kappa\sqrt{3})}\hat{\boldsymbol{\phi}}_0,\end{aligned} \tag{3.34}$$

where $\hat{\boldsymbol{\phi}}_0 \equiv \boldsymbol{\phi}_0/\sqrt{\boldsymbol{\phi}_0^T\boldsymbol{\phi}_0}$ denotes the unit vector in the direction $\boldsymbol{\phi}_0$. We see that after sufficient time has passed, $\mathbf{e}_1$ will be pointing in the direction of the field corresponding with the smallest eigenvalue of $\mathbf{m}^2$. Note also that $F_2\mathbf{m}^4 - F_3\mathbf{m}^2 = 0$ in the single-field limit, so that $\mathbf{e}_2$ does not exist in that case, as expected. Finally the slow-roll functions (3.17), (3.18) are given by the following expressions:

$$\tilde{\epsilon} = \frac{1}{N_\infty}\frac{F_2}{F_1^2}, \quad \tilde{\eta}^{\parallel} = -\frac{1}{2N_\infty}\frac{F_3}{F_2F_1}, \quad \tilde{\eta}^{\perp} = \frac{1}{2N_\infty}\frac{\sqrt{F_4F_2 - F_3^2}}{F_2F_1}, \quad \tilde{\xi}^{\parallel} = \frac{1}{(2N_\infty)^2}\frac{F_4}{F_2F_1^2}. \tag{3.35}$$

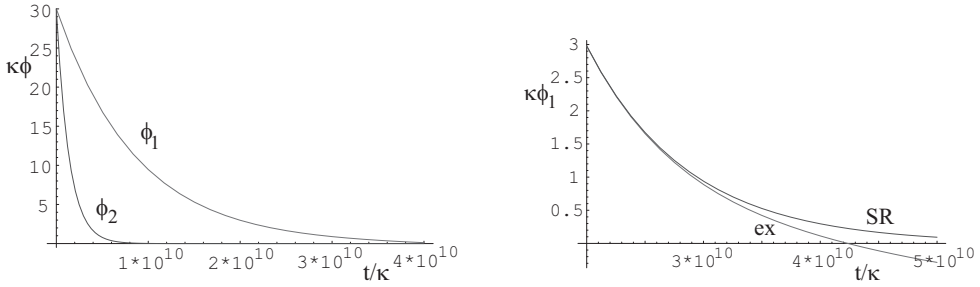

(a) (b)

Figure 3.1: (a) The exact numerical solution for the field $\boldsymbol{\phi}(t)$ in a two-field case with the special quartic potential (3.29), with $\mathbf{m}$ given by the diagonal matrix $(1 \cdot 10^{-5}, 2.5 \cdot 10^{-5})$ and initial condition $\kappa\boldsymbol{\phi}_0 = (30, 30)$. All quantities are expressed in terms of Planck units κ as indicated. In (b) the difference between the exact numerical and the analytical slow-roll solution can be seen for the first component of the field vector near the end of inflation. With exact numerical solution is meant the numerical solution of the exact equation of motion (3.12), while the analytical slow-roll solution is given in (3.30).

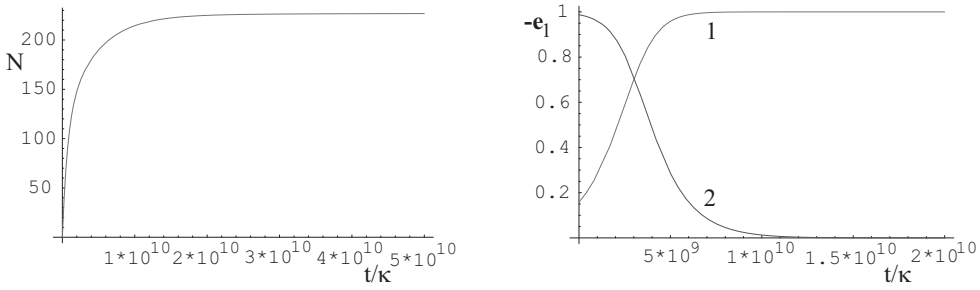

(a) (b)

Figure 3.2: (a) The exact numerical solution for the number of e-folds $N(t)$ in the same situation as in figure 3.1. (b) The two components of the unit basis vector $\mathbf{e}_1$, i.e. those corresponding with the ϕ_1 and ϕ_2 fields.

We see that $\tilde{\xi}^{\parallel}$ is indeed of a smaller order than the other slow-roll functions, as it is suppressed by an additional factor $(1/N_\infty)$. $\tilde{\eta}^{\parallel}$ is negative, while the other three are positive. $\tilde{\epsilon}$, $\tilde{\eta}^{\parallel}$ and $\tilde{\xi}^{\parallel}$ grow very large near the end of inflation, since the F_n go to zero as $\exp(-4m_1^2 t/(\kappa\sqrt{3}))$ with m_1^2 the smallest eigenvalue of $\mathbf{m}^2$. For $\tilde{\eta}^{\perp}$ one has to be a bit more careful because of the subtraction in the numerator and take the next-to-smallest eigenvalue m_2^2 into account as well. The result is that for $m_2^2 < 3m_1^2$, $\tilde{\eta}^{\perp}$ grows very large near the end of inflation, while for $m_2^2 > 3m_1^2$ it goes to zero.

Next we choose a specific situation with two fields and the matrix $\mathbf{m}$ diagonal with eigenvalues $1 \cdot 10^{-5}$ and $2.5 \cdot 10^{-5}$. As initial values we take $\kappa\boldsymbol{\phi}_0 = (30, 30)$. With these initial conditions the total amount of inflation $N_\infty = 225$ is the same as in the examples in section 2.4. The overall normalization of the eigenvalues of $\mathbf{m}$ is chosen for no special reason, but is comparable to the value for m chosen in section 2.4.

In figure 3.1 the exact numerical solution for $\boldsymbol{\phi}(t)$ (i.e. the numerical solution of the

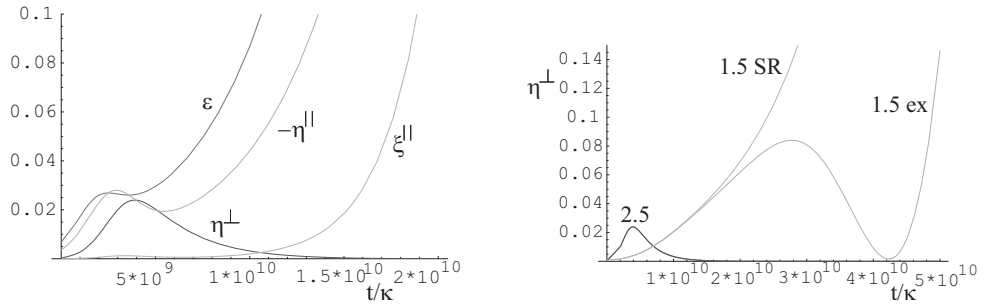

Figure 3.3: (a) The exact numerical solutions for the slow-roll functions $\tilde{\epsilon}$, $\tilde{\eta}^{\parallel}$, $\tilde{\eta}^{\perp}$ and $\tilde{\xi}^{\parallel}$ in the same situation as in figure 3.1. (b) The exact numerical and analytical slow-roll solutions for $\tilde{\eta}^{\perp}$ are compared, both for the situation described in figure 3.1 with $\mathbf{m} = \mathrm{diag}(1 \cdot 10^{-5}, 2.5 \cdot 10^{-5})$ and for the situation where the second eigenvalue has been changed to $1.5 \cdot 10^{-5}$. For the first situation the exact and slow-roll curves lie on top of each other.

exact equation of motion (3.12)) is plotted and compared with the analytical slow-roll solution (3.30).[1] We see that the field corresponding with the largest eigenvalue of $\mathbf{m}$ goes to zero first, and that the slow-roll solution starts to deviate from the exact one only at the end of inflation. In figure 3.2(a) the number of e-folds $N(t)$ is plotted, while figure 3.2(b) shows the behaviour of the unit vector $\mathbf{e}_1$ as a function of time. We see that at first it points mainly in the direction of the second field (the one corresponding with the largest eigenvalue of $\mathbf{m}$), but that after some time, when the second field goes to zero, it changes direction and starts pointing in the direction of the first field.

The slow-roll functions are drawn in figure 3.3(a). Note the structure (bumps) in the solutions around the time that the second field goes to zero. We also see that $\tilde{\xi}^{\parallel}$ is clearly of a smaller order than the other three slow-roll functions, as it should be. As discussed above, $\tilde{\epsilon}$, $\tilde{\eta}^{\parallel}$ and $\tilde{\xi}^{\parallel}$ grow large at the end of inflation, while $\tilde{\eta}^{\perp}$ goes to zero (2.5 is larger than $\sqrt{3}$). Figure 3.3(b) focuses on the behaviour of the slow-roll function $\tilde{\eta}^{\perp}$, comparing the exact numerical and analytical slow-roll results for two cases with different parameter values. For the case of $m_2/m_1 = 2.5$ they are practically identical, but for the smaller parameter ratio of $m_2/m_1 = 1.5 < \sqrt{3}$ the difference becomes large when slow roll breaks down. While the prediction that $\tilde{\eta}^{\perp}$ grows large at the very end of inflation is correct, the analytical slow-roll solution completely misses the features of the exact solution at the end of inflation in this case. Note that with the comoving time t used in these plots the slow-roll approximation breaks down about halfway to the end of inflation (compare figures 3.3(a) and 3.1(b)). However, at that time the total amount of inflation has almost been reached, as can be seen from figure 3.2(a). Hence if the number of e-folds N was used as the time variable instead of comoving time, the end of slow roll would be very close to the end of inflation. This is one of the reasons why N is usually a more convenient time variable, but we used t here because this example could be solved analytically in terms of comoving time.

[1] In the case of the exact equation of motion we also need to specify initial conditions for the field velocity. For these we took the values that are given by the slow-roll solution.

Chapter 4

Perturbations during multiple-field inflation

In the previous chapters we considered a homogeneous situation, both for metric and matter quantities. This was motivated by observations of large-scale homogeneity on the one hand, while on the other hand the enormous expansion of inflation easily removes any initial inhomogeneities, which is one of the reasons why it was proposed in the first place. Hence classically it makes perfect sense to consider a homogeneous background field. However, at the quantum level there are always small inhomogeneous fluctuations. Because of the inflationary expansion something very interesting happens to these fluctuations: their wavelengths are stretched to sizes larger than the Hubble radius (or event horizon), after which they lose their quantum character and become effectively classical perturbations. In this way a classical perturbation spectrum is produced from a quantum origin, and thus inflation solves the density perturbations problem. In this chapter the theory of perturbations during multiple-field slow-roll inflation is developed. It is based on my paper [60].

The outline of this chapter is as follows. Section 4.1 introduces the concepts of scalar, vector and tensor perturbations and discusses coordinate choice (gauge) issues. In section 4.2 the equations of motion for the scalar gravitational and matter perturbations are derived, and the choice of perturbation variables is discussed. Section 4.3 focuses on the quantization of the dynamical scalar perturbations and the choice of initial conditions. The equations are solved in section 4.4 to find expressions for the perturbations, in particular for the gravitational potential, in terms of background quantities only. This section is split into subsections: after discussing the outline of the calculation in §4.4.1 and introducing the concept of slow roll on the perturbations in §4.4.2, the real calculation is performed in §4.4.3. Section 4.5 deals with vector and tensor perturbations. Finally the results of chapters 3 and 4 are summarized in section 4.6.

4.1 Introduction

The theory of the production of density perturbations from inflationary quantum fluctuations has been studied for a long time. First calculations were performed by [179, 67, 63, 9, 140, 88]. Later calculations for the case of a single real scalar field can be found

in [141, 108, 187, 133, 186, 172]. Perturbations in the case of multiple fields have also been considered in the literature. Pioneering work was done in [93, 180]. Using gauge invariant variables the authors of [157, 50, 49, 145, 54] treated two-field inflation models. The fluid flow approach was extended to multiple fields in [125], while a more geometrical approach was used in [170, 144]; both methods assumed several slow-roll-like conditions on the potential. Using slow-roll approximations for both the background and the perturbation equations the authors of [142, 158, 103] were able to find expressions for the metric perturbations in multiple-field inflation. The authors of [83, 85] paid special attention to gauge issues in their discussion of multiple-field perturbations. The case of perturbations in generalized gravity theories was studied in [183, 84, 182].

As explained in section 3.1 it is important to have a general treatment of the inflationary density perturbations that can handle an arbitrary number of scalar fields with an arbitrary field metric and a generic potential. Most of the previous literature on multiple-field inflationary density perturbations is limited with respect to these aspects, usually by considering only two fields and minimal kinetic terms. The exception to this are the papers [170, 144], but these still left a lot of space for improvement, most importantly regarding the treatment of slow roll, the rotation of background fields, the transition region, and the analysis of the particular solution for the gravitational potential caused by the coupling to multiple fields. In our paper [60] we provided a general treatment by computing the scalar gravitational and matter perturbations to first order in slow roll during inflation with multiple real scalar fields that may have non-minimal kinetic terms. Which of these fields acts as inflaton during which part of the inflationary period is determined automatically in our formalism and does not have to be specified beforehand. Central aspects of our formalism are the geometrical setup with quantities that are covariant or invariant under field transformations and the generalized multiple-field slow-roll functions, both discussed in chapter 3.

We consider small inhomogeneous quantum fluctuations on top of a homogeneous classical background. For the scalar matter fields this means

$$\boldsymbol{\phi}^{\mathrm{full}}(\eta, \mathbf{x}) = \boldsymbol{\phi}(\eta) + \boldsymbol{\delta\phi}(\eta, \mathbf{x}). \tag{4.1}$$

For the perturbations the conformal time η is the most convenient time to use, as only with this time coordinate the equations can be solved analytically, see section 4.4. Hence we write all equations in this chapter in terms of conformal time. A very important assumption is that of the perturbations being small. That allows us to linearize all equations in the perturbation quantities, which we will do consistently. This assumption is not made from a practical point of view only (the non-linear equations are much more difficult to solve analytically, if at all possible), but is also motivated by physical observations: the fluctuations we observe in the CMBR are tiny, well within the linear regime. For part of the treatment it is irrelevant whether the perturbations like $\boldsymbol{\delta\phi}$ are classical or quantum objects. This is because we work to linear order in those quantities, so that the quantum nature (such as variables that do not commute) does not play a role. Hence we may derive and manipulate the equations in section 4.2 as if all quantities were classical. Only when we are computing physical quantities, like the correlator of the gravitational potential, do we have to take the quantum nature of the perturbations into account.

Of course we also have fluctuations in the metric. As a symmetric 4 by 4 tensor the

metric has 10 degrees of freedom. Most generally we can write (using the symbols of [141])

$$g_{\mu\nu}^{\rm full}(\eta,\mathbf{x}) = g_{\mu\nu}(\eta) + \delta g_{\mu\nu}(\eta,\mathbf{x}) = a^2\begin{pmatrix}-1 & 0\\ 0 & \delta_{ij}\end{pmatrix} - a^2\begin{pmatrix}2\Phi & -B_{,j}\\ -B_{,i} & 2(\Psi\delta_{ij} - E_{,ij})\end{pmatrix} + a^2\begin{pmatrix}0 & S_j\\ S_i & F_{i,j}+F_{j,i}\end{pmatrix} + a^2\begin{pmatrix}0 & 0\\ 0 & h_{ij}\end{pmatrix}. \tag{4.2}$$

Here $\Phi(\eta,\mathbf{x})$, $\Psi(\eta,\mathbf{x})$, $B(\eta,\mathbf{x})$ and $E(\eta,\mathbf{x})$ are four scalar functions, $\mathbf{S}(\eta,\mathbf{x})$ and $\mathbf{F}(\eta,\mathbf{x})$ are two divergenceless vectors (i.e. $S^i{}_{,i}=0$), and $h_{ij}(\eta,\mathbf{x})$ is a symmetric transverse traceless tensor (i.e. $h_{ij}=h_{ji}$, $h^{ij}{}_{,i}=0$ and $h^i{}_i=0$). Together this gives exactly 10 (=4+4+2) degrees of freedom. One often refers to Φ as the gravitational potential, because the (00) component of the metric in a weak-field approximation can be identified with the potential of Newtonian gravity. The four matrices are, respectively, the background, the scalar perturbations, the vector perturbations and the tensor perturbations. An important result, proved in [8, 188], is that to linear order the scalar, vector and tensor perturbations decouple and can be considered separately, which we will do. Most attention will be paid to the scalar perturbations (sections 4.2, 4.3 and 4.4), as they provide the dominant effect in the CMBR and are also the most interesting from the point of view of multiple-field inflation. Vector and tensor perturbations are discussed in section 4.5. Scalar perturbations are also called density perturbations, since from the observational point of view the energy density is the most important scalar quantity. Tensor perturbations are gravitational wave perturbations.

Although the metric has in principle 10 degrees of freedom, 4 of these are gauge degrees of freedom related to the choice of coordinates. There are basically two ways to deal with this unphysical aspect: either one works only with special gauge-invariant variables, or one simply chooses a specific gauge (choice of coordinates).[1] As long as one works consistently in that gauge, and is interested in physical (gauge-invariant) results, the latter is a viable alternative. With two scalar functions ξ,ξ^0 and a divergenceless vector ξ^i an infinitesimal coordinate transformation can most generally be written as

$$(\eta, x^i) \to (\eta+\xi^0, x^i+\xi^i+\xi^{,i}). \tag{4.3}$$

Under this coordinate transformation the metric perturbations transform as follows (see (B.3) and note that there the divergence has not yet been split off):

$$\begin{aligned}&\Phi\to\Phi-\mathcal{H}\xi^0-(\xi^0)', \qquad \Psi\to\Psi+\mathcal{H}\xi^0, \qquad B\to B+\xi^0-\xi',\\ &E\to E-\xi, \qquad S_i\to S_i-\xi_i', \qquad F_i\to F_i-\xi_i, \qquad h_{ij}\to h_{ij},\end{aligned} \tag{4.4}$$

while the field perturbation transforms as

$$\boldsymbol{\delta\phi}\to\boldsymbol{\delta\phi}-\boldsymbol{\phi}'\xi^0. \tag{4.5}$$

(Note that the signs depend on whether one takes the coordinate transformation passive or active; switching between these is possible by changing all signs at the same time) Hence with ξ,ξ^0 one can eliminate two of the four scalar functions, and ξ^i allows us to

[1] There is another alternative: the fluid flow approach [66, 108, 125]. Here one assumes the universe to be filled with a perfect fluid, which enables one to eliminate the metric perturbations and derive equations for the matter perturbations in closed form. As we want to keep things as general as possible, and also find the metric quantities quite convenient, we will not discuss this method further.

eliminate one of the two divergenceless vectors. The choice that we will make is to set $B = E = 0$ (longitudinal gauge) and $\mathbf{F} = 0$ (vector gauge). In the longitudinal gauge we keep the gravitational (Newtonian) potential Φ, which can in the end be linked directly to the temperature fluctuations in the CMBR (see section 5.4), while the off-diagonal δg_{0i} components are zero, just as for the background metric. One can also construct gauge-invariant combinations [8, 141] that do not change under an infinitesimal coordinate transformation, for example

$$\begin{aligned} \Phi^{(gi)} &= \Phi + \frac{1}{a}\left[(B - E')a\right]', & \Psi^{(gi)} &= \Psi - \mathcal{H}(B - E'), \\ \mathbf{S}^{(gi)} &= \mathbf{S} - \mathbf{F}', & \boldsymbol{\delta\phi}^{(gi)} &= \boldsymbol{\delta\phi} + \boldsymbol{\phi}'(B - E'). \end{aligned} \tag{4.6}$$

The tensor perturbation h_{ij} is automatically gauge invariant. As one can see from these expressions, choosing the longitudinal and vector gauge is equivalent to working with the above gauge-invariant quantities. More information on gauge choices and gauge-invariant combinations can be found in e.g. [84, 129] (note that they call the longitudinal gauge 'zero-shear').

4.2 Scalar perturbations

In this section we start with the treatment of the scalar perturbations, i.e. we take only the first two matrices in (4.2). We begin with the derivation of the perturbed Einstein equation. The scalar metric perturbations are given in appendix B. The matter perturbations for a general theory with multiple scalar fields follow from perturbing and linearizing the energy-momentum tensor in (3.8):

$$\begin{aligned} \delta T^{\mu}_{\ \nu} = g^{\mu\rho}\left(\mathcal{D}_\rho\boldsymbol{\delta\phi}\cdot\partial_\nu\boldsymbol{\phi} + \partial_\rho\boldsymbol{\phi}\cdot\mathcal{D}_\nu\boldsymbol{\delta\phi}\right) + \delta g^{\mu\rho}\,\partial_\rho\boldsymbol{\phi}\cdot\partial_\nu\boldsymbol{\phi} \\ - \delta^\mu_\nu\left(g^{\rho\sigma}\partial_\rho\boldsymbol{\phi}\cdot\mathcal{D}_\sigma\boldsymbol{\delta\phi} + \frac{1}{2}\delta g^{\rho\sigma}\,\partial_\rho\boldsymbol{\phi}\cdot\partial_\sigma\boldsymbol{\phi} + \boldsymbol{\nabla}V\,\boldsymbol{\delta\phi}\right). \end{aligned} \tag{4.7}$$

Using the metric (4.2) this simplifies to

$$\begin{aligned} \delta T^0_{\ 0} &= -\frac{1}{a^2}\left(\boldsymbol{\phi}'\cdot\mathcal{D}_\eta\boldsymbol{\delta\phi} - |\boldsymbol{\phi}'|^2\Phi + a^2\boldsymbol{\nabla}V\,\boldsymbol{\delta\phi}\right) \\ \delta T^0_{\ i} &= -\frac{1}{a^2}\left(\boldsymbol{\phi}'\cdot\boldsymbol{\delta\phi}\right)_{,i} \\ \delta T^i_{\ j} &= \frac{1}{a^2}\,\delta^i_j\,\left(\boldsymbol{\phi}'\cdot\mathcal{D}_\eta\boldsymbol{\delta\phi} - |\boldsymbol{\phi}'|^2\Phi - a^2\boldsymbol{\nabla}V\,\boldsymbol{\delta\phi}\right). \end{aligned} \tag{4.8}$$

An important conclusion that simplifies the calculations considerably can be drawn from the (ij) component of the Einstein equation with $i \neq j$ [141]. We see that $\delta T^i_{\ j} \propto \delta^i_j$. Hence from (B.15) for $\delta G^i_{\ j}$ we find that $(\Phi - \Psi)_{,ij} = 0$ for $i \neq j$. Switching to Fourier modes (see (A.10)) we have $k_i k_j(\Phi - \Psi) = 0$ and we conclude that $\Psi = \Phi$ for a general scalar field theory. (Of course Ψ and Φ might differ by a space-independent function of time, but this can be absorbed in the homogeneous background, so that we can set $\Psi = \Phi$ without loss of generality.)

Using the longitudinal gauge and the fact that $\Psi = \Phi$ the metric for the scalar perturbations simplifies to

$$g_{\mu\nu}(\eta, \mathbf{x}) = a^2(\eta) \begin{pmatrix} -1 & 0 \\ 0 & \delta_{ij} \end{pmatrix} - 2a^2(\eta)\Phi(\eta, \mathbf{x}) \begin{pmatrix} 1 & 0 \\ 0 & \delta_{ij} \end{pmatrix}. \tag{4.9}$$

Combining the (00) and (ii) components of the linearized Einstein equation (see (B.15) and (4.8)) then gives rise to the equation of motion for the gravitational potential:

$$\Phi'' + 6\mathcal{H}\Phi' + 2(\mathcal{H}' + 2\mathcal{H}^2)\Phi - \Delta\Phi = -\kappa^2 a^2 (\boldsymbol{\nabla} V \, \boldsymbol{\delta\phi}). \tag{4.10}$$

The $(0i)$ component on the other hand leads to the constraint equation

$$\Phi' + \mathcal{H}\Phi = \frac{1}{2}\kappa^2 \boldsymbol{\phi}' \cdot \boldsymbol{\delta\phi} = \frac{1}{2}\kappa^2 |\boldsymbol{\phi}'| \delta\phi^{\parallel}. \tag{4.11}$$

Here we have decomposed the vector $\boldsymbol{\delta\phi} = \delta\phi^{\parallel} \, \mathbf{e}_1 + \boldsymbol{\delta\phi}^{\perp}$ in terms of the basis introduced in (3.14). (A similar decomposition in the case of two-field inflation was also discussed in [54].) Because of this constraint, Φ and $\delta\phi^{\parallel}$ are not independent variables. Of course this agrees with the fact that the only physical degrees of freedom of the metric are the two tensor degrees of freedom (corresponding with the two polarizations of the massless graviton), so that the only physical scalar degrees of freedom are the field perturbations $\boldsymbol{\delta\phi}$.

The equation of motion for the scalar field perturbations is derived by perturbing and linearizing the field equation (3.7). As this is a rather long calculation, we give a few intermediate results:

$$g^{\mu\nu}\delta\left(\mathcal{D}_\mu \partial_\nu \phi^a\right) = g^{\mu\nu}\left(\mathcal{D}_\mu \mathcal{D}_\nu \delta^a_d - R^a_{\ bcd}\partial_\mu\phi^b\partial_\nu\phi^c - \Gamma^a_{bd}\partial_\mu\partial_\nu\phi^b - \Gamma^a_{de}\Gamma^e_{bc}\partial_\mu\phi^b\partial_\nu\phi^c\right)\delta\phi^d, \tag{4.12}$$

$$\begin{aligned} -\delta\left(G^{ab}\nabla_b V\right) &= -G^{ab}\nabla_b\nabla_c V \, \delta\phi^c + \Gamma^a_{bd}G^{bc}\nabla_c V \, \delta\phi^d \\ &= -G^{ab}\nabla_b\nabla_c V \, \delta\phi^c \\ &\quad + g^{\mu\nu}\left(\Gamma^a_{bd}\partial_\mu\partial_\nu\phi^b + \Gamma^a_{de}\Gamma^e_{bc}\partial_\mu\phi^b\partial_\nu\phi^c - \Gamma^\lambda_{\mu\nu}\Gamma^a_{bd}\partial_\lambda\phi^b\right)\delta\phi^d, \end{aligned} \tag{4.13}$$

where in the last line we inserted the background equation (3.7). The full equation then reads as

$$\begin{aligned} g^{\mu\nu}\left(\mathcal{D}_\mu\mathcal{D}_\nu - \Gamma^\lambda_{\mu\nu}\mathcal{D}_\lambda - \mathbf{R}(\partial_\mu\boldsymbol{\phi}, \partial_\nu\boldsymbol{\phi})\right)\boldsymbol{\delta\phi} - \mathbf{G}^{-1}\boldsymbol{\nabla}^T\boldsymbol{\nabla}V \, \boldsymbol{\delta\phi} \\ = g^{\mu\nu}\delta\Gamma^\lambda_{\mu\nu}\partial_\lambda\boldsymbol{\phi} - \delta g^{\mu\nu}\left(\mathcal{D}_\mu\partial_\nu\boldsymbol{\phi} - \Gamma^\lambda_{\mu\nu}\partial_\lambda\boldsymbol{\phi}\right), \end{aligned} \tag{4.14}$$

with $\mathbf{R}$ the curvature tensor on the field manifold, $[\mathbf{R}(\partial_\mu\boldsymbol{\phi}, \partial_\nu\boldsymbol{\phi})]^a_{\ d} \equiv R^a_{\ bcd}\partial_\mu\phi^b\partial_\nu\phi^c$, see also appendix A. Inserting the metric quantities for the case of the metric (4.9), which can be found in appendix B, and using the background field equation (3.12) for the terms on the right-hand side, we arrive at the final result:

$$\left(\mathcal{D}_\eta^2 + 2\mathcal{H}\mathcal{D}_\eta - \Delta + a^2\tilde{\mathbf{M}}^2(\boldsymbol{\phi})\right)\boldsymbol{\delta\phi} = 4\Phi'\boldsymbol{\phi}' - 2a^2\Phi \, \mathbf{G}^{-1}\boldsymbol{\nabla}^T V, \tag{4.15}$$

where we have introduced the (effective) mass matrices

$$\tilde{\mathbf{M}}^2 \equiv \mathbf{M}^2 - \mathbf{R}(\dot{\boldsymbol{\phi}}, \dot{\boldsymbol{\phi}}), \qquad \mathbf{M}^2 \equiv \mathbf{G}^{-1}\boldsymbol{\nabla}^T\boldsymbol{\nabla}V. \tag{4.16}$$

This system of perturbation equations must be solved in the background determined by the scalar fields (3.9) and the Friedmann equations (3.10). Decomposing $\boldsymbol{\delta\phi}$ into a parallel and perpendicular part in the same way as in equation (4.11), and making use of the background equation of motion for the scalar fields (3.12) and the constraint equation (4.11), the right-hand side of equation (4.10) for Φ can be rewritten as

$$-\kappa^2 a^2(\boldsymbol{\nabla} V\,\boldsymbol{\delta\phi}) = 2(\Phi' + \mathcal{H}\Phi)\left(\frac{1}{|\boldsymbol{\phi}'|}(\mathcal{D}_\eta\boldsymbol{\phi}')\cdot\mathbf{e}_1 + 2\mathcal{H}\right) + \kappa^2(\mathcal{D}_\eta\boldsymbol{\phi}')\cdot\boldsymbol{\delta\phi}^\perp. \tag{4.17}$$

Inserting this expression in (4.10) and realizing that $|\boldsymbol{\phi}'|'\,|\boldsymbol{\phi}'| = (\mathcal{D}_\eta\boldsymbol{\phi}')\cdot\boldsymbol{\phi}'$ we get

$$\Phi'' + 2\left(\mathcal{H} - \frac{|\boldsymbol{\phi}'|'}{|\boldsymbol{\phi}'|}\right)\Phi' + 2\left(\mathcal{H}' - \mathcal{H}\frac{|\boldsymbol{\phi}'|'}{|\boldsymbol{\phi}'|}\right)\Phi - \Delta\Phi = \kappa^2(\mathcal{D}_\eta\boldsymbol{\phi}')\cdot\boldsymbol{\delta\phi}^\perp. \tag{4.18}$$

In the single-field case the right-hand side is zero because $\boldsymbol{\delta\phi}^\perp$ then vanishes by construction. Using the following relations, which can be derived from the definitions of the slow-roll functions (3.17),

$$\mathcal{H}' = \mathcal{H}^2(1-\tilde{\epsilon}), \quad \frac{|\boldsymbol{\phi}'|'}{|\boldsymbol{\phi}'|} = \mathcal{H}(1+\tilde{\eta}^\parallel), \quad \mathcal{D}_\eta\boldsymbol{\phi}' = \mathcal{H}|\boldsymbol{\phi}'|\,(\tilde{\boldsymbol{\eta}} + \mathbf{e}_1) = \frac{\sqrt{2}}{\kappa}\,\mathcal{H}^2\sqrt{\tilde{\epsilon}}\,(\tilde{\boldsymbol{\eta}} + \mathbf{e}_1)\,, \tag{4.19}$$

the equation for Φ can be rewritten as

$$\Phi'' - 2\mathcal{H}\tilde{\eta}^\parallel\Phi' - 2\mathcal{H}^2(\tilde{\epsilon} + \tilde{\eta}^\parallel)\Phi - \Delta\Phi = \kappa\sqrt{2}\,\mathcal{H}^2\sqrt{\tilde{\epsilon}}\,\tilde{\eta}^\perp\mathbf{e}_2\cdot\boldsymbol{\delta\phi}. \tag{4.20}$$

Note that this equation is still exact; the slow-roll functions are only used as short-hand notation.

The system of perturbations (4.20), (4.11) and (4.15) is quite complicated. To make the physical content more transparent, we introduce new variables u and $\mathbf{q}$ (linearly related to Φ and $\boldsymbol{\delta\phi}$, respectively),

$$u \equiv \frac{a}{\kappa^2|\boldsymbol{\phi}'|}\,\Phi = \frac{\Phi}{\kappa\sqrt{2}\,H\sqrt{\tilde{\epsilon}}}, \qquad\qquad \mathbf{q} \equiv a\left(\boldsymbol{\delta\phi} + \frac{\Phi}{\mathcal{H}}\,\boldsymbol{\phi}'\right), \tag{4.21}$$

which satisfy the following two requirements:

1. The equations of motion for both u and $\mathbf{q}$ do not contain first-order conformal time derivatives;

2. The equation of motion for $\mathbf{q}$ is homogeneous and $\mathbf{q}$ is gauge invariant.

The first requirement makes a direct comparison between the size of the Fourier mode $\mathbf{k}^2 = k^2$ and other physical background quantities in the equation of motion possible. In §4.4.1 we make use of this to distinguish between different regions for the behaviour of the solutions. The other requirement ensures that we can quantize $\mathbf{q}$ in the standard way using the Lagrangean associated with the equation of motion for $\mathbf{q}$. As $\mathbf{q}$ is gauge invariant and linearly related to $\boldsymbol{\delta\phi}$, apart from the shift proportional to $\Phi\boldsymbol{\phi}'$, no non-physical degrees of freedom are quantized. The single-field version of $\mathbf{q}$, including its equation of motion and quantization, was first introduced by Sasaki and Mukhanov [169, 139], which is why

variables of this type are sometimes referred to as Sasaki-Mukhanov variables. The variable u was first introduced in [138], see also [141].

As mentioned below (4.11), Φ and $\delta\phi^{\|}$, or equivalently u and $\mathbf{e}_1\cdot\mathbf{q}$, are not independent variables. Hence we might eliminate one and only consider the other. However, it turns out that during different stages of inflation it will be useful to work with different variables. For the first stages (quantization and initial conditions) one must use the full vector $\mathbf{q}$, but in the end one is interested in the gravitational potential because it is directly linked to the temperature fluctuations in the CMBR. Moreover, during the final stages of inflation the equation of motion for u is simpler to solve than the one for $\mathbf{q}$. Therefore we derive equations for u as well as for the complete vector $\mathbf{q}$ in this section.

The equation of motion for $\mathbf{q}$ is derived as follows. We start by inserting the definition (4.21) of $\mathbf{q}$ into equation (4.15) for $\boldsymbol{\delta\phi}$. Making use of the relation $\mathcal{H}' = \mathcal{H}^2(1-\tilde{\epsilon})$ and the derivative of $\tilde{\epsilon}$ in (3.23) we can write it as

$$\begin{aligned}
&\frac{1}{a}\left[\mathcal{D}_\eta^2 - \mathcal{H}^2(2-\tilde{\epsilon}) + a^2\tilde{\mathbf{M}}^2 - \Delta\right]\mathbf{q} + 2\Phi\left[\mathcal{D}_\eta\boldsymbol{\phi}' + 2\mathcal{H}\boldsymbol{\phi}' + a^2\mathbf{G}^{-1}\boldsymbol{\nabla}^T V\right] \\
&- \frac{\Phi}{\mathcal{H}}\left[\mathcal{D}_\eta^2\boldsymbol{\phi}' - 2\mathcal{H}^2(1+\tilde{\epsilon})\boldsymbol{\phi}' + a^2\tilde{\mathbf{M}}^2\boldsymbol{\phi}'\right] - \frac{\boldsymbol{\phi}'}{\mathcal{H}}\left[\Phi'' - 2\mathcal{H}\tilde{\eta}^{\|}\Phi' - 2\mathcal{H}^2(\tilde{\epsilon}+\tilde{\eta}^{\|})\Phi - \Delta\Phi\right] \\
&- 2\left(\frac{1}{\mathcal{H}}\mathcal{D}_\eta\boldsymbol{\phi}' + (2+\tilde{\epsilon}+\tilde{\eta}^{\|})\boldsymbol{\phi}'\right)\left[\Phi' + \mathcal{H}(1+\tilde{\epsilon})\Phi\right] \;=\; 0. \qquad (4.22)
\end{aligned}$$

The terms between the second pair of brackets form exactly the background field equation in terms of conformal time (3.12) and hence vanish. By differentiating this background equation once more we obtain

$$\mathcal{D}_\eta^2\boldsymbol{\phi}' - 2\mathcal{H}^2(1+\tilde{\epsilon})\boldsymbol{\phi}' + a^2\tilde{\mathbf{M}}^2\boldsymbol{\phi}' = 0, \qquad (4.23)$$

where we used that $\mathcal{D}_\eta(\mathbf{G}^{-1}\boldsymbol{\nabla}^T V) = \mathbf{M}^2\boldsymbol{\phi}' = \tilde{\mathbf{M}}^2\boldsymbol{\phi}'$, with $\mathbf{M}^2$ and $\tilde{\mathbf{M}}^2$ defined in (4.16) (because of the anti-symmetry properties of the curvature tensor, $\mathbf{R}(\dot{\boldsymbol{\phi}},\dot{\boldsymbol{\phi}})\boldsymbol{\phi}' = 0$). This equation can be recognized between the third pair of brackets, so that these terms also vanish. Because of the equation of motion for Φ (4.20) the terms between the fourth pair of brackets cancel as well. Next we rewrite the constraint equation (4.11) by inserting the definition of $\mathbf{q}$:

$$\Phi' + \mathcal{H}(1+\tilde{\epsilon})\Phi = \frac{1}{2}\kappa^2\boldsymbol{\phi}'\cdot\frac{\mathbf{q}}{a}, \qquad (4.24)$$

where we also used the definition of $\tilde{\epsilon}$ written as $\mathcal{H}^2\tilde{\epsilon} = \frac{1}{2}\kappa^2|\boldsymbol{\phi}'|^2$. This equation we recognize between the final pair of brackets. Combining all these results and using once more this relation for $\tilde{\epsilon}$ and the expression for $\mathcal{D}_\eta\boldsymbol{\phi}'$ in (4.19) we finally obtain the (exact) homogeneous equation for the spatial Fourier mode $\mathbf{k}$ of $\mathbf{q}$ (see (A.10)):

$$\mathcal{D}_\eta^2\mathbf{q}_\mathbf{k} + (k^2 + \mathcal{H}^2\boldsymbol{\Omega})\mathbf{q}_\mathbf{k} = 0, \qquad (4.25)$$

with

$$\boldsymbol{\Omega} \equiv \frac{1}{H^2}\tilde{\mathbf{M}}^2 - (2-\tilde{\epsilon})\mathbb{1} - 2\tilde{\epsilon}\Big((3+\tilde{\epsilon})\mathbf{P}^{\|} + \mathbf{e}_1\tilde{\boldsymbol{\eta}}^\dagger + \tilde{\boldsymbol{\eta}}\mathbf{e}_1^\dagger\Big). \qquad (4.26)$$

The $(n1)$ components of $\boldsymbol{\Omega}$ can be expressed completely in terms of the slow-roll functions introduced in section 3.3 using

$$\frac{1}{H^2}\tilde{\mathbf{M}}^2\mathbf{e}_1 = \frac{1}{H^2}\mathbf{M}^2\mathbf{e}_1 = 3\,\tilde{\epsilon}\,\mathbf{e}_1 - 3\,\tilde{\boldsymbol{\eta}} - \tilde{\boldsymbol{\xi}}; \qquad (4.27)$$

in general this is not possible for the other components.

To derive the equation of motion for u it is convenient to introduce the quantity θ,

$$\theta \equiv \frac{\mathcal{H}}{a|\boldsymbol{\phi}'|} = \frac{\kappa}{\sqrt{2}}\frac{1}{a\sqrt{\tilde{\epsilon}}}. \tag{4.28}$$

The resulting (exact) expressions for its first and second-order derivatives are

$$\frac{\theta'}{\theta} = -\mathcal{H}\left(1+\tilde{\epsilon}+\tilde{\eta}^{\parallel}\right), \qquad \frac{\theta''}{\theta} = \mathcal{H}^2\left(2\tilde{\epsilon}+\tilde{\eta}^{\parallel}+2(\tilde{\eta}^{\parallel})^2-(\tilde{\eta}^{\perp})^2-\tilde{\xi}^{\parallel}\right). \tag{4.29}$$

By substituting the definitions of u and $\mathbf{q}$ in (4.20), where we write the relation between Φ and u as $\Phi = \kappa\sqrt{2}\mathcal{H}\sqrt{\tilde{\epsilon}}\,u/a$, and using the derivatives of the slow-roll functions given in (3.23), we obtain the exact (no slow-roll approximation used) equation of motion for u:

$$u_{\mathbf{k}}'' + \left(k^2 - \frac{\theta''}{\theta}\right)u_{\mathbf{k}} = \mathcal{H}\tilde{\eta}^{\perp}\mathbf{e}_2\cdot\mathbf{q}_{\mathbf{k}}. \tag{4.30}$$

From this one can draw the conclusion that at the level of the equations the redefined gravitational potential u decouples from the perpendicular components of the field perturbation $\mathbf{q}^{\perp}$ at leading order, but at first order mixing between these perturbations appears. However, because of integration interval effects it turns out that at the level of the solutions this mixing term can contribute even at leading order, as we will show later on (cf. the discussion around (2.37)).

The equations of motion (4.25) and (4.30) show that the different spatial Fourier modes of both $\mathbf{q}$ and u decouple. From now on we only consider one generic mode $\mathbf{k}$, so that we can drop the subscripts $_{\mathbf{k}}$. Rewriting equation (4.24) in terms of u (using the definition $q_n \equiv \mathbf{e}_n\cdot\mathbf{q}$) and differentiating it once gives

$$u' - \frac{\theta'}{\theta}u = \frac{1}{2}q_1 \qquad \Rightarrow \qquad u'' - \frac{\theta''}{\theta}u = \frac{1}{2}\Big(q_1' + \frac{\theta'}{\theta}q_1\Big), \tag{4.31}$$

where θ and its derivatives are given in (4.28) and (4.29). This second-order differential equation for u can be combined with the equation of motion (4.30) to give

$$k^2 u = \mathcal{H}\tilde{\eta}^{\perp}q_2 - \frac{1}{2}\Big(q_1' + \frac{\theta'}{\theta}q_1\Big). \tag{4.32}$$

After $\mathbf{q}$ has been quantized, this expression can be used to relate it to u.

4.3 Quantization of the scalar perturbations

The Lagrangean associated with the equation of motion (4.25) is

$$L = \frac{1}{2}\mathcal{D}_\eta\mathbf{q}_{\mathbf{k}}^{\dagger}\mathcal{D}_\eta\mathbf{q}_{\mathbf{k}} - \frac{1}{2}\mathbf{q}_{\mathbf{k}}^{\dagger}(k^2+\mathcal{H}^2\boldsymbol{\Omega})\mathbf{q}_{\mathbf{k}}. \tag{4.33}$$

Here the overall normalization follows from the original Lagrangean (3.6). Rewriting it in terms of the basis $\{\mathbf{e}_n\}$ we obtain

$$L = \frac{1}{2}(q'+\mathcal{H}Zq)^T(q'+\mathcal{H}Zq) - \frac{1}{2}q^T(k^2+\mathcal{H}^2\Omega)q, \tag{4.34}$$

where we employ the notation $(\Omega)_{mn} = \mathbf{e}_m^\dagger \mathbf{\Omega} \mathbf{e}_n$ and the matrix Z is given in (3.26). Note that this Lagrangean has the standard canonical normalization of $\frac{1}{2}(q')^T q'$, independent of the field metric $\mathbf{G}$. We maintain the vectorial structure of this multiple-field system and repress the indices n, m as much as possible, which means for example that the non-bold q in this equation is a vector (in the basis $\{\mathbf{e}_n\}$). From the canonical momenta $\pi = \partial L/\partial {q'}^T$ we find the Hamiltonian $H = \pi^T q' - L$ and the Hamilton equations:

$$H = \frac{1}{2}(\pi - \mathcal{H}Zq)^T(\pi - \mathcal{H}Zq) + \frac{1}{2}q^T\Big(k^2 + \mathcal{H}^2(\Omega + Z^2)\Big)q;$$
$$q' = \frac{\partial H}{\partial \pi^T} = \pi - \mathcal{H}Zq, \qquad \pi' = -\frac{\partial H}{\partial q^T} = -(k^2 + \mathcal{H}^2\Omega)q - \mathcal{H}Z\pi. \tag{4.35}$$

In order to avoid writing indices when considering commutation relations we use vectors α, β with components α_m, β_m in the $\mathbf{e}_m$ basis that are independent of q and π. The canonical commutation relations can then be represented as

$$[\alpha^T\hat{q}, \beta^T\hat{q}] = [\alpha^T\hat{\pi}, \beta^T\hat{\pi}] = 0, \qquad [\alpha^T\hat{q}, \beta^T\hat{\pi}] = i\alpha^T\beta. \tag{4.36}$$

Using the Hamilton equations it can be checked that this quantization procedure is time independent. Let Q and Π be complex matrix-valued solutions of the Hamilton equations, such that $q = Qa_0^* + \text{c.c.}$, $\pi = \Pi a_0^* + \text{c.c.}$ is a solution of (4.35) for any constant complex vector a_0 (c.c. denotes the complex conjugate). The Hamilton equations for Q and Π can be combined to give a second-order differential equation for Q:

$$Q'' + 2\mathcal{H}ZQ' + \Big(k^2 + \mathcal{H}^2(\Omega + \frac{1}{\mathcal{H}}Z' + (1-\tilde{\epsilon})Z + Z^2)\Big)Q = 0. \tag{4.37}$$

To remove the first-order time derivative from this equation, we define $Q(\eta) = R(\eta)\tilde{Q}(\eta)$ with R chosen in such a way that the matrix functions $\tilde{Q}$ and R satisfy

$$\tilde{Q}'' + (k^2 + \mathcal{H}^2\tilde{\Omega})\tilde{Q} = 0, \qquad R' + \mathcal{H}ZR = 0, \qquad \tilde{\Omega} \equiv R^{-1}\Omega R. \tag{4.38}$$

The matrix Π is then given by $\Pi = Q' + \mathcal{H}ZQ = R\tilde{Q}'$. We take $R(\eta_i) = \mathbb{1}$ as initial condition, since the initial condition of Q can be absorbed in that of $\tilde{Q}$. The equation of motion for R implies that R^TR and $\det R$ are constant because Z is anti-symmetric and consequently traceless (for $\det R$ the relation $\ln\det R = \operatorname{tr}\ln R$ is used). Taking into account its initial condition, it then follows that R represents a rotation.

Now $\hat{q}$ and $\hat{\pi}$ can be expanded in terms of constant creation ($\hat{a}^\dagger$) and annihilation ($\hat{a}$) operator vectors:

$$\hat{q} = Q\hat{a}^\dagger + Q^*\hat{a} = R\tilde{Q}\hat{a}^\dagger + R\tilde{Q}^*\hat{a}, \qquad \hat{\pi} = \Pi\hat{a}^\dagger + \Pi^*\hat{a}. \tag{4.39}$$

The creation and annihilation operators satisfy

$$[\alpha^T\hat{a}, \beta^T\hat{a}] = [\alpha^T\hat{a}^\dagger, \beta^T\hat{a}^\dagger] = 0, \qquad [\alpha^T\hat{a}, \beta^T\hat{a}^\dagger] = \alpha^T\beta. \tag{4.40}$$

This is consistent with the commutation relations for q and π given above, provided that the matrix functions Q and Π satisfy

$$Q^*\,Q^T - Q\,Q^{*T} = \Pi^*\,\Pi^T - \Pi\,\Pi^{*T} = 0, \qquad Q^*\,\Pi^T - Q\,\Pi^{*T} = i\mathbb{1}. \tag{4.41}$$

These relations hold for all time, as can be checked explicitly by using the equations of motion for Q and Π to show that they are time independent, provided that they hold at some given time.

We assume that the initial state is the vacuum $|0\rangle$ defined by $\hat{a}|0\rangle = 0$ and that there is no initial particle production (some discussion regarding this assumption can be found at the end of this section). This implies that the Hamiltonian initially does not contain any terms with $(\hat{a})^T\hat{a}$ and $(\hat{a}^\dagger)^T\hat{a}^\dagger$, which leads to the condition

$$(\Pi - \mathcal{H}ZQ)^T(\Pi - \mathcal{H}ZQ) + Q^T\Big(k^2 + \mathcal{H}^2(\Omega - Z^TZ)\Big)Q = 0. \tag{4.42}$$

The Hamiltonian is then given by

$$\hat{H} = \frac{1}{2}(\hat{a})^T\left\{(\Pi - \mathcal{H}ZQ)^{*T}(\Pi - \mathcal{H}ZQ) + Q^{*T}\Big(k^2 + \mathcal{H}^2(\Omega - Z^TZ)\Big)Q\right\}\hat{a}^\dagger + \text{c.c.}. \tag{4.43}$$

The solution of equations (4.41) and (4.42) can be parameterized by a unitary matrix U at the beginning of inflation, when the limit that k^2 is much bigger than any other scale is applicable:

$$Q_i = \frac{1}{\sqrt{2k}}\,U, \qquad\qquad \Pi_i = \frac{i\sqrt{k}}{\sqrt{2}}\,U. \tag{4.44}$$

We denote expectation values with respect to the vacuum state $|0\rangle$ by $\langle\ldots\rangle$. Let α, β be two vectors. Then for the expectation value of $(\alpha^TQU\hat{a}^\dagger + \alpha^{*T}Q^*U^*\hat{a})^2$, with U a unitary matrix, we obtain

$$\langle(\alpha^TQU\hat{a}^\dagger + \alpha^{*T}Q^*U^*\hat{a})^2\rangle = \alpha^{*T}Q^*U^*U^TQ^T\alpha = \alpha^{*T}Q^*Q^T\alpha. \tag{4.45}$$

So a unitary matrix in front of the $\hat{a}^\dagger$ will drop out in the computation of this correlator. This is even true if another state than the vacuum is used to compute the correlator. In particular this means that the correlator of the gravitational potential will not depend on the unitary matrix U in (4.44). To draw this conclusion we use relation (4.32) between u and $\mathbf{q}$ and the fact that Q satisfies a linear homogeneous equation of motion. We also see that as long as Q is simply oscillating and hence itself unitary (apart from a normalization factor), its evolution will be irrelevant to the computation of the correlator.

As we work in the Heisenberg picture, states are time independent. Since we have also made the choice of taking the creation and annihilation operators constant (putting the time dependence into the matrix function $Q(\eta)$), this means we can use these same operators and states to compute the correlator at any time. Any evolution effects, like mixing and particle production, will be encoded in the time evolution of the matrix $Q(\eta)$. This is equivalent to, but in our view more simple than, the maybe better-known description in terms of Bogolubov transformations [20, 18]. In that description the creation and annihilation operators are not taken as constants, and although the state is time independent, it will no longer be the vacuum state of the annihilation operator at a later time. Denoting the initial operator vectors by $\hat{a}^\dagger, \hat{a}$, and the ones at a certain later time η_1 by $\hat{b}^\dagger, \hat{b}$, we have the relation $|0\rangle_a = |\psi\rangle_b$ for some state ψ. As $\hat{q}(\eta_1)$ and $\hat{\pi}(\eta_1)$ can be given both in terms of the $\hat{a}$ operators and the $\hat{b}$ operators,

$$\begin{aligned} Q(\eta_1)\hat{a}^\dagger + \text{c.c.} = \hat{q}(\eta_1) &= \frac{1}{\sqrt{2k}}\,V\hat{b}^\dagger(\eta_1) + \text{c.c.} \\ \Pi(\eta_1)\hat{a}^\dagger + \text{c.c.} = \hat{\pi}(\eta_1) &= \frac{i\sqrt{k}}{\sqrt{2}}\,V\hat{b}^\dagger(\eta_1) + \text{c.c.}, \end{aligned} \tag{4.46}$$

with V a unitary matrix, one can solve these expressions for $\hat{b}^\dagger, \hat{b}$ in terms of $\hat{a}^\dagger, \hat{a}$:

$$\hat{b}^\dagger = \frac{V^{-1}}{i\sqrt{2k}} \left((ikQ(\eta_1) + \Pi(\eta_1))\hat{a}^\dagger + (ikQ^*(\eta_1) + \Pi^*(\eta_1))\hat{a} \right),$$
$$\hat{b} = \frac{(V^*)^{-1}}{i\sqrt{2k}} \left((ikQ(\eta_1) - \Pi(\eta_1))\hat{a}^\dagger + (ikQ^*(\eta_1) - \Pi^*(\eta_1))\hat{a} \right). \tag{4.47}$$

Then one finds that correlators like the one in (4.45) are the same, whether calculated in terms of $\hat{b}$ or of $\hat{a}$, and the result is given completely in terms of the matrix function $Q(\eta)$. Moreover, the one in terms of $\hat{b}$ is calculated by using the expressions in terms of $\hat{a}$, so that one can just as well use a description in terms of $\hat{a}^\dagger, \hat{a}$ only, which we will do.

One aspect for which the Bogolubov formalism can be useful is to understand the transition from quantum to classical that occurs when the wavelength of a perturbation mode is stretched to a size larger than the Hubble radius. By calculating the expectation value of the number operator $\hat{b}^\dagger\hat{b}$ at various times η,

$${}_a\langle 0|(\hat{b}^\dagger)^T(\eta)\hat{b}(\eta)|0\rangle_a = \frac{1}{2k} \left(ikQ(\eta) - \Pi(\eta) \right)^{*T} \left(ikQ(\eta) - \Pi(\eta) \right), \tag{4.48}$$

we find that there is an enormous amount of particle creation after this transition, so that the quantum character is lost. (Using the solution (4.69) for Q, and for the sake of simplicity neglecting any multiple-field effects like Z and R, so that we have $\Pi = Q'$, we find that this expectation value grows as $(k\eta)^{-6}$. Here $k\eta \sim -1$ at the transition and goes to zero afterwards, although inflation ends before zero is reached.) A more general discussion of the concept of the quantum to classical transition during inflation can be found in [159, 90] and references therein.

We conclude this section with some remarks on the assumption of taking the vacuum state to compute the correlator. Even though perturbations that we can observe in the CMBR have long wavelengths now, they had very short wavelengths before they crossed the Hubble radius during inflation. Therefore their scale k at the beginning of inflation at t_i is much larger than the Planck scale. It seems a reasonable assumption that modes with momenta very much larger than the Planck scale are not excited at t_i, so that for these modes the vacuum state is a good assumption. (There could be a problem with this approach, because our knowledge of physics beyond the Planck scale is extremely poor. In particular, the dispersion relation $\omega(\mathbf{k}) = k$ that we use implicitly when switching to Fourier modes might not be valid for large k: there might be a cut-off for large momenta. At the level of the equations (4.30) and (4.25) this would mean that the k^2 term is replaced by a more complicated function of $\mathbf{k}$. For a discussion of this trans-Planckian problem and possible cosmological consequences see e.g. [131, 146, 39]. Their results are inconclusive: some modifications to the dispersion relation do change the assumptions about what is a reasonable initial state, while others do not. In the same way some have observational consequences for the spectrum of density perturbations, while others do not. As we do not know the correct modification of the dispersion relation beyond the Planck scale (if any), no definite conclusions can be drawn.)

One can make the previous argument a bit more quantitative by considering another state than the vacuum state and computing the difference in the correlator. For instance one can try a thermal state with a temperature $1/\beta$ of the Planck scale: $\beta \sim \kappa$. Then one

has to compute the correlator in the (mixed) state represented by the density matrix $\hat{\rho}_\beta$

$$\hat{\rho}_\beta = \frac{e^{-\beta \hat{H}_i/a_i}}{\mathrm{Tr}(e^{-\beta \hat{H}_i/a_i})}, \qquad \hat{H}_i = k\,(\hat{a}^\dagger)^T \hat{a}. \tag{4.49}$$

Here $\hat{H}_i$ is simply (4.43) evaluated at the start of inflation (where $k \gg \mathcal{H}$ and (4.44) holds), and neglecting the (infinite) zero-point energy, which drops out in the definition of the density matrix. Since we have included the $\sqrt{-g}$ in the definition of the Lagrangean and Hamiltonian, instead of combining it with the volume element in the expression for the action, the Hamiltonian is not invariant under a change of coordinates and we have to divide by a_i in the above expression because of our use of conformal instead of comoving time. One can easily show that the result of equation (4.45) is multiplied by a factor

$$\left(1 + 2\langle (\hat{a}^\dagger)^T \hat{a}\rangle_{\hat{\rho}_\beta}\right) \qquad \text{with} \qquad \langle (\hat{a}^\dagger)^T \hat{a}\rangle_{\hat{\rho}_\beta} = \frac{1}{e^{\beta k/a_i} - 1}, \tag{4.50}$$

if the expectation value is computed in this thermal state. We are interested in the scale k that crossed the Hubble scale N e-folds after the start of inflation, i.e. $k = \mathcal{H}(N) = a_i H e^N$ with $H \sim \kappa^{-1}$ near the beginning of inflation. Hence the correction to the vacuum result is given by

$$\frac{2}{e^{\beta k/a_i} - 1} \sim \frac{2}{\exp(e^N) - 1}. \tag{4.51}$$

Because of the double exponential this correction term is suppressed very rapidly: even when there have been not more than 2 e-folds of inflation before this scale crossed the horizon, the correction is only of the order 10^{-3}. In explicit inflation models the number of e-folds N can easily be of the order of 100 or larger, so that this thermal effect is completely negligible.

A more extensive discussion on observable effects of non-vacuum initial states can be found in [104, 132]. In the first paper the effects of N-particle states and thermal states are studied, while the second one investigates states with a characteristic scale. Generally they find that these initial states will lead to non-Gaussian statistics in the CMBR power spectrum (see section 5.1 for definitions of these concepts), as well as features at the characteristic scale. However, for wide classes of initial non-vacuum states these effects are too small to be observable (even in principle).

4.4 Solution of the scalar perturbation equations to first order

In this section the perturbation equations are solved. An overview of the various steps in this computation is given in §4.4.1. §4.4.2 discusses the concept of slow roll for the perturbations (as opposed to slow roll for the background), which is needed for certain steps in the calculations. The actual calculations are then performed in §4.4.3.

4.4.1 Setup

We want to determine analytically and accurately up to first order in slow roll during inflation the evolution of the modified gravitational potential u and the quantized field

perturbations $\mathbf{q}$, described by equations (4.30), (4.25) and (4.31). In this section we explain the physical ideas that go into that computation. Since $\mathcal{H}$ grows rapidly, while k is constant for a given mode, the solutions of (4.30) and (4.25) change dramatically around the time $\eta_{\mathcal{H}}$ when a scale crosses the Hubble scale. This time is defined by the relation

$$\mathcal{H}(\eta_{\mathcal{H}}) = k. \tag{4.52}$$

Note that this means that $\eta_{\mathcal{H}}$ depends on k. Hence there are three regions of interest, which are denoted by their conventional names and treated in the following way:

- **sub-horizon ($\mathcal{H} \ll k$)**: This region is irrelevant to the computation of the correlators at the end of inflation (see (4.45)), since solving (4.38) with the $\mathcal{H}^2\tilde{\Omega}$ term neglected with respect to the k^2 term we find

$$Q(\eta) = \frac{1}{\sqrt{2k}}\, R(\eta)\, e^{ik(\eta-\eta_i)} U \qquad \Rightarrow \qquad Q^*(\eta)Q^T(\eta) = \frac{1}{2k}\,\mathbb{1}. \tag{4.53}$$

  (Here the normalization is fixed by the initial condition (4.44).) The end of the sub-horizon period η_- is therefore defined as the moment when this does not hold anymore to first order,[2] leading to the definition $\mathcal{H}^2(\eta_-) = \tilde{\epsilon}^{3/2}k^2$.

- **transition ($\mathcal{H} \sim k$)**: We consider (4.38) for Q, keeping all terms, but using that for a sufficiently small interval around $\eta_{\mathcal{H}}$ the slow-roll functions can be taken to be constant to first order, which makes it possible to obtain solutions for Q valid to first order using Hankel functions. Since the effect of the sub-horizon region is irrelevant, we take the following initial conditions:

$$Q(\eta_-) = \frac{1}{\sqrt{2k}}\,\mathbb{1}, \qquad Q'(\eta_-) = \frac{i\sqrt{k}}{\sqrt{2}}\,\mathbb{1}, \qquad R(\eta_-) = \mathbb{1}. \tag{4.54}$$

- **super-horizon ($\mathcal{H} \gg k$)**: In this region we use u to compute the vacuum correlator of the Newtonian potential Φ, which is related to u via a simple rescaling, see (4.21). As the k^2 dependence can be neglected, the exact solution for u of equation (4.30) is

$$u_{\mathbf{k}}(\eta) = u_{P\,\mathbf{k}} + C_{\mathbf{k}}\theta + D_{\mathbf{k}}\theta \int_{\eta_{\mathcal{H}}}^{\eta} \frac{\mathrm{d}\eta'}{\theta^2(\eta')}, \quad u_{P\,\mathbf{k}} = \theta \int_{\eta_{\mathcal{H}}}^{\eta} \frac{\mathrm{d}\eta'}{\theta^2} \int_{\eta_{\mathcal{H}}}^{\eta'} \mathrm{d}\eta''\, \mathcal{H}\theta\tilde{\eta}^{\perp} q_{2\,\mathbf{k}}, \tag{4.55}$$

  with $C_{\mathbf{k}}$ and $D_{\mathbf{k}}$ integration constants and $u_{P\,\mathbf{k}}$ a particular solution. To work out u_P in a more explicit form and to find solutions for Q slow-roll assumptions are necessary, which are treated in §4.4.2.

As the sub-horizon region is irrelevant to the two-point correlator of the gravitational potential, what remains is the connection between the transition and the super-horizon region. In both these regions we have constructed analytical solutions of the same differential equation for Q. The only thing that must still be computed to determine the

[2] The value 3/2 is chosen here because that is the same order to which the slow-roll background field equation is valid, see (3.20), but the arguments are independent of which specific power (larger than one) is chosen.

super-horizon solution uniquely, is the relative overall normalization between the solutions in these two regions. Instead of the more standard continuously differentiable matching at a specific time scale, we do this by identifying leading-order asymptotic expansions. (The reason for using this method is that there is no single time when one can correctly match the two solutions analytically in the standard way, see the remarks at the end of §4.4.3.)

This procedure works as follows. We can write both these solutions as power series in $k\eta$ and compare them in the transition region. There we find that the leading powers of the transition and super-horizon solutions are the same, separately for both the decaying and the non-decaying independent solution. The ratio of the coefficients in front of these leading powers gives us the relative normalization of the super-horizon solution with respect to the transition (and sub-horizon) solution. Although we need to compute the coefficients accurately to first order in slow roll, zeroth order turns out to be sufficient to distinguish the two independent solutions and identify the exponents of the leading terms in the expansions, see below (4.71). To conclude, we can determine the solution valid in the super-horizon region uniquely from the solution in the transition region around $\eta_{\mathcal{H}}$, even though the solution in the region in between is only known asymptotically. Some remarks on other matching schemes can be found at the end of §4.4.3.

4.4.2 Slow roll for the perturbations

To determine the solution for Q in the super-horizon region, and to rewrite the particular solution u_P in terms of background quantities only, the concept of slow roll on the perturbations is useful. We now justify the use of this concept and make it more precise. Physically it represents the fact that the combination of background and perturbation modes far outside the horizon cannot be distinguished from the background.

We introduce the substitutions

$$\boldsymbol{\phi} \rightarrow \tilde{\boldsymbol{\phi}} = \boldsymbol{\phi} + \boldsymbol{\delta\phi}, \qquad b \rightarrow \tilde{b} = a(1+\Phi), \qquad a \rightarrow \tilde{a} = a(1-\Phi), \tag{4.56}$$

where we have chosen to work with conformal time after substitution to make a direct comparison with section 4.2 possible. Note that in this way the perturbed metric (4.9) is obtained. Applying these substitutions to (3.9) and linearizing gives the perturbation equation (4.15), including the field curvature term, with k^2 set to zero. At the same time, by linearizing the combination

$$\mathcal{D}H_a + 3H_a^2 - \kappa^2 b^2 V = 0 \tag{4.57}$$

of the Friedmann equations (3.10), the equation of motion (4.10) for Φ is obtained. In other words, for the super-horizon modes the system of background equations (3.20) and (4.57) for $(\boldsymbol{\phi}, a, b)$ is also valid for the perturbed fields $(\tilde{\boldsymbol{\phi}}, \tilde{a}, \tilde{b})$. Hence the solutions for $(\boldsymbol{\phi}, a, b)$ and $(\tilde{\boldsymbol{\phi}}, \tilde{a}, \tilde{b})$ can only differ in their initial conditions, so that the perturbation quantities $(\boldsymbol{\delta\phi}, \Phi)$ are obtained by linearizing the background quantities with respect to the initial conditions:

$$\boldsymbol{\delta\phi} = (\boldsymbol{\nabla}_{\boldsymbol{\phi}_0}\boldsymbol{\phi})\boldsymbol{\delta\phi}_0. \tag{4.58}$$

Here we have set the variations of the initial conditions a_0 and b_0 equal to zero, as a simple counting argument shows that this is sufficient to generate a complete set of solutions. This technique of linearizing the background solutions to obtain the super-horizon perturbations

was also used in [191, 171], but our derivation is more complete than the one in [191] and simpler than the one in [171].

Now if slow roll is valid for the background, it follows immediately from the previous result that slow roll also governs the super-horizon perturbations. This assumption has been used previously in the literature, see e.g. [158, 142], but usually without presenting any justification.

Applying slow roll to the equation of motion (4.37) in the super-horizon region and working consistently to first order we find

$$Q' + \mathcal{H}\left(-\delta - (1-\tilde{\epsilon})\mathbb{1} + Z\right) Q = 0. \tag{4.59}$$

Here we have used that $\mathcal{D}Q = Q' - \mathcal{H}Q$ and $\mathcal{D}^2 Q = Q'' - 3\mathcal{H}Q' + \mathcal{H}^2(1+\tilde{\epsilon})Q$, because Q scales with one power of a (see (3.11)). For reasons that will become clear in the next section we have defined δ as

$$\delta = -\frac{1}{3}\left(2\mathbb{1} + \frac{\Omega}{(1-\tilde{\epsilon})^2}\right) = \tilde{\epsilon}\,\mathbb{1} - \frac{\tilde{M}^2}{3H^2} + 2\tilde{\epsilon}\, e_1 e_1^T, \tag{4.60}$$

where the second expression is valid to first order. The (constant) non-bold basis vectors e_n are defined by the simple relation $(e_n)_m = \delta_{nm}$ (being the Kronecker delta, not the matrix defined above). We make the additional assumption that also those components of $\tilde{M}^2/H^2$ that cannot be expressed in terms of the slow-roll functions defined in (3.17) are of first order, so that δ is a first-order quantity. Note that in general this assumption does not just represent a flatness condition on the potential, but also the curvature of the field manifold should not be too large, see (4.16).

It will be useful to define a new quantity $Q_{SR} \equiv \frac{a_{\mathcal{H}}\sqrt{\tilde{\epsilon}_{\mathcal{H}}}}{a\sqrt{\tilde{\epsilon}}}\, Q Q_{\mathcal{H}}^{-1}$. Inserting this definition into (4.59) we find

$$Q_{SR}' + \mathcal{H}\left[-\delta + (2\tilde{\epsilon} + \tilde{\eta}^{\parallel})\mathbb{1} + Z\right] Q_{SR} = 0, \qquad Q_{SR}(\eta_{\mathcal{H}}) = \mathbb{1}. \tag{4.61}$$

The solution of (4.61) is found by integrating:

$$Q_{SR}(\eta) = \exp\left[\int_{\eta_{\mathcal{H}}}^{\eta} \mathrm{d}\eta'\, \mathcal{H}\left(\delta - (2\tilde{\epsilon} + \tilde{\eta}^{\parallel})\mathbb{1} - Z\right)\right]. \tag{4.62}$$

Although the initial conditions are applied at $\eta_{\mathcal{H}}$, this solution is only valid in the super-horizon region because k^2 terms have been neglected. Since slow roll has been used, this result is a priori not expected to be very accurate at the end of inflation. However, we will now show that for the $(m1)$ components ($m \geq 1$) of Q_{SR} the result can be trusted even near the end of slow-roll inflation. First we note that the matrix between the brackets in (4.61) has its $(m1)$ components ($m \geq 1$) all equal to zero to first order in slow roll (using (4.27) and (3.27)). This means that the equations of motion for the $(n1)$ components of Q_{SR}, with here $n > 1$, obtained by multiplying (4.61) with e_n^T from the left and with e_1 from the right, do not couple to the (11) component (nor to any components with the right index unequal to one):

$$(Q_{SR})_{n1}' + \mathcal{H}\left[-\delta + (2\tilde{\epsilon} + \tilde{\eta}^{\parallel})\mathbb{1} + Z\right]_{np} (Q_{SR})_{p1} = 0, \qquad n, p > 1. \tag{4.63}$$

The solution for the vector $(Q_{SR})_{n1}(\eta)$ is then the exponent of a matrix multiplied by a constant vector (this matrix is minus the integral of the matrix in the equation above).

From the initial conditions we have that $(Q_{SR})_{n1}(\eta_{\mathcal{H}}) = 0$, and this can only be true if it is zero at all times (since the exponent of a matrix does not have a zero eigenvalue). Inserting this result into the equation of motion for $(Q_{SR})_{11}$ we find the simple equation $(Q_{SR})'_{11} = 0$, so that it is constant, and because of the initial conditions this constant should be one. Hence we have the solutions $(Q_{SR})_{11} = 1$ and $(Q_{SR})_{n1} = 0$ $(n > 1)$. Since these are constant, it is clear that the slow-roll approximation does not break down for these components and they can be used even near the end of inflation.

4.4.3 Calculation

In this section we perform the calculation that was outlined in §4.4.1. As mentioned there, in a sufficiently small interval around $\eta_{\mathcal{H}}$ in the transition region the slow-roll functions can be regarded as constant. With this approximation we can obtain an expression for $\mathcal{H}(\eta)$ by integrating the relation for $\mathcal{H}'$ in (4.19) with respect to conformal time, while integrating $N' = \mathcal{H}$ gives the number of e-folds to first order around $\eta = \eta_{\mathcal{H}}$:

$$\mathcal{H}(\eta) = \frac{-1}{(1-\tilde{\epsilon}_{\mathcal{H}})\eta}, \qquad N(\eta) = N_{\mathcal{H}} - \frac{1}{1-\tilde{\epsilon}_{\mathcal{H}}} \ln \frac{\eta}{\eta_{\mathcal{H}}}. \tag{4.64}$$

Here we used the freedom in the definition of conformal time to set $\eta_{\mathcal{H}} = -1/[(1-\tilde{\epsilon}_{\mathcal{H}})k]$. From (4.29) we infer that to first order around $\eta = \eta_{\mathcal{H}}$

$$\theta(z) = \theta_{\mathcal{H}} \left(\frac{z}{z_{\mathcal{H}}}\right)^{1+2\tilde{\epsilon}_{\mathcal{H}}+\tilde{\eta}^{\parallel}_{\mathcal{H}}}, \qquad z \equiv k\eta, \qquad \theta_{\mathcal{H}} = \frac{\kappa}{\sqrt{2}} \frac{H_{\mathcal{H}}}{k\sqrt{\tilde{\epsilon}_{\mathcal{H}}}}. \tag{4.65}$$

In these expressions we have made the conventional choice of $\eta_{\mathcal{H}}$ as reference time to compute the constant slow-roll functions, etc., although in principle one could do the complete computation with another reference time scale. However, to be able to take $\tilde{\Omega}$ as a constant (see below), this time should not be much later than $\eta_{\mathcal{H}}$.

With the initial condition (4.54) the solution of (4.38) for the rotation matrix R during the transition region is

$$R(z) = e^{(N-N_-)Z_{\mathcal{H}}} = \left(\frac{z}{z_-}\right)^{-\frac{1}{1-\tilde{\epsilon}_{\mathcal{H}}} Z_{\mathcal{H}}}. \tag{4.66}$$

The only time-dependent terms in the matrix Ω (4.26) are first order, so that we can take $\Omega = \Omega_{\mathcal{H}}$ in the transition region. The matrix $\tilde{\Omega}$ (4.38) on the other hand is given by

$$\tilde{\Omega} = R^{-1}(z)\Omega_{\mathcal{H}}R(z) = \Omega_{\mathcal{H}} - [\Omega_{\mathcal{H}}, Z_{\mathcal{H}}] \ln \frac{z}{z_-} = \Omega_{\mathcal{H}} + 3[\delta_{\mathcal{H}}, Z_{\mathcal{H}}] \left(\ln \frac{z}{z_{\mathcal{H}}} + \frac{3}{4} \ln \tilde{\epsilon}_{\mathcal{H}}\right), \tag{4.67}$$

where we used the definition of η_- given in the text below (4.53) and $\delta_{\mathcal{H}} = \delta(\eta_{\mathcal{H}})$ is defined in (4.60). In this section we are still considering a single, arbitrary mode k (see equation (4.52) and the text above equation (4.31)). However, in the end we are interested in those modes that are visible in the CMBR, which crossed the Hubble scale in a small interval about 60 e-folds before the end of inflation. For those modes we estimate $\tilde{\epsilon}_{\mathcal{H}} \sim 0.01$ (motivated for example by a quadratic potential, see (6.26)), so that $|\ln \tilde{\epsilon}_{\mathcal{H}}|$ is of the order of $\tilde{\epsilon}_{\mathcal{H}}^{-1/2}$. Since both δ and Z are of first order, the time dependence of $\tilde{\Omega}$ caused by the

rotation is then only important at order 3/2 in the region around $z_{\mathcal{H}}$. Hence we take $\tilde{\Omega} = \Omega_{\mathcal{H}}$. From the correction term in equation (4.67) we can always check explicitly if that assumption is justified. (For a smaller value of $\tilde{\epsilon}_{\mathcal{H}}$ the effect is of higher order and hence even less important. On the other hand, for a larger value of $\tilde{\epsilon}_{\mathcal{H}} \sim 0.1$ the above estimate for the logarithm still holds good, but a distinction in half-integer orders is not meaningful anymore then and one should check more carefully whether the commutator term can be neglected. Note that since the term $\frac{9}{4}\ln\tilde{\epsilon}_{\mathcal{H}}[\delta_{\mathcal{H}}, Z_{\mathcal{H}}]$ is constant, it can be included in the expression for $\tilde{\Omega}$ without changing the calculation below in a conceptual way.)

For matching in the region around $z_{\mathcal{H}}$ it will be useful to define $\bar{Q}(z) \equiv R_{\mathcal{H}}\tilde{Q}(z)$ with $R_{\mathcal{H}} \equiv R(z_{\mathcal{H}})$. Then $Q(z) = \bar{Q}(z)$ to first order in a sufficiently small region around $z_{\mathcal{H}}$. Using the same argument as in (4.67) the corresponding $\bar{\Omega} \equiv R_{\mathcal{H}}\tilde{\Omega}R_{\mathcal{H}}^{-1}$ is equal to $\Omega_{\mathcal{H}}$ to first order. Using this result and equation (4.64) for $\mathcal{H}$, equation (4.38) for $\tilde{Q}$ can be rewritten as an equation for $\bar{Q}$:

$$\bar{Q}_{,zz} + \bar{Q} - \frac{\nu_{\mathcal{H}}^2 - \frac{1}{4}}{z^2}\,\bar{Q} = 0, \qquad \nu_{\mathcal{H}}^2 = \frac{9}{4}\mathbb{1} + 3\delta_{\mathcal{H}}. \tag{4.68}$$

The solution of this matrix equation can be written in terms of a Hankel function:[3]

$$\bar{Q}(z) = \sqrt{\frac{\pi}{4k}}\,\sqrt{z}H^{(1)}_{\nu_{\mathcal{H}}}(z), \qquad \nu_{\mathcal{H}} = \frac{3}{2}\mathbb{1} + \delta_{\mathcal{H}}. \tag{4.69}$$

Here the initial conditions (4.54) at the beginning of the transition region have been taken into account, as can be seen by using that for $|z| \gg 1$ the Hankel function can be approximated by $H^{(1)}_{\nu}(z) = \sqrt{2/(\pi z)}\exp i(z - \pi\nu/2 - \pi/4)$ and neglecting unitary matrices (since they are irrelevant to the correlators that we are interested in in the end, see (4.45)). We also need the leading-order term in the expansion in z of this result for $\bar{Q}$:

$$\bar{Q}_{lo} = \frac{1}{i\sqrt{2\pi k}}\,\Gamma(\nu_{\mathcal{H}})\left(\frac{z}{2}\right)^{\frac{1}{2}\mathbb{1}-\nu_{\mathcal{H}}} = -\frac{e^{i\pi\delta_{\mathcal{H}}}}{i\sqrt{2k}}\,E_{\mathcal{H}}\left(\frac{z}{z_{\mathcal{H}}}\right)^{-\mathbb{1}-\delta_{\mathcal{H}}} \tag{4.70}$$

with

$$E_{\mathcal{H}} \equiv (1 - \tilde{\epsilon}_{\mathcal{H}})\mathbb{1} + (2 - \gamma - \ln 2)\delta_{\mathcal{H}}, \tag{4.71}$$

where $\gamma \approx 0.5772$ is the Euler constant. Here we used that for $|z| \ll 1$ we have the relation $H^{(1)}_{\nu}(z) = \frac{1}{i\pi}\Gamma(\nu)(z/2)^{-\nu}$. We expanded $\Gamma(\nu_{\mathcal{H}})$ using the results $\Gamma(\frac{3}{2}) = \frac{1}{2}\sqrt{\pi}$ and $\Gamma'(\frac{3}{2}) = (2 - \gamma - 2\ln 2)\Gamma(\frac{3}{2})$. Furthermore, $(-2)^{\mathbb{1}+\delta} = -2(\mathbb{1} + \delta\ln 2)e^{i\pi\delta}$ and according to equation (4.64), $z_{\mathcal{H}} = -1/(1 - \tilde{\epsilon}_{\mathcal{H}})$. For later convenience we have defined the matrix $E_{\mathcal{H}}$, which to zeroth order in slow roll is equal to the identity. In (4.70) we have taken only the growing solution; the decaying one starts off with a term that is proportional to $z^{\frac{1}{2}\mathbb{1}+\nu_{\mathcal{H}}} = z^{+2\mathbb{1}+\delta_{\mathcal{H}}}$. We see that these two solutions can be distinguished already at zeroth order.

Next we turn to the super-horizon region. Here we have to relate u and Q by means of the first equation of (4.31). The solution for u is given in (4.55). To derive an equation

[3] This Bessel equation and its solution in terms of Hankel functions are well-known in the theory of single-field inflationary density perturbations, see e.g. [119, 133] and references therein. However, in the multiple-field case under consideration the order ν of the Hankel function is matrix valued. This should be considered in the usual way: defined by means of a series expansion.

for q_1 we take the inner product of e_1 with equation (4.59) and use equations (4.27), (3.27) and (4.29). This gives the following result:

$$q_1' - \frac{(1/\theta)'}{1/\theta}\, q_1 = 2\mathcal{H}\tilde{\eta}^\perp q_2 \quad \Rightarrow \quad q_1 = d\,\frac{1}{\theta} + 2\frac{1}{\theta}\int_{\eta_\mathcal{H}}^{\eta} \mathrm{d}\eta'\, \mathcal{H}\theta\tilde{\eta}^\perp q_2, \tag{4.72}$$

where we also gave the solution. By using slow roll we have selected the non-decaying solution for q_1/a. Using (4.31) we then find that the integration constant $D_\mathbf{k}$ in the solution (4.55) for u is given by $D_\mathbf{k} = \frac{1}{2}d$. The constant $C_\mathbf{k}$ is irrelevant because the function θ decays rapidly. The integration constant d can be determined using the procedure of identification of leading-order terms (leading order in the expansion in z, not slow roll) described in §4.4.1. Extrapolating the super-horizon solution for q_1 into the transition region sufficiently close to $\eta_\mathcal{H}$, so that the integral can be neglected and $\delta_\mathcal{H}\ln(z/z_\mathcal{H})$ is smaller than first order, and using (4.65) we find to first order $q_1 = (d/\theta_\mathcal{H})(z/z_\mathcal{H})^{-1}$. Under these conditions $e_1^T E_\mathcal{H}(z/z_\mathcal{H})^{-\mathbb{1}-\delta_\mathcal{H}} = e_1^T E_\mathcal{H}(z/z_\mathcal{H})^{-1}$ so that we can determine the constant d from equation (4.70). (Note that, as mentioned in §4.4.1, the exponents of $z/z_\mathcal{H}$ need only be identified to zeroth order, so that, strictly speaking, the condition that $\delta_\mathcal{H}\ln(z/z_\mathcal{H})$ is smaller than first order is not even necessary.) The final first-order result for $D_\mathbf{k}$ is:

$$\hat{D}_\mathbf{k} = \frac{1}{2}\frac{1}{\sqrt{2k}}\,\theta_\mathcal{H} e_1^T E_\mathcal{H}\hat{a}^\dagger + \text{c.c.}, \tag{4.73}$$

where we have omitted unitary matrices that are irrelevant to the computation of the correlator. For later use we note that this identification procedure can also be used for the complete matrix Q, not just for q_1. Completely analogous to (4.59) and (4.62) one has

$$\begin{aligned} &(\bar{Q}/a)' - \mathcal{H}\, R_\mathcal{H} R^{-1}\,[\delta - \tilde{\epsilon}\mathbb{1}]\, R R_\mathcal{H}^{-1}\,(\bar{Q}/a) = 0 \\ \Rightarrow \qquad &\bar{Q} \propto a\, \exp\left(\int_{\eta_\mathcal{H}}^{\eta} \mathrm{d}\eta'\, \mathcal{H}\, R_\mathcal{H} R^{-1}\,[\delta - \tilde{\epsilon}\mathbb{1}]\, R R_\mathcal{H}^{-1}\right), \end{aligned} \tag{4.74}$$

which behaves like $z^{-\mathbb{1}-\delta_\mathcal{H}}$ when extrapolated into the transition region around $\eta_\mathcal{H}$ using (4.64) and (4.67). Comparing with (4.70) we see that it is exactly the leading-order term in the expansion of the Hankel function in the solution for Q in the transition region that turns into the dominant solution for Q in the super-horizon region.

Combining equations (4.21), (4.55) and (4.73) we can give the gravitational potential Φ as a quantum operator up to first order in slow roll during the later stages of inflation:

$$\hat{\Phi}_\mathbf{k}(t) = \frac{\kappa}{2k^{3/2}}\,\frac{H_\mathcal{H}}{\sqrt{\tilde{\epsilon}_\mathcal{H}}}\,\left(A(t_\mathcal{H}, t)\, e_1^T + \tilde{U}_P^T(t)\right) E_\mathcal{H}\hat{a}_\mathbf{k}^\dagger + \text{c.c.}. \tag{4.75}$$

Here we also used the definition of θ (4.28) and the identity $a_\mathcal{H}H_\mathcal{H} = k$, while we neglected the decaying $C_\mathbf{k}$ term. The function $A(t_\mathcal{H}, t)$ and vector $\tilde{U}_P^T(t)$ are defined as

$$\begin{aligned} A(t_\mathcal{H}, t) &= \frac{H}{a}\int_{\eta_\mathcal{H}}^{\eta} \mathrm{d}\eta'\, a^2\tilde{\epsilon} = \frac{H}{a}\int_{t_\mathcal{H}}^{t} \mathrm{d}t'\, a\left(\frac{1}{H}\right)^\cdot = 1 - \frac{H}{a}\int_{t_\mathcal{H}}^{t} \mathrm{d}t'\, a, \\ \tilde{U}_P^T(t) &= \frac{H}{a}\int_{t_\mathcal{H}}^{t} \mathrm{d}t' a\tilde{\epsilon}\, U_P^T(t'), \qquad U_P^T(t) = 2\sqrt{\tilde{\epsilon}_\mathcal{H}}\int_{t_\mathcal{H}}^{t} \mathrm{d}t'\, H\frac{\tilde{\eta}^\perp}{\sqrt{\tilde{\epsilon}}}\,\frac{a_\mathcal{H}}{a}\, e_2^T Q Q_\mathcal{H}^{-1}. \end{aligned} \tag{4.76}$$

In the calculation of $A(t_{\mathcal{H}}, t)$ we performed an integration by parts in the last step and in the result neglected one term which is exponentially suppressed with the number of e-folds. In this and all following equations $Q_{\mathcal{H}}$ is defined as the leading-order asymptotic expression for Q evaluated at $\eta_{\mathcal{H}}$, i.e. $Q_{\mathcal{H}} = E_{\mathcal{H}}/\sqrt{2k}$. The reason for switching back to comoving time is that we have now expressed everything in terms of background quantities only (for U_P see below), for which comoving time is usually more convenient than conformal time. Remember that $\Phi_{\mathbf{k}}$ depends on k not only explicitly, but also implicitly through the dependence on $\eta_{\mathcal{H}}$ or $t_{\mathcal{H}}$.

Using slow roll on the perturbations and substituting the result for Q_{SR} from (4.62) into the definition for U_P^T we find

$$U_P^T = 2\int_{t_{\mathcal{H}}}^{t} \mathrm{d}t'\, H\tilde{\eta}^{\perp}\, e_2^T \exp\left[\int_{t_{\mathcal{H}}}^{t'} \mathrm{d}t''\, H\left(\delta - (2\tilde{\epsilon} + \tilde{\eta}^{\parallel})\mathbb{1} - Z\right)\right] \tag{4.77}$$

to first order in slow roll. This expression is given in terms of background quantities only. Since to first order $(Q_{SR})_{21} = 0$, U_P has no component in the e_1 direction. In chapter 6 we will show how U_P^T can be computed explicitly for the case of a quadratic potential using the concept of slow roll on the perturbations.

We have been able to determine the integration constant $D_{\mathbf{k}}$ in the solution for u in the super-horizon region to first order in slow roll by using analytic properties of the solutions for Q in the transition region. We did not have to resort to a continuously differentiable matching at a specific time scale; the only time scale that appears in the result is the reference time $\eta_{\mathcal{H}}$, in the neighbourhood of which we have expanded the solutions. In the literature the concept of matching at a specific time is often applied (see e.g. [141, 133]). In most of these cases the time of horizon crossing of either a generic or specific mode k is used. On the one hand matching for the scales of observational interest is then performed at times when $|k\eta| \approx 1$, while on the other hand approximations only valid for small $|k\eta|$ are employed. The identification procedure described in §4.4.1 and used in this subsection shows why the standard (single-field) results in the literature are nonetheless correct: by neglecting the k-dependent corrections and taking $|k\eta| = 1$ (i.e. $|z/z_{\mathcal{H}}| = 1$) one is precisely computing the overall normalization factor that we showed to be the only thing that needs to be determined. (Another possible way to perform a correct matching might seem to be a matching of the transition and super-horizon solutions at a specific time η_+ later than $\eta_{\mathcal{H}}$, so that $|k\eta_+| \ll 1$ is a valid assumption to first order. However, it turns out that the interval between $\eta_{\mathcal{H}}$ and this η_+ is too large to satisfy the requirement that the slow-roll functions can be taken as constants, so that the Hankel solutions are not valid over the whole interval to first order.)

4.5 Vector and tensor perturbations

Having treated scalar perturbations in the previous sections, we now turn to vector and tensor perturbations. We start with vector perturbations, i.e. we consider the first and third matrices in (4.2), and in addition we use the vector gauge $\mathbf{F} = 0$. Vector perturbations turn out to be uninteresting from the point of view of inflation. The reason is that scalar fields, by definition, cannot generate vector perturbations: δT^{μ}_{ν} in (4.8) has no vector perturbation part (remember that by definition the spatial derivative of a scalar is still a scalar perturbation, not a vector perturbation, see (4.2)). And as we will now show,

in the absence of a source the vector perturbations are zero.[4]

The Einstein equation leads to the following two equations for vector perturbations using (B.19):

$$\begin{aligned} \Delta S_i &= 0, \\ (S_{i,j} + S_{j,i})' + 2\mathcal{H}(S_{i,j} + S_{j,i}) &= 0. \end{aligned} \tag{4.78}$$

From the first equation we conclude immediately (after switching to Fourier modes) that there can be no space-dependent vector perturbations in the absence of a vector source.

We can even draw some more general conclusions about vector perturbations, not restricted to inflation. Taking the more general energy-momentum tensor for the case of an arbitrary ideal fluid (2.10), we find for the vector part of the matter perturbations

$$\delta T^0_{\ 0} = 0, \qquad \delta T^0_{\ i} = (\rho + p)\delta u_i, \qquad \delta T^i_{\ j} = 0. \tag{4.79}$$

This means that ΔS_i is no longer zero, but the second equation of (4.78) is unchanged. It can be rewritten as

$$\left[a^2(k_j S_i + k_i S_j)\right]' = 0. \tag{4.80}$$

Contracting the solution with k^j and realizing that $k^j S_j = 0$ (by definition for a divergenceless vector) we obtain

$$S_i = \frac{k^j C_{ij}}{k^2 a^2}, \tag{4.81}$$

with C_{ij} a constant matrix. We conclude that even if there is some ideal fluid vector source at a certain time in the history of the universe (which cannot be of (scalar) inflationary origin), the vector perturbations will in general decay because of the expansion of the universe.

Next we consider the tensor perturbations, that is the fourth matrix in (4.2) (and of course the first matrix, the background, is also taken into account). Actually the two tensor degrees of freedom of the metric are the only physical ones, i.e. the only ones that are also present without any matter sources. They represent the two polarizations of the graviton. Hence, as opposed to vector perturbations, tensor perturbations are important from the point of view of inflation, even though the scalar fields provide no sources for them. However, precisely because the scalar fields do not generate the tensor perturbations, there is no difference between the treatment of these perturbations in multiple-field or in single-field inflation (or in any other era of an ideal fluid universe, see (2.10)). Inflation enters only by way of the background quantities. Hence the results derived here are not new (see e.g. [141, 133] and references therein), but we use the method described in section 4.4 in our derivation, including our improved matching technique.

Using (B.23) we find only one equation from the Einstein equation:

$$h''_{ij} + 2\mathcal{H}h'_{ij} - \Delta h_{ij} = 0. \tag{4.82}$$

[4] While the conclusions below for vector perturbations are often mentioned in the literature, we were unable to find a paper where they are actually derived.

Because h_{ij} is symmetric, transverse and traceless, it has only two independent components. Hence we can write

$$h_{ij}(\eta,\mathbf{x}) = \sum_{A=1}^{2} \frac{2\kappa}{a}\,\psi_A(\eta,\mathbf{x}) e_{ij}^A. \tag{4.83}$$

We have taken out a factor of $2\kappa/a$ to simplify the equation of motion and obtain the correct normalization of the Lagrangean, see below. The e_{ij}^A, $A = 1, 2$, are two constant polarization tensors, normalized as $e_{ij}^A e^{ij\,B} = \delta^{AB}$. They are symmetric, transverse ($k^i e_{ij}^A = 0$) and traceless. To be more explicit, in a coordinate system where the gravitational wave is traveling in the z-direction, i.e. the unit vector $\hat{\mathbf{k}}^T$ is given by $(0, 0, 1)$, the two polarization tensors are usually defined as

$$e_{ij}^{+} = \frac{1}{\sqrt{2}} \begin{pmatrix} 1 & 0 & 0 \\ 0 & -1 & 0 \\ 0 & 0 & 0 \end{pmatrix}, \qquad e_{ij}^{\times} = \frac{1}{\sqrt{2}} \begin{pmatrix} 0 & 1 & 0 \\ 1 & 0 & 0 \\ 0 & 0 & 0 \end{pmatrix}. \tag{4.84}$$

After switching to Fourier modes we find the following equation of motion for the mode functions $\psi_{A\,\mathbf{k}}(\eta)$:

$$\psi''_{A\,\mathbf{k}} + \left(k^2 - \frac{a''}{a}\right)\psi_{A\,\mathbf{k}} = 0. \tag{4.85}$$

This equation is similar to equation (4.30) for $u_{\mathbf{k}}$, but without an inhomogeneous term. An important difference between ψ_A and u is that the ψ_A represent two physical degrees of freedom and can be quantized directly, while u is not a physical degree of freedom, and had to be quantized indirectly by means of the scalar field degrees of freedom $\mathbf{q}$. There is no coupling at all between the two different polarizations $A = 1$ and $A = 2$, as can be seen from (4.85). This means that it is not necessary to introduce a 2 by 2 matrix analogous to Q as we had to do in section 4.3 (as there is no coupling, this matrix would remain diagonal and can therefore be represented by a vector just as well). The Lagrangean associated with the equation of motion (4.85) is

$$L = \frac{1}{2}(\psi'_{A\,\mathbf{k}})^2 - \frac{1}{2}\left(k^2 - \frac{a''}{a}\right)(\psi_{A\,\mathbf{k}})^2. \tag{4.86}$$

To derive the overall normalization of the Lagrangean we had to go back to the original action (2.6) and expand it to second order in the tensor perturbations. Since only the overall normalization had to be determined, it was sufficient to consider one type of terms, which simplified the calculation considerably. Only with the definition (4.83) of ψ_A does the Lagrangean have the standard canonical normalization. (A different overall normalization factor would change the expression for the canonical momentum and hence affect the quantization and the determination of the initial conditions.) Quantization is now straightforward:

$$\hat{h}_{ij\,\mathbf{k}}(\eta) = \sum_{A=1}^{2} \frac{2\kappa}{a}\, e_{ij}^A \left(\psi_{A\,\mathbf{k}}(\eta)\,\hat{a}^\dagger_{A\,\mathbf{k}} + \text{c.c.}\right), \tag{4.87}$$

with the creation and annihilation operators satisfying the usual relations,

$$[\hat{a}_{A\,\mathbf{k}}, \hat{a}^\dagger_{B\,\mathbf{k}'}] = \delta_{AB}\,\delta(\mathbf{k} - \mathbf{k}') \tag{4.88}$$

and all other commutators zero. The $\psi_{A\,\mathbf{k}}(\eta)$ are now simply functions satisfying the classical equation of motion (4.85). Since the different Fourier modes, as well as the different polarizations, do not couple, we drop the subscripts A and $\mathbf{k}$ for notational simplicity and consider one generic polarization and Fourier mode in the rest of this section.

In a way analogous to section 4.3 we can derive the initial conditions for ψ and the canonical momentum $\partial L/\partial\psi' = \psi'$ by using the canonical commutation relations between ψ and ψ' and the condition that the Hamiltonian does not contain any particle creation or annihilation terms initially, when k^2 is still much bigger than any other scale. This leads to the relations

$$\psi^*\psi' - \psi\psi'^* = i, \qquad (\psi')^2 + k^2\psi^2 = 0 \tag{4.89}$$

with the solution

$$\psi_i = \frac{1}{\sqrt{2k}}\, e^{i\alpha}, \qquad \psi_i' = \frac{i\sqrt{k}}{\sqrt{2}}\, e^{i\alpha}. \tag{4.90}$$

Here α is an arbitrary phase factor, which in a way completely analogous to section 4.3 can be shown to be irrelevant to the physical correlator, just as the whole sub-horizon region, where ψ is simply oscillating, is irrelevant. Hence we take $\alpha = 0$ without loss of generality.

Realizing that $a''/a = \mathcal{H}^2(2-\tilde{\epsilon})$ we see that the whole treatment of §4.4.3 is easily applied to this case as well. In a sufficiently small interval around $\eta_\mathcal{H}$ (the time when $k = \mathcal{H}$) we find to first order in slow roll with $z = k\eta$:

$$\psi(z) = \sqrt{\frac{\pi}{4k}}\sqrt{z}\, H^{(1)}_{3/2+\tilde{\epsilon}_\mathcal{H}}(z) = -\frac{e^{i\pi\tilde{\epsilon}_\mathcal{H}}}{i\sqrt{2k}}\left[1+\tilde{\epsilon}_\mathcal{H}(1-\gamma-\ln 2)\right]\left(\frac{z}{z_\mathcal{H}}\right)^{-1-\tilde{\epsilon}_\mathcal{H}}, \tag{4.91}$$

where the expression after the last equals sign is only valid for $|z| \ll 1$. On the other hand, the solution in the super-horizon region where $k \ll \mathcal{H}$ is given by (cf. (4.55))

$$\psi(z) = Ca + Da\int_{z_\mathcal{H}}^{z}\frac{\mathrm{d}z'}{a^2}. \tag{4.92}$$

Integrating expression (4.64) for $\mathcal{H} = (\ln a)'$ we find the following first-order approximation for $a(z)$ around $\eta = \eta_\mathcal{H}$:

$$a(z) = a_\mathcal{H}\left(\frac{z}{z_\mathcal{H}}\right)^{-1-\tilde{\epsilon}_\mathcal{H}}. \tag{4.93}$$

Using the identification procedure described in §4.4.1 we see that again it is the leading-order term in the expansion in z of the Hankel function in the solution for ψ in the transition region that turns into the dominant solution for ψ in the super-horizon region, i.e. the C term in (4.92). From this we derive an expression for C:

$$C = \frac{1}{\sqrt{2k}\, a_\mathcal{H}}\left[1+\tilde{\epsilon}_\mathcal{H}(1-\gamma-\ln 2)\right]. \tag{4.94}$$

Here we omitted some unitary factors that are irrelevant to the calculation of the correlator of the tensor perturbations. As the D term in (4.92) rapidly decays compared to the

C term, we do not have to determine D. Using (4.87) we then obtain the final result for h_{ij} at later times (i.e. when we can neglect the D term) to first order in slow roll for super-horizon modes that crossed the horizon during slow-roll inflation:

$$\hat{h}_{ij\,\mathbf{k}} = \frac{\sqrt{2}\,\kappa}{k^{3/2}}\, H_{\mathcal{H}}\,[1 + \tilde{\epsilon}_{\mathcal{H}}(1 - \gamma - \ln 2)] \sum_{A=1}^{2} e_{ij}^{A}\, \hat{a}^{\dagger}_{A\,\mathbf{k}} + \text{c.c.}, \tag{4.95}$$

where we used the identity $k = a_{\mathcal{H}} H_{\mathcal{H}}$. This result is also valid after inflation, as long as the mode $\mathbf{k}$ remains super-horizon. We see that this expression for h_{ij} is independent of time: the super-horizon h_{ij} is simply constant. Of course this could be seen directly from (4.82) for k^2 negligibly small. Comparing this tensor expression with the scalar result (4.75) we find that the tensor perturbations miss the overall factor of $1/\sqrt{\tilde{\epsilon}_{\mathcal{H}}}$, so that they will be smaller than the scalar perturbations in general.

4.6 Summary and conclusion

We have given a general analytical treatment for scalar, vector and tensor perturbations on a spatially flat Robertson-Walker spacetime in the presence of an arbitrary number of scalar fields that take values on a curved field manifold during slow-roll inflation. These are the kind of systems that one typically obtains from (string-inspired) high-energy models. The main part of the treatment is about the scalar perturbations. They were calculated to first order in slow roll. In particular we computed the gravitational potential in terms of background quantities only. Special attention was paid to multiple-field effects. In chapter 5 we will show that it is the correlator of the gravitational potential that is related to the temperature fluctuations that are observed in the CMBR. An explicit example to illustrate and check the results of this chapter will be treated in chapter 6.

A discussion of the background scalar fields in chapter 3 served as the foundation for this analysis. The first of three central ingredients for this discussion was the manifestly covariant treatment with respect to reparameterizations of the field manifold and of the time variable. Secondly, the field dynamics (the field velocity, acceleration, etc.) naturally induce an orthonormal basis $(\mathbf{e}_1, \mathbf{e}_2, \dots)$ on the field manifold. This makes a separation between effectively single-field and truly multiple-field contributions possible and is also an important ingredient of the quantization scheme. Finally, we modified the definitions of the well-known slow-roll parameters to define slow-roll functions in terms of derivatives of the Hubble parameter and the background field velocity for the case of multiple-scalar-field inflation. These slow-roll functions (except $\tilde{\epsilon}$) are vectors, which can be decomposed in the basis induced by the field dynamics. For example, the slow-roll function $\tilde{\eta}^{\perp}$ measures the size of the acceleration perpendicular to the field velocity. Because we did not make the assumption that slow roll is valid in the definition of the slow-roll functions, it is often possible to identify these slow-roll functions in exact equations of motion and make decisions about neglecting some of the terms. In this context we introduced the slow-roll derivative, which is very useful to keep track of orders in slow roll while switching between different time variables and which is also a necessary ingredient to write the equations in a form that is independent of the specific choice of time variable. For precision calculations estimates of the accuracy of the solutions of these approximated slow-roll equations are very important; it turns out that if the size of the region of integration is too large this accuracy may be compromised.

Our calculation of the scalar perturbations accurate to first order in slow roll is based on the following principles. We generalized the combined system of gravitational and matter perturbations of Mukhanov et al. [141] by defining the Mukhanov-Sasaki variables as a vector on the scalar-field manifold. The decomposition of these variables in the basis induced by the background field dynamics is field space reparameterization invariant, and the corresponding Lagrangean takes the standard canonical form, making quantization straightforward. The gravitational potential only couples to the scalar field perturbation in the direction $\mathbf{e}_2$ with a slow-roll factor $\tilde{\eta}^{\perp}$.

To obtain analytical solutions for the scalar perturbations to first order in slow roll it is crucial to divide the inflationary epoch into three different regimes, which reflects the change of behaviour for a given mode when it crosses the Hubble scale. These regimes are conventionally called sub-horizon, horizon-crossing (transition), and super-horizon. Within all three regions analytical solutions for the perturbations valid to first order could be found. The sub-horizon region is irrelevant to the correlator of the gravitational potential. Relating the transition and super-horizon regions is not trivial, as there is no analytical result that is valid to first order at the boundary between them. Using the procedure identifying leading-order asymptotic expansions we could determine the relative normalization of the super-horizon solution with respect to the solution in the sub-horizon region using analytical properties.

To determine the solution for the scalar perturbations other than the gravitational potential in the super-horizon region we need a final principle: the application of slow roll to the perturbations. For this it was essential that we treated the background using an arbitrary time variable, since the perturbed metric has to be rewritten in terms of a changed background metric. In particular this method was used to obtain an integral expression for the particular solution U_P of the gravitational potential in terms of background quantities only. Although this expression is a priori not expected to hold good near the end of (slow-roll) inflation, it can actually be a very good approximation if $\tilde{\eta}^{\perp}$ goes to zero at the end of inflation (since U_P is an integral over $\tilde{\eta}^{\perp}$, contributions at the end of inflation are then negligible).

As will be discussed in more detail in chapter 5, multiple-field effects are important in the gravitational potential if $\tilde{\eta}^{\perp}$ is sizable during the last 60 e-folds of inflation. The most important source of multiple-field effects is the particular solution U_P of the gravitational potential. In the example in chapter 6 we will show that this term can contribute even at leading order. This contribution is included implicitly in the function $N(\boldsymbol{\phi})$ of [144], but we derived an explicit expression. If $\tilde{\eta}^{\perp}$ peaks in the transition region, the rotation of the basis induced by the background field dynamics during the transition region can be another source of multiple-field effects, but in generic situations we found it to be beyond the level of first order in slow roll.

Next to the scalar perturbations we also considered vector and tensor perturbations. Vector perturbations turn out to be absent in the case of scalar field matter. The tensor perturbations were treated in a way analogous to the scalar perturbations, and an expression for the gravitational wave perturbation in terms of background quantities only was derived. As is discussed in chapter 5, the correlator of this quantity is also of some importance for the temperature fluctuations in the CMBR. However, there are no explicit multiple-field effects in the tensor perturbations.

Chapter 5

Perturbations after inflation and the link with observations

One of the greatest successes of the concept of inflation is that it can give an explanation for the existence of small density fluctuations in an otherwise homogeneous universe. These small fluctuations, which are the gravitational seeds for the formation of large-scale structures, are observed in the cosmic microwave background radiation (CMBR). Of course this is a two-way interaction: the observed amplitude and slope of the fluctuation spectrum give us some observational constraints on the otherwise rather elusive parameters in the inflation models, and hence on the parameters in the underlying high-energy theories. This was exactly our main motivation for working on the theory of inflationary density perturbations. In chapter 4 this theory was developed, resulting in expressions for the gravitational and matter perturbations at the end of inflation. In this chapter we discuss how these quantities evolve after inflation and how they are linked to the fluctuations we observe in the CMBR.

In section 5.1 the discussion of section 1.3 is continued in more detail with a (mostly qualitative) overview of the temperature anisotropies in the CMBR. §5.1.1 defines some quantities used to describe these anisotropies. §5.1.2 discusses the main features of the CMBR power spectrum and gives a qualitative explanation for them, introducing the most important physical processes that play a role here. §5.1.3 gives a brief overview of the various additional physical processes that affect the spectrum as we observe it, and explains which processes are the most important from the point of view of inflation (the most important ones together form the Sachs-Wolfe effect). The behaviour of the superhorizon perturbations from inflation during radiation and matter domination is derived in section 5.2. The gravitational potential is the subject of §5.2.1, where also the concepts of adiabatic and entropy/isocurvature perturbations are introduced. The latter are then further treated in §5.2.2.

In section 5.3 the results from chapter 4 and section 5.2 are combined to derive expressions for the spectral amplitudes and indices at the time of recombination in terms of inflationary background quantities. The amplitudes are basically the correlators of the gravitational potential and of the tensor perturbation. There are four amplitudes and indices: three for the scalar perturbations (adiabatic, total isocurvature and mixing) and one for the tensor perturbations. The resulting expressions are discussed in detail. Section 5.4

explains the relation between these spectral amplitudes and indices and the observed temperature fluctuations. In §5.4.1 an expression for the Sachs-Wolfe effect is derived as well as the relation between Fourier modes and spherical harmonics. Observational values for the scalar and tensor amplitudes and spectral indices are given in §5.4.2. The results of this chapter are summarized in section 5.5, where also the various aspects that still have to be studied are pointed out.

Sections 5.1 and 5.4 are mainly based on work by other authors, as indicated in those sections. Of those two only the generalized expression (5.55) for the Sachs-Wolfe effect in the presence of hot dark matter and quintessence is my own work. Parts of section 5.3 can be found in my papers [60, 195]. The other new results in this chapter are to be included in another paper [194].

5.1 Temperature fluctuations in the CMBR

This section gives a (mainly qualitative) overview of results from the literature regarding the CMBR, with the main focus on those that are important from the point of view of inflation. First some quantities relevant for the description of temperature anisotropies are defined in §5.1.1. A qualitative discussion of the CMBR power spectrum and of the physical processes that play a role are the subjects of §5.1.2 and §5.1.3 (a quantitative treatment of the effects most important for inflation follows later in section 5.4). This section is mainly based on [2, 21, 74, 76, 77, 106, 136, 192].

5.1.1 Temperature anisotropies

As discussed in section 1.3 the cosmic microwave background radiation consists of the photons left over from the early universe. At the early stages of the universe the photons were tightly coupled to the baryons by means of (mainly Compton) scattering with free electrons [149]. The protons and electrons were also tightly coupled by means of Compton scattering. Because of this coupling there was thermal equilibrium and the photons were distributed according to a Planck distribution, which can be characterized by a single temperature T. But when the universe was about 300 000 years old, with a temperature of about 3500 K, the protons and electrons combined into neutral hydrogen atoms and the universe became transparent for photons. Hence the CMBR shows the universe as it was at that time, although the photons have been redshifted to a temperature of about 3 K (2.725 to be exact, see table 1.1) because of the expansion of the universe. Note that a Planck (or black body) spectrum remains a Planck spectrum during expansion. This can be seen as follows. The number of photons $\mathrm{d}N$ in a comoving volume V with a wavelength between λ and $\lambda + \mathrm{d}\lambda$ is given by

$$\mathrm{d}N(\lambda) = Vn(\lambda)\mathrm{d}\lambda, \qquad \text{with} \quad n(\lambda) = \frac{8\pi}{\lambda^4}\frac{1}{\exp\left(\frac{2\pi}{\lambda T}\right) - 1} \tag{5.1}$$

(the Planck function). Changing the scale factor a to $\tilde{a}$ we see that $\tilde{\lambda} = (\tilde{a}/a)\lambda$ and $\tilde{V} = (\tilde{a}/a)^3 V$. Since the number of photons does not change we know that $\mathrm{d}\tilde{N} = \mathrm{d}N$. That can only be true if $\tilde{T} = (a/\tilde{a})T$. In that case we see that $\tilde{n}(\tilde{\lambda}) \equiv \mathrm{d}\tilde{N}/(\tilde{V}\mathrm{d}\tilde{\lambda})$ is also a Planck function, with temperature $\tilde{T}$.

In this very homogeneous background spectrum small anisotropies have been observed, and it is these we are interested in. They can be represented by specifying a direction-

dependent temperature. Subtracting the monopole (or direction-independent, i.e. background) temperature T_0, and dividing by T_0 to normalize, we obtain the temperature fluctuation $\Delta T/T$, which we expand in spherical harmonics Y_{lm}:

$$\frac{\Delta T}{T}(\theta,\varphi) \equiv \frac{T(\theta,\varphi)-T_0}{T_0} = \sum_{l=1}^{\infty}\sum_{m=-l}^{+l} a_{lm}Y_{lm}(\theta,\varphi). \tag{5.2}$$

In principle the coefficients a_{lm} are measured by CMBR experiments like the COBE satellite [30]. The dipole component $l = 1$ is completely dominated by our own motion with respect to the last scattering surface, but the other components can give information about physical processes occuring during various eras in the evolution of the universe, most importantly (from our point of view) about inflation.

The multipole l can be related to the wave number k of features in the CMBR. A detailed treatment of the relation between spherical harmonics and Fourier modes is given in §5.4.1, but here we give a simple argument to find a rough estimate. If $x_{\rm ls}$ is the coordinate (or comoving) distance to the last scattering surface, the angular size α (in radians) of a feature of comoving size $r \ll x_{\rm ls}$ in a flat universe is $\alpha = r/x_{\rm ls}$. The relation between the wave number k and comoving size r of a structure is $k = 2\pi/r$. So we find that $k = 2\pi/(x_{\rm ls}\alpha)$ for sufficiently small angles. Furthermore the relation between the angular size α and the multipole l that dominates it is $\alpha = \pi/l$, which leads to the relation $k = 2l/x_{\rm ls}$. We can use this to estimate the multipole l corresponding with the horizon size at recombination. Using the formulae for a flat matter-dominated universe we find from (2.22) that the present angular size of the horizon at recombination and the corresponding multipole are given by

$$\alpha_H = \frac{d_H(t_{\rm rec})/a_{\rm rec}}{d_H(t_0)/a_0} = \left(\frac{t_{\rm rec}}{t_0}\right)^{1/3} \approx 0.03 = 1.7^\circ \qquad \Rightarrow \qquad l_H = \frac{\pi}{\alpha_H} \approx 100. \tag{5.3}$$

In this thesis we restrict ourselves to Gaussian fluctuations. In single-field inflation one can show that non-Gaussianity can only be caused by non-linearities and their backreaction, and is necessarily small because they are constrained by the slow-roll conditions [200]. In multiple-field inflation with correlations between the different field perturbations the non-linearities might be larger, leading to non-negligible non-Gaussianity [13]. At present observations have not led to any evidence for non-Gaussianity [101], but the new satellites MAP [130] and Planck [155] will be able to detect smaller deviations from Gaussianity. If indeed a non-Gaussian signature is detected, it will offer more experimental data to constrain inflationary parameters, so that this aspect is well worth future study, but beyond the scope of this thesis. Note that non-Gaussianity is a rather broad notion, and that the exact type is important as well. Some types, for example coherent spatial structures like line discontinuities, simply cannot be produced by inflation at all, and would point in the direction of another mechanism, like topological defects, being at least partially responsible for the origin of the perturbations [106].

For Gaussian fluctuations all information is contained in the two-point correlation function. Moreover, perturbations from inflation are statistically isotropic (i.e. all correlation functions are rotationally invariant), since in the whole treatment there is never a preferred direction. This means that we only need consider the correlation function

$$C(\alpha) \equiv \left\langle \frac{\Delta T}{T}(\hat{\mathbf{e}})\frac{\Delta T}{T}(\hat{\mathbf{e}}')\right\rangle, \tag{5.4}$$

which depends exclusively on the angle α between the two directions $\hat{\mathbf{e}}$ and $\hat{\mathbf{e}}'$, given by $\cos\alpha = \hat{\mathbf{e}}\cdot\hat{\mathbf{e}}'$, because of statistical isotropy. Here we represent the direction (θ,φ) by the unit vector $\hat{\mathbf{e}}$. Inserting the definition (5.2) into the correlation function we find

$$C(\alpha) = \sum_{l,m}\sum_{l',m'} \langle a_{lm} a^*_{l'm'}\rangle Y_{lm}(\hat{\mathbf{e}}) Y^*_{l'm'}(\hat{\mathbf{e}}'). \tag{5.5}$$

It follows from statistical isotropy that $\langle a_{lm} a^*_{l'm'}\rangle$ can be written as $C_l \delta_{ll'}\delta_{mm'}$. Using this as well as the addition theorem for spherical harmonics we obtain

$$C(\alpha) = \sum_l \frac{2l+1}{4\pi} C_l P_l(\cos\alpha), \tag{5.6}$$

where P_l is the Legendre polynomial of degree l.

Theoretically the correlation function is an ensemble-average over all possible skies, while experimentally we only have access to the single sky we see from Earth. (Using the ergodic theorem the ensemble-average can also be seen as an average over all observer positions.) This means that even in the hypothetical case of whole-sky coverage and perfect resolution there would still be statistical errors in the observed C_l. This effect is called cosmic variance, and is most important for observables that depend only on a small number of a_{lm}, like the C_l with small l. More quantitatively, for a given experiment the accuracy of the determination of the C_l can approximately be given by [136, 92]:

$$\frac{\Delta C_l}{C_l} = \sqrt{\frac{2}{(2l+1) f_{\rm sky}}} \left(1 + \frac{\sigma^2_{\rm pixel}\Omega_{\rm pixel}}{C_l}\, \exp(l^2\sigma^2_{\rm beam})\right), \tag{5.7}$$

where $f_{\rm sky}$ is the sky coverage fraction, $\sigma_{\rm beam}$ is the angular resolution (beam size), $\sigma_{\rm pixel}$ is the experimental noise per pixel and $\Omega_{\rm pixel}$ is the area per pixel. In the case of a perfect experiment a factor $\sqrt{2/(2l+1)}$ remains, which is the cosmic variance.

5.1.2 The CMBR power spectrum

The quantity C_l is called the power spectrum of the CMBR. A plot of the theoretical power spectrum as a function of l (with a certain normalization of C_l that is explained in §5.4.1), numerically computed with the CMBFAST code [173], is shown in figure 5.1. The present best-fit cosmological parameters have been used as input, as well as flat scalar and tensor spectra with adiabatic initial conditions (see §5.2.1). For clarity in the figure, a large tensor to scalar quadrupole ratio of 0.5 has been chosen (see the remark at the end of §5.4.1). In generic inflation models this ratio is much smaller, but then the tensor spectrum would not be visible in the plot. The current observational results are given in figure 5.2.

Basically we see three different regions for the scalar perturbations. At the largest angular sizes (smallest l) the spectrum is more or less flat, at intermediate sizes there are a series of peaks, while at the largest values of l the spectrum goes to zero. For the tensor perturbations the spectrum goes to zero right after the first flat region. In the remainder of this subsection we give a qualitative explanation for this behaviour.

The first region is both the simplest and, from the point of view of inflation, the most interesting. As derived in (5.3), the multipoles with $l \lesssim 100$ correspond with scales that

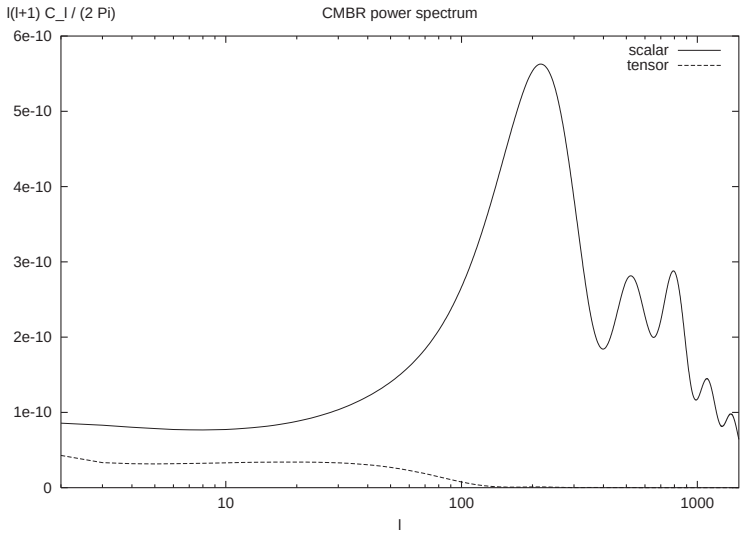

Figure 5.1: The CMBR power spectrum (a plot of $l(l+1)C_l/(2\pi)$ against l) in the range of $l = 2 \ldots 1500$ (note the logarithmic axis), numerically computed with the CMBFAST computer code [173]. Both the contributions from the scalar and the tensor perturbations are shown, assuming flat initial spectra for both, adiabatic initial conditions and a tensor to scalar quadrupole ratio of 0.5. The cosmological parameters of table 1.1 have been used, except that all neutrino species were taken to be massless. Furthermore, a helium mass fraction of 0.24 was assumed and the effect of global reionization was neglected. The CMBFAST code automatically normalizes the spectrum to the COBE data at small l.

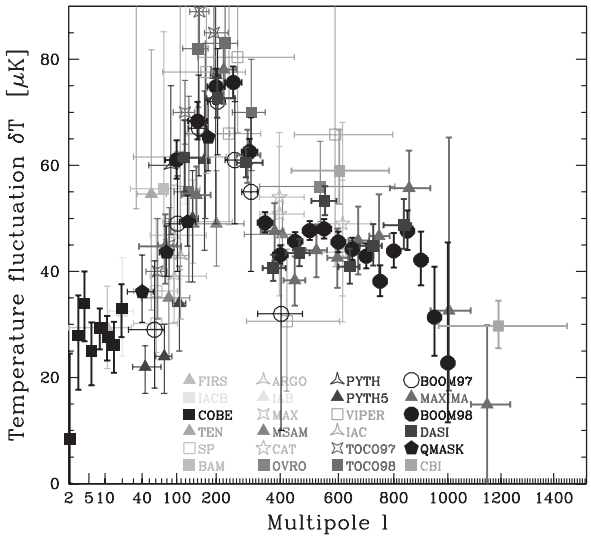

Figure 5.2: The observational results for the CMBR power spectrum from a large number of experiments. The quantity plotted on the vertical axis is equal to $\sqrt{l(l+1)C_l/(2\pi)}\,T_0$. Figure taken from [201], with permission.

were still outside the horizon at the time of recombination. Hence at these smallest values of l we still see the primordial inflationary spectrum. With the normalization chosen this corresponds to a flat region. In §5.4.1 the relation between the C_l and the inflationary perturbations is described and the normalization factor is explained.

At values of $l \gtrsim 100$ we start to see angular sizes that correspond to scales that reentered the horizon before recombination. Already before recombination the universe had been matter-dominated for some time. As soon as a mode reentered the horizon during matter domination, gravity made the matter density increase in gravitational wells and decrease on gravitational hills. However, before recombination the baryons were tightly coupled to the photons by scattering processes, and the photon pressure resisted the compression of the baryons, which led to acoustic oscillations in the baryon-photon plasma. At the time of recombination this coupling suddenly fell away and in the CMBR we see the oscillations as they were at that time. The wave number k of a perturbation determines the time when it entered the horizon and thus the amount of time it spent oscillating, as well as the frequency of the oscillations. Hence the scale of a perturbation mode determines the phase of oscillation at the time of recombination. Certain modes were exactly at the extremum of an oscillation at the time of recombination, and at the corresponding multipole we see a peak in the CMBR power spectrum, since a region of compression (rarefaction) has a higher (lower) than average temperature (note that in the power spectrum we have basically squared the temperature fluctuations, so that the sign is irrelevant). So the first peak corresponds to a scale that has had exactly sufficient time between horizon reentry and recombination for a single compression or rarefaction, the second peak corresponds to a scale that has undergone both a compression and a rarefaction, etc.

The perturbations are generally divided into two types: adiabatic and isocurvature. They are properly defined in §5.2.1, but basically the adiabatic perturbation is that part of the gravitational potential that comes directly from inflation, while the isocurvature perturbations are those parts of Φ generated by multiple-component effects during matter domination. This means that while the adiabatic gravitational perturbation was fully developed at horizon reentry, this was not the case for the isocurvature ones. Hence there is a phase shift between the acoustic oscillations in an adiabatic model and those in an isocurvature one, so that the positions of the peaks are different in both models. See [77, 78], to which papers the reader is referred for more details. Observations have by now ruled out pure isocurvature perturbations, while pure adiabatic perturbations are still allowed [41].

As the peaks are not the most important part of the power spectrum from the point of view of inflation, we will not go into any more detail here. A detailed treatment of the acoustic peaks can be found in e.g. [74, 75] and references therein. Very roughly the peaks are located at $l_n \approx 200\, n$ [74]. However, the positions and heights of the peaks turn out to depend on the basic cosmological parameters in many different combinations, so that the main importance of detailed observations of the acoustic peaks is the accurate determination of these parameters. A simple example of this is that an object at a certain fixed distance has a larger angular size in a closed universe than in a flat one. Hence the acoustic peaks appear at larger angles, i.e. lower l, in a closed universe. The converse is true for an open universe. Other dependences, for example on the baryon density, are caused by the details of the acoustic oscillation mechanism during the plasma era before recombination. See e.g. [192, 77]; animations of the parameter dependences of the peaks can be found at [73].

Finally, the disappearance of the oscillations at the largest $l \gtrsim 1000$ can be understood

as follows. As mentioned above it was the pressure of the tightly coupled photons that resisted gravitational compression and led to acoustic oscillations. However, since recombination was not an instantaneous process, there was a transition period when the photons were no longer perfectly coupled to the baryons, but had a certain (short) mean free path. When this mean free path became larger than the oscillation wavelength, the photons diffused out of regions of compression into regions of rarefaction and thus smoothed out the differences instead of generating oscillations. This is called Silk damping [175], and the details again depend on the cosmological parameters.

As opposed to the behaviour of the scalar perturbations, tensor perturbations were destroyed by Thomson scattering as soon as they entered the horizon, see [74] and references therein. Hence for multipoles $l \gtrsim 100$ the tensor perturbations are strongly suppressed. However, for smaller l they behave just like the scalar perturbations, leading to a degeneracy in the parameter dependences. This degeneracy will disappear as soon as the polarization spectrum of the CMBR is observed in addition to the temperature anisotropy spectrum [79, 89]: scalar and tensor (and vector) perturbations have very different polarization characteristics. Unfortunately, sufficient accuracy will probably only be achieved by the Planck satellite [155]. The influence of the inflationary tensor perturbations on the CMBR spectrum is discussed at the end of §5.4.1.

In the discussion of the acoustic peaks we have assumed that all perturbations of the same scale had the same temporal phase during the oscillations. This is indeed the case for inflationary perturbations: these were generated during the inflation era as decoupled perturbation modes, and at the time of horizon reentry all perturbation modes $\mathbf{k}$ with the same $k = |\mathbf{k}|$ were given by a single 'growing mode' solution (the decaying mode is suppressed by factors of $1/a$ and had disappeared by this time, see e.g. (4.55)). The phase of the oscillation at the time of recombination, when the oscillations suddenly stopped, is then completely determined by k, with the spectrum of acoustic peaks as a result. This is contrary to the case where the perturbations are caused by topological defects, see [2, 3, 156]. Defect fluctuations are continuously seeded by defect evolution, which is a nonlinear process. The Fourier modes are then coupled and the various decoherent sources cause modes with the same value of k, but different $\mathbf{k}$, to behave differently. Hence the simple relation between temporal oscillation phase and scale is destroyed, with the result that the spectrum of acoustic peaks is smeared to a single broad hump. This is a very distinct difference between models of the CMBR spectrum based on inflation and those based on topological defects. As can be concluded from figure 5.2 (see [201]), the data have become sufficiently accurate that we can see a series of acoustic peaks, which rules out topological defects as the dominant source of perturbations, and means that inflation has passed an observational test.

5.1.3 Sources of the anisotropies

The effects discussed thus far are the so-called primary sources of anisotropies, acting right at recombination. As mentioned in secion 1.3 there are also secondary and tertiary sources of anisotropies, which acted on the photons after they had left the last scattering surface. A rather extensive list, taken from [192], is given in table 5.1. Three of the primary sources, density fluctuations, damping and defects, were discussed in §5.1.2. Because of the oscillations, the baryons had certain velocities, leading to Doppler shifts of the photons that were scattered by them, which is the Doppler source in the table. Finally, gravitational fluctuations, apart from causing density fluctuations, have the additional

Primary (acting at decoupling)	Gravity	
	Doppler	
	Density fluctuations	
	Damping	
	Defects	Strings
		Textures
Secondary (acting after decoupling)	Gravity	Early Integrated Sachs-Wolfe
		Late ISW
		Rees-Sciama
		Lensing
	Local reionization	Thermal Sunyaev-Zeldovich
		Kinematic SZ
	Global reionization	Suppression
		New Doppler
		Vishniac
Tertiary (foregrounds)	Extra-galactic	Radio point sources
		IR point sources
	Galactic	Dust
		Free-free
		Synchrotron
	Local	Solar system
		Atmosphere
		Noise, etc.

Table 5.1: The different sources of anisotropies in the CMBR according to [192].

effect that photons climbing out of a potential well experience a gravitational redshift, which corresponds with a lower temperature. This means that gravitational wells caused two opposite effects: a lower temperature because of the redshift, and a higher temperature because of the higher density. The combined effect of the three primary sources gravity, Doppler and density perturbations on the largest angular sizes is called the Sachs-Wolfe effect [167] and is derived in §5.4.1.

Those effects that played a role when the photons were travelling from the last scattering surface towards our detectors are called secondary sources of temperature anisotropies [192]:

Gravity Gravity influences photons in two ways: by means of the integrated Sachs-Wolfe effect and gravitational lensing. The former is caused by the fact that, if the gravitational potential is not constant in time, potential wells that the photons are travelling through change while the photons are crossing them. (This integrated Sachs-Wolfe effect should not be confused with the Sachs-Wolfe effect, which is a combination of primary sources of anisotropies and is discussed in detail in §5.4.1.) Depending on the cause of this time dependence, the ISW effect is divided into three parts: early ISW, late ISW and Rees-Sciama.

Early ISW Right after recombination the photon contribution to the density of the universe was not yet completely negligible, so that the gravitational potential was somewhat higher than later on (see (5.16)).

Late ISW At later times (close to the present) the cosmological constant (or dark energy) started to contribute significantly to the density of the universe, causing a change in the gravitational potential.

Rees-Sciama Gravitational collapse leading to the formation of both large and small-scale structures causes a time-dependent gravitational potential as well [164].

Lensing Gravitational lensing is not a form of the ISW effect. It changes the direction of photon trajectories, thus producing a certain kind of smearing at small scales.

Local reionization The Sunyaev-Zeldovich effect [208] is caused by hot gas in individual clusters. A moving cluster of galaxies causes a Doppler shift in the CMBR photons because of Thomson scattering with the free electrons in the hot intra-cluster gas (kinematic SZ effect). Independent of the cluster velocity, interaction with these hot electrons distorts the Planck spectrum (thermal SZ effect).

Global reionization During the evolution of the universe there was a time when because of gravitational collapse the density perturbations had grown to become the first galaxy-like objects emitting radiation. Since these early objects (quasars) appear to have been very bright, they may have led to a substantial reionization of the matter in the universe on a global scale. Depending on the amount of global reionization this could have had quite an impact on the CMBR. In the first place, a new phase of scattering, where the photons were not free, would have caused a smearing and suppression of small scales, the exact smallness of which depends on the time between decoupling and reionization. Of course this new phase of scattering would also have caused new Doppler shifts. Finally, the Vishniac effect [197] is a second-order effect that would have generated new fluctuations at very small scales.

Tertiary sources of anisotropies are not really sources of anisotropies, just sources of contamination of the data. More information on these tertiary sources and how to remove them from the data can be found in [24, 193] and references therein.

As mentioned before, from the point of view of inflation we are mostly interested in the fluctuations at the largest angular sizes in the CMBR. By means of the Sachs-Wolfe effect the observed CMBR spectrum at those largest sizes is directly related to the primordial inflationary perturbations. However, we should take care that, apart from removing the contamination of the tertiary sources, the data at these scales are not influenced by the secondary sources as well. Fortunately, most of the secondary sources of anisotropies are local processes affecting only the fluctuations at smaller sizes. The exceptions are the early and late ISW effects and global reionization. Global reionization affected sizes smaller than the horizon at the time of reionization, so it could not affect the very smallest multipoles $l \lesssim 10$ [192]. More information on global reionization can be found in [10, 57]. The ISW effects peak at the scales corresponding with the horizon scale at the time when they are important [192, 74, 99]. For the early ISW effect this means the horizon scale at recombination, so that it did not affect the largest sizes with the primordial inflationary perturbations. The late ISW effect, on the other hand, is important at the very largest angular sizes $l \lesssim 5$, since observations show our universe to be in the process of moving from matter domination to cosmological constant domination right now. In fact, this is the cause of the slight tilt in figure 5.1 at the smallest values of l. For a rough estimate

one can neglect all the secondary effects if one looks at values $l \sim 10$ (the lowest values of l are inaccurate anyway because of cosmic variance), but in the observational values quoted in §5.4.2 for the amplitude and tilt of the spectrum global reionization and late ISW effect have been taken into account.

5.2 Perturbations after inflation

In this section the equations for the perturbations during radiation and matter domination are derived, valid after inflation (and reheating) all the way up to recombination. We start with the gravitational potential in §5.2.1, where we also define the concepts of adiabatic and isocurvature perturbations. The treatment of the latter is the subject of §5.2.2.

5.2.1 Gravitational potential

The equation of motion for the gravitational potential during radiation and matter domination is derived in a way analogous to the one during inflation. We make the assumption that we have ideal fluids, i.e. no anisotropic stress. Then there are no non-diagonal space-space components in the energy-momentum-stress tensor T^μ_ν and the argument for the relation $\Psi = \Phi$ given in section 4.2 remains valid. Adding the (00) component of the Einstein equation, multiplied by c_s^2, to 1/3 times the summed (ii) components we obtain from (B.15) after switching to Fourier modes:

$$\Phi'' + 3\mathcal{H}(1+c_s^2)\Phi' + \kappa^2 a^2(\rho c_s^2 - p)\Phi + c_s^2 k^2 \Phi = -2\kappa^2 a^2(\rho c_s^2 - p)\tilde{S} \tag{5.8}$$

with

$$\begin{aligned} &\rho \equiv -T^0_{\ 0} = \frac{3}{\kappa^2 a^2}\mathcal{H}^2, \qquad p \equiv \frac{1}{3}T^i_{\ i} = -\frac{1}{\kappa^2 a^2}(2\mathcal{H}' + \mathcal{H}^2), \qquad c_s^2 \equiv \frac{p'}{\rho'} = \frac{\dot{p}}{\dot{\rho}}, \\ &\delta\rho \equiv -\delta T^0_{\ 0}, \qquad\qquad \delta p \equiv \frac{1}{3}\delta T^i_{\ i}, \qquad\qquad \tilde{S} \equiv \frac{1}{4}\frac{\delta p - c_s^2 \delta\rho}{p - c_s^2 \rho}. \end{aligned} \tag{5.9}$$

Here ρ and p are the energy density and isotropic pressure, c_s^2 is the sound velocity and $\tilde{S}$ is the total (gauge-invariant) entropy perturbation (more about this entropy perturbation later on). The expressions after the second equality sign in the definitions of ρ and p follow from the background Einstein equation, see (2.12) and (2.13). For super-horizon modes, which are the only ones we consider, the k^2 term can be neglected. Equation (5.8) can also be found in [141]. The multiplication of the (00) component of the Einstein equation by c_s^2 in the derivation of (5.8) might seem rather arbitrary, but is necessary to obtain the gauge-invariant quantity $\tilde{S}$ on the right-hand side. (As $\delta\rho \to \delta\rho - \rho'\xi^0$ and $\delta p \to \delta p - p'\xi^0$ under the coordinate transformation (4.3), see [85], $\delta p - c_s^2\delta\rho$ is exactly the correct gauge-invariant combination.) The following definition and relations will also be useful:

$$w \equiv \frac{p}{\rho}, \qquad \rho' + 3\mathcal{H}\rho(1+w) = 0, \qquad w' = -3\mathcal{H}(c_s^2 - w)(1+w). \tag{5.10}$$

The second expression is just a rewriting of equation (2.14), while the last follows by writing $w' = (p'/\rho' - p/\rho)\rho'/\rho$.

From equation (5.8) we see a situation that resembles the situation during inflation: the equation of motion for Φ has an inhomogeneous source term. Moreover, just as during

inflation, the source term is zero in the case of a single component, since in that case $\delta p/\delta\rho = p'/\rho' = c_s^2$. (Of course this is not surprising, since the inflationary case (4.20) is just a special example of equation (5.8), see (5.32) ff.). We can rewrite this equation in terms of the same u and θ that we used in chapter 4 during inflation [141]. The definitions (4.21) and (4.28) become

$$u \equiv \frac{\Phi}{\kappa\sqrt{2}\,H\sqrt{\tilde{\epsilon}}} = \frac{\Phi}{\kappa^2\sqrt{\rho(1+w)}}, \qquad \theta \equiv \frac{\kappa}{\sqrt{2}}\frac{1}{a\sqrt{\tilde{\epsilon}}} = \frac{\kappa}{a\sqrt{3}}\frac{1}{\sqrt{1+w}}, \tag{5.11}$$

where we used (4.19) and (5.9). From this we find

$$\frac{\theta'}{\theta} = -\mathcal{H}\left(1+\frac{3}{2}w-\frac{3}{2}c_s^2\right), \qquad \frac{\theta''}{\theta} = \frac{3}{2}\mathcal{H}^2\left(1+\frac{1}{2}w+\frac{1}{2}c_s^2-\frac{3}{2}wc_s^2+\frac{3}{2}c_s^4+\frac{1}{\mathcal{H}}(c_s^2)'\right). \tag{5.12}$$

Rewriting equation (5.8) in terms of u and θ for super-horizon modes gives

$$u'' - \frac{\theta''}{\theta}u = -2\sqrt{3}\,\frac{a\mathcal{H}}{\kappa}\,\frac{c_s^2-w}{\sqrt{1+w}}\,\tilde{S}. \tag{5.13}$$

The solution is derived analogously to (4.55), and after switching back to Φ and to comoving time reads as

$$\Phi = \kappa^2\tilde{C}\frac{H}{a} + 3\tilde{D}\frac{H}{a}\int_{t_*}^{t}\mathrm{d}t'\,a(1+w) - 6\frac{H}{a}\int_{t_*}^{t}\mathrm{d}t' a(1+w)\int_{t_*}^{t'}\mathrm{d}t''\,H\frac{c_s^2-w}{1+w}\,\tilde{S}. \tag{5.14}$$

The last (double integral) term is the particular solution. At this moment t_* is just an arbitrary reference time, the choice of which is related to the values of the integration constants $\tilde{C}$ and $\tilde{D}$. Using the relations (5.9) and (5.10) between w, c_s^2 and H this solution can also be written as

$$\Phi = \left(\kappa^2\tilde{C}+2\tilde{D}\frac{a_*}{H_*}\right)\frac{H}{a} + 2\tilde{D}A(t_*,t) - 2\frac{H}{a}\int_{t_*}^{t}\mathrm{d}t'\frac{1+w}{\frac{5}{6}+\frac{1}{2}w}\left(\frac{a}{H}\right)^{\cdot}\int_{t_*}^{t'}\mathrm{d}t''\,\tilde{S}\left(\frac{\frac{5}{6}+\frac{1}{2}w}{1+w}\right)^{\cdot} \tag{5.15}$$

where we defined $A(t_*,t) = 1 - H/a\int_{t_*}^{t}\mathrm{d}t' a$ using integration by parts as in (4.76). We see that if $\tilde{S}$ is constant, $\Phi_P = -2\tilde{S}$ is a particular solution. Of course this could also be determined directly from (5.8).

During radiation and matter domination we have $a \propto t^{1/2}$, $w = 1/3$ and $a \propto t^{2/3}$, $w = 0$, respectively. The non-decaying part of $A(t_*,t)$ is then equal to $2/3$ during radiation domination and equal to $3/5$ during matter domination. For the homogeneous part of Φ this means that

$$\Phi_{\mathrm{hom}}^{\mathrm{rad}} = \frac{4}{3}\tilde{D} + \mathcal{O}(t^{-3/2}), \qquad \Phi_{\mathrm{hom}}^{\mathrm{mat}} = \frac{6}{5}\tilde{D} + \mathcal{O}(t^{-5/3}). \tag{5.16}$$

We see that, except for a quickly decaying part, Φ goes to a constant value during radiation and matter domination. However, this value decreases by a factor $9/10$ during the transition from radiation to matter domination. Note that in the matter-dominated era, where $c_s^2 = 0$, this constant solution is also valid for modes that have reentered the

horizon, as the k^2 term then drops out in (5.8). This is the reason why there is only an integrated Sachs-Wolfe effect (ISW, see §5.1.3) when matter domination is not absolute, even though all visible modes have reentered the horizon by now.

In the literature the curvature perturbation $\mathcal{R}$ or ζ is often used instead of the gravitational potential. It is defined as $\mathcal{R} = -\zeta = \Phi - (H/\dot{H})(\dot{\Phi} + H\Phi)$ (see e.g. [54]; for ζ this expression is only correct on super-horizon scales). Note that the term curvature here means the curvature of the comoving three-dimensional spatial hypersurfaces, not the curvature of spacetime. Looking at the homogeneous non-decaying solution for Φ in (5.15), i.e. the $2\tilde{D}A(t_*, t)$ term, we see that this definition of the curvature perturbation precisely removes the time-dependent A factor. Hence in the absence of entropy perturbations (i.e. $\tilde{S} = 0$), the curvature perturbation remains constant, independent of the exact time dependence of the scale factor (but assuming an expanding universe, otherwise the so-called decaying terms do not decay at all). A very general derivation of this fact can be found in [199]. In the end, to relate these quantities to the temperature fluctuations in the CMBR, one has to switch to Φ, during which process the so-called transfer function is used, which for super-horizon modes is basically just the factor $9/10$ mentioned above, see [108, 103] and references therein. However, since the time dependence of Φ in the form of the function A is well-defined and easily evaluated at recombination, one can just as well keep working with the gravitational potential and not bother with $\mathcal{R}$ and ζ at all, which is how we will proceed.

Two more terms used in the literature need to be introduced: adiabatic and isocurvature [93, 116, 94, 95, 96, 103, 85]. Adiabatic initial conditions set $\tilde{S} = 0$ (no entropy perturbations, hence the name adiabatic) and isocurvature initial conditions set $\Phi = 0$ (no curvature perturbation). For this reason the homogeneous solution for Φ is called the adiabatic perturbation, while the particular solution corresponding with the $\tilde{S}$ source term is called the (total) isocurvature perturbation. Of course, this distinction depends on the time at which one considers the system. Conventionally the time selected is the beginning of the radiation-dominated era. This means that the adiabatic gravitational potential perturbation at the time of recombination is defined as the homogeneous solution of (5.8) at that time, where as initial conditions one has matched to the total solution for Φ at the beginning of the radiation-dominated era. Hence according to this conventional definition the adiabatic perturbation does include the possible effects of entropy perturbations during inflation and (p)reheating, i.e. the particular solution U_P in (4.75). The isocurvature contribution to the gravitational potential at the time of recombination is then defined as the particular solution of (5.8) at that time, with the initial conditions that it is zero and has zero derivative at the beginning of the radiation-dominated era. These definitions mean that in the solution for Φ (5.15) one should take t_* as the beginning of the radiation-dominated era. Assuming a constant $\tilde{S}$ (see §5.2.2 for a discussion) and neglecting the decaying solution, the isocurvature perturbation is then given by

$$\Phi_{\text{iso}} = -2\tilde{S}\left(1 - 2\,\frac{\frac{5}{6} + \frac{1}{2}w_*}{1 + w_*}\,A(t_*, t)\right) = -2\tilde{S}\left(1 - \frac{3}{2}A(t_*, t)\right). \tag{5.17}$$

During radiation domination this gives zero, as expected (since Φ and $\tilde{S}$ are constant), while during matter domination one finds $\Phi_{\text{iso}} = -\frac{1}{5}\tilde{S}$.

5.2.2 Entropy perturbations

In this subsection we derive expressions for the behaviour of the total entropy perturbation $\tilde{S}$ during radiation and matter domination. We consider an arbitrary number N of components, labeled by the subscript i. The different components each have a pressure p_i and an energy density ρ_i, as well as pressure and density perturbations. Analogously to the total w and c_s^2 we define these parameters also for the separate components (see e.g. [85]): $w_i \equiv p_i/\rho_i$ and $c_i^2 \equiv p_i'/\rho_i' = \dot{p}_i/\dot{\rho}_i$. Note that in general $w \neq \sum_i w_i$ and $c_s^2 \neq \sum_i c_i^2$. Equations (2.19) and (5.10) for the components read as

$$\rho_i' + 3\mathcal{H}\rho_i(1+w_i) = aX_i, \qquad w_i' = -3\mathcal{H}(c_i^2 - w_i)(1+w_i) + (c_i^2 - w_i)\frac{aX_i}{\rho_i}, \tag{5.18}$$

with X_i a measure of the interactions between the different components. In the following we make two assumptions regarding the separate components, which for the rest are completely arbitrary:

1. All components behave as ideal fluids with a constant w_i;
2. There are no interactions: $X_i = 0$ for all i.

From equation (5.18) we see that this automatically means that $c_i^2 = w_i$ (the square in c_i^2 is just convention; c_i^2 can be negative). Moreover, a constant w_i also means that $\delta p_i/\delta\rho_i = w_i$.

Let us remark briefly on the assumption of no interactions with regard to a real model. One can think of the following situation. Of the multiple scalar fields during inflation one has decayed to all the Standard Model particles, so that there are no entropy perturbations between those components (see the definition of S_{kl} below) and the absence or presence of interactions is irrelevant. The other fields have decayed to different kinds of dark matter, which makes the assumption of no interactions between these components quite plausible. It is usually assumed (see e.g. [158, 103]) that including interactions will have the effect of wiping out the isocurvature perturbations. However, it will be interesting to check this more carefully in the near future.

To rewrite $\tilde{S}$ (defined in (5.9)) we need some auxiliary results. In the first place we have that $p = \sum_i w_i\rho_i$, so that

$$c_s^2 = \frac{p'}{\rho'} = \sum_i \frac{\rho_i(1+w_i)}{\rho(1+w)}\, w_i, \tag{5.19}$$

where we used (5.18) and (5.10) for ρ_i' and ρ'. Using this result the numerator of $\tilde{S}$ is rewritten as follows:

$$\begin{aligned}
\delta p - c_s^2\delta\rho &= \sum_k (w_k - c_s^2)\delta\rho_k \\
&= \frac{1}{\rho(1+w)} \sum_{k,l} \rho_l(1+w_l)(w_k - w_l)\delta\rho_k \\
&= \frac{1}{\rho(1+w)} \frac{1}{2} \sum_{k,l} \rho_k\rho_l(1+w_k)(1+w_l)(w_k - w_l)S_{kl}
\end{aligned} \tag{5.20}$$

with

$$S_{kl} \equiv \frac{\delta\rho_k}{\rho_k(1+w_k)} - \frac{\delta\rho_l}{\rho_l(1+w_l)}. \tag{5.21}$$

In the last step of (5.20) we symmetrized the expression in k and l. Completely analogously we find for the denominator

$$\begin{aligned} p - c_s^2\rho &= \sum_k (w_k - c_s^2)\rho_k \\ &= \frac{1}{\rho(1+w)}\frac{1}{2}\sum_{k,l}\rho_k\rho_l(1+w_k)(1+w_l)(w_k-w_l)\left(\frac{1}{1+w_k} - \frac{1}{1+w_l}\right) \\ &= -\frac{1}{\rho(1+w)}\frac{1}{2}\sum_{k,l}\rho_k\rho_l(w_k-w_l)^2, \end{aligned} \tag{5.22}$$

so that

$$\tilde{S} = -\frac{1}{4}\frac{\sum_{k,l}\rho_k\rho_l(1+w_k)(1+w_l)(w_k-w_l)S_{kl}}{\sum_{k,l}\rho_k\rho_l(w_k-w_l)^2}. \tag{5.23}$$

Because we have symmetrized the expressions in k and l, and the terms with $k = l$ are zero, one can just as well sum only over $l > k$ and remove the factors $\frac{1}{2}$ in (5.20) and (5.22).

The S_{kl} are the individual entropy (or isocurvature) perturbations [85, 93, 54]. They are antisymmetric in k and l, and in addition one has $S_{kl} = S_{km} - S_{lm}$. This means that S_{kl} contains $N-1$ independent components. One can take a single reference component 0 and define $S_k \equiv S_{k0}$, so that $S_{kl} = S_k - S_l$, with of course $S_0 = 0$. Hence if we have a system of N components, there are in general 1 adiabatic and $N-1$ entropy perturbations. The combination $\tilde{S}$ of these $N-1$ entropy perturbations that enters as the source term into the equation for Φ is what we call the total entropy perturbation. In the case of a two-component system the total entropy perturbation is simply the only entropy perturbation. For example, in the case of inflation with N fields the adiabatic perturbation corresponds with the e_1 direction in our basis, while the perturbations in the $N-1$ other directions are isocurvature perturbations. The total entropy perturbation that enters as the source term for the adiabatic perturbation corresponds exactly with the e_2 direction in our basis, see for example (4.30) (an exact derivation can be found in section 5.3). In the literature (e.g. [103]) one often sees the statement that the adiabatic perturbation corresponds with a perturbation in the total energy density, while the entropy perturbations are relative fluctuations of the energy densities of the various components that leave the total energy density constant. However, since energy density perturbations are gauge-dependent quantities, this is a gauge-dependent statement, which is valid in the total comoving gauge (this gauge has $B = 0$ in (4.2), as well as a zero velocity perturbation in the matter). Since we use only the longitudinal gauge, this does not apply here. (Contrary to the adiabatic perturbation, the entropy perturbations S_{kl} are gauge-invariant by definition in the absence of interactions. This can be seen from the behaviour $\delta\rho_k \to \delta\rho_k - \rho_k'\xi^0$ under the coordinate transformation (4.3), see [85], in combination with equation (5.18) for ρ_k'.)

Working out (5.23) in the case of an arbitrary number of matter components (e.g. baryons or cold dark matter with $w = 0$) and an arbitrary number of radiation components

(e.g. photons or hot dark matter with $w = 1/3$) we obtain

$$\tilde{S} = \frac{\sum_{\mathrm{m,r}} \rho_{\mathrm{m}} \rho_{\mathrm{r}} S_{\mathrm{mr}}}{\sum_{\mathrm{m,r}} \rho_{\mathrm{m}} \rho_{\mathrm{r}}} = \frac{\sum_{\mathrm{m}} \rho_{\mathrm{m}} S_{\mathrm{m}}}{\sum_{\mathrm{m}} \rho_{\mathrm{m}}} - \frac{\sum_{\mathrm{r}} \rho_{\mathrm{r}} S_{\mathrm{r}}}{\sum_{\mathrm{r}} \rho_{\mathrm{r}}}, \tag{5.24}$$

where m denotes matter components and r radiation components. In the last step we have singled out one of the radiation components, for example the photons γ, as the reference component, so that $S_{\mathrm{m}} = S_{\mathrm{m}\gamma}$ and $S_{\mathrm{r}} = S_{\mathrm{r}\gamma}$. (One could just as well choose one of the matter components as reference. The only difference with (5.24) is then an overall minus sign.) The first expression of (5.24) has the form of a statistical average of the quantities S_{mr} over the normalized distribution $\rho_{\mathrm{m}}\rho_{\mathrm{r}}$. To be more general one can also consider a quintessence component with $-1 < w_Q < 0$, but the resulting expression is rather complicated. Note however, that a pure cosmological constant ($w = -1$) does not contribute to the numerator of $\tilde{S}$ (see (5.23)) and only adds some weight to the denominator, which should be negligible at recombination and before as the cosmological constant becomes important only at the present epoch ($\rho_\Lambda \ll \rho_{\mathrm{r}}, \rho_{\mathrm{m}}$ at recombination and before).

In the case of a simple two-component system consisting of photons γ and one cold dark matter component C, which is the case usually considered in inflationary literature (see e.g. [158, 103, 54, 12]), this result simplifies to

$$\tilde{S} = S_C = \frac{\delta\rho_C}{\rho_C} - \frac{3}{4}\frac{\delta\rho_\gamma}{\rho_\gamma}. \tag{5.25}$$

For photons the entropy density s is proportional to T^3, while the energy density is proportional to T^4. Hence $\delta s_\gamma/s_\gamma = 3/4\,\delta\rho_\gamma/\rho_\gamma$. On the other hand, since the mass of the cold dark matter particles is constant, their number density contrast and energy density contrast are equal: $\delta n_C/n_C = \delta\rho_C/\rho_C$. This means that S_C can also be written as the fluctuations in the entropy per matter particle: $S_C = \delta(s_\gamma/n_C)/(s_\gamma/n_C)$, so that it indeed represents an entropy perturbation as its name suggests.

Finally we derive an expression for the time derivative of $\tilde{S}$. First we need an equation of motion for $\delta\rho_i$. This equation can be derived by working out the condition $D_\mu T^\mu_0 = 0$ to first order in the perturbations. However, as we are only interested in the super-horizon modes, it is simpler to use the method of varying the background equation, which was derived in the context of inflation in §4.4.2, but is valid more generally. From (5.18), with the two assumptions of ideal fluids without interactions, we then find

$$\delta\rho_i' + 3\mathcal{H}\delta\rho_i(1+w_i) - 3\Phi'\rho_i(1+w_i) = 0, \tag{5.26}$$

using $\delta\mathcal{H} = (\delta \ln a)' = -\Phi'$. This equation can also be found in [85]. From this result together with (5.18) we easily derive that

$$S_{kl}' = \frac{\delta\rho_k}{\rho_k(1+w_k)}\left(\frac{\delta\rho_k'}{\delta\rho_k} - \frac{\rho_k'}{\rho_k}\right) - (k \leftrightarrow l) = 0. \tag{5.27}$$

When differentiating $\tilde{S}$, given in (5.23), this means that the time dependence is completely determined by the background quantities. We find

$$\begin{aligned}\tilde{S}' &= \frac{3}{4}\mathcal{H}\frac{\sum_{i,j,k,l}[(w_k+w_l)-(w_i+w_j)](w_k-w_l)(w_i-w_j)^2(1+w_k)(1+w_l)\rho_i\rho_j\rho_k\rho_l S_{kl}}{\left(\sum_{i,j}(w_i-w_j)^2\rho_i\rho_j\right)^2} \\ &= \frac{3}{4}\mathcal{H}\frac{\sum_{i,j,k} w_i(w_i-w_j)[w_k^2-w_iw_k+w_iw_j]\rho_i\rho_j\delta\rho_k}{(1+w)(w-c_s^2)^2\rho^3}. \end{aligned} \tag{5.28}$$

The second form of the result comes about after inserting the definition of S_{kl} (5.21), substantial index manipulation in the numerator and using (5.22) in the denominator. It is more compact, but in some ways the first expression is more useful. From the first expression we can see immediately that $\tilde{S}'$ will be zero in the case of components with only two different values of w_i (one cannot make all three of $[(w_k+w_l)-(w_i+w_j)]$, (w_i-w_j) and (w_k-w_l) unequal to zero in that case). Hence we can draw the important conclusion that in a universe consisting only of matter and radiation components $\tilde{S}$ remains constant on super-horizon scales, irrespective of how many kinds of matter and radiation there are (provided that the two assumptions of constant w_i and no interactions are valid). This includes a universe with an arbitrary number of hot and cold dark matter components. Only if we have quintessence as well, $\tilde{S}'$ is no longer zero. However, as such a quintessence or cosmological constant component only seems to become important at the present time, it is expected to have been completely negligible at recombination and before. It will be interesting to check this conjecture by working out the time dependence of $\tilde{S}$ in the presence of quintessence.

5.3 Spectral amplitudes and indices from inflation

Having determined the evolution of Φ and $\tilde{S}$ after inflation during the radiation and matter-dominated eras in section 5.2 we can now compute the correlators of these quantities at the time of recombination. We define the quantities $|\delta_{\mathbf{k}}^X|^2$, with X denoting adiabatic, isocurvature, mixing, or tensor, as

$$\begin{aligned}|\delta_{\mathbf{k}}^{\mathrm{ad}}|^2 = \frac{2k^3}{9\pi^2}\langle\hat{\Phi}^2_{\mathbf{k}\,\mathrm{ad}}\rangle_{t_{\mathrm{rec}}}, \qquad |\delta_{\mathbf{k}}^{\mathrm{iso}}|^2 = \frac{2k^3}{9\pi^2}\langle\hat{\Phi}^2_{\mathbf{k}\,\mathrm{iso}}\rangle_{t_{\mathrm{rec}}}, \qquad |\delta_{\mathbf{k}}^{\mathrm{tens}}|^2 = \frac{2k^3}{9\pi^2}\langle\hat{h}_{ij\,\mathbf{k}}\hat{h}^{ij}_{\mathbf{k}}\rangle_{t_{\mathrm{rec}}}, \\ |\delta_{\mathbf{k}}^{\mathrm{mix}}|^2 = \frac{2k^3}{9\pi^2}\left(\langle\hat{\Phi}_{\mathbf{k}\,\mathrm{iso}}\hat{\Phi}_{\mathbf{k}\,\mathrm{ad}}\rangle_{t_{\mathrm{rec}}} + \langle\hat{\Phi}_{\mathbf{k}\,\mathrm{ad}}\hat{\Phi}_{\mathbf{k}\,\mathrm{iso}}\rangle_{t_{\mathrm{rec}}}\right).\end{aligned} \tag{5.29}$$

In section 5.4 the exact link between these correlators and the observational quantities C_l is derived, and then the reason for choosing these specific combinations will become clear. Unfortunately there are different conventions in the literature regarding the normalization factor. The normalization used here corresponds with [108, 28], so that the fitting formulae provided there can be used immediately. The normalization factor in [133], which was used in the table with numerical values in our paper [60] as well, is 9/4 times larger.

If $|\delta_{\mathbf{k}}^X|^2$ depends only weakly on k, we can make the following approximation:

$$|\delta_{\mathbf{k}}^X|^2 = |\delta_{\mathbf{k}_0}^X|^2\left(\frac{k}{k_0}\right)^{n_X-1} \tag{5.30}$$

with k_0 a certain reference scale, which in explicit calculations we take to be the scale corresponding with the present horizon, which crossed the horizon (or Hubble scale) during inflation about 60 e-folds before the end of inflation. $|\delta^X_{\mathbf{k}_0}|^2$ and n_X are two constants, called the amplitude of the spectrum and the spectral index respectively. This approximation holds good over a wide range of k if $n_X - 1$ is close to zero. As we will find below, this turns out to be the case for slow-roll inflation. The above expression (5.30) is the correct definition for the scalar perturbations. For historical reasons one writes n_{tens} instead of $n_{\text{tens}} - 1$ in the exponent for the tensor perturbations. This is a rather unfortunate source of confusion, but since it is the standard definition used in the literature we adopt it here as well.

The rest of this section is devoted to the calculation of these amplitudes and spectral indices. As defined in §5.2.1, the adiabatic perturbation is the homogeneous solution for Φ with the initial condition that the particular solution is zero and has zero derivative at the beginning of the radiation-dominated era. Hence we have to match the homogeneous part of (5.15) to the complete solution (4.75) at the end of reheating. Of course (4.75) was given as the solution at the end of inflation, but the $A(t_{\mathcal{H}}, t)$ part also remains valid for super-horizon modes during (p)reheating (for this homogeneous part of the solution no assumptions about the background were necessary), while the $\tilde{U}^T_P(t)$ part remains valid as long as there is only scalar matter. However, in the following we will ignore the presence of (p)reheating, and make the approximation of an immediate transition to a radiation-dominated universe at the end of inflation. Especially for the isocurvature perturbations this is a crude approximation (see below), which should certainly be improved upon, but the treatment of the perturbations during a more realistic transition at the end of inflation as well as during an epoch of (p)reheating is still under investigation and beyond the scope of this thesis.[1]

Demanding continuity and continuous differentiability at the end of inflation for Φ, given by (4.75) before the matching and by the homogeneous part of (5.15) after the matching, we find expressions for $\tilde{C}$ and $\tilde{D}$. The term with $\tilde{C}$ rapidly decays, so that we are only interested in the expression for $\tilde{D}$. The result, valid at later times when the decaying terms have disappeared, is

$$\hat{\Phi}_{\mathbf{k}\,\text{ad}}(t) = \frac{\kappa}{2k^{3/2}} \frac{H_{\mathcal{H}}}{\sqrt{\tilde{\epsilon}_{\mathcal{H}}}} A(t_e, t) \left(e^T_1 + U^T_{P\,e}\right) E_{\mathcal{H}} \hat{a}^\dagger_{\mathbf{k}} + \text{c.c.} \tag{5.31}$$

The function A and vector $U_{P\,e} = U_P(t_e)$ are defined in (4.76). Some interesting simplifications occurred: the $A(t_{\mathcal{H}}, t_e)$ terms dropped out during the calculation, and the double integral expression $\tilde{U}_P$ has been replaced by the single integral expression U_P.

Just as for the adiabatic contribution we can compute the correlator for the isocurvature contribution and for the mixing between them. Under the assumption that $\tilde{S}$ is constant (see §5.2.2 for a discussion), the isocurvature part of the gravitational potential is given by (5.17), which at recombination simplifies to $\Phi_{\text{iso}} = -\frac{1}{5}\tilde{S}$. As we are assuming an immediate transition to a radiation-dominated universe at the end of inflation, we set $\tilde{S}(\text{after inflation}) = \tilde{S}(\text{end of inflation})$. During inflation $\tilde{S}$ can be computed from its definition in (5.9), $\tilde{S} = \frac{1}{4}(\delta p - c_s^2 \delta\rho)/(p - c_s^2\rho)$. The density and pressure (perturbations), being components of the (perturbed) energy-momentum tensor as defined in (5.9), can

[1] Some study on the effects of preheating on the scalar perturbations has been done for specific models, see [14, 199, 43, 129, 68, 196] and references therein, but different authors do not yet agree regarding the conclusions.

easily be determined during inflation from (3.8) (cf. (2.27)) and (4.8):

$$\rho = \frac{1}{2}|\dot{\boldsymbol{\phi}}|^2 + V = \frac{3H^2}{\kappa^2}, \qquad p = \frac{1}{2}|\dot{\boldsymbol{\phi}}|^2 - V = -\frac{3H^2}{\kappa^2}\left(1 - \frac{2}{3}\tilde{\epsilon}\right),$$
$$w = \frac{p}{\rho} = -1 + \frac{2}{3}\tilde{\epsilon}, \qquad c_s^2 = \frac{\dot{p}}{\dot{\rho}} = -1 - \frac{2}{3}\tilde{\eta}^{\parallel}, \tag{5.32}$$

$$\begin{aligned}\delta\rho &= \dot{\boldsymbol{\phi}}\cdot\mathcal{D}_t\boldsymbol{\delta\phi} - |\dot{\boldsymbol{\phi}}|^2\Phi + \mathbf{G}^{-1}\boldsymbol{\nabla}^T V\cdot\boldsymbol{\delta\phi}\\ &= \frac{H|\dot{\boldsymbol{\phi}}|}{a}\left[\frac{1}{H}\mathbf{e}_1\cdot\mathcal{D}_t\mathbf{q} - \tilde{\boldsymbol{\eta}}\cdot\mathbf{q} - 4\mathbf{e}_1\cdot\mathbf{q}\right] - \frac{|\dot{\boldsymbol{\phi}}|^2}{H}\left(\dot{\Phi} + H(-2+\tilde{\epsilon})\Phi\right), \qquad (5.33)\\ \delta p &= \dot{\boldsymbol{\phi}}\cdot\mathcal{D}_t\boldsymbol{\delta\phi} - |\dot{\boldsymbol{\phi}}|^2\Phi - \mathbf{G}^{-1}\boldsymbol{\nabla}^T V\cdot\boldsymbol{\delta\phi}\\ &= \frac{H|\dot{\boldsymbol{\phi}}|}{a}\left[\frac{1}{H}\mathbf{e}_1\cdot\mathcal{D}_t\mathbf{q} + \tilde{\boldsymbol{\eta}}\cdot\mathbf{q} + 2\mathbf{e}_1\cdot\mathbf{q}\right] - \frac{|\dot{\boldsymbol{\phi}}|^2}{H}\left(\dot{\Phi} + H(4+\tilde{\epsilon}+2\tilde{\eta}^{\parallel})\Phi\right). \qquad (5.34)\end{aligned}$$

To rewrite $\delta\rho$ and δp we used the background equation of motion (3.12) and the definitions of $\mathbf{q}$ (4.21) and the slow-roll functions (3.17). Working out $\delta p - c_s^2\delta\rho$ we find

$$\begin{aligned}\delta p - c_s^2\delta\rho &= \frac{H^2\sqrt{2\tilde{\epsilon}}}{\kappa a}\left[\left(2+\frac{2}{3}\tilde{\eta}^{\parallel}\right)\frac{1}{H}\mathbf{e}_1\cdot\mathcal{D}_t\mathbf{q} - \frac{2}{3}\tilde{\eta}^{\parallel}\tilde{\eta}^{\perp}q_2 - \left(2+\frac{8}{3}\tilde{\eta}^{\parallel}+\frac{2}{3}(\tilde{\eta}^{\parallel})^2\right)q_1\right]\\ &\quad - 2\left(1+\frac{1}{3}\tilde{\eta}^{\parallel}\right)\frac{|\dot{\boldsymbol{\phi}}|^2}{H}\left(\dot{\Phi} + H(1+\tilde{\epsilon})\Phi\right)\\ &= \frac{2\sqrt{2}}{\kappa}H^2\sqrt{\tilde{\epsilon}}\,\tilde{\eta}^{\perp}\frac{q_2}{a}. \qquad (5.35)\end{aligned}$$

Here we used (4.24) to eliminate Φ and the relation

$$\mathbf{e}_1\cdot\mathcal{D}_t\mathbf{q} = \dot{q}_1 - H\tilde{\eta}^{\perp}q_2 = H\tilde{\eta}^{\perp}q_2 + H(1+\tilde{\epsilon}+\tilde{\eta}^{\parallel})q_1. \tag{5.36}$$

The latter is derived using (3.24) and, to eliminate $\dot{q}_1$, (4.32) (for super-horizon modes the u term in (4.32) can be neglected). The final result for $\tilde{S}$ is:

$$\tilde{S} = \frac{\kappa}{2\sqrt{2}}\frac{\sqrt{\tilde{\epsilon}}}{\tilde{\epsilon}+\tilde{\eta}^{\parallel}}\,\tilde{\eta}^{\perp}\,\frac{q_2}{a}. \tag{5.37}$$

This is not a slow-roll approximated expression; the slow-roll functions are merely shorthand notation. The only approximation made was to consider super-horizon modes. We see that the total entropy perturbation depends only on the q_2 component in our basis during inflation. Although this was to be expected (compare for example (4.20) and (5.8)), it is still an important result. Moreover, $\tilde{S}$ is proportional to $\tilde{\eta}^{\perp}$, indicating once more the key role this slow-roll function plays in determining the importance of multiple-field effects. Note that during inflation $\tilde{S}$ is not a convenient quantity to use, as it becomes singular when $\dot{\tilde{\epsilon}} = 2H\tilde{\epsilon}(\tilde{\epsilon}+\tilde{\eta}^{\parallel})$ is zero. It is only after inflation, when it remains constant (as discussed in §5.2.2), that $\tilde{S}$ becomes very useful.

With the results (5.31) and (5.37) for Φ and $\tilde{S}$ after inflation, as well as (4.95) for h_{ij} (which is independent of time and also valid after inflation), we can now compute the

correlators (5.29) valid up to and including first order in slow roll:

$$|\delta_{\mathbf{k}}^{\rm ad}|^2 = \frac{1}{\alpha_{\rm ad}}\frac{\kappa^2}{50\pi^2}\frac{H_{\mathcal{H}}^2}{\tilde\epsilon_{\mathcal{H}}}\Big[(1-2\tilde\epsilon_{\mathcal{H}})(1+U_{P\,e}^T U_{P\,e}) + 2B\left((2\tilde\epsilon_{\mathcal{H}}+\tilde\eta_{\mathcal{H}}^{\parallel}) + 2\tilde\eta_{\mathcal{H}}^{\perp} e_2^T U_{P\,e} + U_{P\,e}^T \delta_{\mathcal{H}} U_{P\,e}\right)\Big], \tag{5.38}$$

$$|\delta_{\mathbf{k}}^{\rm iso}|^2 = \frac{1}{\alpha_{\rm iso}}\frac{\kappa^2}{50\pi^2}\frac{H_{\mathcal{H}}^2}{\tilde\epsilon_{\mathcal{H}}}\Big[(1-2\tilde\epsilon_{\mathcal{H}})V_e^T V_e + 2B V_e^T \delta_{\mathcal{H}} V_e\Big], \tag{5.39}$$

$$|\delta_{\mathbf{k}}^{\rm mix}|^2 = \frac{1}{\alpha_{\rm mix}}\frac{\kappa^2}{50\pi^2}\frac{H_{\mathcal{H}}^2}{\tilde\epsilon_{\mathcal{H}}}\Big[(1-2\tilde\epsilon_{\mathcal{H}})V_e^T U_{P\,e} + 2B\left(\tilde\eta_{\mathcal{H}}^{\perp} e_2^T V_e + V_e^T \delta_{\mathcal{H}} U_{P\,e}\right)\Big], \tag{5.40}$$

$$|\delta_{\mathbf{k}}^{\rm tens}|^2 = \frac{8\kappa^2}{9\pi^2} H_{\mathcal{H}}^2 \left(1+2(B-1)\tilde\epsilon_{\mathcal{H}}\right). \tag{5.41}$$

Several ingredients went into this computation. The calculation of the expectation values was performed using (4.45). The definition of $E_{\mathcal{H}}$ is given in (4.71), the one for $\delta_{\mathcal{H}}$ in (4.60), and the expression for $\tilde M^2 e_1$ in (4.27). The vector V_e is defined as[2]

$$V_e^T = \sqrt{\tilde\epsilon_{\mathcal{H}}}\,\frac{\sqrt{\tilde\epsilon_e}\,\tilde\eta_e^{\perp}}{\tilde\epsilon_e+\tilde\eta_e^{\parallel}}\frac{a_{\mathcal{H}}}{a_e}\, e_2^T Q_e Q_{\mathcal{H}}^{-1}. \tag{5.42}$$

From (4.45) we find that, apart from the scalar factors in front, the adiabatic, isocurvature and mixing amplitudes are given by the expressions $(e_1+U_{P\,e})^T E_{\mathcal{H}}^2 (e_1+U_{P\,e})$, $V_e^T E_{\mathcal{H}}^2 V_e$ and $2V_e^T E_{\mathcal{H}}^2(e_1+U_{P\,e})$. As mentioned above (5.16), $A(t_e,t_{\rm rec})=3/5$. We have defined the constants B and α_X as

$$B = 2-\gamma-\ln 2 \approx 0.7296, \qquad \alpha_{\rm ad}=1, \qquad \alpha_{\rm iso}=36, \qquad \alpha_{\rm mix}=6, \tag{5.43}$$

where γ is the Euler constant. Furthermore, we used the fact that the quantities $U_{P\,e}$ and V_e have no components in the e_1 direction since $(a_{\mathcal{H}}/a)(QQ_{\mathcal{H}}^{-1})_{21}=0$, see the text below (4.63). We assume V_e to be of order 1 at most, otherwise other terms have to be included in the correlators to give the complete results to first order in slow roll.

The spectral indices n_X can be calculated from the expressions for $|\delta_{\mathbf{k}}^X|^2$ above:

$$n_X - 1 = \left.\frac{\partial \ln|\delta_{\mathbf{k}}^X|^2}{\partial \ln k}\right|_{\mathbf{k}=\mathbf{k}_0} = \frac{\partial \ln|\delta_{\mathbf{k}}^X|^2}{\partial t_{\mathcal{H}}}\frac{\partial t_{\mathcal{H}}}{\partial \ln k} = \frac{\partial \ln|\delta_{\mathbf{k}}^X|^2}{\partial t_{\mathcal{H}}}\frac{1}{H_{\mathcal{H}}(1-\tilde\epsilon_{\mathcal{H}})}. \tag{5.44}$$

Here we omitted the explicit $\mathbf{k}=\mathbf{k}_0$ from the last two steps, but of course it should be applied there as well. In the last step we used $\partial t_{\mathcal{H}}/\partial\ln k = (\partial \ln k/\partial t_{\mathcal{H}})^{-1}$ and $\mathcal{H}_{\mathcal{H}}=k$. For the tensor perturbations the left-hand side of the equation should read $n_{\rm tens}$ instead of $n_{\rm tens}-1$. To work out this expression we need the derivatives of $U_{P\,e}$ and V_e with respect to $t_{\mathcal{H}}$:

$$\begin{aligned}\frac{\partial U_{P\,e}^T}{\partial t_{\mathcal{H}}} &= \frac{1}{2}\frac{\dot{\tilde\epsilon}_{\mathcal{H}}}{\tilde\epsilon_{\mathcal{H}}}U_{P\,e}^T - 2H_{\mathcal{H}}\tilde\eta_{\mathcal{H}}^{\perp} e_2^T + \frac{\dot a_{\mathcal{H}}}{a_{\mathcal{H}}}U_{P\,e}^T + U_{P\,e}^T Q_{\mathcal{H}}(Q_{\mathcal{H}}^{-1})^{\bullet}\\ &= H_{\mathcal{H}} U_{P\,e}^T\left(2\tilde\epsilon_{\mathcal{H}}+\tilde\eta_{\mathcal{H}}^{\parallel}-\delta_{\mathcal{H}}\right) - 2H_{\mathcal{H}}\tilde\eta_{\mathcal{H}}^{\perp} e_2^T,\end{aligned} \tag{5.45}$$

$$\frac{\partial V_e^T}{\partial t_{\mathcal{H}}} = H_{\mathcal{H}} V_e^T\left(2\tilde\epsilon_{\mathcal{H}}+\tilde\eta_{\mathcal{H}}^{\parallel}-\delta_{\mathcal{H}}\right). \tag{5.46}$$

[2]To show the similarities between the correlators more clearly, we have removed a factor $\frac{1}{2}$ compared with our original definition in [60].

Here we used $(Q_{\mathcal{H}}^{-1})^{\bullet} = -Q_{\mathcal{H}}^{-1}\dot{Q}_{\mathcal{H}}Q_{\mathcal{H}}^{-1}$ and $\dot{Q}_{\mathcal{H}} = H_{\mathcal{H}}(1 - \tilde{\epsilon}_{\mathcal{H}} + \delta_{\mathcal{H}})Q_{\mathcal{H}}$, which can be derived from (4.70). The final results to first order in slow roll are:

$$n_{\rm ad} - 1 = -4\tilde{\epsilon}_{\mathcal{H}} - 2\tilde{\eta}_{\mathcal{H}}^{\parallel} + \frac{2U_{P\,e}^T(2\tilde{\epsilon}_{\mathcal{H}} + \tilde{\eta}_{\mathcal{H}}^{\parallel} - \delta_{\mathcal{H}})U_{P\,e} - 4\tilde{\eta}_{\mathcal{H}}^{\perp}e_2^T U_{P\,e}}{1 + U_{P\,e}^T U_{P\,e}}, \tag{5.47}$$

$$n_{\rm iso} - 1 = -2\,\frac{V_e^T\delta_{\mathcal{H}}V_e}{V_e^T V_e}, \tag{5.48}$$

$$n_{\rm mix} - 1 = -2\,\frac{V_e^T\delta_{\mathcal{H}}U_{P\,e} + \tilde{\eta}_{\mathcal{H}}^{\perp}e_2^T V_e}{V_e^T U_{P\,e}}, \tag{5.49}$$

$$n_{\rm tens} = -2\tilde{\epsilon}_{\mathcal{H}} + \Big[-2\tilde{\epsilon}_{\mathcal{H}}^2 + 4(B-1)\tilde{\epsilon}_{\mathcal{H}}(\tilde{\epsilon}_{\mathcal{H}} + \tilde{\eta}_{\mathcal{H}}^{\parallel})\Big]. \tag{5.50}$$

For the tensor spectral index we have added the second-order slow-roll terms between the square brackets. For the other spectral indices the second-order terms can also be determined, but we have omitted those expressions here as they are very long and do not change the conclusions below (because the spectral indices are proportional to the slow-roll derivatives of the amplitudes, one automatically finds results of one order higher in slow roll). We see that the $n_X - 1$ contain only slow-roll terms, and thus the $|\delta_{\mathbf{k}}^X|^2$ do indeed depend on k very weakly. In other words, the spectrum predicted by slow-roll inflation is nearly scale-invariant. Of course if $V_e = 0$ there are no isocurvature perturbations and $n_{\rm iso}$ and $n_{\rm mix}$ become meaningless.

The explicit multiple-field terms in the amplitudes and the spectral indices are the contributions of the terms $U_{P\,e}$ and V_e, which are absent in the single-field case (setting them equal to zero we obtain the well-known single-field results, see e.g. [133]). There are no isocurvature and mixing contributions in the single-field case. Since both $U_{P\,e}$ and V_e are to a large extent determined by $\tilde{\eta}^{\perp}$ (see their definitions in (4.76) and (5.42)), we can draw the important conclusion that the behaviour of $\tilde{\eta}^{\perp}$ during the last 60 e-folds of inflation is crucial in order to determine whether multiple-field effects are important. For example, one can immediately see that in assisted inflation [110] — where one quickly goes to an attractor solution with all $\dot{\phi}_i$ equal to each other apart from constant factors, so that $\tilde{\eta}^{\perp} = 0$ — there will be no explicit multiple-field contributions to the gravitational potential.

The fact that the entropy perturbations act as sources for the adiabatic perturbation (the U_P term) naturally leads to correlations between adiabatic and isocurvature perturbations (described by the mixing amplitude), as has been realized before, see [103, 54]. Note that even if $U_{P\,e} = 0$ there is still one other term in the mixing amplitude, although merely of first order in slow roll. Only if $\tilde{\eta}_{\mathcal{H}}^{\perp}$ vanishes as well, the correlations are completely absent. However, at least in the context of slow roll the situation where $U_{P\,e} = 0$ while $\tilde{\eta}_{\mathcal{H}}^{\perp}, V_e \neq 0$ is not possible, because the $e_2^T Q/a$ under the integral in the definition of $U_{P\,e}$ cannot change sign. It would be interesting to see if (p)reheating effects can change this conclusion. Anyhow, if $\tilde{\eta}^{\perp} = 0$ everywhere during the last 60 e-folds, there are certainly no correlations. (The authors of [54] studied the two-field case and found the derivative of the angle that parameterizes the influence of the second field on the background trajectory to be the relevant parameter. In the two-field limit this parameter corresponds with $\tilde{\eta}^{\perp}$, but our result is valid for an arbitrary number of fields.)

Using the concept of slow roll on the perturbations, introduced in §4.4.2, the quantity $U_{P\,e}$ can be rewritten in terms of background quantities only, as was done in (4.77). Because we have used slow roll in the derivation, this expression is in principle not valid

at the very end of inflation. If (4.77) does indeed give a bad approximation for U_{Pe}, for example if $\tilde{\eta}^{\perp}$ grows very large, a more careful treatment of the transition at the end of inflation is necessary. However, in other cases the contribution to the integral near the end of inflation can be negligible, for example if $\tilde{\eta}^{\perp}$ goes sufficiently rapidly to zero. In those cases (4.77) gives a very good approximation for U_{Pe} and the details of the transition are unimportant for the adiabatic amplitude (5.38). An important example of this latter case is discussed in section 6.2. Unfortunately V_e depends very much on the details of the transition at the end of inflation, so that for an accurate calculation a model of this transition has to be assumed, which is beyond the scope of this thesis. However, one can still draw the conclusion that, if $\tilde{\eta}^{\perp}$ goes to zero at the end of inflation, the isocurvature perturbations are expected to be negligible compared with the adiabatic one (neglecting possible amplifying mechanisms during the transition and preheating).

Compared with the scalar amplitudes, an overall factor of $1/\tilde{\epsilon}_{\mathcal{H}}$ is missing in the expression for the tensor amplitude, showing that the tensor contribution to the CMBR from slow-roll inflation will generically be smaller than the scalar one. Defining the tensor to scalar ratio r we find the following relation to leading order:

$$r \equiv \frac{|\delta_{\mathbf{k}}^{\mathrm{tens}}|^2}{|\delta_{\mathbf{k}}^{\mathrm{ad}}|^2} = \frac{400}{9}\frac{\tilde{\epsilon}_{\mathcal{H}}}{1+U_{Pe}^T U_{Pe}} = -\frac{200}{9}\frac{n_{\mathrm{tens}}}{1+U_{Pe}^T U_{Pe}}. \tag{5.51}$$

The last relation is the multiple-field generalization of the single-field result known as the consistency relation [108, 113], and it is a very important result. Note that in the two-field case one can rewrite the factor $(1+U_{Pe}^T U_{Pe})^{-1}$ as $(1-r_{\mathrm{mix}}^2)$, where r_{mix} is defined as $r_{\mathrm{mix}} \equiv |\delta_{\mathbf{k}}^{\mathrm{mix}}|^2/(|\delta_{\mathbf{k}}^{\mathrm{ad}}||\delta_{\mathbf{k}}^{\mathrm{iso}}|)$. In terms of this quantity the above multiple-field consistency relation was also derived in [12]. However, not only is their result restricted to the case of two fields, their derivation is also more complicated. Here we have given a very simple derivation and our result is valid for an arbitrary number of fields without additional assumptions. Once observations have become good enough to determine the tensor amplitude and spectral index independently, this relation is an excellent means to check if multiple-field effects are important or not.[3]

5.4 Linking inflation and the CMBR

In this section the relation between the spectral amplitudes and indices of the previous section and the observations of the temperature fluctuations (in the form of the quantities C_l) is derived. As discussed in §5.1.3, the dominant effect at the largest angular sizes, which are the most important from the point of view of inflation, is the Sachs-Wolfe effect. A derivation of this effect is given in §5.4.1, as well as a treatment of the relation between Fourier modes and spherical harmonics, leading to expressions for the C_l as functions of the scalar spectral amplitudes and indices. Analogous expressions for the tensor perturbations are also given, but for a derivation of these the reader is referred to the literature. §5.4.2 gives the values for the spectral amplitudes and indices (in the form of a so-called fitting function) that have been determined from the observations.

[3] There are two other effects that might lead to corrections to this formula: higher-order slow-roll terms and non-vacuum initial states [81]. However, both of these are expected to be small: higher-order slow-roll terms are small by construction, and deviations from the vacuum initial state should not be too large, otherwise the particle background dominates over the potential energy of the inflaton and there is no (standard) inflation [190]. Hence a large deviation from the single-field result is a clear proof of multiple-field effects being important during the last 60 e-folds of inflation.

5.4.1 The Sachs-Wolfe effect

We start with a derivation of the Sachs-Wolfe effect [167], which is the dominant effect relating the scalar inflationary perturbations to the observed temperature fluctuations in the CMBR. A discussion of the tensor perturbations follows at the end of this subsection. The Sachs-Wolfe effect is a combination of primary effects acting at recombination, causing temperature fluctuations at the largest scales in the CMBR. The relevant primary effects are gravity (gravitational redshift (blueshift) because of gravitational wells (hills)), Doppler (Doppler shift of the photons because of the peculiar velocity distribution of the scattering baryons) and density fluctuations (higher density corresponds with a higher intrinsic temperature). Although the total effect is of course gauge invariant, the specifics of the division of the Sachs-Wolfe effect into these three individual effects, and even the physical interpretation of the terms, depends on the choice of coordinates. A clear discussion of gauge issues in the derivation of the Sachs-Wolfe effect and the danger of Newtonian heuristic arguments is given in [86]. The derivation we give here uses the longitudinal gauge (which was used in chapter 4 as well), and generalizes the usual two-component assumptions to a multi-component system consisting of photons, baryons, an arbitrary number of cold and hot dark matter components, and dark energy (quintessence). Derivations of the Sachs-Wolfe effect in two-component systems in various other gauges can be found in many places, see e.g. [108, 149]. In our derivation we only consider the terms that are important at the largest scales (barring the late ISW effect), i.e. the regular Sachs-Wolfe effect, and work these out for a more general case than is usually considered in inflationary literature. On the other hand, a more complete treatment regarding terms like the ISW and other, sub-dominant, effects can be found in [82], where the gauge issue is carefully treated as well.

We denote the various components with the following subscripts: γ for the photons, m for the baryons, C for cold dark matter (CDM), H for hot dark matter (HDM) and Q for quintessence. (There might be an arbitrary number of cold and hot dark matter components, but for the following derivation this does not matter: ρ_C and ρ_H should just be seen as a sum over the various components in those cases.) Moreover we use the fact that $w_m = w_C = 0$ and $w_\gamma = w_H = 1/3$, while w_Q is a fixed number with $-1 \leq w_Q < 0$. We still assume that there are no interactions. For the dark matter and quintessence components this seems reasonable, while for the photons and the baryons we use the fact that we are considering super-horizon scales. (At smaller scales there are of course interactions between the photons and the baryons, which is precisely the cause of the acoustic peaks in the spectrum.) Using the relations $\rho_\gamma = (\pi^2/15)T^4$ and $\rho_\gamma = \rho_{\gamma,\mathrm{rec}}\,(a/a_{\mathrm{rec}})^{-4}$ we obtain

$$\frac{\delta T}{T} = \frac{1}{4}\frac{\delta\rho_\gamma}{\rho_\gamma} = \frac{1}{4}\frac{\delta\rho_{\gamma,\mathrm{rec}}}{\rho_{\gamma,\mathrm{rec}}} - \frac{\delta a}{a} = \frac{1}{4}\frac{\delta\rho_{\gamma,\mathrm{rec}}}{\rho_{\gamma,\mathrm{rec}}} + \Phi, \tag{5.52}$$

where we used (4.56) in the last step.

To derive an expression for $\delta\rho_{\gamma,\mathrm{rec}}/\rho_{\gamma,\mathrm{rec}}$ we start from the definition of $\tilde{S}$, this time not in terms of the S_{kl}, but the original definition in (5.9). (To simplify the notation, we omit the explicit rec subscripts in the equations.) First we need c_s^2:

$$c_s^2 = \frac{p'}{\rho'} = \frac{1}{\rho}\left(\frac{4}{9}(\rho_\gamma + \rho_H) + w_Q(1+w_Q)\rho_Q\right). \tag{5.53}$$

Here we used that the time dependence of the energy density ρ_i of a component i with an equation of state characterized by w_i is given by $\rho_i(t) \propto a(t)^{-3(1+w_i)}$, which can be derived from (5.18). We also neglected the total pressure p with respect to the total energy density ρ, since at recombination we have matter domination. Using this we find for $\tilde{S}$:

$$\begin{aligned}\tilde{S} &= -\frac{3}{4}\frac{\delta\rho_\gamma + \delta\rho_H + 3w_Q\delta\rho_Q - \frac{4}{3}\left(\rho_\gamma + \rho_H + \frac{9}{4}w_Q(1+w_Q)\rho_Q\right)\delta\rho/\rho}{\rho_\gamma + \rho_H + 9w_Q^2\rho_Q} \\ &= -\frac{3}{4}\frac{\left(\rho_\gamma + \rho_H + \frac{9}{4}w_Q(1+w_Q)\rho_Q\right)(\delta\rho_\gamma/\rho_\gamma - \frac{4}{3}\delta\rho/\rho) + \frac{4}{3}\rho_H S_H + 3w_Q(1+w_Q)\rho_Q S_Q}{\rho_\gamma + \rho_H + 9w_Q^2\rho_Q}.\end{aligned} \tag{5.54}$$

In the last step we have introduced the individual entropy perturbations of HDM and quintessence relative to the photons, $S_H = S_{H\gamma}$ and $S_Q = S_{Q\gamma}$. Taking this as an equation for $\delta\rho_{\gamma,\mathrm{rec}}/\rho_{\gamma,\mathrm{rec}}$ we obtain the final result

$$\frac{\Delta T}{T} = \frac{1}{3}\Phi - \frac{1}{3}\frac{\rho_\gamma + \rho_H + 9w_Q^2\rho_Q}{\rho_\gamma + \rho_H + \frac{9}{4}w_Q(1+w_Q)\rho_Q}\tilde{S} - \frac{1}{3}\frac{\rho_H S_H + \frac{9}{4}w_Q(1+w_Q)\rho_Q S_Q}{\rho_\gamma + \rho_H + \frac{9}{4}w_Q(1+w_Q)\rho_Q}. \tag{5.55}$$

Here we used the relation $\delta\rho/\rho = -2\Phi$ which follows from the (00) components of the perturbed and background Einstein equations (see (B.15) and (5.9)) using the fact that Φ is constant (see (5.16) and (5.17)). To follow conventions we write ΔT instead of δT, but that is just notation.

From (5.55) we can draw the conclusion that, if there is no hot dark matter and no quintessence, but an arbitrary number of cold dark matter components, the temperature fluctuations in the CMBR according to the Sachs-Wolfe effect are given by

$$\frac{\Delta T}{T} = \frac{1}{3}\Phi - \frac{1}{3}\tilde{S}, \tag{5.56}$$

i.e. completely in terms of the gravitational potential and the total entropy perturbation. If hot dark matter and/or quintessence is present the total entropy perturbation $\tilde{S}$ is no longer sufficient to describe the Sachs-Wolfe effect and some of the individual entropy perturbations are needed as well. Remembering that $\Phi = \Phi_{\mathrm{ad}} + \Phi_{\mathrm{iso}}$ and $\Phi_{\mathrm{iso}} = -\frac{1}{5}\tilde{S}$ (see (5.17)), we can also write the previous equation in the following two forms:

$$\frac{\Delta T}{T} = \frac{1}{3}\Phi_{\mathrm{ad}} - \frac{2}{5}\tilde{S} = \frac{1}{3}\Phi_{\mathrm{ad}} + 2\Phi_{\mathrm{iso}}. \tag{5.57}$$

The latter form shows the well-known result that an isocurvature perturbation leads to an anisotropy in the CMBR that is six times bigger than in the adiabatic case, see e.g. [108].

Taking into account the quantum origin of the perturbations the correct way to make the final link between the inflationary perturbations and the temperature fluctuations in the CMBR is by way of the correlators (see e.g. [104]). The calculation of the correlators from inflation in Fourier space was the subject of section 5.3. Here we conclude with a computation to relate such a Fourier quantity to the temperature correlator (5.6) in terms of Legendre polynomials. The remainder of this subsection is based on [108].

The vacuum correlator of a quantity $\hat{f}(\mathbf{x})$ in terms of Fourier modes $\hat{f}_{\mathbf{k}}$ given by (A.10), with $\hat{f}_{\mathbf{k}}$ a quantum operator proportional to the creation operator $\hat{a}^\dagger_{\mathbf{k}}$ and $\hat{f}^*_{\mathbf{k}}$ proportional

to the annihilation operator $\hat{a}_{\mathbf{k}}$, is given by

$$\begin{aligned}\langle\hat{f}(\mathbf{x})\hat{f}(\mathbf{y})\rangle &= \frac{1}{(2\pi)^3}\int \mathrm{d}\mathbf{k}\int \mathrm{d}\mathbf{k}'\left\langle\left(\hat{f}_{\mathbf{k}}e^{-i\mathbf{k}\cdot\mathbf{x}}+\hat{f}^*_{\mathbf{k}}e^{i\mathbf{k}\cdot\mathbf{x}}\right)\left(\hat{f}_{\mathbf{k}'}e^{-i\mathbf{k}'\cdot\mathbf{y}}+\hat{f}^*_{\mathbf{k}'}e^{i\mathbf{k}'\cdot\mathbf{y}}\right)\right\rangle \\ &= \frac{1}{(2\pi)^3}\int \mathrm{d}\mathbf{k}\langle\hat{f}^*_{\mathbf{k}}\hat{f}_{\mathbf{k}}\rangle e^{i\mathbf{k}\cdot(\mathbf{x}-\mathbf{y})}. \end{aligned} \tag{5.58}$$

Of course the quantity we are interested in is the gravitational potential, and the Fourier correlator $\langle\hat{f}^*_{\mathbf{k}}\hat{f}_{\mathbf{k}}\rangle = \langle\hat{\Phi}^2_{\mathbf{k}}\rangle$ with $\hat{\Phi}_{\mathbf{k}}$ given in (4.75). However, to relate this correlator to the C_l that are measured in the CMBR we need to rewrite the exponential in terms of spherical harmonics, using (see e.g. equation [7.78] of [26])

$$e^{i\mathbf{k}\cdot\mathbf{x}} = 4\pi\sum_{l=0}^{\infty}\sum_{m=-l}^{+l} i^l j_l(kx)Y^*_{lm}(\hat{\mathbf{k}})Y_{lm}(\hat{\mathbf{x}}). \tag{5.59}$$

In this expression j_l is a spherical Bessel function. In our case both $\mathbf{x}$ and $\mathbf{y}$ point to the last scattering surface, with $\hat{\mathbf{x}} = \hat{\mathbf{e}}$ and $\hat{\mathbf{y}} = \hat{\mathbf{e}}'$ in terms of the directions defined in (5.4) and $y = x = x_{\mathrm{ls}}$ the comoving distance to the last scattering surface. Inserting this expansion both for $e^{i\mathbf{k}\cdot\mathbf{x}}$ and $e^{-i\mathbf{k}\cdot\mathbf{y}}$, the angular part of the integral can be performed using the orthonormality relations of the $Y_{lm}(\hat{\mathbf{k}})$ (the Fourier correlator only depends on the length of $\mathbf{k}$, not on the angles, as was shown in section 5.3). Using the addition theorem on the remaining spherical harmonics the result is

$$\langle\hat{f}(x_{\mathrm{ls}}\hat{\mathbf{e}})\hat{f}(x_{\mathrm{ls}}\hat{\mathbf{e}}')\rangle = \frac{2}{\pi}\sum_l \frac{2l+1}{4\pi}P_l(\cos\alpha)\int_0^\infty k^2\mathrm{d}k\, j_l^2(kx_{\mathrm{ls}})\langle\hat{f}^*_{\mathbf{k}}\hat{f}_{\mathbf{k}}\rangle. \tag{5.60}$$

Comparison with (5.6) now allows us to determine the C_l: using (5.57) we find

$$C_l^X = \pi\alpha_X\int_0^\infty \frac{\mathrm{d}k}{k} j_l^2(kx_{\mathrm{ls}})|\delta^X_{\mathbf{k}}|^2, \tag{5.61}$$

with X here denoting adiabatic, isocurvature, or mixing. The $|\delta^X_{\mathbf{k}}|^2$ are defined in (5.29) and the α_X in (5.43). Here we assumed that there are only cold dark matter components and no hot dark matter and quintessence ones, so that equation (5.57) is valid. If that is not the case, one has to include additional amplitudes for the S_H and S_Q isocurvature terms and for the corresponding mixing terms. Let us stress that this assumption is only used to simplify the treatment of the isocurvature perturbations; the treatment of the adiabatic perturbation is completely general and independent of it. Using the assumption of weak k dependence (5.30) we can simplify the expression for C_l^X some more [108, 109]:

$$\begin{aligned} C_l^X &= \pi\alpha_X|\delta^X_{\mathbf{k}_0}|^2(k_0x_{\mathrm{ls}})^{1-n_X}\int_0^\infty \mathrm{d}z\, j_l^2(z)z^{n_X-2} \\ &= \frac{\pi^{3/2}}{4}\alpha_X|\delta^X_{\mathbf{k}_0}|^2(k_0x_{\mathrm{ls}})^{1-n_X}\frac{\Gamma(\frac{3}{2}-\frac{n_X}{2})\Gamma(l-\frac{1}{2}+\frac{n_X}{2})}{\Gamma(2-\frac{n_X}{2})\Gamma(l+\frac{5}{2}-\frac{n_X}{2})}. \end{aligned} \tag{5.62}$$

In the case of a scale-invariant spectrum ($n_X = 1$) this simplifies to

$$C_l^X = \frac{2\pi}{l(l+1)}\frac{1}{4}\alpha_X|\delta^X_{\mathbf{k}_0}|^2. \tag{5.63}$$

This is the reason for the normalization factor $l(l+1)/(2\pi)$ in the plots of the power spectrum, see e.g. figure 5.1.

Tensor perturbations enter into the temperature spectrum of the CMBR by their effect on the spacetime through which the photons travel, in a way comparable to the scalar ISW effect. The resulting expression for $\Delta T/T$ was already given in the original paper by Sachs and Wolfe [167] and can also be found in [82]:

$$\frac{\Delta T_{\rm tens}}{T} = -\frac{1}{2}\int_E^O \mathrm{d}y\, h'_{ij}\hat{\mathbf{e}}^i\hat{\mathbf{e}}^j. \tag{5.64}$$

Here $\mathrm{d}/\mathrm{d}y = \partial/\partial\eta - \hat{\mathbf{e}}^i\partial/\partial x^i$, i.e. the integral is along the photon's null-geodesic path, from the emission event E to the observation event O (the unit vector $\hat{\mathbf{e}}$ gives the direction to the last scattering surface, as before).

The relation between the correlator of $\Delta T/T$ in terms of Legendre polynomials (5.6) and the tensor amplitude (5.41) by way of (5.64) is more complicated than the scalar case treated above. This is caused both by the integral in (5.64) and by the fact that tensor spherical harmonics have to be introduced to expand $h_{ij}(\eta,\mathbf{x})$. The calculation was performed in [181]; the result is (see also [133]):

$$C_l^{\rm tens} = \frac{81\pi}{16}|\delta_{\mathbf{k}_0}^{\rm tens}|^2(k_0x_{\rm ls})^{-n_t}(l-1)l(l+1)(l+2)\int_0^\infty \mathrm{d}z\, z^{n_t-1}\left|\int_0^z \mathrm{d}y\,\frac{j_2(y)j_l(z-y)}{y(z-y)^2}\right|^2 \tag{5.65}$$

(where expression (5.30) with $n_X - 1 = n_{\rm tens}$ was used and we wrote n_t instead of $n_{\rm tens}$ for notational simplicity). The integrals in (5.65) can in general not be performed analytically, except in the limit for both large l and $n_t = 0$. In the case of a scale-invariant spectrum ($n_t = 0$) (5.65) can be written as [181]:

$$C_l^{\rm tens} = \frac{\pi}{16}\left(1+\frac{48\pi^2}{385}\right)\frac{c_l}{l(l+1)}\,|\delta_{\mathbf{k}_0}^{\rm tens}|^2, \tag{5.66}$$

where the c_l are constants that have to be determined numerically: $c_2 = 1.118$, $c_3 = 0.878$, $c_4 = 0.819$ and $c_\infty = 1$.

In the (older) literature we often find a definition for the tensor to scalar ratio that is different from the r defined in (5.51) (see e.g. [108, 133]):

$$R_l \equiv \frac{C_l^{\rm tens}}{C_l^{\rm ad}} = \frac{1}{8}\left(1+\frac{48\pi^2}{385}\right)c_l\, r. \tag{5.67}$$

In the last expression scale invariance has been assumed and (5.66) and (5.63) were used. Usually either the limit for large l (R with $c_l = 1$, in practice this is reached for $l \gtrsim 10$) or the quadrupole $l = 2$ (R_2 with $c_l = 1.118$) is employed. The disadvantage of R_l is that its value will deviate from the above pure Sachs-Wolfe expression as soon as additional effects are important, e.g. the late ISW effect, which is especially important for the quadrupole. This is the reason why r is used more in the newer literature. The CMBFAST computer code employed in figure 5.1 works with the quadrupole ratio R_2. The value $R_2 = 0.5$ in that figure corresponds with the large value $r = 1.6$.

5.4.2 Observational values

In this subsection we complete the link between inflation and the observations by specifying the observational values for the amplitudes and indices of the CMBR spectrum, following [28, 109, 57]. The results in these papers are given in terms of a so-called fitting function, which gives the amplitude as defined in (5.29) and (5.30) as a function of certain additional variables. These represent the remaining freedom in the assumptions made to derive the fitting function. As reference scale k_0 the scale of the presently observable universe is chosen.

The basic observational value for the amplitude of the scalar perturbations is given by $|\delta_{\mathbf{k}_0}| = 1.94 \cdot 10^{-5}$, see [109] (this is the square root of the quantity defined in (5.30)). In this result all other degrees of freedom have been set to certain default values: it is derived assuming a flat universe, a scale-invariant inflationary spectrum, the absence of a cosmological constant (no late ISW effect), no gravitational wave contribution and a negligible effect of global reionization. Below a more general expression is given in which some of these constraints are relaxed. Of course it is especially the assumption of no cosmological constant that needs to be changed. The above expression is the sum of adiabatic, isocurvature and mixing terms (in the sense that $|\delta_{\mathbf{k}_0}|^2 = |\delta^{\mathrm{ad}}_{\mathbf{k}_0}|^2 + |\delta^{\mathrm{iso}}_{\mathbf{k}_0}|^2 + |\delta^{\mathrm{mix}}_{\mathbf{k}_0}|^2$), but, as is shown in [41], according to the observations the adiabatic contribution dominates. The 1σ error of the results is estimated at 9% [109].

A more general expression for the observed value of the scalar amplitude, which includes the possibility of a tilted scalar spectrum ($n \neq 1$), a cosmological constant ($\Omega_\Lambda \neq 0$), a tensor contribution ($r > 0$) and a non-negligible global reionization (parameterized by the optical depth for rescattering $\tau > 0$), is given in [28, 57]:[4]

$$|\delta_{\mathbf{k}_0}| = 1.91 \cdot 10^{-5} \, \frac{\exp[1.01(1-n)]}{\sqrt{1 + (0.21 - 0.036\Omega_\Lambda^2)r}} \, (1-\Omega_\Lambda)^{-0.80-0.05\ln(1-\Omega_\Lambda)} \\ \times (1 - 0.18(1-n)\Omega_\Lambda - 0.008 r \Omega_\Lambda) \left(1 + 0.76\tau - 1.96\tau^2 + 1.46\tau^3\right). \tag{5.68}$$

(The fact that (5.68) does not reduce exactly to the value given above in the limit $n = 1$ and $\Omega_\Lambda = r = \tau = 0$ is caused by fitting errors.) In the derivation of this expression the single-field version of the consistency relation (5.51) between r and n_{tens} has been assumed. Since at the moment it is not possible to determine n_{tens} from the observations, this is the simplest assumption. However, it would be interesting to see the changes to the fitting function if this constraint is relaxed, but to our knowledge this has not yet been derived.

The best-fit value for Ω_Λ ($\Omega_\Lambda = 0.7$) can be found in table 1.1. Best-fit values for the other three parameters are given in [201]:

$$n = 0.93^{+0.12}_{-0.09}, \qquad r = 0.0^{+0.5}, \qquad \tau = 0.0^{+0.3}. \tag{5.69}$$

Inserting these preferred values leads to the result

$$|\delta_{\mathbf{k}_0}| = 5.0 \cdot 10^{-5}. \tag{5.70}$$

The main cause of the change from the value of $1.9 \cdot 10^{-5}$ given above is the factor $(1-\Omega_\Lambda)^{-0.8}$, so that the rather large error in Ω_Λ dominates the uncertainty in the result.

[4] The r defined in these papers is given by the Sachs-Wolfe formula for R (i.e. (5.67) for large l), which differs from our definition of r. Hence the numerical changes compared with the formula in [28].

Hence it is meaningless to give more decimals. A maximal tensor to scalar ratio of $r = 0.5$ changes this value to $4.7 \cdot 10^{-5}$.

Unfortunately there is an additional source of inaccuracy when making the final link between inflation and observations. This is the time, usually expressed in terms of the number of e-folds, when the present horizon scale k_0 crossed the Hubble scale during inflation, i.e. the time that has to be used in the evaluation of the slow-roll functions like $\tilde{\epsilon}_{\mathcal{H}}$ in the amplitude and spectral indices of section 5.3. As derived in section 2.2 this is about 60 e-folds before the end of inflation, but the exact number depends (logarithmically) on the temperature after reheating (see [108] for details). Of course the slow-roll functions are supposed to change slowly, so that a slight change in the number of e-folds should not lead to a very big change in the computed amplitude, but for more accurate calculations one must have a complete inflation model, including a reheating phase, to determine this number more precisely. In our treatment of the examples in chapter 6 we will keep working with a general $N_k \equiv N_{\rm end} - N_{\mathcal{H}=k_0}$ as long as possible, and only insert a value of $N_k = 60$ when we want to compute a numerical value. It should be kept in mind that this value can be smaller in the case of a specific model for reheating with a lower reheating temperature (lower than the 10^{15} GeV assumed in section 2.2).

From the relation $k = aH = a_0\, e^N H$ we see that k enters logarithmically into the relation giving the number of e-folds when the scale corresponding with k crossed the Hubble scale during inflation. As derived above (5.3), k is proportional to the multipole l, which means that the scale that reentered the horizon at recombination (with $l \sim 100$) left the horizon about $\ln 100 = 4.6$ e-folds after the scale k_0. The scale corresponding with $l = 2000$, which is the largest l that is expected to be measured by experiments in the near future, left $\ln 2000 = 7.6$ e-folds after k_0. Hence all observable scales crossed the Hubble scale in a relatively small interval during inflation.

5.5 Summary and conclusion

In this chapter we discussed the relation between the inflationary density perturbations of chapter 4 and the observed temperature fluctuations in the cosmic microwave background radiation. The ultimate objective is a complete formalism for the treatment of the super-horizon perturbations during the long period starting right at the end of inflation and ending at recombination. Although this aim will not be attained until a lot of additional research has been performed, this chapter offers a number of interesting results and analyses.

The end result of such a formalism is formed by the spectral amplitudes and indices of the various perturbation components as a function of the inflationary input parameters. We have derived expressions for the scalar adiabatic, isocurvature and mixing amplitudes and spectral indices, as well as for the tensor ones. A number of ingredients and assumptions went into this calculation, which are summarized below. For completeness' sake we have also given an overview of a number of results from the literature regarding the next step, i.e. relating these amplitudes and indices to the real observations. This field of physics of the CMBR and observational data analysis is a separate area of research, which is by now quite well understood, although actual calculations usually require a numerical treatment.

An important ingredient of the calculations was the observation that, although there may be many individual isocurvature perturbations in a multi-component system, only

the total entropy perturbation $\tilde{S}$ enters into the equation of motion for the gravitational potential Φ. With the assumptions that the various components behave as ideal fluids and have no interactions the time derivative of $\tilde{S}$ was worked out. It was found that, if there are only two different types of matter in the universe (i.e. two different equations of state, e.g. baryons and cold dark matter with $p = 0$ and photons and hot dark matter with $p = \frac{1}{3}\rho$), $\tilde{S}$ is simply constant during radiation and matter domination.

The primary temperature fluctuations at the largest angular sizes are not only determined by the gravitational potential, but also by the density perturbations at the time of recombination. It was shown that if there are only baryons, photons and cold dark matter, it is still sufficient to consider only the gravitational potential and the total entropy perturbation. However, if there is also hot dark matter and/or quintessence, it becomes necessary to include the individual entropy perturbations of these components in the calculations.

An important part of the expressions for the scalar spectral amplitudes and indices are the multiple-field effects, written in the form of the vectors $U_{P\,e}$ (adiabatic) and V_e (isocurvature). In all multiple-field terms the slow-roll function $\tilde{\eta}^{\perp}$ plays a key role: if it is negligible during the last 60 e-folds of inflation, multiple-field effects are unimportant. Unfortunately an accurate determination of these vectors, especially V_e, requires a careful analysis of the transition at the end of inflation as well as of the era of (p)reheating. Both are still to be done. However, there is a wide class of models where $\tilde{\eta}^{\perp}$ goes to zero at the end of inflation. Then $U_{P\,e}$ can be determined accurately without knowing the details of the transition and V_e is negligibly small (barring possible amplification mechanisms during preheating), so that isocurvature perturbations are expected to be unimportant. Explicit examples to illustrate the results of this chapter will be treated in chapter 6.

Finally we derived a multiple-field generalization of what is known as the consistency relation in slow-roll inflation: an explicit relation between the ratio of the tensor and scalar adiabatic amplitudes and the tensor spectral index. The resulting expression is valid for an arbitrary number of scalar fields and a possibly non-trivial field metric. Once observations have become good enough to determine the tensor amplitude and spectral index independently, this will allow for a definite measurement to see whether we have multiple-field inflation or (effectively) single-field inflation during the observable part of the inflation era.

The basic formalism developed in this chapter still leaves a lot of room for future research to improve and extend it. Most importantly the formalism will not be complete without a full treatment of the perturbations during the transition at the end of inflation and during the era of (p)reheating. Regarding the total entropy perturbation $\tilde{S}$, it would be interesting to determine its behaviour with time if one (or more) quintessence fields are included, as well as the effects of relaxing the assumptions of ideal fluids and no interactions. Moreover, as discussed above, for a complete picture of the temperature fluctuations the individual hot dark matter and quintessence entropy perturbations should be studied (some work on individual components including interactions has been done in [27]). Finally two subjects we barely touched upon (except to give some references) are polarization and non-Gaussianity. Since polarization is only important for the tensor perturbations, which are unaffected by the complications of multiple-field inflation, this area is already well covered by the present literature. On the other hand, a systematic study of non-Gaussianity from multiple-field inflation might very well lead to interesting new results.

Chapter 6

Inflation models with a quadratic potential

In this chapter inflation models with a quadratic potential are discussed and analyzed thoroughly. This is both to illustrate the general theory of the previous chapters and to check our analytical results numerically. In section 6.1 we consider a quadratic potential where all scalar field components have equal masses, while in section 6.2 we focus on the more complicated case of a quadratic potential with an arbitrary mass matrix. In both these sections we assume a flat field manifold. Section 6.2 is divided into subsections: §6.2.1 and §6.2.2 deal with analytical expressions for the background and the perturbations, respectively, while in §6.2.3 an explicit two-field model is treated numerically. In section 6.3 we generalize to a curved field manifold, deriving some general expressions not restricted to a quadratic potential. Proceeding to the special case of a spherical field manifold we treat examples with a quadratic potential with equal masses in section 6.4. The case of a general mass matrix on a curved field manifold is the subject of section 6.5. The results of this chapter are summarized and discussed in section 6.6. The discussion of the examples in this chapter is based on, but more extensive than, the treatment in my papers [59, 60].

6.1 Flat field manifold and equal masses

We start by considering some models of slow-roll inflation with a quadratic potential and with the scalar fields living on a flat manifold. Since all flat manifolds are locally isomorphic to a subset of $\mathbb{R}^N$, we assume that the N scalar fields live in the $\mathbb{R}^N$ itself and we use the standard basis for $\mathbb{R}^N$. The first-order slow-roll equation of motion and Friedmann equation for the background quantities are given by

$$\dot{\boldsymbol{\phi}} = -\frac{2}{\sqrt{3}\,\kappa}\,\boldsymbol{\partial}^T\sqrt{V(\boldsymbol{\phi})} \quad \Leftrightarrow \quad \boldsymbol{\phi}_{,N} = -\frac{1}{\kappa^2}\boldsymbol{\partial}^T \ln V(\boldsymbol{\phi}), \qquad H = \frac{\kappa}{\sqrt{3}}\sqrt{V(\boldsymbol{\phi})}\left(1+\frac{\tilde{\epsilon}}{6}\right). \tag{6.1}$$

We make use of the hat to indicate a unit vector: $\hat{\boldsymbol{\phi}} \equiv \boldsymbol{\phi}/\phi$, with $\phi \equiv \sqrt{\boldsymbol{\phi}^T\boldsymbol{\phi}}$ the length of the vector $\boldsymbol{\phi}$.

In the example in this section all masses are assumed to be equal to $\kappa^{-1}m$, with m a dimensionless mass parameter, while the next section treats the case of a general mass matrix. With equal masses the mass matrix is proportional to the identity matrix and the potential reads as

$$V(\boldsymbol{\phi}) = \frac{1}{2}\kappa^{-2}m^2\phi^2. \tag{6.2}$$

The slow-roll equation of motion for the background fields simplifies to

$$\dot{\boldsymbol{\phi}} = \dot{\phi}\,\hat{\boldsymbol{\phi}} + \phi\,\dot{\hat{\boldsymbol{\phi}}} = -\sqrt{\frac{2}{3}}\,\frac{m}{\kappa^2}\,\hat{\boldsymbol{\phi}} \qquad \Rightarrow \qquad \dot{\phi} = -\sqrt{\frac{2}{3}}\,\frac{m}{\kappa^2} \quad \text{and} \quad \dot{\hat{\boldsymbol{\phi}}} = 0. \tag{6.3}$$

Here we have used the fact that $\hat{\boldsymbol{\phi}}$ and $\dot{\hat{\boldsymbol{\phi}}}$ are perpendicular, as can be seen by differentiating the relation $\hat{\boldsymbol{\phi}}^T\hat{\boldsymbol{\phi}} = 1$. This means that the direction of $\boldsymbol{\phi}$ is fixed in time; only its magnitude changes. The scalar equation can of course be solved easily, and we obtain

$$\boldsymbol{\phi}(t) = \left(1 - \frac{t}{t_\infty}\right)\boldsymbol{\phi}_0, \qquad\qquad t_\infty = \sqrt{\frac{3}{2}}\frac{\kappa^2\phi_0}{m}, \tag{6.4}$$

where we used the initial condition $\boldsymbol{\phi}(0) = \boldsymbol{\phi}_0$. Here t_∞ is the time when $\boldsymbol{\phi} = 0$ if slow roll would be valid until the end of inflation. Note the similarity to the single-field result (2.42), as expected.

The leading-order expression for the number of e-folds can be computed in two ways: solving the equation of motion for $\boldsymbol{\phi}$ in terms of N and inverting the result, or integrating the leading-order expression for H with respect to t. The latter method is simpler here:

$$H(t) = \frac{m}{\sqrt{6}}\,\phi = \frac{m\phi_0}{\sqrt{6}}\left(1 - \frac{t}{t_\infty}\right), \qquad N(t) = \int_0^t H\mathrm{d}t' = N_\infty\left(1 - \left(1 - \frac{t}{t_\infty}\right)^2\right), \tag{6.5}$$

where $N_\infty = \frac{1}{4}\kappa^2\phi_0^2$ is the slow-roll estimate for the total amount of inflation. This means that

$$\boldsymbol{\phi}(N) = \sqrt{1 - \frac{N}{N_\infty}}\,\boldsymbol{\phi}_0, \qquad\qquad H(N) = \frac{2N_\infty}{t_\infty}\sqrt{1 - \frac{N}{N_\infty}}. \tag{6.6}$$

Next we calculate the slow-roll functions. Since $\boldsymbol{\phi}(t)$ is linear in time to this order in slow roll, $\tilde{\eta}^{\parallel}$ and $\tilde{\eta}^{\perp}$ are zero. Hence

$$\tilde{\epsilon} = \left(H^{-1}\right)^{\bullet} = \frac{1}{2N_\infty}\left(1 - \frac{t}{t_\infty}\right)^{-2} = \frac{1}{2(N_\infty - N)}, \qquad \tilde{\eta}^{\parallel} = 0, \qquad \tilde{\eta}^{\perp} = 0. \tag{6.7}$$

Clearly, $\tilde{\epsilon}$ becomes infinite when $t \to t_\infty$ or $N \to N_\infty$, which is in contradiction with the bound $\tilde{\epsilon} < 3$ derived in section 3.3. But of course slow roll has certainly stopped when

$$t \geq t_1 \equiv t_\infty - \frac{\sqrt{3}\,\kappa}{m} \qquad \Leftrightarrow \qquad N \geq N_1 \equiv N_\infty - \frac{1}{2}, \tag{6.8}$$

because then $\tilde{\epsilon} \geq 1$, so that results obtained from equations valid only within slow roll cannot be trusted. Notice that we do not have a slow-roll period at all if $\phi_0 \leq \sqrt{2}/\kappa$, since then $t_1, N_1 \leq 0$, so that $\tilde{\epsilon}$ is never smaller than 1.

We conclude this section with a calculation of the amplitudes and spectral indices of the CMBR spectrum in this model. Since $\tilde{\eta}^{\perp} = 0$ there are no multiple-fields effects here: $U_{P\,e} = V_e = 0$, so that there are only adiabatic scalar perturbations. Defining $N_k = N_\infty - N_{\mathcal{H}}$ (i.e. N_k is the number of e-folds between the moment when the reference scale k leaves the horizon and the end of inflation) we obtain from (5.38), (5.47), (5.41) and (5.50)

$$|\delta_{\mathbf{k}}^{\rm ad}|^2 = \frac{2}{75\pi^2}\, m^2 N_k^2 \left(1 + \frac{2B - \frac{5}{6}}{N_k}\right), \qquad n_{\rm ad} - 1 = -\frac{2}{N_k},$$
$$|\delta_{\mathbf{k}}^{\rm tens}|^2 = \frac{16}{27\pi^2}\, m^2 N_k \left(1 + \frac{B - \frac{5}{6}}{N_k}\right), \qquad n_{\rm tens} = -\frac{1}{N_k}. \tag{6.9}$$

Here we included the factor $(1 + \tilde{\epsilon}/6)$ in the expression for H to get the first-order result. Hence the spectral indices are completely fixed, while the amplitudes depend on the single parameter m. (As before, B is the constant $2 - \gamma - \ln 2 \approx 0.7296$.) The consistency relation (5.51) is satisfied with $r = 200/(9N_k)$ and we see that in this example there is a relation $n_{\rm ad} - 1 = 2n_{\rm tens}$. Taking $N_k = 60$ we have $r = 0.37$ and m can be determined by fitting to the observations (5.68): $m = 1.5 \cdot 10^{-5}$ in units of the reduced Planck mass κ^{-1}.

6.2 Flat field manifold and general mass matrix

Next we consider a more general symmetric mass matrix $\kappa^{-1}\mathbf{m}$ in the potential,

$$V_2 = \frac{1}{2}\kappa^{-2}\, \boldsymbol{\phi}^T \mathbf{m}^2 \boldsymbol{\phi}. \tag{6.10}$$

The matrix $\mathbf{m}^2$ does not necessarily have to be diagonalized, but because it is symmetric we can always bring it in diagonal form. As a further assumption we take all eigenvalues of $\mathbf{m}^2$ to be positive, otherwise the potential would not be bounded from below. First we derive analytical results for the general case, both for the background (§6.2.1) and for the perturbations (§6.2.2). In §6.2.3 we treat an explicit two-field example numerically in order to illustrate and check our results.

6.2.1 Analytical expressions for the background

With the potential (6.10) the slow-roll equation of motion (6.1) reduces to

$$\boldsymbol{\phi}_{,N} = -\frac{2}{\kappa^2}\, \frac{\mathbf{m}^2 \boldsymbol{\phi}}{\boldsymbol{\phi}^T \mathbf{m}^2 \boldsymbol{\phi}}. \tag{6.11}$$

Independent of the actual number of scalar fields the solution of this vector equation can be written in terms of only one dimensionless scalar function $\psi(N)$ as

$$\boldsymbol{\phi}(N) = e^{-\frac{1}{2}\mathbf{m}^2 \psi(N)} \boldsymbol{\phi}_0. \tag{6.12}$$

Here $\boldsymbol{\phi}_0 = \boldsymbol{\phi}(0)$ is the initial starting point of the field $\boldsymbol{\phi}$, which implies that $\psi(0) = 0$. In other words, we have determined the trajectory that the field $\boldsymbol{\phi}$ follows through field space starting from point $\boldsymbol{\phi}_0$. The function ψ has to satisfy the differential equation

$$\psi_{,N} = \frac{4}{\kappa^2} \frac{1}{\boldsymbol{\phi}_0^T \mathbf{m}^2 e^{-\mathbf{m}^2\psi} \boldsymbol{\phi}_0}, \qquad \psi(0) = 0. \tag{6.13}$$

This means that ψ always increases with time.

An important role in our further analyses is played by the functions F_n, defined by

$$F_n(\psi) = \frac{\boldsymbol{\phi}_0^T \mathbf{m}^{2n} e^{-\mathbf{m}^2\psi} \boldsymbol{\phi}_0}{\phi_0^2}, \tag{6.14}$$

with ϕ_0 the length of $\boldsymbol{\phi}_0$: $\phi_0^2 = \boldsymbol{\phi}_0^T \boldsymbol{\phi}_0$. The functions $F_n(\psi)$ are positive and monotonously decreasing for all ψ, tending to zero in the limit $\psi \to \infty$, because we have assumed that all mass eigenvalues squared are positive. The functions F_n do not depend on the length of $\boldsymbol{\phi}_0$, only on its direction. Next we discuss some additional properties of the functions F_n. The definition of F_n can also be written as

$$F_n = \frac{\boldsymbol{\phi}_0^T e^{-\frac{1}{2}\mathbf{m}^2\psi} \mathbf{m}^{n-p} \mathbf{m}^{n+p} e^{-\frac{1}{2}\mathbf{m}^2\psi} \boldsymbol{\phi}_0}{\phi_0^2}, \tag{6.15}$$

for any integer $-n \leq p \leq n$. Using the Green-Schwarz inequality $(\mathbf{A}^T\mathbf{B})^2 \leq (\mathbf{A}^T\mathbf{A})(\mathbf{B}^T\mathbf{B})$ for arbitrary vectors $\mathbf{A}$ and $\mathbf{B}$ we obtain

$$F_n{}^2 \leq F_{n-p}\, F_{n+p}. \tag{6.16}$$

From the definition of the F_n we also see that

$$\frac{\mathrm{d}}{\mathrm{d}\psi} F_n(\psi) = -F_{n+1}(\psi). \tag{6.17}$$

We can express many important quantities in the functions F_n. The differential equation for ψ can be rewritten as

$$\psi_{,N} = \frac{1}{N_\infty F_1(\psi)}, \qquad \psi(0) = 0. \tag{6.18}$$

Here $N_\infty = \frac{1}{4}\kappa^2\phi_0^2$ as in section 6.1. Inverting this relation, $\partial N/\partial\psi = (\partial\psi/\partial N)^{-1}$, and using (6.17) to integrate we obtain an expression for the number of e-folds as a function of ψ:

$$N(\psi) = N_\infty \left(1 - F_0(\psi)\right). \tag{6.19}$$

Hence we see that N_∞ does indeed have the same interpretation as in section 6.1: the slow-roll estimate for the total amount of inflation. Finally, the leading-order Hubble parameter (6.1) and the slow-roll functions (3.17) can now be written as

$$\begin{aligned} H &= \frac{\sqrt{6N_\infty}}{3\kappa}\sqrt{F_1}, & \tilde{\epsilon} &= \frac{1}{2N_\infty}\frac{F_2}{F_1^2}, \\ \tilde{\eta}^{\parallel} &= -\frac{1}{2N_\infty}\frac{F_3F_1 - F_2^2}{F_2F_1^2}, & \tilde{\eta}^{\perp} &= \frac{1}{2N_\infty}\frac{\sqrt{F_4F_2 - F_3^2}}{F_2F_1}. \end{aligned} \tag{6.20}$$

Using the Green-Schwarz inequality (6.16) we see that $\tilde{\eta}^{\parallel}$ is always negative, while $\tilde{\eta}^{\perp}$ is real, as it should be. Observe that if $\mathbf{m}$ is proportional to the identity, the inequality is saturated and $\tilde{\eta}^{\parallel}$ and $\tilde{\eta}^{\perp}$ are zero, in agreement with the results of section 6.1. Since the functions $F_n(\psi)$ are independent of the length ϕ_0, this dependence enters only through the factor N_∞.

Before going on to discuss estimates for the functions F_n, we need to introduce some additional notation. We define a semi-positive-definite matrix norm:

$$||\mathbf{C}||^2 = \frac{|\mathbf{C}\boldsymbol{\phi}_0|^2}{\phi_0^2}, \tag{6.21}$$

for any arbitrary d by d matrix $\mathbf{C}$ (with d the number of scalar fields). The reason that $||\cdot||$ does not define a regular norm is that $||\mathbf{C}||^2 = 0$ does not imply that $\mathbf{C} = 0$; we can only infer that $\mathbf{C}\boldsymbol{\phi}_0 = 0$. Indeed, if $\mathbf{C}$ has determinant zero and $\boldsymbol{\phi}_0$ is one of $\mathbf{C}$'s zero modes, $\mathbf{C}\boldsymbol{\phi}_0 = 0$ is satisfied without $\mathbf{C}$ being the zero matrix. With this norm the definition of $F_n(\psi)$ can also be written as

$$F_n(\psi) = ||\mathbf{m}^n e^{-\frac{1}{2}\mathbf{m}^2\psi}||^2. \tag{6.22}$$

We order the eigenvalues of $\mathbf{m}^2$ from smallest to largest, $m_1^2 < m_2^2 < \ldots < m_\ell^2$. Here we only look at distinct eigenvalues, so that ℓ is smaller than d if there are degenerate eigenvalues. The projection operator $\mathbf{E}_n$ projects on the eigenspace with eigenvalue m_n^2. These operators are mutually orthogonal and sum to the identity: $\sum_n \mathbf{E}_n = \mathbb{1}$, while the norm satisfies $||\mathbf{E}_n|| \leq 1$.

Above we have been able to write all kinds of important quantities for the slow-roll period in terms of the functions $F_n(\psi)$. Unfortunately these functions are rather complicated as they depend both on an (exponentiated) mass matrix $\mathbf{m}^2$ and on the direction of the initial vector $\boldsymbol{\phi}_0$. However, to get some information about the behaviour of these functions during the last stages of inflation, which are the most important from an observational point of view, we now study the asymptotic behaviour for large ψ. As can be seen from the definition of F_n in (6.14), in the limit $\psi \to \infty$ the smallest mass eigenvalue will start to dominate in the exponential. We denote the smallest eigenvalue by μ, $\mu \equiv |m_1|$, while the ratio of the next-to-smallest and smallest masses squared is called ρ: $\rho \equiv m_2^2/m_1^2 > 1$. Furthermore, the operator $\mathbf{E} \equiv \mathbf{E}_1$ projects on the eigenspace of the smallest eigenvalue,[1] and we define $\chi \equiv ||\mathbf{E}_2||^2/||\mathbf{E}_1||^2$. Using these definitions we find the following asymptotic behaviour for the functions $F_n(\psi)$ in the limit $\psi \to \infty$:

$$F_n \to ||\mathbf{E}||^2\mu^{2n}e^{-\mu^2\psi}\left(1 + \chi\rho^n e^{-(\rho-1)\mu^2\psi}\right) \to ||\mathbf{E}||^2\mu^{2n}e^{-\mu^2\psi}, \tag{6.23}$$

where the first limit contains both leading and next-to-leading-order terms, while the second contains only the leading-order term. Both these asymptotic expressions for F_n are needed to obtain the non-vanishing leading-order behaviour of ratios and differences of ratios of the functions F_n:

$$\frac{F_p}{F_q} \to \mu^{2(p-q)}, \qquad \frac{F_{n+1}}{F_n} - \frac{F_n}{F_{n-1}} \to \mu^2\rho^{n-1}(\rho-1)^2\chi e^{-(\rho-1)\mu^2\psi}. \tag{6.24}$$

Using these expressions we find the asymptotic behaviour for the number of e-folds (6.19),

[1] Here we assume that $||\mathbf{E}_1|| \neq 0$. If $||\mathbf{E}_1||$ is zero, it means that $\boldsymbol{\phi}_0$ has no component in the subspace corresponding with this eigenvalue. As can be seen from the differential equation for this quadratic case (6.11), this means that $\boldsymbol{\phi}$ will never obtain a component in the directions corresponding to this subspace. Hence we remove these directions from the system, consider $\boldsymbol{\phi}$ to be a vector of appropriate, lower dimension, and take m_1^2 to be the smallest remaining eigenvalue, etc.

the Hubble parameter and the slow-roll functions (6.20):

$$N \to N_\infty \left(1 - ||\mathbf{E}||^2 e^{-\mu^2\psi}\right), \qquad H \to \frac{\sqrt{6N_\infty}}{3\kappa}\,\mu||\mathbf{E}||e^{-\frac{1}{2}\mu^2\psi},$$
$$\tilde{\epsilon} \to \frac{1}{2N_\infty||\mathbf{E}||^2}\,e^{\mu^2\psi}, \qquad \tilde{\eta}^{\parallel} \to -\frac{\chi}{2N_\infty||\mathbf{E}||^2}\,\rho(\rho-1)^2 e^{-(\rho-2)\mu^2\psi},$$
$$\tilde{\eta}^{\perp} \to \frac{\sqrt{\chi}}{2N_\infty||\mathbf{E}||^2}\,\rho(\rho-1)e^{-\frac{1}{2}(\rho-3)\mu^2\psi}. \tag{6.25}$$

Note that $\tilde{\eta}^{\parallel}$ goes to zero for $\rho > 2$, while for $\rho < 2$ it diverges. The same holds true for $\tilde{\eta}^{\perp}$, but there the critical value is $\rho = 3$. Since $\rho > 1$ by definition, the slow-roll function $\tilde{\epsilon}$ always grows faster than $\tilde{\eta}^{\parallel}$ and $\tilde{\eta}^{\perp}$ in the limit $\psi \to \infty$.

We can solve the asymptotic expressions above for ψ and $\tilde{\epsilon}$ in terms of N:

$$e^{-\mu^2\psi(N)} = \frac{1}{||\mathbf{E}||^2}\frac{N_\infty - N}{N_\infty}, \qquad \tilde{\epsilon}(N) = \frac{1}{2(N_\infty - N)}. \tag{6.26}$$

The approximation in (6.23) for large ψ, and hence (6.25), is good when

$$e^{-m_2^2\psi} \ll e^{-m_1^2\psi} \qquad \Rightarrow \qquad \left(\frac{1}{||\mathbf{E}||^2}\frac{N_\infty - N}{N_\infty}\right)^{\rho-1} \ll 1, \tag{6.27}$$

that is when $N_\infty \gg N_\infty - N$ and ρ not too close to one. For $N_\infty - N \approx 60$, i.e. when the observationally interesting scales leave the horizon, we find from this approximation that $\tilde{\epsilon} \sim 0.01$.

6.2.2 Analytical expressions for the perturbations

We continue by computing the particular solution $U_{P\,e} = U_P(t_e)$, defined in (4.76). It turns out that in this case we can work out the integral analytically in slow roll, making use of the fact that we have obtained the slow-roll trajectories in (6.12). The velocity and acceleration are given by

$$\dot{\boldsymbol{\phi}} = -\frac{1}{2}\dot{\psi}\,\mathbf{m}^2\boldsymbol{\phi}, \qquad \ddot{\boldsymbol{\phi}} = -\frac{1}{2}\ddot{\psi}\,\mathbf{m}^2\boldsymbol{\phi} + \frac{1}{4}\dot{\psi}^2\,\mathbf{m}^4\boldsymbol{\phi}. \tag{6.28}$$

To derive an expression for the field perturbation we use the fact that for super-horizon modes $\boldsymbol{\delta\phi}$ is given by the variation of the background field $\boldsymbol{\phi}$ generated by a variation in the initial conditions $\boldsymbol{\phi}_0$, see §4.4.2 and especially (4.58). Hence

$$\boldsymbol{\delta\phi} = -\frac{1}{2}\delta\psi\,\mathbf{m}^2\boldsymbol{\phi} + e^{-\frac{1}{2}\mathbf{m}^2\psi}\boldsymbol{\delta\phi}_0, \tag{6.29}$$

where $\delta\psi$ is short-hand notation for $(\boldsymbol{\nabla}_{\boldsymbol{\phi}_0}\psi)\boldsymbol{\delta\phi}_0$. The projector parallel to the velocity is given by $\mathbf{P}^{\parallel} = \mathbf{m}^2\boldsymbol{\phi}\,\boldsymbol{\phi}^T\mathbf{m}^2/(\boldsymbol{\phi}^T\mathbf{m}^4\boldsymbol{\phi})$, and therefore we find that

$$\ddot{\boldsymbol{\phi}}^T\,\mathbf{P}^{\perp}\boldsymbol{\delta\phi} = \frac{1}{4}\dot{\psi}^2\,\boldsymbol{\phi}^T\left[\mathbf{m}^4 - \frac{\boldsymbol{\phi}^T\mathbf{m}^6\boldsymbol{\phi}}{\boldsymbol{\phi}^T\mathbf{m}^4\boldsymbol{\phi}}\mathbf{m}^2\right]e^{-\frac{1}{2}\mathbf{m}^2\psi}\boldsymbol{\delta\phi}_0. \tag{6.30}$$

Here we have used that the first terms of $\ddot{\boldsymbol{\phi}}$ and $\boldsymbol{\delta\phi}$ are proportional to $\dot{\boldsymbol{\phi}}$ and hence are projected away, so that $\delta\psi$ and $\ddot{\psi}$ drop out. We rewrite $U^T_{P\,e}$ in such a way that we can apply this result:

$$U^T_{P\,e} q_{\mathcal{H}} = 2\sqrt{\tilde{\epsilon}_{\mathcal{H}}} \int_{t_{\mathcal{H}}}^{t_e} \mathrm{d}t \, \frac{H}{\sqrt{\tilde{\epsilon}}} \, \tilde{\boldsymbol{\eta}}^T \mathbf{P}^{\perp} a_{\mathcal{H}} \boldsymbol{\delta\phi}. \tag{6.31}$$

Substituting the definition (3.17) for $\tilde{\boldsymbol{\eta}}$ and using (6.20) for $\tilde{\epsilon}$ and (6.28) to determine $|\dot{\boldsymbol{\phi}}|$ the integral takes the form

$$U^T_{P\,e} q_{\mathcal{H}} = \frac{\kappa\sqrt{\tilde{\epsilon}_{\mathcal{H}}}}{\sqrt{2}} \int_{\psi_{\mathcal{H}}}^{\psi_e} \mathrm{d}\psi \, \frac{\boldsymbol{\phi}^T \mathbf{m}^2 \boldsymbol{\phi}}{\boldsymbol{\phi}^T \mathbf{m}^4 \boldsymbol{\phi}} \, \boldsymbol{\phi}^T \mathbf{m}^4 \mathbf{P}^{\perp} e^{-\frac{1}{2}\mathbf{m}^2(\psi - \psi_{\mathcal{H}})} \, a_{\mathcal{H}} \boldsymbol{\delta\phi}_{\mathcal{H}}. \tag{6.32}$$

By writing out the projector $\mathbf{P}^{\perp}$ we can employ

$$\frac{1}{\boldsymbol{\phi}^T \mathbf{m}^4 \boldsymbol{\phi}} \left[\boldsymbol{\phi}^T \mathbf{m}^4 - \frac{\boldsymbol{\phi}^T \mathbf{m}^6 \boldsymbol{\phi}}{\boldsymbol{\phi}^T \mathbf{m}^4 \boldsymbol{\phi}} \boldsymbol{\phi}^T \mathbf{m}^2 \right] e^{-\frac{1}{2}\mathbf{m}^2\psi} = -\frac{\mathrm{d}}{\mathrm{d}\psi} \left[\frac{\boldsymbol{\phi}^T \mathbf{m}^2 e^{-\frac{1}{2}\mathbf{m}^2\psi}}{\boldsymbol{\phi}^T \mathbf{m}^4 \boldsymbol{\phi}} \right] \tag{6.33}$$

to perform an integration by parts to express $U^T_{P\,e}$ as

$$U^T_{P\,e} q_{\mathcal{H}} = \frac{\kappa\sqrt{\tilde{\epsilon}_{\mathcal{H}}}}{\sqrt{2}} \left[\boldsymbol{\phi}^T \mathbf{P}^{\perp} e^{-\frac{1}{2}\mathbf{m}^2(\psi - \psi_{\mathcal{H}})} \right]_{\psi_{\mathcal{H}}}^{\psi_e} a_{\mathcal{H}} \boldsymbol{\delta\phi}_{\mathcal{H}}. \tag{6.34}$$

To determine $a_{\mathcal{H}}\delta\phi_{\mathcal{H}}$ we use the definition of q in (4.21): $q_{\mathcal{H}} = a_{\mathcal{H}}(\delta\phi_{\mathcal{H}} + (\sqrt{2\tilde{\epsilon}_{\mathcal{H}}}/\kappa)\, \Phi_{\mathcal{H}} e_1)$, where we also inserted the definition of $\tilde{\epsilon}$. Using (4.21) and (4.32) to relate $\Phi_{\mathcal{H}}$ to $q_{\mathcal{H}}$ we obtain

$$a_{\mathcal{H}}\delta\phi_{\mathcal{H}} = \left[1 - \tilde{\epsilon}_{\mathcal{H}} \left(2\tilde{\eta}^{\perp}_{\mathcal{H}} e_2 + \left(2\tilde{\epsilon}_{\mathcal{H}} + \tilde{\eta}^{\parallel}_{\mathcal{H}} - \delta_{\mathcal{H}} \right) e_1 \right) e_1^T \right]^T q_{\mathcal{H}}, \tag{6.35}$$

where we made use of the relation $Q'_{\mathcal{H}} = \mathcal{H}_{\mathcal{H}}(1 - \tilde{\epsilon}_{\mathcal{H}} + \delta_{\mathcal{H}}) Q_{\mathcal{H}}$ that follows from (4.70). Hence $a_{\mathcal{H}}\delta\phi_{\mathcal{H}} = q_{\mathcal{H}}$ to first order in slow roll, or equivalently $a_{\mathcal{H}}\boldsymbol{\delta\phi}_{\mathcal{H}} = \mathbf{q}_{\mathcal{H}}$. With this we find our final result for $U^T_{P\,e}$:

$$U^T_{P\,e} = \frac{\kappa\sqrt{\tilde{\epsilon}_{\mathcal{H}}}}{\sqrt{2}} \left(-\phi^{\perp}_{\mathcal{H}} + e^{-\frac{1}{2}\mathbf{m}^2(\psi_e - \psi_{\mathcal{H}})} \phi^{\perp}_e \right)^T. \tag{6.36}$$

Here everything is written in terms of the basis $\{\mathbf{e}_n\}$: $\phi^{\perp}$ denotes the vector with components $\mathbf{e}_n^T \mathbf{P}^{\perp} \boldsymbol{\phi}$. Because of the time dependence of the unit vectors $\mathbf{e}_n$ the definition of the matrix in this formula is not trivial: $\exp(-\frac{1}{2}\mathbf{m}^2(\psi_e - \psi_{\mathcal{H}}))$ denotes the matrix with components $\mathbf{e}_m^T(t_e) \exp(-\frac{1}{2}\mathbf{m}^2(\psi_e - \psi_{\mathcal{H}}))\mathbf{e}_n(t_{\mathcal{H}})$. The second term within the parentheses in the expression for $U^T_{P\,e}$ is in general very small. In the first place all fields except the least massive one have reached zero near the end of inflation, so that $\phi^{\perp}_e$ is small. In the second place this term is suppressed by a large negative exponential, since ψ_e is very large near the end of inflation, even though we may not be able to take the limit of $\psi_e \to \infty$ because slow roll is then no longer valid.

For a complete picture one should also work out the expression for the vector V_e, defined in (5.42) and necessary to compute the isocurvature perturbations. Using the relations (6.28) to (6.30) above, as well as the relation $\tilde{\epsilon} = \frac{1}{2}\kappa^2 |\dot{\boldsymbol{\phi}}|^2 / H^2$, we find

$$V_e^T q_{\mathcal{H}} = \frac{\sqrt{2\tilde{\epsilon}_{\mathcal{H}}}}{\kappa} \frac{\tilde{\epsilon}_e}{\tilde{\epsilon}_e + \tilde{\eta}^{\parallel}_e} \frac{1}{\boldsymbol{\phi}_e^T \mathbf{m}^4 \boldsymbol{\phi}_e} \boldsymbol{\phi}_e^T \mathbf{m}^4 \mathbf{P}^{\perp}_e e^{-\frac{1}{2}\mathbf{m}^2(\psi_e - \psi_{\mathcal{H}})} \mathbf{q}_{\mathcal{H}}. \tag{6.37}$$

However, the problem with this expression is that it must be evaluated at the end of inflation, where slow roll is no longer a valid approximation. Moreover, isocurvature perturbations might well be influenced by the details of (p)reheating. Therefore a careful analysis of the end of inflation and the subsequent epoch of (p)reheating is needed to obtain a reliable expression for the isocurvature and mixing amplitudes and spectral indices. Although under investigation, that is beyond the scope of this thesis. Hence in this chapter we only consider adiabatic scalar perturbations (and tensor perturbations). Note, however, that, if $\tilde{\eta}^\perp$ goes to zero at the end of inflation, which according to (6.25) happens if $m_2^2 > 3m_1^2$, isocurvature perturbations are expected to be unimportant compared with the adiabatic one, since $V_e \propto \tilde{\eta}_e^\perp$.

Assuming a situation where $\tilde{\eta}^\perp$ goes to zero at the end of inflation, i.e. where the second term in the expression (6.36) for U_{Pe} can be neglected, the complete results for $|\delta_{\mathbf{k}}^{\rm ad}|^2$ (5.38) and $n_{\rm ad}$ (5.47) can be given in terms of background quantities evaluated at the time of horizon crossing $t_{\mathcal{H}}$:

$$|\delta_{\mathbf{k}}^{\rm ad}|^2 = \frac{\kappa^2}{50\pi^2}\frac{H_{\mathcal{H}}^2}{\tilde{\epsilon}_{\mathcal{H}}}\Bigg[(1-2\tilde{\epsilon}_{\mathcal{H}})\left(1+\frac{1}{2}\kappa^2\tilde{\epsilon}_{\mathcal{H}}|\phi_{\mathcal{H}}^\perp|^2\right) + 2B\left((2\tilde{\epsilon}_{\mathcal{H}}+\tilde{\eta}_{\mathcal{H}}^{\parallel}) - \kappa\sqrt{2}\,\tilde{\eta}_{\mathcal{H}}^\perp\sqrt{\tilde{\epsilon}_{\mathcal{H}}}\,e_2^T\phi_{\mathcal{H}}^\perp + \frac{1}{2}\kappa^2\tilde{\epsilon}_{\mathcal{H}}(\phi_{\mathcal{H}}^\perp)^T\delta_{\mathcal{H}}\phi_{\mathcal{H}}^\perp\right)\Bigg], \quad (6.38)$$

$$n_{\rm ad}-1 = -4\tilde{\epsilon}_{\mathcal{H}} - 2\tilde{\eta}_{\mathcal{H}}^{\parallel} + \frac{\kappa^2\tilde{\epsilon}_{\mathcal{H}}(\phi_{\mathcal{H}}^\perp)^T(2\tilde{\epsilon}_{\mathcal{H}}+\tilde{\eta}_{\mathcal{H}}^{\parallel}-\delta_{\mathcal{H}})\phi_{\mathcal{H}}^\perp + 2\kappa\sqrt{2\tilde{\epsilon}_{\mathcal{H}}}\,\tilde{\eta}_{\mathcal{H}}^\perp e_2^T\phi_{\mathcal{H}}^\perp}{1+\frac{1}{2}\kappa^2\tilde{\epsilon}_{\mathcal{H}}|\phi_{\mathcal{H}}^\perp|^2}.$$

Using the expressions in (6.20) for H and the slow-roll functions (but multiplying the expression for H with a factor $(1+\tilde{\epsilon}/6)$ to get a first-order result) this can be rewritten in terms of the functions F_n defined in (6.14). Terms containing $\phi_{\mathcal{H}}^\perp$ are rewritten using $\mathbf{P}^\perp = \mathbb{1} - \mathbf{m}^2\boldsymbol{\phi}\,\boldsymbol{\phi}^T\mathbf{m}^2/(\phi_0^2F_2)$ and the definition of the F_n. Note that the $\tilde{M}_{\mathcal{H}}^2$ in the expression (4.60) for $\delta_{\mathcal{H}}$ is simply given by $\tilde{\mathbf{M}}_{\mathcal{H}}^2 = \kappa^{-2}\mathbf{m}^2$ for this potential. The basis vector $\mathbf{e}_2$ is defined in (3.14). The final results are:

$$|\delta_{\mathbf{k}}^{\rm ad}|^2 = \frac{2}{75\pi^2}N_k^2\frac{F_1}{F_0}\left[1+\frac{1}{N_k}\left(B+\left(B-\frac{5}{6}\right)\frac{F_2F_0}{F_1^2}\right)\right], \quad n_{\rm ad}-1 = \frac{-1}{N_k}\left(1+\frac{F_2F_0}{F_1^2}\right),$$
$$|\delta_{\mathbf{k}}^{\rm tens}|^2 = \frac{16}{27\pi^2}N_k\frac{F_1}{F_0}\left(1+\frac{B-\frac{5}{6}}{N_k}\frac{F_2F_0}{F_1^2}\right), \quad n_{\rm tens} = \frac{-1}{N_k}\frac{F_2F_0}{F_1^2}, \quad (6.39)$$

where we also gave the tensor quantities (5.41) and (5.50). The factor F_2F_0/F_1^2 is exactly the multiple-field term $(1+U_{Pe}^TU_{Pe})$. Here all functions F_n must be evaluated at the time of horizon crossing $t_{\mathcal{H}}$. We used relation (6.19) to rewrite $N_\infty F_0 = N_\infty - N_{\mathcal{H}} \equiv N_k$. The leading-order expression for the ratio of tensor and scalar adiabatic perturbations (5.51) is

$$r = \frac{200}{9}\frac{1}{N_k} = -\frac{200}{9}\frac{F_1^2}{F_2F_0}\,n_{\rm tens}. \quad (6.40)$$

In the single-field limit $F_2F_0/F_1^2 \to 1$ and $F_1/F_0 \to m^2$, so that these results then agree with (6.9).

It is interesting to note that where the individual quantities in (6.38) contain different combinations of the F_n's up to F_4, the end results (6.39) only contain the combinations

$N_k F_1/F_0 = \frac{3}{2}\kappa^2 (H^{(0)}_{\mathcal{H}})^2$ and $F_2 F_0/F_1^2 = 2N_k \tilde{\epsilon}_{\mathcal{H}}$. The deviations from the single-field values of these quantities are sufficient to determine whether multiple-field effects are important for the scalar adiabatic and tensor perturbations (given the assumption that $\tilde{\eta}^{\perp}$ goes to zero, so that end-of-inflation contributions to $U_{P\,e}$ can be neglected).[2] It is a nice result that the complicated expressions (5.38) and (5.47) for the adiabatic spectral quantities reduce to the simple expressions (6.39) in the case of a quadratic potential with an arbitrary number of scalar fields.

6.2.3 Numerical example

We now treat a numerical example, not only to illustrate the theory, but also to check our analytical results. We take the situation of two fields, with (diagonalized) masses $m_1 = 1{\cdot}10^{-5}$ and $m_2 = 2.5{\cdot}10^{-5}$ in units of the reduced Planck mass. As initial conditions we choose $\kappa\phi_1 = 20$ and $\kappa\phi_2 = 25$. Then $N_\infty = 256.25$, while an exact numerical calculation gives a total amount of inflation of 257.8 e-folds before the oscillations start. We have chosen the overall normalization of the masses in such a way that we get the correct order of magnitude for the amplitude of the density perturbations. The relative mass ratio is chosen large enough that $\tilde{\eta}^{\perp}$ goes to zero at the end of inflation and contributions to $U_{P\,e}$ at the end of inflation are negligible (this is checked below). Apart from giving sufficient inflation, the specific choice of initial conditions has no special meaning. To solve the exact equation of motion we also need initial conditions for the field velocity, for which we take the values given by the slow-roll solution.

We compare three different sets of results for the adiabatic scalar perturbations:

1. The numerical solutions of the exact equations of motion, without any slow-roll approximations; denoted as the exact solution;

2. The solutions constructed by computing all background quantities numerically from the exact equations, and then inserting them in our analytical slow-roll results for the perturbations (6.38); denoted as the half-slow-roll solution;

3. The analytical slow-roll solutions (6.39), i.e. slow-roll approximated analytical expressions have been used for both background and perturbations (only the function $\psi(N)$ is determined numerically as it cannot be done analytically); denoted as the total-slow-roll solution.

Moreover, the results are divided into a homogeneous part (all terms without $U_{P\,e}$) and a particular part (the rest). Comparing the second and the first sets of results determines the relative error introduced in the results of chapter 4 by the slow-roll approximation used in the transition region and in the calculation of $U_{P\,e}$ in §6.2.2. Only the first source of error is present in the homogeneous part, and it should be of order 0.001 or smaller, as we took care in our treatment of the transition region that our results should be valid to first order in slow roll at the level of the solutions. On the other hand, to derive the third set of results slow roll has been used over the whole epoch of inflation, and integration interval effects, as discussed in section 2.3, may then very well have increased the relative error beyond first order at the level of the solutions (i.e. made it of order 0.01 or larger).

[2] From the relation $F_2 F_0/F_1^2 = 2N_k \tilde{\epsilon}_{\mathcal{H}}$ we see that importance of multiple-field effects corresponds exactly with the situation that the estimate (6.26) for $\tilde{\epsilon}_{\mathcal{H}}$ becomes bad. As this expression was meant only as a rough order of magnitude estimate, there is no problem. See also the plot of $\tilde{\epsilon}(N)$ in figure 6.2(a).

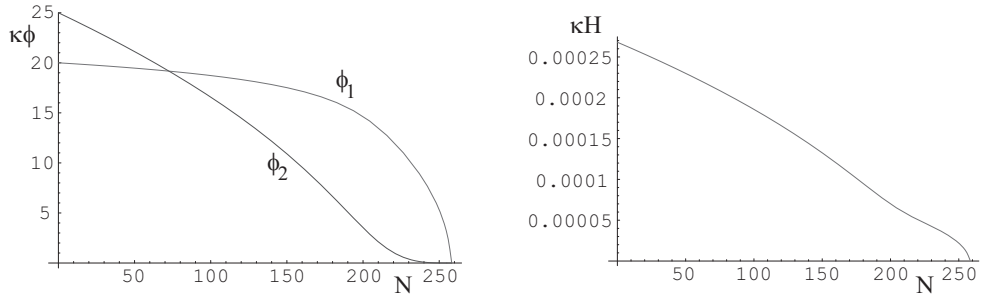

(a) (b)

Figure 6.1: The exact solution for (a) the background fields and (b) the Hubble parameter as a function of the number of e-folds in the model with two fields on a flat manifold with a quadratic potential with masses $m_1 = 1 \cdot 10^{-5}$, $m_2 = 2.5 \cdot 10^{-5}$ in reduced Planck units and initial conditions $\kappa\phi_1 = 20$, $\kappa\phi_2 = 25$.

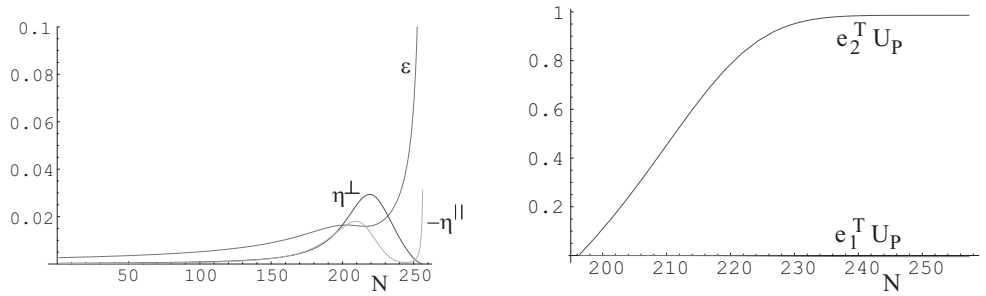

(a) (b)

Figure 6.2: (a) Exact solutions for the slow-roll functions as a function of the number of e-folds in the same model as in figure 6.1. (b) The particular part U_P (4.76) of the solution for the gravitational potential (see (5.31)) as a function of the number of e-folds during the super-horizon region.

In figure 6.1 we have plotted the fields and the Hubble parameter as a function of the number of e-folds. We see that the more massive field goes to zero more quickly than the less massive field, as expected from (6.12). Figure 6.2(a) shows the slow-roll functions as a function of the number of e-folds. Around the time that the second field reaches zero, all slow-roll functions show a bump. For the chosen masses and initial conditions the bumps are located during the last 60 e-folds. As discussed in section 5.3, for multiple-field effects to be important we need $\tilde{\eta}^{\perp}$ to be substantial during the last 60 e-folds. Hence this is a good model to look for multiple-field effects. Moreover, as we see from the figure, $\tilde{\eta}^{\perp}$ goes to zero at the end of inflation, in agreement with the slow-roll prediction (6.25). (For $\tilde{\eta}^{\parallel}$ we see a deviation from the slow-roll result, as it starts growing again at the very end of inflation.) A priori expression (6.36) for U_{Pe} might be a bad approximation because of the break-down of slow roll at the end of inflation, but because of the behaviour of $\tilde{\eta}^{\perp}$ we expect the contribution to U_{Pe} at the end of inflation to be small. Indeed, figure 6.2(b) shows that the contribution to U_{Pe} during the last few e-folds of inflation is negligible, so

	Exact value	Contribution	Error half-SR	Error total-SR
Homogeneous	$6.902 \cdot 10^{-10}$	0.505	0.00008	0.018
Particular	$6.771 \cdot 10^{-10}$	0.495	0.0005	0.030
Total	$1.367 \cdot 10^{-9}$	1	0.0003	0.024

Table 6.1: The scalar adiabatic spectral amplitude $|\delta^{\rm ad}_{\mathbf{k}}|^2$ for the mode k that crossed the horizon 60 e-folds before the end of inflation is separated into a purely homogeneous and a (mixed) particular part. The first two columns give their values and their relative contributions to the total correlator according to the exact numerical solution in the same model as in figure 6.1. The third column shows the relative error between the half-slow-roll solution and the exact one (in the half-slow-roll solution the background is computed numerically from the exact equations and is then inserted into the analytical slow-roll expressions for the perturbations). The final column shows the relative error for the total-slow-roll solution (where analytical slow-roll results are used both for the background and the perturbations) with respect to the exact one.

	Exact value	Contribution	Error half-SR	Error total-SR
Homogeneous	-0.0385	0.787	0.019	0.022
Particular	-0.0104	0.213	0.060	0.113
Total	-0.0489	1	0.002	0.007

Table 6.2: The same as table 6.1, but for the spectral index $n_{\rm ad} - 1$ of the adiabatic scalar perturbations instead of the amplitude. Note that, since $n_{\rm ad} - 1$ has no zeroth-order slow-roll contribution, the relative errors are automatically a slow-roll order of magnitude larger (i.e. about a factor 100).

that (6.36) is a very good approximation in this case.

The results for the amplitude and the spectral index of the scalar adiabatic perturbation spectrum are summarized in tables 6.1 and 6.2. Everything is evaluated for the mode k that crossed the horizon 60 e-folds before the end of inflation. The columns respectively give the exact value of $|\delta^{\rm ad}_{\mathbf{k}}|^2$ and $n_{\rm ad} - 1$, the relative contribution to the total of the homogeneous and particular parts, the relative error of the half-slow-roll solution compared with the exact solution, and the relative error of the total-slow-roll solution compared with the exact one. From the second column we can draw the important conclusion that the particular solution terms are responsible for a considerable part of the total result in this model. Hence neglecting these terms to leading order, which might naively be done because they couple with an $\tilde{\eta}^{\perp}$ in (4.30), can be dangerous.

The results in the third column of the tables agree with our claim that the calculation of the perturbations is valid to first order in slow roll:[3] the relative errors are (much) smaller than $\mathcal{O}(\tilde{\epsilon}_{\mathcal{H}})$. (Note that, as the results for the spectral index $n - 1$ start off with first-order terms instead of zeroth-order terms as is the case for the amplitude, the relative error is automatically larger, and a correction of order $\tilde{\epsilon}_{\mathcal{H}}^{3/2}$ here corresponds with an error of order 0.1.) We also see that our slow-roll approximation for U_{Pe} is indeed very good (since the error in the particular part of the third column is small). The errors of the total-slow-roll solution are larger, since integration interval effects play a role for

[3] In particular this means that the commutator term in (4.67) could indeed be neglected to first order. Explicitly we have $(9/4) \ln \tilde{\epsilon}_{\mathcal{H}} [\delta_{\mathcal{H}}, Z_{\mathcal{H}}]_{11} = -0.0035$ (and comparable or smaller values for the other components), which is of order 3/2.

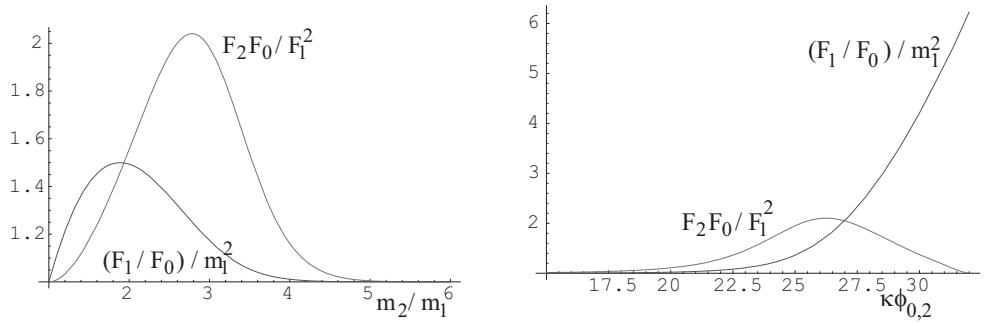

(a) (b)

Figure 6.3: (a) The multiple-field factors F_2F_0/F_1^2 and F_1/F_0 (see (6.39)), evaluated at the horizon-crossing time $t_{\mathcal{H}}$, as a function of the mass ratio m_2/m_1. The model is the same as in figure 6.1, except that m_2 is allowed to vary. The factor F_1/F_0 has been normalized to one by dividing it by its single-field value m_1^2. (b) The same factors, but this time as a function of the initial condition $\phi_{0,2}$. The other initial condition $\phi_{0,1}$ also varies, in such a way that the length of the vector $\boldsymbol{\phi}_0$ remains constant.

the slow-roll background solutions. The numerical calculation of the exact background equations does not last very long (and one has to compute $\psi(N)$ numerically anyway even for the total-slow-roll solution), but the numerical computation of the exact perturbation equations takes a lot of computer time. Hence the half-slow-roll solution (numerical exact background and analytical slow-roll perturbations) seems to be the optimal combination of accuracy and speed.

For (significantly) larger or smaller mass ratios the contribution of the explicit multiple-field terms to the amplitude and spectral index is less important, as can be seen from figure 6.3(a). There we have plotted the two multiple-field factors F_2F_0/F_1^2 and F_1/F_0 (see (6.39)) as a function of the mass ratio m_2/m_1, while keeping the initial conditions and m_1 constant. The factor F_1/F_0 is divided by its single-field value, so that both factors go to one in the limit that multiple-field effects are negligible. The fact that the importance of multiple-field effects is smaller for both larger and smaller mass ratios could also be expected a priori. A much larger mass ratio means that the heavy field has already reached zero before the last 60 e-folds, and the situation is effectively single-field. On the other hand, a much smaller mass ratio means that we approach the limit of equal masses that was treated in section 6.1, which is also effectively single-field. As can be computed from (5.68), the model with the parameters of figure 6.1 does not quite give the correct amplitude of the density perturbations. This can be cured by a slight change of m_1 to $m_1 = 1.2 \cdot 10^{-5}$, keeping all other parameters constant. It is not possible to get the correct amplitude by only changing m_2 (with $m_2/m_1 = 2.5$ one is very near the maximum value that can be obtained by changing only m_2, as can be seen from figure 6.3(a)).

The influence of the direction $\hat{\boldsymbol{\phi}}_0$ of the initial-condition vector on the importance of multiple-field effects is shown in figure 6.3(b). The same two multiple-field factors are plotted, but this time as a function of the initial condition $\phi_{0,2}$. The masses and the length of the vector $\boldsymbol{\phi}_0$ are kept constant, which means that $\phi_{0,1}$ also varies. As expected, multiple-field effects are only important in the middle of the range of values for $\phi_{0,2}$. For a small value of $\phi_{0,2}$ we have effectively single-field inflation with the field ϕ_1. On the other

hand, if $\phi_{0,2}$ is close to ϕ_0 it means that $\phi_{0,1}$ is small: then we have effectively single-field inflation with the field ϕ_2. Note that, since the factor F_1/F_0 has been normalized with m_1^2, it does not go to one in the latter case, but grows to the value $(m_2/m_1)^2$. Instead of changing m_1, another way to make this model fit the observations (5.68) would be to change $(\kappa\phi_{0,1}, \kappa\phi_{0,2})$ to $(17, 27)$, keeping the length ϕ_0 and the masses constant.

The effect of the tensor perturbations can be computed from (6.39) (total-slow-roll solution), or more accurately by inserting the exact expressions for the background quantities into (5.41) and (5.50) (half-slow-roll solution). The latter computation gives

$$|\delta_{\mathbf{k}}^{\text{tens}}|^2 = 4.939 \cdot 10^{-10}, \qquad n_{\text{tens}} = -0.0323, \tag{6.41}$$

again for the mode that crossed the Hubble scale 60 e-folds before the end of inflation. (Including the second-order corrections, i.e. the terms between the brackets in (5.50), changes the result for n_{tens} to -0.0329.) Hence the ratio r of tensor and scalar perturbations is $r = 0.36$, while the single-field consistency relation (5.51) gives $-(200/9)n_{\text{tens}} = 0.72$. This means that multiple-field effects cause r to deviate from the single-field result by a factor of two in this model.

6.3 Curved field manifold: general remarks

Now we turn to the slow-roll behaviour of scalar fields that parameterize a curved manifold that is isotropic around a point. We start with setting up the general framework, which we will illustrate and expand upon in the special cases discussed in the next sections. Consider a manifold of arbitrary dimension d with coordinates $\boldsymbol{\phi}$ and metric $\mathbf{G}(\boldsymbol{\phi})$ given by

$$\mathbf{G}(\boldsymbol{\phi}) = g(\phi)\left(\mathbb{1} + \frac{\lambda(\phi)}{1-\lambda(\phi)}\,\mathbf{P}_0\right), \tag{6.42}$$

with $g(\phi) \neq 0$ and $\lambda(\phi) \neq 1$. Here $\phi \equiv \sqrt{\boldsymbol{\phi}^T\boldsymbol{\phi}}$ represents the coordinate length of the vector $\boldsymbol{\phi}$. The matrix $\mathbf{P}_0$ is the projection operator defined by

$$\mathbf{P}_0 \equiv \mathbf{e}_0\mathbf{e}_0^T, \qquad \mathbf{e}_0 \equiv \frac{\boldsymbol{\phi}}{\phi}. \tag{6.43}$$

This is the most general metric for a manifold of Euclidean signature (all eigenvalues of the metric are positive) that is isotropic around a point, chosen as the origin of the coordinates. (This can most easily be seen in spherical coordinates: $\mathrm{d}s_G^2 = g(\phi)[f(\phi)\mathrm{d}\phi^2 + \phi^2\mathrm{d}\Omega^2]$ corresponds with (6.42) after switching to cartesian coordinates and making the identification $\lambda/(1-\lambda) = f - 1$.) The restriction of isotropy around the origin has been assumed for simplicity, but it covers some general, interesting cases, e.g. the sphere and the hyperbolic space. The inverse of the metric (6.42) and its determinant are given by

$$\mathbf{G}^{-1} = \frac{1}{g}\left(\mathbb{1} - \lambda\mathbf{P}_0\right), \qquad \det\mathbf{G} = \frac{g^d}{1-\lambda}. \tag{6.44}$$

For the determinant we used the relation $\ln\det\mathbf{G} = \mathrm{tr}\ln\mathbf{G}$ and the fact that $\mathrm{tr}\,\mathbf{P}_0 = 1$. For the metric connection we find

$$\Gamma^a_{bc} = \frac{1}{2}\frac{g_{,\phi}}{g}\left(\frac{\phi_c}{\phi}\,\delta^a_b + \frac{\phi_b}{\phi}\,\delta^a_c - \frac{\phi^a}{\phi}\,\delta_{bc}\right) + \lambda\left(\frac{1}{2}\frac{g_{,\phi}}{g} + \frac{1}{\phi}\right)\frac{\phi^a}{\phi}(\mathbf{P}_0^\perp)_{bc} + \frac{1}{2}\frac{\lambda_{,\phi}}{1-\lambda}\frac{\phi^a}{\phi}(\mathbf{P}_0)_{bc}, \tag{6.45}$$

where $\mathbf{P}_0^\perp \equiv \mathbb{1} - \mathbf{P}_0$.

Inserting this metric into the first-order slow-roll equation of motion for $\boldsymbol{\phi}$ gives:

$$\dot{\boldsymbol{\phi}} = -\frac{2}{\sqrt{3}\,\kappa}\,\mathbf{G}^{-1}\boldsymbol{\partial}^T\sqrt{V} = -\frac{1}{\sqrt{3}}\frac{1}{\kappa g}\left(\frac{\boldsymbol{\partial}^T V}{\sqrt{V}} - \frac{\lambda}{\phi^2}\frac{\boldsymbol{\phi}^T\boldsymbol{\partial}^T V}{\sqrt{V}}\boldsymbol{\phi}\right)$$

$$\Leftrightarrow \qquad \boldsymbol{\phi}_{,N} = -\frac{1}{\kappa^2}\,\mathbf{G}^{-1}\boldsymbol{\partial}^T \ln V = -\frac{1}{\kappa^2 g}\left(\frac{\boldsymbol{\partial}^T V}{V} - \frac{\lambda}{\phi^2}\frac{\boldsymbol{\phi}^T\boldsymbol{\partial}^T V}{V}\boldsymbol{\phi}\right). \tag{6.46}$$

Note that $\boldsymbol{\phi}^T\boldsymbol{\partial}^T V = \phi^a\partial_a V$ is a scalar. In general this vector equation may be hard to solve, but in practice we often have some information from the corresponding flat case that we can use. In particular, we can sometimes determine the trajectories that the scalar fields follow through the flat field space. It is much harder to calculate exactly how the scalar fields move along these trajectories as a function of time or number of e-folds, but this still means that we have reduced the system of d differential equations for $\boldsymbol{\phi}$ to a single one, which gives the velocity along the trajectories. In other words, the trajectories of the slow-roll equation of motion for the flat case can be written as

$$\boldsymbol{\phi}_{\text{flat}}(N) = \mathbf{T}(\psi(N), \boldsymbol{\phi}_0), \qquad \mathbf{T}(0, \boldsymbol{\phi}_0) = \boldsymbol{\phi}_0, \qquad \psi(0) = 0 \tag{6.47}$$

(with $\mathbf{T}$ a known function), where the function $\psi(N)$ has to satisfy the differential equation

$$\psi_{,N} = -\frac{1}{\kappa^2 V}\frac{\mathbf{T}_{,\psi}^T\boldsymbol{\partial}^T V}{\mathbf{T}_{,\psi}^T\mathbf{T}_{,\psi}} \qquad \text{(flat case)}. \tag{6.48}$$

An example of this was given in (6.12) and (6.18) for the case of a quadratic potential. This flat solution can be generalized to curved manifolds with a metric of the form (6.42) by defining

$$\boldsymbol{\phi}_{\text{curved}}(N) = s(\psi(N))\,\mathbf{T}(\psi(N), \boldsymbol{\phi}_0). \tag{6.49}$$

Here $\mathbf{T}$ is the same function as for the flat case, while the differential equation (6.48) for ψ is slightly modified to

$$\psi_{,N} = -\frac{1}{g s}\frac{1}{\kappa^2 V}\frac{\mathbf{T}_{,\psi}^T\boldsymbol{\partial}^T V}{\mathbf{T}_{,\psi}^T\mathbf{T}_{,\psi}} \qquad \text{(curved case)}. \tag{6.50}$$

By inserting the ansatz (6.49) into the equation of motion (6.46) we find that the factor $s(\psi)$ has to satisfy

$$\frac{s_{,\psi}}{s} = -\lambda\,\frac{\mathbf{T}_{,\psi}^T\mathbf{T}_{,\psi}}{\mathbf{T}^T\mathbf{T}}\frac{\mathbf{T}^T\boldsymbol{\partial}^T V}{\mathbf{T}_{,\psi}^T\boldsymbol{\partial}^T V}, \qquad s(0) = 1. \tag{6.51}$$

Next we discuss the slow-roll functions $\tilde{\epsilon}$, $\tilde{\eta}^\parallel$ and $\tilde{\eta}^\perp$. To this end we define functions $C_n(V)$ as follows:

$$C_1(V) = \kappa^2\,\frac{2V}{\phi_0^2}, \qquad C_n(V) = \kappa^{2n}\,\frac{\boldsymbol{\nabla}V(\mathbf{G}^{-1}\boldsymbol{\nabla}^T\boldsymbol{\nabla}V)^{n-2}\mathbf{G}^{-1}\boldsymbol{\nabla}^T V}{\phi_0^2}, \quad n \geq 2. \tag{6.52}$$

The functions $C_n(V)$ are not simply the curved generalizations of the functions F_n defined in (6.14): the C_n are defined for an arbitrary potential, while in the definition of the F_n we have assumed a quadratic potential and made use of the fact that we can determine the trajectories of the fields in this case. Using the Green-Schwarz inequality we can derive the following relation for positive integers n, p with $0 < p < n$:

$$C_n^2 \leq C_{2p} C_{2(n-p)}, \tag{6.53}$$

which follows by writing $\phi_0^2 C_n = \kappa^{2n} \boldsymbol{\nabla} V (\mathbf{G}^{-1} \boldsymbol{\nabla}^T \boldsymbol{\nabla} V)^{p-1} \mathbf{G}^{-1} (\boldsymbol{\nabla}^T \boldsymbol{\nabla} V \mathbf{G}^{-1})^{n-p-1} \boldsymbol{\nabla}^T V$. The slow-roll functions to leading order, i.e. using the expressions given by (3.22), can now be written as

$$\tilde{\epsilon} = \frac{2}{\kappa^2 \phi_0^2} \frac{C_2}{C_1^2}, \qquad \tilde{\eta}^{\parallel} = -\frac{2}{\kappa^2 \phi_0^2} \frac{C_3 C_1 - C_2^2}{C_2 C_1^2}, \qquad \tilde{\eta}^{\perp} = \frac{2}{\kappa^2 \phi_0^2} \frac{\sqrt{C_4 C_2 - C_3^2}}{C_2 C_1}. \tag{6.54}$$

These expressions are quite general, and include the cases discussed in sections 6.2 and 3.4, in the limits of a trivial field metric and a quadratic or quartic potential, respectively. For a flat field metric and a quadratic potential, the relation is simply $C_n = F_n$, cf. (6.20). For a quartic potential on a flat field manifold the relation is more complicated: one has $C_1 = \frac{1}{2}\kappa^2 \phi_0^2 F_1^2$, $C_2 = \kappa^4 \phi_0^4 F_2 F_1^2$ and $C_3 = \kappa^6 \phi_0^6 F_1^2 (F_3 F_1 + 2F_2^2)$ with the quartic F_n defined in (3.32), leading to the expressions (3.35). The only inequality for the functions C_n that is directly applicable is for $n = 3, p = 1$: $C_3^2 \leq C_2 C_4$, which implies that $\tilde{\eta}^{\perp}$ is real, as it should be.

We conclude this section with some general results in the case of a central potential, i.e. a potential $V_c(\phi)$ that is a function of the coordinate length ϕ only. Basically this means that we have an effectively single-field situation, but because of the non-trivial curvature some effects that are absent in a truly single-field situation will come into play. The first and second-order gradients $\boldsymbol{\partial}^T V_c$ and $\boldsymbol{\partial}^T \boldsymbol{\partial} V_c$ are given by

$$\boldsymbol{\partial}^T V_c = V_{c,\phi} \mathbf{e}_0, \qquad \boldsymbol{\partial}^T \boldsymbol{\partial} V_c = V_{c,\phi\phi}\, \mathbf{P}_0 + \frac{V_{c,\phi}}{\phi}\, \mathbf{P}_0^{\perp}, \tag{6.55}$$

which leads to the following expression for the covariant second-order derivative of the potential, $\mathbf{M}^2 \equiv \mathbf{G}^{-1} \boldsymbol{\nabla}^T \boldsymbol{\nabla} V_c$:

$$\mathbf{M}^2 = \frac{1-\lambda}{g} \left[\left(V_{c,\phi\phi} - \frac{1}{2} V_{c,\phi} \left(\frac{g_{,\phi}}{g} + \frac{\lambda_{,\phi}}{1-\lambda} \right) \right) \mathbf{P}_0 + V_{c,\phi} \left(\frac{1}{2} \frac{g_{,\phi}}{g} + \frac{1}{\phi} \right) \mathbf{P}_0^{\perp} \right]. \tag{6.56}$$

As in our first example of scalar fields with equal masses on a flat manifold in section 6.1, we find that the vector slow-roll equation of motion reduces to a scalar equation. The direction of the vector $\boldsymbol{\phi}$ does not change in time, while its length satisfies the differential equation

$$\phi_{,N} = -\frac{1-\lambda}{\kappa^2 g} \frac{V_{c,\phi}}{V_c}. \tag{6.57}$$

Next we work out the expressions for the slow-roll functions to leading order, given in (6.54):

$$\begin{aligned} \tilde{\epsilon} &= \frac{1-\lambda}{2\kappa^2 g} \left(\frac{V_{c,\phi}}{V_c} \right)^2, \qquad \tilde{\eta}^{\perp} = 0, \\ \tilde{\eta}^{\parallel} &= -\frac{1-\lambda}{\kappa^2 g} \left[\frac{V_{c,\phi\phi}}{V_c} - \frac{1}{2} \left(\frac{g_{,\phi}}{g} + \frac{\lambda_{,\phi}}{1-\lambda} \right) \frac{V_{c,\phi}}{V_c} - \frac{1}{2} \left(\frac{V_{c,\phi}}{V_c} \right)^2 \right]. \end{aligned} \tag{6.58}$$

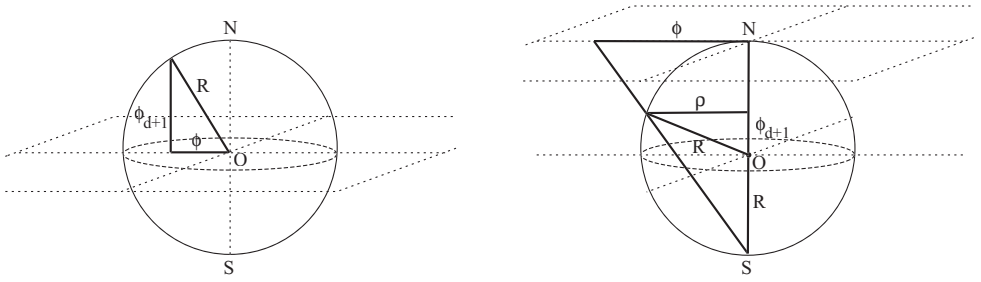

Figure 6.4: A figure to clarify the construction of (a) embedding and (b) stereographical coordinates for the d-dimensional sphere. With embedding coordinates one describes a point $(\boldsymbol{\phi}, \phi_{d+1})$ that lies on the sphere in the $(d+1)$-dimensional embedding space by its perpendicular projection on the hyperplane $\phi_{d+1} = 0$. Stereographical coordinates (in this example) are constructed by a stereographical projection of a point of the sphere on the hyperplane that is tangent to the sphere at the north pole, with the projection source at the south pole.

The fact that $\tilde{\eta}^{\perp} = 0$ can most easily be seen by realizing that since $\mathbf{e}_0$ is an eigenvector of both $\mathbf{G}^{-1}$ and $\mathbf{M}^2$, the vectors $\mathbf{G}^{-1}\boldsymbol{\nabla}^T V_c$ and $\mathbf{M}^2\mathbf{G}^{-1}\boldsymbol{\nabla}^T V_c$ are parallel, so that the Green-Schwarz inequality (6.53) is saturated ($C_3^2 = C_2 C_4$).

6.4 Spherical field manifold and equal masses

After the general discussion in the previous section, we now move on to some explicit examples. In this section we consider a quadratic central potential with mass $\kappa^{-1}m$, i.e. $V(\boldsymbol{\phi}) = \frac{1}{2}\kappa^{-2}m^2\phi^2$. The scalar fields are the local coordinates on a d-dimensional sphere with radius R. We consider two situations:

1. Embedding coordinates induced by embedding the sphere in a $(d+1)$-dimensional Euclidean space;

2. Stereographical coordinates, where the same embedding is made, but coordinates are then defined by means of a stereographical projection on a plane.

Note that even though these coordinates describe the same sphere, we are not in the same physical situation since the potential distribution on the sphere is different (because we choose the same function of the coordinates in both cases).

The construction of these two sets of coordinates is illustrated in figure 6.4. The embedding coordinates are the simplest. Here one parameterizes a point on the sphere by its projection parallel to the ϕ_{d+1} axis on the $\phi_{d+1} = 0$ hyperplane. In other words, of the $d+1$ cartesian coordinates of the embedding space one eliminates the coordinate ϕ_{d+1} by means of the equation for the sphere: $\sum_{j=1}^{d+1} \phi_j^2 = R^2$. Using this constraint on the line element of the embedding space, $\mathrm{d}s^2 = \sum_{j=1}^{d+1} \mathrm{d}\phi_j^2$, gives the metric of the sphere in embedding coordinates:

$$\mathbf{G} = \mathbb{1} + \frac{\boldsymbol{\phi}\boldsymbol{\phi}^T}{R^2 - \phi^2} \qquad \Rightarrow \qquad g = 1, \qquad \lambda = \frac{\phi^2}{R^2}, \tag{6.59}$$

with $\boldsymbol{\phi}$ a d-dimensional vector. By construction $\phi^2 \equiv \boldsymbol{\phi}^T\boldsymbol{\phi} < R^2$. With this procedure one can describe either the northern or the southern hemisphere, but not both at the same time. In the slow-roll discussion here we stay within one hemisphere, because the quadratic potential is minimal in the origin of this set of coordinates (i.e. on the north/south pole of the sphere).

With the construction of the stereographical coordinates we do not use a projection parallel to the ϕ_{d+1} axis, but a stereographical projection from the south pole of the sphere on the tangent plane of the sphere at the north pole. This means that one draws a line through the south pole and a certain point on the sphere, and the point where this line crosses the tangent plane gives the coordinates in the plane that correspond with this point on the sphere, see figure 6.4(b). In these coordinates one can describe the whole sphere, except for the south pole itself. The northern hemisphere is coordinatized by points on the tangent plane with $\phi < 2R$, while the southern hemisphere has $\phi > 2R$ (ϕ is the length of the d-dimensional vector $\boldsymbol{\phi}$ that lies completely within the d-dimensional tangent plane, so not including ϕ_{d+1}). To derive the metric of the sphere in stereographical coordinates it is simplest to write the line element of the embedding space in a kind of generalized cylindrical coordinates: $\mathrm{d}s^2 = \mathrm{d}\rho^2 + \rho^2\mathrm{d}\Omega^2_{(d-1)} + \mathrm{d}\phi^2_{d+1}$. From the figure we see the following relation: $\rho/(R \pm \phi_{d+1}) = \phi/(2R)$, where the plus sign is for the northern hemisphere and the minus sign for the southern one. Using the constraint relation $\phi^2_{d+1} + \rho^2 = R^2$ to eliminate ϕ_{d+1} leads to the following expression for ρ as a function of ϕ: $\rho = 4\phi R^2/(4R^2 + \phi^2)$. Inserting this expression and the constraint relation into the metric in cylindrical coordinates of the embedding space we obtain the metric of the sphere in stereographical coordinates:

$$\mathbf{G} = \left(\frac{4R^2}{4R^2+\phi^2}\right)^2 \mathbb{1} \qquad \Rightarrow \qquad g = \left(\frac{4R^2}{4R^2+\phi^2}\right)^2, \qquad \lambda = 0. \tag{6.60}$$

The choice of projection source and plane is certainly not unique, but this is one of the choices where the limit of $R \to \infty$ exactly gives the usual flat metric with $g = 1$.

Having constructed the field metrics we now treat the corresponding inflation models. First we consider the case of embedding coordinates. Inserting the metric quantities (6.59) and a quadratic central potential into the slow-roll equation of motion (6.57) we find

$$\begin{aligned} &\phi\,\phi_{,N} = -\frac{2}{\kappa^2}\left(1 - \frac{\phi^2}{R^2}\right) \\ \Rightarrow \qquad &\boldsymbol{\phi}(N) = R\sqrt{1 - \exp\left(-\frac{4(N_\infty - N)}{\kappa^2 R^2}\right)}\,\hat{\boldsymbol{\phi}}_0 = \sqrt{\frac{1 - \exp\left(-\frac{4(N_\infty - N)}{\kappa^2R^2}\right)}{1 - \exp\left(-\frac{4N_\infty}{\kappa^2R^2}\right)}}\,\boldsymbol{\phi}_0, \end{aligned} \tag{6.61}$$

with $N_\infty = -\frac{1}{4}\kappa^2R^2\ln(1-\phi_0^2/R^2)$. Here the initial condition $\boldsymbol{\phi}(0) = \boldsymbol{\phi}_0$ has been applied.[4] Note that we can also determine the solution for $\boldsymbol{\phi}$ by using our knowledge from the flat case and the method described in (6.49) ff., but in this particular case that is more complicated.

[4] In this case the equation of motion can also be solved in terms of comoving time t, with the result $\boldsymbol{\phi}(t) = R\,\tanh[\beta(t_\infty - t)]\,\hat{\boldsymbol{\phi}}_0$, with $\beta = \sqrt{\frac{2}{3}}\,\frac{m}{\kappa^2 R}$ and $t_\infty = \frac{1}{2\beta}\ln\frac{R+\phi_0}{R-\phi_0}$.

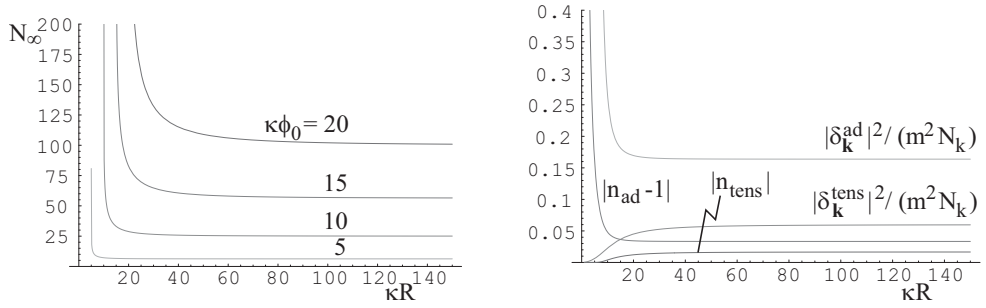

(a) (b)

Figure 6.5: (a) The total amount of inflation N_∞ as a function of the radius R, for the inflation model with a quadratic potential with equal masses on a spherical field manifold with embedding coordinates (6.59). Shown are the graphs for four different values of the length ϕ_0 of the initial condition vector, which must be smaller than R by construction. (b) The scalar adiabatic and tensor spectral amplitudes and indices (6.63) as a function of R. The amplitudes have been normalized by $m^2 N_k$, both to remove the dependence on m and to make them of the same order of magnitude as the spectral indices. Since the latter are negative, the absolute value has been taken. A value of $N_k = 60$ has been assumed.

The slow-roll functions follow immediately from (6.58):

$$\tilde{\epsilon} = \frac{2}{\kappa^2 R^2} \frac{1}{\exp\left(\frac{4(N_\infty - N)}{\kappa^2 R^2}\right) - 1}, \qquad \tilde{\eta}^{\parallel} = \frac{2}{\kappa^2 R^2}, \qquad \tilde{\eta}^{\perp} = 0. \tag{6.62}$$

For slow roll to be valid we see first, from the expression for $\tilde{\eta}^{\parallel}$, that the curvature should not be too large (i.e. R too small): spheres with a radius of the Planck scale or smaller do not satisfy the slow-roll conditions. In the second place we find, from the expression for $\tilde{\epsilon}$, that $\phi_0^2/R^2 > 2/(\kappa^2 R^2 + 2)$ to allow slow roll initially (at $N = 0$). Combining this with the other condition and keeping in mind that $\phi_0^2 < R^2$ always, we find that slow roll works best if ϕ_0 is sufficiently close to R (the equator of the sphere). From the expression for N_∞ we see that this also gives the most inflation. A plot of N_∞ as a function of R for different values of ϕ_0 is given in figure 6.5(a).

Using the expression for H, $H = (m\phi/\sqrt{6})(1 + \tilde{\epsilon}/6)$, and the fact that U_{Pe} and V_e are zero because $\tilde{\eta}^{\perp} = 0$, we find the following expressions for the amplitudes and spectral indices (5.38), (5.41), (5.47) and (5.50):

$$\begin{aligned}
|\delta_{\mathbf{k}}^{\mathrm{ad}}|^2 &= \frac{\kappa^4 R^4 m^2}{300\pi^2}\left(\cosh\frac{4N_k}{\kappa^2R^2} - 1\right)\left[1 + \frac{4}{\kappa^2R^2}\frac{1}{\exp\frac{4N_k}{\kappa^2R^2} - 1}\left[B - \frac{5}{6} + B\exp\frac{4N_k}{\kappa^2R^2}\right]\right], \\
|\delta_{\mathbf{k}}^{\mathrm{tens}}|^2 &= \frac{4\kappa^2R^2m^2}{27\pi^2}\left(1 - \exp\left(-\frac{4N_k}{\kappa^2R^2}\right)\right)\left[1 + \frac{4(B - \frac{5}{6})}{\kappa^2R^2}\frac{1}{\exp\frac{4N_k}{\kappa^2R^2} - 1}\right], \\
n_{\mathrm{ad}} - 1 &= -\frac{4}{\kappa^2R^2}\frac{\exp\frac{4N_k}{\kappa^2R^2} + 1}{\exp\frac{4N_k}{\kappa^2R^2} - 1}, \qquad n_{\mathrm{tens}} = -\frac{4}{\kappa^2R^2}\frac{1}{\exp\frac{4N_k}{\kappa^2R^2} - 1},
\end{aligned} \tag{6.63}$$

with $N_k \equiv N_\infty - N_{\mathcal{H}}$. In the limit $R \to \infty$ all results agree with those we found in the flat case in section 6.1. As $U_{Pe} = 0$, the standard single-field consistency relation

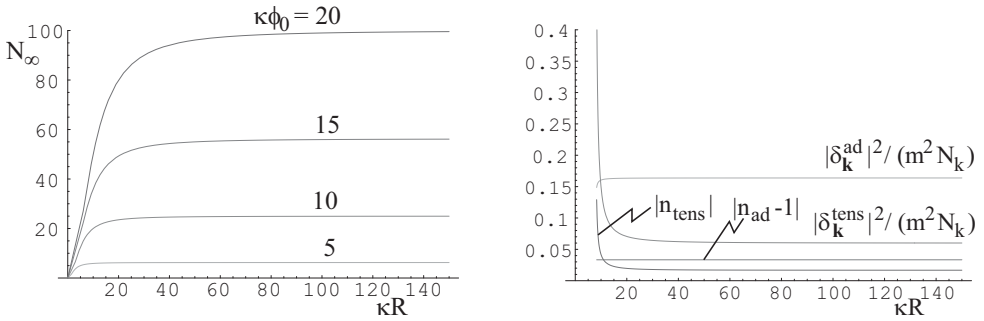

(a) (b)

Figure 6.6: The same plots as in figure 6.5, but for the model with stereographical coordinates (6.60). In this model ϕ_0 can in principle take all values, although the slow-roll conditions lead to the restriction (6.66). For slow roll to be valid, as well as to satisfy the necessary condition $N_\infty > N_k$, the radius κR has to be larger than $\sqrt{N_k} \approx 8$.

(5.51) $r = -(200/9)n_{\rm tens}$ is valid to leading order. The amplitudes and indices are plotted as a function of R in figure 6.5(b). For sufficiently small R, $\kappa R \lesssim 30$, all amplitudes and indices are affected by the curvature effects, but for $\kappa R \gtrsim 50$ the results become practically indistinguishable from the flat case (of course the exact values depend on the accuracy). Moreover, while curvature effects make the scalar quantities larger, the tensor quantities become smaller.

As opposed to the flat case discussed in section 6.1, we now have two free parameters in the model: m and R. Taking the best-fit value for $n_{\rm ad}$ from (5.69), $n_{\rm ad} = 0.93$, and using $N_k = 60$ we can solve the above expression for $n_{\rm ad}$ in terms of R to find $\kappa R = 7.7$. Note that, if we assume that this is the correct inflation model, observations seem to favour a curved field manifold over a flat one, although the uncertainty in the observations of $n_{\rm ad}$ is still far too large to draw any definite conclusions. On the other hand, as can be seen from figure 6.5(a), for this model with such a small value of R to give sufficient inflation, the initial condition ϕ_0 has to be extremely close to R. Using this value for R we find for the tensor to scalar ratio $r = 0.03$, which is a lot smaller than in the flat case. Inserting these values into the fitting function (5.68) and comparing with the above expression for $|\delta^{\rm ad}_{\mathbf{k}}|$ we obtain a value for the mass: $m = 8.4 \cdot 10^{-6}$ in units of κ^{-1}, which is significantly smaller than in the flat case.

Now we proceed to the case of the stereographical coordinates (6.60). Then the equation of motion for the length of the vector $\boldsymbol{\phi}$ reads as

$$\phi\,\phi_{,N} = -\frac{2}{\kappa^2}\left(\frac{4R^2+\phi^2}{4R^2}\right)^2 \qquad \Rightarrow \qquad \boldsymbol{\phi}(N) = \sqrt{\frac{\left(\frac{\kappa^2R^2}{N_\infty}-1\right)(N_\infty - N)}{\kappa^2R^2-(N_\infty-N)}}\,\boldsymbol{\phi}_0, \quad (6.64)$$

with the initial condition $\boldsymbol{\phi}(0) = \boldsymbol{\phi}_0$ and N_∞ given by $N_\infty = \kappa^2R^2\phi_0^2/(4R^2+\phi_0^2)$. Note that this means that $N_\infty \leq \kappa^2R^2$, so that the radius of the sphere in units of κ^{-1} should not be smaller than $\sqrt{N_k}$ in order to have sufficient inflation to solve the horizon problem. A plot of N_∞ as a function of R for different values of ϕ_0 is given in figure 6.6(a). For the

slow-roll functions we find

$$\tilde{\epsilon} = \frac{\frac{1}{2}\kappa^2 R^2}{(N_\infty - N)(\kappa^2 R^2 - (N_\infty - N))}, \qquad \tilde{\eta}^{\parallel} = \frac{-1}{\kappa^2 R^2 - (N_\infty - N)}, \qquad \tilde{\eta}^{\perp} = 0. \quad (6.65)$$

From the remarks above it follows that if N_∞ is large enough, $|\tilde{\eta}^{\parallel}|$ is always small. From the condition $\tilde{\epsilon}(N=0) < 1$ we find

$$(\kappa^2 R^2 - 1) - \sqrt{(\kappa^2 R^2 - 1)^2 - 1} < \frac{\phi_0^2}{4R^2} < (\kappa^2 R^2 - 1) + \sqrt{(\kappa^2 R^2 - 1)^2 - 1}, \quad (6.66)$$

which in the limit of $R \to \infty$ simplifies to $2/\kappa^2 < \phi_0^2 < \infty$, as it should. For smaller R the lower limit is larger.

Once again the multiple-field effects U_{Pe} and V_e are zero and we find for the amplitudes and spectral indices:

$$\begin{aligned} |\delta_{\mathbf{k}}^{\mathrm{ad}}|^2 &= \frac{2}{75\pi^2}\, m^2 N_k^2 \left[1 + \frac{2B}{N_k} - \frac{5}{6}\frac{1}{N_k}\frac{\kappa^2 R^2}{\kappa^2 R^2 - N_k}\right], \\ |\delta_{\mathbf{k}}^{\mathrm{tens}}|^2 &= \frac{16}{27\pi^2}\, m^2 N_k \frac{\kappa^2 R^2}{\kappa^2 R^2 - N_k}\left[1 + \frac{B - \frac{5}{6}}{N_k}\frac{\kappa^2 R^2}{\kappa^2 R^2 - N_k}\right], \\ n_{\mathrm{ad}} - 1 &= -\frac{2}{N_k}, \qquad\qquad n_{\mathrm{tens}} = -\frac{1}{N_k}\frac{\kappa^2 R^2}{\kappa^2 R^2 - N_k}. \end{aligned} \quad (6.67)$$

The single-field consistency relation $r = -(200/9)n_{\mathrm{tens}}$ is satisfied to leading order. All results agree with those of section 6.1 in the limit $R \to \infty$. The amplitudes and spectral indices are plotted as a function of R in figure 6.6(b). From the figure as well as from the expressions (6.67) we see that the scalar adiabatic results are independent of R to leading order, but this is not true for the tensor results. While in the case of the embedding coordinates the tensor quantities become smaller for smaller R, here they become larger. Because of the independence of R to leading order for the scalar amplitude, the value of m that satisfies the observational constraints does not differ significantly from the flat case. However, as soon as the tensor quantities can be observed, this model will be observationally distinguishable from the flat case for not too large values of R, $\kappa R \lesssim 30$.

6.5 Curved field manifold and general mass matrix

In this final example we generalize the quadratic potential with equal masses of the previous section to the case of a general mass matrix: $V_2 = \frac{1}{2}\kappa^{-2}\,\boldsymbol{\phi}^T \mathbf{m}^2 \boldsymbol{\phi}$, the same potential as (6.10), but this time on a curved field manifold. We start with a few expressions using the metric (6.42), but after that we make the further simplification of taking $\lambda = 0$, as in that case one can work out the important multiple-field quantity U_{Pe} explicitly. An example of the latter case is the sphere with stereographical coordinates (6.60).

We use the knowledge of the trajectory in the flat case to derive results about the curved case, i.e. the method described in (6.49) ff. Hence we have

$$\boldsymbol{\phi}(N) = s(\psi(N))\, e^{-\frac{1}{2}\mathbf{m}^2 \psi(N)} \boldsymbol{\phi}_0, \quad (6.68)$$

where s and ψ satisfy the equations

$$\frac{s_{,\psi}}{s} = \frac{1}{2}\lambda(\phi(\psi))\frac{F_1(\psi)}{F_0(\psi)}, \qquad \psi_{,N} = \frac{4}{\kappa^2 \phi_0^2}\frac{1}{g(\phi(\psi))s^2(\psi)F_1(\psi)}. \quad (6.69)$$

Here the F_n are the functions defined in (6.14). It is useful to express everything in terms of these functions F_n, as their behaviour as a function of ψ was studied in §6.2.1. Working out the expressions for the C_n (with a quadratic potential) in terms of the F_n we find for the first two:

$$C_1(V_2) = s^2 F_1, \qquad C_2(V_2) = \frac{s^2}{g}\left(F_2 - \lambda\frac{F_1^2}{F_0}\right), \tag{6.70}$$

so that the expression for $\tilde{\epsilon}$ is

$$\tilde{\epsilon} = \frac{2}{\kappa^2\phi_0^2}\frac{1}{gs^2}\left(\frac{F_2}{F_1^2} - \frac{\lambda}{F_0}\right). \tag{6.71}$$

The expressions for the higher $C_n(V_2)$ and the other slow-roll functions become very long, so we do not give them here. Instead we now make the further simplification of taking $\lambda = 0$.

With the assumption $\lambda = 0$ things simplify considerably.[5] In the first place we see from (6.69) (or (6.51)) that $s = 1$ for all values of ψ. Using the expression for the covariant second-order derivative of the potential,

$$\mathbf{M}^2 \equiv \mathbf{G}^{-1}\boldsymbol{\nabla}^T\boldsymbol{\nabla}V_2 = \frac{1}{\kappa^2 g}\left[\mathbf{m}^2 - \frac{1}{2}\frac{\phi g_{,\phi}}{g}\frac{1}{F_0}\left(\frac{\mathbf{m}^2\boldsymbol{\phi}\,\boldsymbol{\phi}^T}{\phi_0^2} + \frac{\boldsymbol{\phi}\,\boldsymbol{\phi}^T\mathbf{m}^2}{\phi_0^2} - F_1\mathbb{1}\right)\right], \tag{6.72}$$

the first four $C_n(V_2)$ are given by

$$\begin{aligned} C_1(V_2) &= F_1, & C_3(V_2) &= \frac{1}{g^2}\left(F_3 - \frac{1}{2}\frac{\phi g_{,\phi}}{g}\frac{F_2F_1}{F_0}\right), \\ C_2(V_2) &= \frac{1}{g}F_2, & C_4(V_2) &= \frac{1}{g^3}\left(F_4 - \frac{\phi g_{,\phi}}{g}\frac{F_2^2}{F_0}\left(1 - \frac{1}{4}\frac{\phi g_{,\phi}}{g}\right)\right), \end{aligned} \tag{6.73}$$

which leads to the following expressions for the slow-roll functions:

$$\begin{aligned} \tilde{\epsilon} &= \frac{2}{\kappa^2\phi_0^2}\frac{1}{g}\frac{F_2}{F_1^2}, & \tilde{\eta}^{\parallel} &= -\frac{2}{\kappa^2\phi_0^2}\frac{1}{g}\left(\frac{F_3}{F_2F_1} - \frac{F_2}{F_1^2} - \frac{1}{2}\frac{\phi g_{,\phi}}{g}\frac{1}{F_0}\right), \\ \tilde{\eta}^{\perp} &= \frac{2}{\kappa^2\phi_0^2}\frac{1}{g}\frac{\sqrt{F_4F_2 - F_3^2 + \frac{\phi g_{,\phi}}{gF_0}(F_3F_2F_1 - F_2^3) + \frac{1}{4}\left(\frac{\phi g_{,\phi}}{gF_0}\right)^2(F_2^3F_0 - F_2^2F_1^2)}}{F_2F_1}. \end{aligned} \tag{6.74}$$

Next we derive an explicit expression for U_{Pe} (defined in (4.76)) in a way analogous to the derivation in §6.2.2. The field velocity, acceleration and perturbation are given by

$$\begin{aligned} \dot{\boldsymbol{\phi}} &= -\frac{1}{2}\dot{\psi}\,\mathbf{m}^2\boldsymbol{\phi}, & \boldsymbol{\delta\phi} &= -\frac{1}{2}\delta\psi\,\mathbf{m}^2\boldsymbol{\phi} + e^{-\frac{1}{2}\mathbf{m}^2\psi}\boldsymbol{\delta\phi}_0, \\ \mathcal{D}_t\dot{\boldsymbol{\phi}} &= -\frac{1}{2}\ddot{\psi}\,\mathbf{m}^2\boldsymbol{\phi} + \frac{1}{4}\dot{\psi}^2\,\mathbf{m}^4\boldsymbol{\phi} - \frac{1}{4}\dot{\psi}^2\frac{\phi g_{,\phi}}{g}\left(\frac{1}{2}\frac{\boldsymbol{\phi}^T\mathbf{m}^4\boldsymbol{\phi}}{\boldsymbol{\phi}^T\boldsymbol{\phi}}\boldsymbol{\phi} - \frac{\boldsymbol{\phi}^T\mathbf{m}^2\boldsymbol{\phi}}{\boldsymbol{\phi}^T\boldsymbol{\phi}}\mathbf{m}^2\boldsymbol{\phi}\right). \end{aligned} \tag{6.75}$$

[5] As an aside let us remark that in the case of embedding coordinates, where $g = 1$ and $\lambda = \phi^2/R^2$, one can also compute the function $s(\psi)$ explicitly: $s^2 = [1 - (\phi_0^2/R^2)(1 - F_0)]^{-1}$.

The projector parallel to the velocity is given by $\mathbf{P}^{\parallel} = \mathbf{m}^2\boldsymbol{\phi}\,\boldsymbol{\phi}^T\mathbf{m}^2/(\boldsymbol{\phi}^T\mathbf{m}^4\boldsymbol{\phi})$ because the factors g cancel, and therefore we find that

$$\mathcal{D}_t\dot{\boldsymbol{\phi}}^T\,\mathbf{G}\,\mathbf{P}^{\perp}\boldsymbol{\delta\phi} = \frac{1}{4}\dot{\psi}^2\,g\boldsymbol{\phi}^T\Bigg[\mathbf{m}^4 - \frac{\boldsymbol{\phi}^T\mathbf{m}^6\boldsymbol{\phi}}{\boldsymbol{\phi}^T\mathbf{m}^4\boldsymbol{\phi}}\mathbf{m}^2 + \frac{1}{2}\frac{\phi g_{,\phi}}{g}\left(\frac{\boldsymbol{\phi}^T\mathbf{m}^2\boldsymbol{\phi}}{\boldsymbol{\phi}^T\boldsymbol{\phi}}\mathbf{m}^2 - \frac{\boldsymbol{\phi}^T\mathbf{m}^4\boldsymbol{\phi}}{\boldsymbol{\phi}^T\boldsymbol{\phi}}\right)\Bigg]e^{-\frac{1}{2}\mathbf{m}^2\psi}\boldsymbol{\delta\phi}_0. \quad (6.76)$$

Here we have used that the first term of $\boldsymbol{\delta\phi}$ and the first and last terms of $\mathcal{D}_t\dot{\boldsymbol{\phi}}$ are proportional to $\dot{\boldsymbol{\phi}}$ and hence are projected away. With these results we find for $U^T_{P\,e}$:

$$\begin{aligned} U^T_{P\,e}q_{\mathcal{H}} &= 2\sqrt{\tilde{\epsilon}_{\mathcal{H}}}\int_{t_{\mathcal{H}}}^{t_e}\mathrm{d}t\,\frac{H}{\sqrt{\tilde{\epsilon}}}\,\tilde{\boldsymbol{\eta}}^T\mathbf{G}\,\mathbf{P}^{\perp}\,a_{\mathcal{H}}\boldsymbol{\delta\phi} \\ &= \frac{\kappa\sqrt{\tilde{\epsilon}_{\mathcal{H}}}}{\sqrt{2}}\int_{\psi_{\mathcal{H}}}^{\psi_e}\mathrm{d}\psi\,g\,\frac{\boldsymbol{\phi}^T\mathbf{m}^2\boldsymbol{\phi}}{\boldsymbol{\phi}^T\mathbf{m}^4\boldsymbol{\phi}}\,\boldsymbol{\phi}^T\Bigg[\mathbf{m}^4 - \frac{\boldsymbol{\phi}^T\mathbf{m}^6\boldsymbol{\phi}}{\boldsymbol{\phi}^T\mathbf{m}^4\boldsymbol{\phi}}\mathbf{m}^2 \\ &\qquad + \frac{1}{2}\frac{\phi g_{,\phi}}{g}\left(\frac{\boldsymbol{\phi}^T\mathbf{m}^2\boldsymbol{\phi}}{\boldsymbol{\phi}^T\boldsymbol{\phi}}\mathbf{m}^2 - \frac{\boldsymbol{\phi}^T\mathbf{m}^4\boldsymbol{\phi}}{\boldsymbol{\phi}^T\boldsymbol{\phi}}\right)\Bigg]e^{-\frac{1}{2}\mathbf{m}^2(\psi-\psi_{\mathcal{H}})}\,a_{\mathcal{H}}\boldsymbol{\delta\phi}_{\mathcal{H}}. \quad (6.77)\end{aligned}$$

Next we use the two relations

$$\begin{aligned} \frac{g\,\boldsymbol{\phi}^T}{\boldsymbol{\phi}^T\mathbf{m}^4\boldsymbol{\phi}}\left[\mathbf{m}^4 - \frac{\boldsymbol{\phi}^T\mathbf{m}^6\boldsymbol{\phi}}{\boldsymbol{\phi}^T\mathbf{m}^4\boldsymbol{\phi}}\mathbf{m}^2 + \frac{1}{2}\frac{\phi g_{,\phi}}{g}\frac{\boldsymbol{\phi}^T\mathbf{m}^2\boldsymbol{\phi}}{\boldsymbol{\phi}^T\boldsymbol{\phi}}\mathbf{m}^2\right]e^{-\frac{1}{2}\mathbf{m}^2\psi} &= -\frac{\mathrm{d}}{\mathrm{d}\psi}\left[g\,\frac{\boldsymbol{\phi}^T\mathbf{m}^2e^{-\frac{1}{2}\mathbf{m}^2\psi}}{\boldsymbol{\phi}^T\mathbf{m}^4\boldsymbol{\phi}}\right], \\ g\,\boldsymbol{\phi}^T\left[\mathbf{m}^2 + \frac{1}{2}\frac{\phi g_{,\phi}}{g}\frac{\boldsymbol{\phi}^T\mathbf{m}^2\boldsymbol{\phi}}{\boldsymbol{\phi}^T\boldsymbol{\phi}}\right]e^{-\frac{1}{2}\mathbf{m}^2\psi} &= -\frac{\mathrm{d}}{\mathrm{d}\psi}\left[g\,\boldsymbol{\phi}^Te^{-\frac{1}{2}\mathbf{m}^2\psi}\right], \quad (6.78)\end{aligned}$$

the first to perform an integration by parts on the first three terms of (6.77) and the second to perform the remaining integral. The result is

$$U^T_{P\,e}q_{\mathcal{H}} = \frac{\kappa\sqrt{\tilde{\epsilon}_{\mathcal{H}}}}{\sqrt{2}}\left[g\,\boldsymbol{\phi}^T\mathbf{P}^{\perp}e^{-\frac{1}{2}\mathbf{m}^2(\psi-\psi_{\mathcal{H}})}\right]_{\psi_{\mathcal{H}}}^{\psi_e}a_{\mathcal{H}}\boldsymbol{\delta\phi}_{\mathcal{H}} = \frac{\kappa\sqrt{\tilde{\epsilon}_{\mathcal{H}}}}{\sqrt{2}}\left[\boldsymbol{\phi}^{\perp}\cdot e^{-\frac{1}{2}\mathbf{m}^2(\psi-\psi_{\mathcal{H}})}\right]_{\psi_{\mathcal{H}}}^{\psi_e}\mathbf{q}_{\mathcal{H}}. \quad (6.79)$$

Here we used the fact that relation (6.35) remains unchanged, so that $a_{\mathcal{H}}\boldsymbol{\delta\phi}_{\mathcal{H}} = \mathbf{q}_{\mathcal{H}}$ to first order. The final expression for $U^T_{P\,e}$ is then equal to (6.36):

$$U^T_{P\,e} = \frac{\kappa\sqrt{\tilde{\epsilon}_{\mathcal{H}}}}{\sqrt{2}}\left(-\phi^{\perp}_{\mathcal{H}} + e^{-\frac{1}{2}\mathbf{m}^2(\psi_e-\psi_{\mathcal{H}})}\phi^{\perp}_e\right)^T. \quad (6.80)$$

The effects of the non-trivial field metric are hidden in the background quantities and the inner products: $\phi^{\perp}$ denotes the vector with components $\mathbf{e}_n\cdot\mathbf{P}^{\perp}\boldsymbol{\phi} = g\,\mathbf{e}_n^T\mathbf{P}^{\perp}\boldsymbol{\phi}$ and $\exp(-\frac{1}{2}\mathbf{m}^2(\psi_e-\psi_{\mathcal{H}}))$ the matrix with components $g_e\,\mathbf{e}_m^T(t_e)\exp(-\frac{1}{2}\mathbf{m}^2(\psi_e-\psi_{\mathcal{H}}))\mathbf{e}_n(t_{\mathcal{H}})$. For the same reasons as discussed below (6.36) the second term within the parentheses in the expression for $U^T_{P\,e}$ is in general expected to be very small.

Assuming that $\tilde{\eta}^{\perp}$ goes to zero at the end of inflation, so that we can neglect the second term in the expression for $U_{P\,e}$, as well as the isocurvature and mixing components, the expressions (6.38) for $|\delta^{\mathrm{ad}}_{\mathbf{k}}|^2$ and $n_{\mathrm{ad}}-1$ are valid here as well. One additional complication

in the curved case under consideration is that $\delta_{\mathcal{H}}$ in those expressions now contains the curvature tensor $\mathbf{R}(\dot{\boldsymbol{\phi}}, \dot{\boldsymbol{\phi}})$ next to the mass matrix $\mathbf{M}^2$ (see (4.60) and (4.16)). It is given by

$$\begin{aligned}\mathbf{R}(\dot{\boldsymbol{\phi}}, \dot{\boldsymbol{\phi}}) = \frac{\tilde{\epsilon}}{3}\frac{1}{\kappa^2 g F_0}\Bigg[\frac{1}{2}\left(\frac{\phi^2 g_{,\phi\phi}}{g} - \frac{3}{2}\left(\frac{\phi g_{,\phi}}{g}\right)^2 - \frac{\phi g_{,\phi}}{g}\right)\frac{F_1^2}{F_2 F_0} \\ \times\left(F_1 \mathbb{1} - \frac{\mathbf{m}^2 \boldsymbol{\phi}\,\boldsymbol{\phi}^T}{\phi_0^2} - \frac{\boldsymbol{\phi}\,\boldsymbol{\phi}^T \mathbf{m}^2}{\phi_0^2} + \frac{F_2}{F_1}\frac{\boldsymbol{\phi}\,\boldsymbol{\phi}^T}{\phi_0^2}\right) \\ + \left(\frac{1}{4}\left(\frac{\phi g_{,\phi}}{g}\right)^2 + \frac{\phi g_{,\phi}}{g}\right)\left(F_1\mathbb{1} - \frac{F_1}{F_2}\frac{\mathbf{m}^2\boldsymbol{\phi}\,\boldsymbol{\phi}^T\mathbf{m}^2}{\phi_0^2}\right)\Bigg]. \qquad (6.81)\end{aligned}$$

The most important thing to note is the overall factor of $\tilde{\epsilon}$ when comparing this expression with the one for $\mathbf{M}^2$ in (6.72). Unless the metric factors become very large, which in the case of stereographical coordinates on the sphere, for example, is not the case (see below), this means that the $\mathbf{R}(\dot{\boldsymbol{\phi}}, \dot{\boldsymbol{\phi}})$ can be neglected in the expression for $\delta_{\mathcal{H}}$, as it leads only to corrections of second order in slow roll. Using this result, as well as (6.72) for $\mathbf{M}^2$, the slow-roll functions (6.74) and the expression $H^2 = (\phi_0^2 F_1/6)(1+\tilde{\epsilon}/3)$, we can work out the expressions for the scalar adiabatic and tensor amplitudes and spectral indices in a way analogous to the derivation of (6.39). The result is:

$$\begin{aligned}|\delta_{\mathbf{k}}^{\mathrm{ad}}|^2 &= \frac{2}{75\pi^2}\left(\frac{1}{4}\kappa^2\phi_0^2\right)^2 g F_0 F_1\left[1 + \frac{1}{\frac{1}{4}\kappa^2\phi_0^2\, g F_0}\left(B + \frac{1}{2}B\frac{\phi g_{,\phi}}{g} + \left(B - \frac{5}{6}\right)\frac{F_2 F_0}{F_1^2}\right)\right], \\ |\delta_{\mathbf{k}}^{\mathrm{tens}}|^2 &= \frac{16}{27\pi^2}\left(\frac{1}{4}\kappa^2\phi_0^2\right) F_1\left[1 + \frac{B - \frac{5}{6}}{\frac{1}{4}\kappa^2\phi_0^2\, g F_0}\,\frac{F_2 F_0}{F_1^2}\right], \qquad (6.82) \\ n_{\mathrm{ad}} - 1 &= \frac{-1}{\frac{1}{4}\kappa^2\phi_0^2\, g F_0}\left[1 + \frac{1}{2}\frac{\phi g_{,\phi}}{g} + \frac{F_2 F_0}{F_1^2}\right], \qquad n_{\mathrm{tens}} = \frac{-1}{\frac{1}{4}\kappa^2\phi_0^2\, g F_0}\,\frac{F_2 F_0}{F_1^2}.\end{aligned}$$

Here all functions F_n must be evaluated at the time of horizon crossing $t_{\mathcal{H}}$. Just as in the flat case no functions higher than F_2 occur in the final results and the factor $F_2 F_0/F_1^2$ is equal to the multiple-field term $(1 + U_{Pe}^T U_{Pe})$. This means that the leading-order expression for the ratio of tensor and scalar adiabatic perturbations is given by the same expression as in the flat case: $r = -(200/9) n_{\mathrm{tens}} F_1^2/(F_2 F_0)$. In the limit of $g \to 1$ the results agree with the flat case (6.39).

To go any further with the calculations we need an explicit expression for the function $g(\phi)$. We take the case of the sphere with stereographical coordinates, as given in (6.60): $g(\phi) = (4R^2/(4R^2+\phi^2))^2$ with R the radius of the sphere. Note that in the limit $\phi \to 0$, i.e. $\psi \to \infty$, the function g goes to its flat value: $g \to 1$. Hence the asymptotic results in (6.25) are valid here as well, so that $\tilde{\eta}^{\perp}$ goes to zero at the end of inflation for $m_2/m_1 > \sqrt{3}$.

The relation (6.69) for $\psi_{,N}$ can now be inverted and integrated to give an explicit expression for $N(\psi)$:

$$N(\psi) = \frac{N_\infty(1 - F_0(\psi))}{1 + \frac{N_\infty F_0(\psi)}{\kappa^2 R^2 - N_\infty}}, \qquad N_\infty = \frac{\kappa^2 R^2 \phi_0^2}{4R^2 + \phi_0^2}. \qquad (6.83)$$

	$\lvert\delta^{\rm ad}_{\mathbf{k}}\rvert^2$	$n_{\rm ad}-1$	$\lvert\delta^{\rm tens}_{\mathbf{k}}\rvert^2$	$n_{\rm tens}$	N_∞
$\kappa R = 10$	$3.08\cdot10^{-9}$	-0.060	$2.88\cdot10^{-9}$	-0.068	72
$\kappa R = 15$	$1.86\cdot10^{-9}$	-0.057	$0.93\cdot10^{-9}$	-0.047	120
$\kappa R = 20$	$1.60\cdot10^{-9}$	-0.054	$0.68\cdot10^{-9}$	-0.041	156
$\kappa R = 50$	$1.40\cdot10^{-9}$	-0.050	$0.52\cdot10^{-9}$	-0.034	232
$\kappa R \to \infty$	$1.37\cdot10^{-9}$	-0.049	$0.49\cdot10^{-9}$	-0.032	256

Table 6.3: The scalar adiabatic and tensor spectral amplitudes and indices for the mode k that crossed the Hubble scale 60 e-folds before the end of inflation, in the two-field model with a quadratic potential with masses $(m_1, m_2) = (1\,,\,2.5)\cdot10^{-5}$ and initial conditions $\kappa\boldsymbol{\phi}_0 = (20, 25)$ on a spherical field manifold with radius R using stereographical coordinates. Given are the values of the spectral quantities for five different values of κR, as well as the total amount of inflation in those cases. To compute the values the half-slow-roll solution has been used (i.e. exact numerical background and analytical first-order slow-roll perturbations).

Using this equation at time $t_{\mathcal{H}}$, we can view it as a relation giving $F_0(\psi_{\mathcal{H}})$ in terms of $N_k \equiv N_\infty - N_{\mathcal{H}}$:

$$F_0(\psi_{\mathcal{H}}) = \frac{\phi^2_{\mathcal{H}}}{\phi_0^2} = \frac{N_k(\kappa^2R^2 - N_\infty)}{N_\infty(\kappa^2R^2 - N_k)}, \tag{6.84}$$

leading to the following results:

$$\sqrt{g} = \frac{\kappa^2R^2 - N_k}{\kappa^2R^2}, \qquad \frac{1}{4}\kappa^2\phi_0^2\sqrt{g}\,F_0 = N_k, \qquad 1 + \frac{1}{2}\frac{\phi g_{,\phi}}{g} = 2\sqrt{g} - 1. \tag{6.85}$$

Here the explicit argument $\psi_{\mathcal{H}}$ has been omitted, but it should be kept in mind that these relations are only valid at $t_{\mathcal{H}}$. With these results the expressions in (6.82) simplify to

$$\begin{aligned}
\lvert\delta^{\rm ad}_{\mathbf{k}}\rvert^2 &= \frac{2}{75\pi^2}N_k^2\frac{F_1}{F_0}\left[1 + \frac{2B}{N_k} + \frac{1}{N_k}\frac{\kappa^2R^2}{\kappa^2R^2 - N_k}\left(-B + \left(B - \frac{5}{6}\right)\frac{F_2F_0}{F_1^2}\right)\right],\\
\lvert\delta^{\rm tens}_{\mathbf{k}}\rvert^2 &= \frac{16}{27\pi^2}N_k\frac{F_1}{F_0}\frac{\kappa^2R^2}{\kappa^2R^2 - N_k}\left[1 + \frac{B - \frac{5}{6}}{N_k}\frac{\kappa^2R^2}{\kappa^2R^2 - N_k}\frac{F_2F_0}{F_1^2}\right],\\
n_{\rm ad} - 1 &= -\frac{2}{N_k}\left[1 + \frac{1}{2}\frac{\kappa^2R^2}{\kappa^2R^2 - N_k}\left(\frac{F_2F_0}{F_1^2} - 1\right)\right], \qquad n_{\rm tens} = -\frac{1}{N_k}\frac{\kappa^2R^2}{\kappa^2R^2 - N_k}\frac{F_2F_0}{F_1^2}.
\end{aligned} \tag{6.86}$$

In the limit of equal masses, where $F_2F_0/F_1^2 \to 1$ and $F_1/F_0 \to m^2$, these results agree with (6.67). Hence we find a combination of the results (6.39) for a general mass matrix on a flat field manifold and (6.67) for equal masses on a spherical field manifold with stereographical coordinates: the multiple-field effects are encoded in the two combinations F_1/F_0 and F_2F_0/F_1^2, as well as in the non-trivial curvature factor $\kappa^2R^2/(\kappa^2R^2 - N_k)$.

As a numerical illustration we consider the specific two-field example with initial conditions $\kappa\boldsymbol{\phi}_0 = (20, 25)$ and mass values $m_1 = 1\cdot10^{-5}$ and $m_2 = 2.5\cdot10^{-5}$. Taking $N_k = 60$ the results for the spectral amplitudes and indices using the half-slow-roll solution (exact numerical background and analytical first-order slow-roll perturbations) are given in table 6.3 for several values of the radius R. In the limit $R \to \infty$ this is the same model as was considered in §6.2.3. The slow-roll estimates N_∞ for the total amount of inflation are also given. We see that especially the tensor quantities increase very rapidly with smaller R, as was also the case for equal masses, see figure 6.6(b). The total amount of

inflation decreases for smaller R. In contrast to the case of equal masses, the scalar adiabatic quantities are also influenced by the change in R, increasing for smaller R, although not as much as the tensor quantities.

6.6 Summary and conclusion

In this chapter we studied the example of inflation with a quadratic potential in various settings: equal masses and general mass matrix, flat field manifold and curved field space. The basic purpose was to illustrate the general theory of chapters 3 to 5 and check our analytical results numerically. However, some of the results in this chapter are interesting in their own right.

We started with the simple model of equal masses and a flat field space, to be used as a reference model. As expected this situation is identical to the single-field case. The generalization to the case of a general mass matrix gave the following results. In the first place it turns out to be possible to solve the slow-roll background field equation in terms of a single scalar function ψ, independently of the actual number of scalar fields. In other words, we determined the trajectory of the scalar-field vector through field space, and it is only the way in which this trajectory is traversed that in general cannot be determined analytically. Secondly, we defined the functions $F_n(\psi)$, which further depend on the mass matrix and the direction of the initial-condition vector $\boldsymbol{\phi}_0$. In terms of these functions all background quantities, like the slow-roll functions, can be given explicitly. Studying the asymptotic behaviour of these functions we found that, if the mass ratio between the two smallest mass eigenvalues is larger than $\sqrt{3}$, the slow-roll function $\tilde{\eta}^{\perp}$ goes to zero at the end of inflation. As a third result it was found that the expression for the vector U_{Pe}, which represents the multiple-field effects in the adiabatic perturbations, can be worked out explicitly in this example. If end-of-inflation effects can be neglected, for example if $\tilde{\eta}^{\perp}$ goes to zero, the spectral amplitudes and indices for the scalar adiabatic and the tensor perturbations can all be given completely in terms of the F_n (evaluated at horizon crossing) as well. The multiple-field effects then turn out to be encoded in only two explicit combinations of the three quantities F_0, F_1 and F_2.

To check our analytical results, we treated an explicit two-field example numerically. The analytical perturbation results were found to be very accurate, easily justifying our claim of first-order slow-roll accuracy at the level of the solutions. On the other hand, the accuracy of the analytical slow-roll background results was found to be less, as was expected because of the large integration intervals involved. As the exact background equations can be solved numerically very quickly, while the perturbation equations demand much more computer time, computing the background numerically (exact) and the perturbations analytically (slow roll) seems to give the optimal combination of accuracy and speed (for models where end-of-inflation effects can be neglected). Furthermore, it was found that multiple-field effects can be the source of no less than half the total result, so that they should merit serious consideration, even for leading-order estimates.

To study the effects of a non-trivial field metric we considered the case of a curved field manifold that is isotropic around the origin. For a general potential we found that if one has an expression for the trajectory of the fields in the corresponding flat case in terms of a single function ψ, then one can give the slow-roll solution for the background fields in the curved case in terms of ψ and one additional scalar function s. Defining functions C_n in terms of the potential and its derivatives it is also possible to give general leading-order

expressions for the slow-roll functions.

Proceeding to the specific case of a quadratic potential with equal masses on a spherical field manifold we considered two situations: embedding coordinates and stereographical coordinates. (Note that, as the potential in the two cases was given by the same function of the coordinates, they represent two different physical configurations.) Although the results in the two situations were rather different, one can draw the conclusion that, for a small enough radius of the sphere ($\kappa R \lesssim 30$), they differ significantly from the single-field case.

Finally we treated the example of a general mass matrix on a curved field manifold. For certain situations the function $s(\psi)$ was determined explicitly, and then all background quantities could be given in terms of the same functions $F_n(\psi)$ as in the flat case. For the case of a field metric that is proportional to the identity matrix the vector U_{Pe} was worked out explicitly and, neglecting end-of-inflation effects, the scalar adiabatic and tensor spectral amplitudes and indices were determined explicitly in terms of the F_n as well. The effect of the curvature tensor on the mass matrix was found to be negligible to first order in slow roll. For a spherical field manifold with stereographical coordinates the results turn out to be a combination of the cases treated before: multiple-field effects are encoded in the same two combinations of F_0, F_1 and F_2 as in the flat case, as well as in the same R-dependent factors we find in the case of equal masses with stereographical coordinates. It will be very interesting to apply the general formalism to models with more realistic potentials and field metrics from specific high-energy theories.

Chapter 7

Conclusion and outlook

Inflation not only offers a solution for the horizon, flatness, topological defects and large-scale homogeneity problems of the standard Big Bang theory, it also provides a mechanism to explain the tiny fluctuations that are observed in the cosmic microwave background radiation (CMBR). These fluctuations are the gravitational seeds for the formation of the large-scale structures of the universe at later times. The simplest models for inflation only need a single scalar field as dominant form of energy in the universe, with a potential satisfying certain flatness (slow-roll) conditions. Of course for realistic models of inflation this scalar field and its potential should be part of a theoretical high-energy model. Present high-energy theories, like supersymmetry or effective supergravity from string theory, usually contain not one but many scalar fields, with the additional complication that these fields may live in a curved field space with a non-trivial field metric. Motivated by these facts we have, in the work presented in this thesis, developed an analytical formalism to describe slow-roll inflation in the very general setting of multiple scalar fields, an arbitrary potential and a non-trivial field metric. Special attention was paid to the production of the density fluctuations.

There are two main reasons to emphasize an analytical treatment (as opposed to a numerical one). In the first place analytical expressions provide more insight into the underlying physics: one can immediately see the dependence on the various variables and parameters in the results. Secondly there is a practical reason: numerical calculations can take a very long time (and they typically do for the perturbation equations), especially if they have to be repeated for different parameter values. The disadvantage of the analytical treatment is that in most cases the exact equations are too complicated to solve and one has to use the slow-roll approximation. Then one must take care that the end results are of sufficient accuracy.

To be able to distinguish and identify the various directions in field space one needs a basis. We introduced a special basis, induced by the dynamics of the background fields, that is especially useful when dealing with the perturbations, see below. We also generalized the slow-roll conditions by defining multiple-field slow-roll functions as functions of the field velocity and Hubble parameter and their derivatives. For slow-roll inflation to be possible these functions have to be small, which offers the opportunity of setting up a slow-roll expansion. To leading order in this expansion the slow-roll functions can be written in terms of only the potential and field metric and their derivatives, but our definition makes it possible to go beyond leading order. Regarding the solutions of slow-roll

approximated equations of motion one has to keep in mind that a too large interval of integration might compromise the accuracy of the results. We introduced the concept of a slow-roll derivative, which is very useful to keep track of orders in slow roll while switching between different time variables, and which makes it possible to write the equations in a form that is independent of the specific choice of time variable.

Perturbations can be divided into three types: scalar, vector and tensor. Vector perturbations are not produced by inflation, while the production of tensor perturbations follows the standard theory and depends only on inflation through the background. On the other hand, scalar perturbations depend very much on the details of inflation, and the existence of multiple fields adds quite some complications. There are two basic scalar perturbation quantities: the gravitational potential and the scalar field perturbation vector. One of the components of this vector is not independent of the gravitational potential; using our basis it is the $\mathbf{e}_1$ component. Moreover, with our basis it is only the $\mathbf{e}_2$ component of the field perturbation that enters as an inhomogeneous source term into the equation of motion for the gravitational potential. Using a specific redefinition of the field perturbation vector in combination with our basis the perturbations can be quantized in a straightforward way.

During inflation there is a sudden transition in the behaviour of a perturbation mode when the corresponding wavelength becomes of the order of the Hubble length. To be able to treat the perturbations analytically during this transition, one needs the assumption of slow roll. We studied the transition region very carefully, to make sure that even in the presence of multiple fields we can guarantee an accuracy to first order in slow roll. We also found that the method used in the literature for the single-field case, although giving the right result, is not completely correct. The end results of our treatment are expressions for the gravitational potential, the field perturbation vector and the tensor perturbation at the end of (slow-roll) inflation, valid to first order in slow roll.

We also studied what happens with these perturbations after inflation. The equation of motion for the gravitational potential after inflation is similar to the one during inflation, with again a single inhomogeneous source term, called the total entropy perturbation. It is related to the $\mathbf{e}_2$ component of the scalar field perturbation at the end of inflation. In the case that the existence of quintessence can be neglected and that there are no interactions between the various (ideal fluid) components at super-horizon scales, the total entropy perturbation was found to be constant after inflation. The final results are expressions for the spectral amplitudes and indices for the different perturbation components (scalar adiabatic, isocurvature and mixing, and tensor), which relate the inflationary perturbations to the observed temperature fluctuations in the CMBR.

The two main consequences of the presence of multiple scalar fields during inflation regarding these observational quantities are: the existence of isocurvature and mixing components, and additional terms in the adiabatic component. All multiple-field terms show a crucial dependence on the slow-roll function $\tilde{\eta}^{\perp}$. If it is zero during the last 60 e-folds of inflation, multiple-field effects are not observable. We derived a relation between the ratio of the tensor and scalar adiabatic amplitudes on the one side, and the tensor spectral index on the other, that will clearly show whether multiple-field effects are significant once both quantities can be observed with sufficient accuracy.

To illustrate the general theory and check our results numerically we worked out the example of a quadratic potential with multiple fields in great detail, both in a flat and a curved field space. In the flat case we found explicit first-order expressions for the background quantities, like the slow-roll functions, as well as for the scalar and tensor amplitudes and spectral indices, in terms of a single scalar function that in general cannot

be determined analytically. (For the perturbations we made the assumption that $\tilde{\eta}^{\perp}$ goes to zero at the end of inflation, which turns out to be correct for most mass values.) Taking a specific two-field model to compute some numbers we found that multiple-field effects can account for about half the total result. Hence the possible influence of multiple-field effects should be taken very seriously. Moreover, we found that our analytical results for the perturbations are indeed accurate up to and including first order in slow roll (which here means a relative error of order 0.001 or smaller for the amplitudes).

To study the influence of a non-trivial field metric, we also worked out the example of a quadratic potential on a spherical field space. Of course the radius of the sphere is an additional parameter in these models. We found that the background quantities can still be given explicitly to first order, although there is now an additional, a priori unknown, scalar function. However, for the two different configurations we studied this second function was determined analytically. A completely explicit analytical expression for the perturbations is not always possible. From the cases where we found such an expression we see that, depending on the model, the effects of the non-trivial curvature can vary between being of leading-order importance and being negligible. Moreover, they may lead to an increase or a decrease and can affect scalar and tensor perturbations differently. Hence even the relatively simple models considered in this thesis can differ significantly from the single-field case in various ways. It will be very interesting to apply our theory to more realistic models from high-enery theory.

The analytical formalism of the background and the perturbations during multiple-field slow-roll inflation described in this thesis is quite complete. However, it is always possible to find some areas where it might be extended. It might be nice to extend the analytical treatment of the transition region and of the perpendicular field perturbations in the super-horizon region beyond first order in slow roll, but it seems highly unlikely that this can be done. Moreover, before embarking on such a project one has to consider if an advantage with respect to an exact numerical treatment is still to be expected. Another possible addition to the formalism would be to try and include effects of non-vacuum initial states and trans-Planckian effects on the dispersion relation, as was mentioned briefly when we discussed quantization, but at present ideas about this are still very speculative.

On the contrary, the treatment of the perturbations after inflation is still far from complete. Most importantly, a systematic formalism for the perturbations during the transition at the end of inflation and (p)reheating is still missing, although under investigation. Especially for an accurate treatment of the isocurvature perturbations this will be very important. (An additional bonus is that such a formalism will also be applicable in the case of inflation with a break: a brief period during the inflation era when the slow-roll conditions are no longer satisfied.) As long as one only considers models where $\tilde{\eta}^{\perp}$ goes to zero at the end of inflation, one gets around this problem. Although models like that still leave room for interesting multiple-field effects, as shown in the examples, it would be nice to lift this restriction. Other aspects that should be investigated are: the inclusion of quintessence, the effects of interactions, and the influence of a possible individual hot dark matter entropy perturbation on the CMBR.

My view of the future regarding observational constraints on the inflationary parameters is moderately optimistic. The new satellite missions MAP (from the end of this year) and especially Planck (from 2007) will provide very accurate values for the spectral amplitudes and indices. As mentioned above this will clearly establish whether multiple-field effects are of significant importance during the observable part of inflation (assuming that the tensor perturbations are large enough to be observed). It also offers at least four

constraint relations (scalar adiabatic and tensor) for the inflationary parameters. If the theories of isocurvature perturbations and of non-Gaussianity from inflation are brought to a sufficient level of accuracy, the observational data will offer even more useful information. However, and this is one of the reasons for the qualifier 'moderately', that might be quite a difficult task. Moreover, inflation models, especially multiple-field ones with a non-trivial field metric, may easily have many more free parameters than there are observational constraint relations. This leads to degeneracies in the determination of inflationary parameters. In particular, if there are more than 60 e-folds of inflation, any features in the potential that only play a role before those last 60 e-folds are basically unobservable. Here it will be the task of high-energy theorists, e.g. string theorists, to determine from other considerations which types of inflation models are realistic. Anyhow, the next years will certainly be very interesting for (inflationary) cosmology because of the wealth of new observational data.

Appendix A

Conventions and definitions

In this appendix the conventions applied throughout this thesis are described. For units we use the so-called natural units, as employed in almost all papers and books in high-energy physics and cosmology. In this system one sets

$$\hbar = c = k_B = 1. \tag{A.1}$$

By using

$$\begin{aligned} \hbar &= 1.054571596 \cdot 10^{-34}\ \mathrm{J \cdot s}, \\ c &= 2.99792458 \cdot 10^{8}\ \mathrm{m/s}, \\ k_B &= 1.3806503 \cdot 10^{-23}\ \mathrm{J/K}, \end{aligned} \tag{A.2}$$

and $E = mc^2$ one finds that in this system only one unit need be chosen. This unit is often called [mass]. Hence

$$[\text{energy}] = [\text{temperature}] = [\text{mass}], \qquad [\text{time}] = [\text{length}] = [\text{mass}]^{-1}.$$

Taking as this one unit the GeV, the following table (which can be calculated directly from the expressions given above) can be used to convert these natural units to the SI units:

1 GeV corresponds with:	$1.602 \cdot 10^{-10}$ J	(energy);
	$1.160 \cdot 10^{13}$ K	(temperature);
	$1.783 \cdot 10^{-27}$ kg	(mass).
1 $(\mathrm{GeV})^{-1}$ corresponds with:	$6.582 \cdot 10^{-25}$ s	(time);
	$1.973 \cdot 10^{-16}$ m	(length).

In natural units Newton's constant of gravitation, $G = 6.673 \cdot 10^{-11}\ \mathrm{m^3\ kg^{-1}\ s^{-2}}$, can be written as $G = 1/M_P^2$. Here M_P is the Planck mass, defined as that mass at which the Schwarzschild radius and the Compton wavelength are approximately equal, i.e. $GM_P/c^2 = \hbar/(M_P c)$, so that $M_P = 1 \cdot 10^{19}$ GeV. As one usually encounters the combination $8\pi G$, the so-called inverse reduced Planck mass κ is defined as

$$\kappa^2 \equiv 8\pi G = \frac{8\pi}{M_P^2}; \qquad \kappa^{-1} = 2.435 \cdot 10^{18}\ \mathrm{GeV}. \tag{A.3}$$

Especially in numerical examples we often present quantities in Planck units, i.e. in units of some power of κ (depending on the dimension of the quantity under consideration). For example, instead of plotting comoving time t the dimensionless quantity t/κ is used.

Next we discuss the conventions used for the relativistic quantities. In the field of general relativity many different conventions are used side by side. Although they mostly differ only in an overall minus sign, it is necessary to know which convention is being used. To combine expressions from authors using different conventions without knowing that they do can lead to disaster! For the metric tensor we use the sign convention $(-,+,+,+)$. Hence, in Minkowski space:

$$\mathrm{d}s^2 = -\mathrm{d}t^2 + \mathrm{d}x^2 + \mathrm{d}y^2 + \mathrm{d}z^2. \tag{A.4}$$

For a general spacetime with metric tensor $g_{\mu\nu}$ and inverse $g^{\mu\nu}$, we find the Christoffel symbols (or affine/metric connection fields):

$$\Gamma^{\alpha}_{\beta\gamma} = \frac{1}{2} g^{\alpha\delta} \left(g_{\delta\beta,\gamma} + g_{\delta\gamma,\beta} - g_{\beta\gamma,\delta} \right). \tag{A.5}$$

Here $_{,\beta}$ means differentiating with respect to x^{β}, also denoted by ∂_{β}. The Riemann curvature tensor is defined as follows:

$$R^{\alpha}_{\ \beta\gamma\delta} = \Gamma^{\alpha}_{\beta\delta,\gamma} - \Gamma^{\alpha}_{\beta\gamma,\delta} + \Gamma^{\alpha}_{\gamma\epsilon}\Gamma^{\epsilon}_{\beta\delta} - \Gamma^{\alpha}_{\delta\epsilon}\Gamma^{\epsilon}_{\beta\gamma}, \tag{A.6}$$

while for the Ricci tensor the following contraction is used:

$$R_{\mu\nu} \equiv R^{\alpha}_{\ \mu\alpha\nu} = \Gamma^{\alpha}_{\mu\nu,\alpha} - \Gamma^{\alpha}_{\mu\alpha,\nu} + \Gamma^{\alpha}_{\mu\nu}\Gamma^{\beta}_{\alpha\beta} - \Gamma^{\alpha}_{\mu\beta}\Gamma^{\beta}_{\nu\alpha}. \tag{A.7}$$

Finally the Ricci scalar curvature and the Einstein tensor are defined by

$$R = g^{\mu\nu}R_{\mu\nu}, \qquad G_{\mu\nu} = R_{\mu\nu} - \frac{1}{2}g_{\mu\nu}R. \tag{A.8}$$

In our notation Greek indices $\alpha, \beta, \gamma, \ldots$ run from 0 to 3; Roman indices $i, j, k, \ldots$ run from 1 to 3, thus indicating only space components. The Roman indices $a, b, c, \ldots$ are used to label the components in the internal field space, see below, and their range depends on the number of fields.

Starting from section 2.2 we only work in a spatially flat background spacetime, as is explained there. The symbol Δ is used for the spatial Laplacean, which in a flat background is given by:

$$\Delta \equiv \sum_{i=1}^{3} \partial_i^2. \tag{A.9}$$

In our treatment of the space-dependent perturbations we often switch to complex Fourier modes $f_{\mathbf{k}}(t)$, defined by

$$f(t, \mathbf{x}) = \frac{1}{(2\pi)^{3/2}} \int \mathrm{d}^3\mathbf{k} \left(f_{\mathbf{k}}(t) e^{-i\mathbf{k}\mathbf{x}} + f^*_{\mathbf{k}}(t) e^{i\mathbf{k}\mathbf{x}} \right), \tag{A.10}$$

where f is any real quantity that depends on both time and space coordinates. After this switch equations for $f(t, \mathbf{x})$ become equations for $f_{\mathbf{k}}(t)$ and the spatial Laplacean $-\Delta$ is

replaced by $k^2 = |\mathbf{k}|^2$. This expansion in Fourier modes is only possible for a spatially flat background; for a curved space one must use different expansion functions.

Next to the four-dimensional spacetime, the internal field space plays an important role in this thesis. It is a real manifold $\mathcal{M}$ with a metric $\mathbf{G}$ and local coordinates $\boldsymbol{\phi} = (\phi^a)$. From the components of this metric G_{ab} the metric connection Γ^a_{bc} and the curvature tensor R^a_{bcd} of the field manifold are obtained according to the definitions (A.5) and (A.6). Using tangent vectors $\mathbf{B}, \mathbf{C}$ the curvature tensor can be written without taking explicit components:

$$[\mathbf{R}(\mathbf{B}, \mathbf{C})]^a_{\ d} \equiv R^a_{\ bcd}\, B^b C^c. \tag{A.11}$$

One should realize that for notational convenience (see e.g. (4.16)) we have introduced the matrix $\mathbf{R}(\mathbf{B}, \mathbf{C})$ instead of the more standard vector $\mathbf{R}(\mathbf{C}, \mathbf{D}, \mathbf{B})$ (see e.g. [143]); that vector is equal to $\mathbf{R}(\mathbf{B}, \mathbf{C})\,\mathbf{D}$ in our notation.

The definition of the manifold $\mathcal{M}$ is coordinate independent, therefore the description of this manifold should be invariant under non-singular local coordinate transformations

$$\phi^a \to \tilde{\phi}^a = X^a(\phi). \tag{A.12}$$

A vector $\mathbf{A} = (A^a)$ is called a vector in the tangent space $T_p\mathcal{M}$ at a point $p \in \mathcal{M}$ if it transforms as

$$A^a \to \tilde{A}^a = X^a_{\ b}(\phi) A^b, \qquad\qquad X^a_{\ b}(\phi) = X^a_{\ ,b}(\phi), \tag{A.13}$$

where the comma denotes differentiation with respect to local coordinates. The cotangent space is the dual of the tangent space. Its elements are linear operators on the tangent space,

$$\begin{array}{rccc} {}^*\mathbf{C}: & T_p\mathcal{M} & \to & \mathbb{R} \\ & \mathbf{A} & \mapsto & C_a A^a \end{array} \tag{A.14}$$

As $C_a A^a$ is a scalar object, the cotangent vector ${}^*\mathbf{C}$ transforms as

$$C_a \to \tilde{C}_a = C_b (X^{-1})^b_{\ a}. \tag{A.15}$$

The metric G_{ab} can be used to construct a cotangent vector $(\mathbf{A}^\dagger)_a \equiv A^b G_{ba}$ from the tangent vector $\mathbf{A}$. Using index-free notation this reads as $\mathbf{A}^\dagger = \mathbf{A}^T\mathbf{G}$, where the superscript T denotes the transpose. The notion of (co)tangent vectors defined at a point $p \in \mathcal{M}$ can be extended over the whole manifold $\mathcal{M}$ by interpreting them as sections of the (co)tangent bundle.

The metric $\mathbf{G}$ introduces an inner product and the corresponding norm on the tangent bundle of the manifold:

$$\mathbf{A} \cdot \mathbf{B} \equiv \mathbf{A}^\dagger \mathbf{B} = \mathbf{A}^T \mathbf{G} \mathbf{B} = A^a G_{ab} B^b, \qquad\qquad |\mathbf{A}| \equiv \sqrt{\mathbf{A} \cdot \mathbf{A}}, \tag{A.16}$$

for any two vector fields $\mathbf{A}$ and $\mathbf{B}$. The Hermitean conjugate $\mathbf{L}^\dagger$ of a linear operator $\mathbf{L} : T_p\mathcal{M} \to T_p\mathcal{M}$ with respect to this inner product is defined by

$$\mathbf{B} \cdot (\mathbf{L}^\dagger \mathbf{A}) \equiv (\mathbf{L}\mathbf{B}) \cdot \mathbf{A}, \tag{A.17}$$

so that $\mathbf{L}^\dagger = \mathbf{G}^{-1}\mathbf{L}^T\mathbf{G}$. A Hermitean operator $\mathbf{H}$ satisfies $\mathbf{H}^\dagger = \mathbf{H}$. An important example of Hermitean operators are the projection operators. Apart from being Hermitean, a projection operator $\mathbf{P}$ is idempotent: $\mathbf{P}^2 = \mathbf{P}$.

To complete the discussion on conventions and definitions we define different types of derivatives. Next to the normal spacetime derivative there is the covariant spacetime derivative (denoted by $_{;\nu}$ or D_ν), defined on a general mixed tensor in spacetime as

$$D_\nu T^{\alpha\beta\cdots}_{\gamma\delta\cdots} = \partial_\nu T^{\alpha\beta\cdots}_{\gamma\delta\cdots} + \Gamma^\alpha_{\mu\nu} T^{\mu\beta\cdots}_{\gamma\delta\cdots} + \Gamma^\beta_{\mu\nu} T^{\alpha\mu\cdots}_{\gamma\delta\cdots} + \cdots - \Gamma^\mu_{\gamma\nu} T^{\alpha\beta\cdots}_{\mu\delta\cdots} - \Gamma^\mu_{\delta\nu} T^{\alpha\beta\cdots}_{\gamma\mu\cdots} - \cdots . \tag{A.18}$$

The covariant derivative on the field manifold, denoted by ∇_a, is defined in a completely equivalent way. On a vector A^a in field space it acts as

$$\nabla_b A^a \equiv A^a_{,b} + \Gamma^a_{bc} A^c, \tag{A.19}$$

while on a scalar function V the derivative $\boldsymbol{\partial}$ and the covariant derivative $\boldsymbol{\nabla}$ are equal: $(\boldsymbol{\nabla} V)_a = (\boldsymbol{\partial} V)_a \equiv V_{,a} \equiv \partial V/\partial\phi^a$. If we represent $\mathrm{d}\boldsymbol{\phi}$ as a column vector, $\boldsymbol{\nabla}$ and $\boldsymbol{\partial}$ are row vectors and therefore $\boldsymbol{\nabla}^T$ and $\boldsymbol{\partial}^T$ are column vectors. The second covariant derivative of a scalar function V is a matrix with two lower indices: $(\boldsymbol{\nabla}^T\boldsymbol{\nabla} V)_{ab} = \nabla_a\nabla_b V$. Finally we also need the concept of a spacetime derivative that is covariant with respect to the field space, e.g. to take the time derivative of a quantity that is a scalar in spacetime, but a vector in field space. This covariant derivative is denoted by $\mathcal{D}_\mu$ and it acts on a vector $\mathbf{A}$ of the tangent bundle as follows:

$$\mathcal{D}_\mu A^a = \partial_\mu A^a + \Gamma^a_{bc}\partial_\mu\phi^b A^c, \tag{A.20}$$

while $\mathcal{D}_\mu$ acting on a scalar is simply equal to ∂_μ.

Appendix B

Explicit expressions for the metric quantities

Infinitesimal coordinate transformations

$$x^\mu \to \tilde{x}^\mu = x^\mu + \xi^\mu \quad \Rightarrow \quad g_{\mu\nu}(x) \to \tilde{g}_{\mu\nu}(\tilde{x}) = (X^{-1})^\rho_\mu (X^{-1})^\sigma_\nu g_{\rho\sigma}(x), \quad X^\mu_\nu \equiv \frac{\partial \tilde{x}^\mu}{\partial x^\nu} \tag{B.1}$$

$$\tilde{g}_{\mu\nu}(x) = g_{\mu\nu}(x) - g_{\mu\nu,\rho}\xi^\rho - g_{\mu\rho}\xi^\rho_{,\nu} - g_{\rho\nu}\xi^\rho_{,\mu} = g_{\mu\nu}(x) - D_\mu\xi_\nu - D_\nu\xi_\mu \tag{B.2}$$

$$= a^2 \begin{pmatrix} -1 & 0 \\ 0 & \delta_{ij} \end{pmatrix} - a^2 \begin{pmatrix} -2(\xi^0)' - 2\mathcal{H}\xi^0 & -\xi^0_{,i} + \delta_{ik}(\xi^k)' \\ -\xi^0_{,j} + \delta_{jk}(\xi^k)' & 2\mathcal{H}\xi^0\delta_{ij} + \delta_{ik}\xi^k_{,j} + \delta_{jk}\xi^k_{,i} \end{pmatrix} \quad \text{(for flat RW)} \tag{B.3}$$

Background metric quantities

$$g_{00} = -b(\tau)^2 \qquad g_{0i} = 0 \qquad g_{ij} = a(\tau)^2 \left(\delta_{ij} + \frac{K x^i x^j}{1 - K r^2} \right) \quad \text{(see (2.2))} \tag{B.4}$$

$$\begin{aligned} &\Gamma^0_{00} = H_b \qquad \Gamma^0_{0i} = 0 \qquad \Gamma^0_{ij} = \frac{H_a}{b^2}\, g_{ij} \\ &\Gamma^i_{00} = 0 \qquad \Gamma^i_{0j} = H_a \delta^i_j \quad \Gamma^i_{jk} = \frac{K x^i}{a^2}\, g_{jk} \end{aligned} \tag{B.5}$$

$$R_{00} = 3H_aH_b - 3\frac{a^{;;}}{a} \quad R_{0i} = 0 \qquad R_{ij} = \left(\frac{1}{b^2}\frac{a^{;;}}{a} + \frac{H_a(2H_a - H_b)}{b^2} + \frac{2K}{a^2} \right) g_{ij} \tag{B.6}$$

$$R = 6\left(\frac{1}{b^2}\frac{a^{;;}}{a} + \frac{H_a(H_a - H_b)}{b^2} + \frac{K}{a^2} \right) \tag{B.7}$$

$$G_{00} = 3H_a^2 + 3K\frac{b^2}{a^2} \qquad G_{0i} = 0 \qquad G_{ij} = -\left(\frac{2}{b^2}\frac{a^{\cdot\cdot}}{a} + \frac{H_a(H_a - 2H_b)}{b^2} + \frac{K}{a^2}\right) g_{ij} \tag{B.8}$$

with $H_a \equiv a^{\cdot}/a$, $H_b \equiv b^{\cdot}/b$ and $^{\cdot} \equiv \frac{\partial}{\partial\tau}$.

Perturbed metric quantities

$$\delta g^{\mu\nu} = -g^{\mu\rho}g^{\nu\sigma}\delta g_{\rho\sigma} \qquad\qquad \delta\sqrt{-g} = \frac{1}{2}\sqrt{-g}\, g^{\mu\nu}\delta g_{\mu\nu} \tag{B.9}$$

$$g_{\mu\nu} = a^2\begin{pmatrix}-1 & 0\\ 0 & \delta_{ij}\end{pmatrix} - 2a^2\begin{pmatrix}\Phi & 0\\ 0 & \Psi\delta_{ij}\end{pmatrix} + a^2\begin{pmatrix}0 & S_j\\ S_i & 0\end{pmatrix} + a^2\begin{pmatrix}0 & 0\\ 0 & h_{ij}\end{pmatrix} \tag{B.10}$$

(flat universe, longitudinal & vector gauge, see (4.2))

Scalar perturbations

$$\begin{aligned}
&\delta\Gamma^0_{00} = \Phi' && \delta\Gamma^0_{0i} = \Phi_{,i} && \delta\Gamma^0_{ij} = -\left(\Psi' + 2\mathcal{H}(\Phi+\Psi)\right)\delta_{ij}\\
&\delta\Gamma^i_{00} = \delta^{ij}\Phi_{,j} && \delta\Gamma^i_{0j} = -\Psi'\delta^i_j && \delta\Gamma^i_{jk} = -\Psi_{,k}\delta^i_j - \Psi_{,j}\delta^i_k + \delta^{il}\Psi_{,l}\delta_{jk}
\end{aligned} \tag{B.11}$$

$$\begin{aligned}
&\delta R_{00} = 3\Psi'' + \Delta\Psi + 3\mathcal{H}(\Phi' + \Psi') && \delta R_{0i} = 2(\Psi' + \mathcal{H}\Phi)_{,i}\\
&\delta R_{ij} = -\left[\Psi'' - \Delta\Psi + \mathcal{H}(\Phi' + 5\Psi') + 2(\mathcal{H}' + 2\mathcal{H}^2)(\Phi+\Psi)\right]\delta_{ij} - (\Phi - \Psi)_{,ij}
\end{aligned} \tag{B.12}$$

$$\delta R = -\frac{2}{a^2}\left[3\Psi'' + \Delta(\Phi - 2\Psi) + 3\mathcal{H}(\Phi' + 3\Psi') + 6(\mathcal{H}' + \mathcal{H}^2)\Phi\right] \tag{B.13}$$

$$\begin{aligned}
&\delta G_{00} = 2(\Delta\Psi - 3\mathcal{H}\Psi') && \delta G_{0i} = 2(\Psi' + \mathcal{H}\Phi)_{,i}\\
&\delta G_{ij} = 2\left[\Psi'' + \frac{1}{2}\Delta(\Phi - \Psi) + \mathcal{H}(\Phi' + 2\Psi') + (2\mathcal{H}' + \mathcal{H}^2)(\Phi+\Psi)\right]\delta_{ij} - (\Phi - \Psi)_{,ij}
\end{aligned} \tag{B.14}$$

$$\begin{aligned}
&\delta G^0_{\ 0} = \frac{2}{a^2}\left(-\Delta\Psi + 3\mathcal{H}(\Psi' + \mathcal{H}\Phi)\right) && \delta G^0_{\ i} = -\frac{2}{a^2}(\Psi' + \mathcal{H}\Phi)_{,i}\\
&\delta G^i_{\ j} = \frac{2}{a^2}\left[\Psi'' + \frac{1}{2}\Delta(\Phi - \Psi) + \mathcal{H}(\Phi' + 2\Psi') + (2\mathcal{H}' + \mathcal{H}^2)\Phi\right]\delta^i_j - \frac{\delta^{ik}}{a^2}(\Phi - \Psi)_{,kj}
\end{aligned} \tag{B.15}$$

Vector perturbations

$$\begin{aligned}
&\delta\Gamma^0_{00} = 0 && \delta\Gamma^0_{0i} = \mathcal{H}S_i && \delta\Gamma^0_{ij} = -\frac{1}{2}(S_{i,j} + S_{j,i})\\
&\delta\Gamma^i_{00} = \delta^{ik}(S_k' + \mathcal{H}S_k) && \delta\Gamma^i_{0j} = \frac{1}{2}\delta^{ik}(S_{k,j} - S_{j,k}) && \delta\Gamma^i_{jk} = -\mathcal{H}\delta^{il}S_l\delta_{jk}
\end{aligned} \tag{B.16}$$

$$\delta R_{00} = 0 \qquad \delta R_{0i} = -\frac{1}{2}\Delta S_i + (\mathcal{H}' + 2\mathcal{H}^2)S_i$$
$$\delta R_{ij} = -\frac{1}{2}(S_{i,j} + S_{j,i})' - \mathcal{H}(S_{i,j} + S_{j,i}) \qquad \delta R = 0 \tag{B.17}$$

$$\delta G_{00} = 0 \quad \delta G_{0i} = -\frac{1}{2}\Delta S_i - (2\mathcal{H}' + \mathcal{H}^2)S_i \quad \delta G_{ij} = -\frac{1}{2}(S_{i,j} + S_{j,i})' - \mathcal{H}(S_{i,j} + S_{j,i}) \tag{B.18}$$

$$\delta G^0_{\ 0} = 0 \quad \delta G^0_{\ i} = \frac{1}{2a^2}\,\Delta S_i \qquad \delta G^i_{\ j} = -\frac{\delta^{ik}}{2a^2}\left[(S_{k,j} + S_{j,k})' + 2\mathcal{H}(S_{k,j} + S_{j,k})\right] \tag{B.19}$$

Tensor perturbations

$$\delta\Gamma^0_{00} = 0 \qquad \delta\Gamma^0_{0i} = 0 \qquad \delta\Gamma^0_{ij} = \frac{1}{2}h'_{ij} + \mathcal{H}h_{ij}$$
$$\delta\Gamma^i_{00} = 0 \qquad \delta\Gamma^i_{0j} = \frac{1}{2}\delta^{ik}h'_{kj} \qquad \delta\Gamma^i_{jk} = \frac{1}{2}\delta^{il}\left(h_{lj,k} + h_{lk,j} - h_{jk,l}\right) \tag{B.20}$$

$$\delta R_{00} = 0 \quad \delta R_{0i} = 0 \quad \delta R_{ij} = \frac{1}{2}h''_{ij} - \frac{1}{2}\Delta h_{ij} + \mathcal{H}h'_{ij} + (\mathcal{H}' + 2\mathcal{H}^2)h_{ij} \quad \delta R = 0 \tag{B.21}$$

$$\delta G_{00} = 0 \qquad \delta G_{0i} = 0 \qquad \delta G_{ij} = \frac{1}{2}h''_{ij} - \frac{1}{2}\Delta h_{ij} + \mathcal{H}h'_{ij} - (2\mathcal{H}' + \mathcal{H}^2)h_{ij} \tag{B.22}$$

$$\delta G^0_{\ 0} = 0 \qquad \delta G^0_{\ i} = 0 \qquad \delta G^i_{\ j} = \frac{\delta^{ik}}{2a^2}\left(h''_{kj} + 2\mathcal{H}h'_{kj} - \Delta h_{kj}\right) \tag{B.23}$$

Bibliography

[1] F.C. Adams *et al.*, Phys. Rev. **D47**, 426 (1993) hep-ph/9207245.

[2] A. Albrecht in: *Critical Dialogues in Cosmology*, ed. by N. Turok. World Scientific, Singapore (1997) p.265, astro-ph/9612017.

[3] A. Albrecht, D. Coulson, P. Ferreira, and J. Magueijo, Phys. Rev. Lett. **76**, 1413 (1996) astro-ph/9505030.

[4] A. Albrecht and P.J. Steinhardt, Phys. Rev. Lett. **48**, 1220 (1982).

[5] R. Allahverdi, Phys. Rev. **D62**, 063509 (2000) hep-ph/0004035.

[6] R.A. Alpher and R.C. Herman, Nature **162**, 774 (1948).

[7] T. Asaka and M. Kawasaki, Phys. Rev. **D60**, 123509 (1999) hep-ph/9905467.

[8] J.M. Bardeen, Phys. Rev. **D22**, 1882 (1980).

[9] J.M. Bardeen, P.J. Steinhardt, and M.S. Turner, Phys. Rev. **D28**, 679 (1983).

[10] R. Barkana and A. Loeb, Phys. Rep. **349**, 125 (2001) astro-ph/0010468.

[11] J.D. Barrow and K. Maeda, Nucl. Phys. **B341**, 294 (1990).

[12] N. Bartolo, S. Matarrese, and A. Riotto, Phys. Rev. **D64**, 123504 (2001) astro-ph/0107502.

[13] N. Bartolo, S. Matarrese, and A. Riotto, Phys. Rev. **D65**, 103505 (2002) hep-ph/0112261.

[14] B.A. Bassett, F. Tamburini, D.I. Kaiser, and R. Maartens, Nucl. Phys. **B561**, 188 (1999) hep-ph/9901319.

[15] C.L. Bennett *et al.*, Astrophys. J. **464**, L1 (1996) astro-ph/9601067.

[16] A. Berera, Phys. Rev. Lett. **75**, 3218 (1995) astro-ph/9509049.

[17] A. Berera, M. Gleiser, and R.O. Ramos, Phys. Rev. Lett. **83**, 264 (1999) hep-ph/9809583.

[18] N.D. Birrell and P.C.W. Davies. *Quantum Fields in Curved Space* (Cambridge monographs on mathematical physics). Cambridge University Press, Cambridge, UK (1982).

[19] N.W. Boggess *et al.*, Astrophys. J. **397**, 420 (1992).

[20] N.N. Bogolubov, Sov. Phys. JETP **7**, 51 (1958).

[21] J.R. Bond in: *Cosmology and Large Scale Structure*, ed. by R. Schaeffer *et al.* Elsevier, New York, USA (1996) p.469.

[22] BOOMERanG website: `http://www.physics.ucsb.edu/~boomerang`.

[23] G. Börner. *The Early Universe, Facts and Fiction* (third corrected and enlarged edition). Springer-Verlag, New York, USA (1993).

[24] F.R. Bouchet, J.-L. Puget, and J.M. Lamarre in: *The Primordial Universe*, ed. by P. Binétruy *et al.* Springer-Verlag, Berlin, Germany (2000) p.103.

[25] C. Brans and C.H. Dicke, Phys. Rev. **124**, 925 (1961).

[26] B.H. Bransden and C.J. Joachain. *Introduction to Quantum Mechanics*. Longman Scientific & Technical, Harlow, UK (1989).

[27] M. Bucher, K. Moodley, and N. Turok, Phys. Rev. **D62**, 083508 (2000) astro-ph/9904231.

[28] E.F. Bunn, A.R. Liddle, and M. White, Phys. Rev. **D54**, R5917 (1996) astro-ph/9607038.

[29] K. Cahill, *Elements of supersymmetry*, hep-ph/9907295.

[30] COBE website: `http://space.gsfc.nasa.gov/astro/cobe`. The COBE datasets were developed by the NASA Goddard Space Flight Center under the guidance of the COBE Science Working Group and were provided by the NSSDC.

[31] S. Coleman and E. Weinberg, Phys. Rev. **D7**, 1888 (1973).

[32] P. Coles and F. Lucchin. *Cosmology, The Origin and Evolution of Cosmic Structure*. John Wiley & Sons, Chichester, UK (1995).
[33] C.B. Collins and S.W. Hawking, Astrophys. J. **180**, 317 (1973).
[34] E.J. Copeland, E.W. Kolb, A.R. Liddle, and J.E. Lidsey, Phys. Rev. **D48**, 2529 (1993) hep-ph/9303288.
[35] E. Cremmer, S. Ferrara, L. Girardello, and A. van Proeyen, Nucl. Phys. **B212**, 413 (1983).
[36] R. Crittenden and P.J. Steinhardt, Phys. Lett. **B293**, 32 (1992) astro-ph/9207002.
[37] A. Dekel and J.P. Ostriker (ed.). *Formation of Structure in the Universe*. Cambridge University Press, Cambridge, UK (1999).
[38] R.H. Dicke, P.J.E. Peebles, P.G. Roll, and D.T. Wilkinson, Astrophys. J. **142**, 414 (1965).
[39] R. Easther, B.R. Greene, W.H. Kinney, and G. Shiu, *A generic estimate of trans-Planckian modifications to the primordial power spectrum in inflation*, hep-th/0204129.
[40] A. Einstein, Ann. Phys. **49**, 769 (1916).
[41] K. Enqvist, H. Kurki-Suonio, and J. Väliviita, Phys. Rev. **D65**, 043002 (2002) astro-ph/0108422.
[42] J.E. Felten and R. Isaacman, Rev. Mod. Phys. **58**, 689 (1986).
[43] F. Finelli and R. Brandenberger, Phys. Rev. **D62**, 083502 (2000) hep-ph/0003172.
[44] D.Z. Freedman, P. van Nieuwenhuizen, and S. Ferrara, Phys. Rev. **D13**, 3214 (1976).
[45] K. Freese, J.A. Frieman, and A.V. Olinto, Phys. Rev. Lett. **65**, 3233 (1990).
[46] A. Friedmann, Z. Phys. **10**, 377 (1922).
[47] G. Gamow, Phys. Rev. **70**, 572 (1946).
[48] J. García-Bellido and A.D. Linde, Phys. Rev. **D55**, 7480 (1997) astro-ph/9701173.
[49] J. García-Bellido, A.D. Linde, and D. Wands, Phys. Rev. **D54**, 6040 (1996) astro-ph/9605094.
[50] J. García-Bellido and D. Wands, Phys. Rev. **D53**, 5437 (1996) astro-ph/9511029.
[51] H. Georgi and S.L. Glashow, Phys. Rev. Lett. **32**, 438 (1974).
[52] H. Georgi, H.R. Quinn, and S. Weinberg, Phys. Rev. Lett. **33**, 451 (1974).
[53] S.L. Glashow, Nucl. Phys. **22**, 579 (1961).
[54] C. Gordon, D. Wands, B.A. Bassett, and R. Maartens, Phys. Rev. **D63**, 023506 (2001) astro-ph/0009131.
[55] A.M. Green and A.R. Liddle, Phys. Rev. **D55**, 609 (1997) astro-ph/9607166.
[56] M.B. Green, J.H. Schwarz, and E. Witten. *Superstring theory* (Cambridge monographs on mathematical physics, 2 volumes). Cambridge University Press, Cambridge, UK (1987).
[57] L.M. Griffiths and A.R. Liddle, Mon. Not. Roy. Astron. Soc. **324**, 769 (2001) astro-ph/0101149.
[58] S. Groot Nibbelink, *Supersymmetric non-linear unification in particle physics: Kähler manifolds, bundles for matter representations and anomaly cancellation*, Ph.D. thesis (2000).
[59] S. Groot Nibbelink and B.J.W. van Tent, *Density perturbations arising from multiple-field slow-roll inflation*, hep-ph/0011325.
[60] S. Groot Nibbelink and B.J.W. van Tent, Class. Quantum Grav. **19**, 613 (2002) hep-ph/0107272.
[61] A.H. Guth, Phys. Rev. **D23**, 347 (1981).
[62] A.H. Guth and B. Jain, Phys. Rev. **D45**, 426 (1992).
[63] A.H. Guth and S.-Y. Pi, Phys. Rev. Lett. **49**, 1110 (1982).
[64] A.H. Guth and E.J. Weinberg, Nucl. Phys. **B212**, 321 (1983).
[65] S. Hannestad, S.H. Hansen, F.L. Villante, and A.J.S. Hamilton, Astropart. Phys. **17**, 375 (2002) astro-ph/0103047.
[66] S.W. Hawking, Astrophys. J. **145**, 544 (1966).
[67] S.W. Hawking, Phys. Lett. **115**, 295 (1982).
[68] A.B. Henriques and R.G. Moorhouse, Phys. Rev. **D65**, 103524 (2002) hep-ph/0109218.
[69] M. Herrero, *The Standard Model*, hep-ph/9812242.
[70] P.W. Higgs, Phys. Rev. **145**, 1156 (1966).
[71] G. 't Hooft, Nucl. Phys. **B33**, 173 (1971).

[72] G. 't Hooft, Nucl. Phys. **B35**, 167 (1971).
[73] Website of W. Hu: `http://background.uchicago.edu`.
[74] W. Hu and S. Dodelson, *Cosmic microwave background anisotropies*, astro-ph/0110414.
[75] W. Hu and N. Sugiyama, Phys. Rev. **D51**, 2599 (1995) astro-ph/9411008.
[76] W. Hu, N. Sugiyama, and J. Silk, Nature **386**, 37 (1997) astro-ph/9604166.
[77] W. Hu and M. White, Astrophys. J. **471**, 30 (1996) astro-ph/9602019.
[78] W. Hu and M. White, Phys. Rev. Lett. **77**, 1687 (1996) astro-ph/9602020.
[79] W. Hu and M. White, New Astron. **2**, 323 (1997) astro-ph/9706147.
[80] E. Hubble, Proc. Nat. Acad. Sci. **15**, 168 (1929).
[81] L. Hui and W.H. Kinney, Phys. Rev. **D65**, 103507 (2002) astro-ph/0109107.
[82] J.-C. Hwang and H. Noh, Phys. Rev. **D59**, 067302 (1999) astro-ph/9812007.
[83] J.-C. Hwang and H. Noh, Phys. Lett. **B495**, 277 (2000) astro-ph/0009268.
[84] J.-C. Hwang and H. Noh, Phys. Rev. **D65**, 023512 (2002) astro-ph/0102005.
[85] J.-C. Hwang and H. Noh, Class. Quantum Grav. **19**, 527 (2002) astro-ph/0103244.
[86] J.-C. Hwang, T. Padmanabhan, O. Lahav, and H. Noh, Phys. Rev. **D65**, 043005 (2002) astro-ph/0107307.
[87] J.N. Islam. *An Introduction to Mathematical Cosmology*. Cambridge University Press, Cambridge, UK (1992).
[88] R. Kahn and R.H. Brandenberger, Phys. Lett. **B141**, 317 (1984).
[89] M. Kamionkowski, A. Kosowsky, and A. Stebbins, Phys. Rev. **D55**, 7368 (1997) astro-ph/9611125.
[90] C. Kiefer, D. Polarski, and A.A. Starobinsky, Int. J. Mod. Phys. **D7**, 455 (1998) gr-qc/9802003.
[91] W.H. Kinney, A. Melchiorri, and A. Riotto, Phys. Rev. **D63**, 023505 (2001) astro-ph/0007375.
[92] L. Knox, Phys. Rev. **D52**, 4307 (1995) astro-ph/9504054.
[93] H. Kodama and M. Sasaki, Prog. Theor. Phys. Suppl. **78**, 1 (1984).
[94] H. Kodama and M. Sasaki, Int. J. Mod. Phys. **A1**, 265 (1986).
[95] H. Kodama and M. Sasaki, Int. J. Mod. Phys. **A2**, 491 (1987).
[96] L.A. Kofman and A.D. Linde, Nucl. Phys. **B282**, 555 (1987).
[97] L.A. Kofman, A.D. Linde, and A.A. Starobinsky, Phys. Rev. Lett. **73**, 3195 (1994) hep-th/9405187.
[98] L.A. Kofman, A.D. Linde, and A.A. Starobinsky, Phys. Rev. **D56**, 3258 (1997) hep-ph/9704452.
[99] L.A. Kofman and A.A. Starobinsky, Sov. Astron. Lett. **11**, 271 (1985).
[100] E.W. Kolb and M.S. Turner. *The Early Universe*. Addison-Wesley Publishing Company, Reading, USA (1990).
[101] E. Komatsu *et al.*, Astrophys. J. **566**, 19 (2002) astro-ph/0107605.
[102] D. La and P.J. Steinhardt, Phys. Rev. Lett. **62**, 376 (1989).
[103] D. Langlois, Phys. Rev. **D59**, 123512 (1999) astro-ph/9906080.
[104] J. Lesgourgues, D. Polarski, and A.A. Starobinsky, Nucl. Phys. **B497**, 479 (1997) gr-qc/9611019.
[105] A.R. Liddle, Phys. Lett. **B220**, 502 (1989).
[106] A.R. Liddle, *Inflationary cosmology: status and prospects*, astro-ph/0111556.
[107] A.R. Liddle and D.H. Lyth, Phys. Lett. **B291**, 391 (1992) astro-ph/9208007.
[108] A.R. Liddle and D.H. Lyth, Phys. Rep. **231**, 1 (1993) astro-ph/9303019.
[109] A.R. Liddle and D.H. Lyth. *Cosmological Inflation and Large-Scale Structure*. Cambridge University Press, Cambridge, UK (2000).
[110] A.R. Liddle, A. Mazumdar, and F.E. Schunck, Phys. Rev. **D58**, 061301 (1998) astro-ph/9804177.
[111] A.R. Liddle, P. Parsons, and J.D. Barrow, Phys. Rev. **D50**, 7222 (1994) astro-ph/9408015.
[112] A.R. Liddle and D. Wands, Phys. Rev. **D45**, 2665 (1992).
[113] J.E. Lidsey *et al.*, Rev. Mod. Phys. **69**, 373 (1997) astro-ph/9508078.
[114] A.D. Linde, Phys. Lett. **B108**, 389 (1982).

[115] A.D. Linde, Phys. Lett. **B129**, 177 (1983).
[116] A.D. Linde, JETP Lett. **40**, 1333 (1984).
[117] A.D. Linde, Mod. Phys. Lett. **A1**, 81 (1986).
[118] A.D. Linde, Phys. Lett. **B175**, 395 (1986).
[119] A.D. Linde. *Particle Physics and Inflationary Cosmology* (contemporary concepts in physics volume 5). Harwood Academic Publishers, Chur, Switzerland (1990).
[120] A.D. Linde, Phys. Lett. **B259**, 38 (1991).
[121] A.D. Linde, Phys. Rev. **D49**, 748 (1994) astro-ph/9307002.
[122] A.D. Linde and A. Mezhlumian, Phys. Rev. **D52**, 6789 (1995) astro-ph/9506017.
[123] C.H. Lineweaver, *Cosmological parameters*, astro-ph/0112381.
[124] F. Lucchin and S. Matarrese, Phys. Rev. **D32**, 1316 (1985).
[125] D.H. Lyth and A. Riotto, Phys. Rep. **314**, 1 (1999) hep-ph/9807278.
[126] D.H. Lyth and E.D. Stewart, Phys. Rev. Lett. **75**, 201 (1995) hep-ph/9502417.
[127] D.H. Lyth and E.D. Stewart, Phys. Rev. **D53**, 1784 (1996) hep-ph/9510204.
[128] J.M.F. Maia and J.A.S. Lima, Phys. Rev. **D60**, 101301 (1999) astro-ph/9910568.
[129] K.A. Malik, *Cosmological perturbations in an inflationary universe*, Ph.D. thesis (2001) astro-ph/0101563.
[130] MAP website: `http://map.gsfc.nasa.gov`.
[131] J. Martin and R.H. Brandenberger, Phys. Rev. **D63**, 123501 (2001) hep-th/0005209.
[132] J. Martin, A. Riazuelo, and M. Sakellariadou, Phys. Rev. **D61**, 083518 (2000) astro-ph/9904167.
[133] J. Martin and D.J. Schwarz, Phys. Rev. **D62**, 103520 (2000) astro-ph/9911225.
[134] MAXIMA website: `http://cosmology.berkeley.edu/group/cmb/index.html`.
[135] J. McDonald, Phys. Rev. **D61**, 083513 (2000) hep-ph/9909467.
[136] A. Melchiorri, *Multiple peaks in the CMB*, astro-ph/0201237.
[137] L.E. Mendes and A.R. Liddle, Phys. Rev. **D62**, 103511 (2000) astro-ph/0006020.
[138] V.F. Mukhanov, JETP Lett. **41**, 493 (1985).
[139] V.F. Mukhanov, Sov. Phys. JETP **67**, 1297 (1988).
[140] V.F. Mukhanov and G.V. Chibisov, Sov. Phys. JETP **56**, 258 (1982).
[141] V.F. Mukhanov, H.A. Feldman, and R.H. Brandenberger, Phys. Rep. **215**, 203 (1992).
[142] V.F. Mukhanov and P.J. Steinhardt, Phys. Lett. **B422**, 52 (1998) astro-ph/9710038.
[143] M. Nakahara. *Geometry, Topology and Physics* (graduate student series in physics). Institute of Physics Publishing, Bristol, UK (1996).
[144] T.T. Nakamura and E.D. Stewart, Phys. Lett. **B381**, 413 (1996) astro-ph/9604103.
[145] Y. Nambu and A. Taruya, Class. Quantum Grav. **15**, 2761 (1998) gr-qc/9801021.
[146] J.C. Niemeyer, Phys. Rev. **D63**, 123502 (2001) astro-ph/0005533.
[147] P. van Nieuwenhuizen, Phys. Rep. **68**, 189 (1981).
[148] H.P. Nilles, Phys. Rep. **110**, 1 (1984).
[149] T. Padmanabhan. *Structure Formation in the Universe*. Cambridge University Press, Cambridge, UK (1993).
[150] R.B. Partridge. *3K: The Cosmic Microwave Background Radiation* (Cambridge astrophysics series 25). Cambridge University Press, Cambridge, UK (1995).
[151] J.A. Peacock. *Cosmological Physics*. Cambridge University Press, Cambridge, UK (1999).
[152] A.A. Penzias and R.W. Wilson, Astrophys. J. **142**, 419 (1965).
[153] M.E. Peskin in: *Proc. 1996 European School of High-Energy Physics*, ed. by N. Ellis *et al.* CERN, Geneva, Switzerland (1997) p.49, hep-ph/9705479.
[154] A. Pich in: *The Standard Model and Beyond*, ed. by J.A. Villar *et al.* Editions Frontieres, Gif-sur-Yvette, France (1995) p.1, hep-ph/9412274.
[155] Planck website: `http://astro.estec.esa.nl/Planck`.
[156] L. Pogosian, Int. J. Mod. Phys. **A16S1C**, 1043 (2001) astro-ph/0009307.
[157] D. Polarski and A.A. Starobinsky, Nucl. Phys. **B385**, 623 (1992).
[158] D. Polarski and A.A. Starobinsky, Phys. Rev. **D50**, 6123 (1994) astro-ph/9404061.
[159] D. Polarski and A.A. Starobinsky, Class. Quantum Grav. **13**, 377 (1996) gr-qc/9504030.

[160] J. Polchinski. *String Theory* (Cambridge monographs on mathematical physics, 2 volumes). Cambridge University Press, Cambridge, UK (1998).
[161] J.P. Preskill, Phys. Rev. Lett. **43**, 1365 (1979).
[162] F. Quevedo in: *Proc. 5th Mexican workshop of particles and fields and phenomenology of fundamental interactions*, ed. by J.C. D'Olivo *et al.* American Institute of Physics, Woodbury, USA (1996) p.202, hep-th/9603074.
[163] L. Randall, M. Soljačić, and A.H. Guth, Nucl. Phys. **B472**, 377 (1996) hep-ph/9512439.
[164] M.J. Rees and D.W. Sciama, Nature **217**, 511 (1968).
[165] H.P. Robertson, Proc. Nat. Acad. Sci. Washington **15**, 822 (1929).
[166] G.G. Ross. *Grand Unified Theories*. Benjamin/Cummings, Reading, USA (1984).
[167] R.K. Sachs and A.M. Wolfe, Astrophys. J. **147**, 73 (1967).
[168] A. Salam in: *Elementary Particle Theory*, ed. by N. Svartholm. Almqvist and Wiksell, Stockholm, Sweden (1968) p.367.
[169] M. Sasaki, Prog. Theor. Phys. **76**, 1036 (1986).
[170] M. Sasaki and E.D. Stewart, Prog. Theor. Phys. **95**, 71 (1996) astro-ph/9507001.
[171] M. Sasaki and T. Tanaka, Prog. Theor. Phys. **99**, 763 (1998) gr-qc/9801017.
[172] D.J. Schwarz, C.A. Terrero-Escalante, and A.A. Garcia, Phys. Lett. **B517**, 243 (2001) astro-ph/0106020.
[173] U. Seljak and M. Zaldarriaga, Astrophys. J. **469**, 437 (1996) astro-ph/9603033. CMBFAST website: `http://physics.nyu.edu/matiasz/CMBFAST/cmbfast.html`.
[174] M. Shifman, Int. J. Mod. Phys. **A11**, 5761 (1996) hep-ph/9606281.
[175] J. Silk, Astrophys. J. **151**, 459 (1968).
[176] J. Silk. *The Big Bang* (revised and updated edition). W.H. Freeman and Company, New York, USA (1989).
[177] G.F. Smoot *et al.*, Astrophys. J. **360**, 685 (1990).
[178] A.A. Starobinsky, Phys. Lett. **B91**, 99 (1980).
[179] A.A. Starobinsky, Phys. Lett. **B117**, 175 (1982).
[180] A.A. Starobinsky, JETP Lett. **42**, 152 (1985).
[181] A.A. Starobinsky, Sov. Astron. Lett. **11**, 133 (1985).
[182] A.A. Starobinsky, S. Tsujikawa, and J. Yokoyama, Nucl. Phys. **B610**, 383 (2001) astro-ph/0107555.
[183] A.A. Starobinsky and J. Yokoyama in: *Proc. 4th Workshop on General Relativity and Gravitation (Kyoto)*, ed. by K. Nakao *et al.* Kyoto University Press, Kyoto, Japan (1995) p.381, gr-qc/9502002.
[184] P.J. Steinhardt and F.S. Accetta, Phys. Rev. Lett. **64**, 2740 (1990).
[185] P.J. Steinhardt and M.S. Turner, Phys. Rev. **D29**, 2162 (1984).
[186] E.D. Stewart and J.-O. Gong, Phys. Lett. **B510**, 1 (2001) astro-ph/0101225.
[187] E.D. Stewart and D.H. Lyth, Phys. Lett. **B302**, 171 (1993) gr-qc/9302019.
[188] J.M. Stewart, Class. Quantum Grav. **7**, 1169 (1990).
[189] L. Susskind, Phys. Rep. **104**, 181 (1984).
[190] T. Tanaka, *A comment on trans-Planckian physics in inflationary universe*, astro-ph/0012431.
[191] A. Taruya and Y. Nambu, Phys. Lett. **B428**, 37 (1998) gr-qc/9709035.
[192] M. Tegmark, *Doppler peaks and all that: CMB anisotropies and what they can tell us*, astro-ph/9511148.
[193] M. Tegmark, D.J. Eisenstein, W. Hu, and A. de Oliveira-Costa, Astrophys. J. **530**, 133 (2000) astro-ph/9905257.
[194] B.J.W. van Tent, in preparation.
[195] B.J.W. van Tent and S. Groot Nibbelink, *Inflationary perturbations with multiple scalar fields*, hep-ph/0111370.
[196] S. Tsujikawa and B.A. Bassett, Phys. Lett. **B536**, 9 (2002) astro-ph/0204031.
[197] E.T. Vishniac, Astrophys. J. **322**, 597 (1987).
[198] A.G. Walker, Proc. London Math. Soc. 2nd Ser. **42**, 90 (1936).

[199] D. Wands, K.A. Malik, D.H. Lyth, and A.R. Liddle, Phys. Rev. **D62**, 043527 (2000) astro-ph/0003278.
[200] L. Wang and M. Kamionkowski, Phys. Rev. **D61**, 063504 (2000) astro-ph/9907431.
[201] X. Wang, M. Tegmark, and M. Zaldarriaga, Phys. Rev. **D65**, 123001 (2002) astro-ph/0105091.
[202] S. Weinberg, Phys. Rev. Lett. **19**, 1264 (1967).
[203] S. Weinberg. *Gravitation and Cosmology: principles and applications of the general theory of relativity*. John Wiley & Sons, New York, USA (1972).
[204] J. Wess and J. Bagger. *Supersymmetry and Supergravity* (revised edition). Princeton University Press, Princeton, USA (1992).
[205] J. Wess and B. Zumino, Nucl. Phys. **B70**, 39 (1974).
[206] E. Witten, Phys. Lett. **B155**, 151 (1985).
[207] J. Yokoyama and A.D. Linde, Phys. Rev. **D60**, 083509 (1999) hep-ph/9809409.
[208] Y.B. Zeldovich and R.A. Sunyaev, Astrophys. Space Sci. **4**, 301 (1969).
[209] B. Zumino, Phys. Lett. **B87**, 203 (1979).

Samenvatting

De geschiedenis en evolutie van het heelal worden beschreven door de Oerknaltheorie (*Big Bang*). In 1929 wist Edwin Hubble uit waarnemingen af te leiden dat het heelal uitdijt en deze uitdijing is het belangrijkste ingredient van de Oerknaltheorie. Het betekent dat het heelal vroeger kleiner was dan nu en dus een hogere dichtheid en temperatuur had. Als men dit helemaal doortrekt, vindt men dat volgens deze theorie het heelal begonnen is als één punt met een oneindig hoge temperatuur, vandaar de naam Oerknal. Het feit dat de temperatuur vroeger hoger was, leidt tot een aantal belangrijke voorspellingen, waarvan hier twee. In de eerste plaats voorspelt de theorie dat toen het heelal ongeveer een minuut oud was de omstandigheden zodanig waren dat er kernfusie mogelijk was: waterstofkernen smolten samen tot voornamelijk helium en deuterium. Dit proces wordt nucleosynthese genoemd. Waarnemingen van deze elementen in onverstoorde gebieden van het heelal (waar geen sterren zijn die deze stoffen kunnen aanmaken of vernietigen) zijn in overeenstemming met de Oerknaltheorie.

In de tweede plaats voorspelt de theorie dat toen het heelal ongeveer 300 000 jaar oud was uit protonen en elektronen neutrale waterstofatomen gevormd konden worden (dit proces wordt recombinatie genoemd). Bij hogere temperaturen (vroegere tijden) bevatte het heelal een plasma van losse protonen en elektronen. Dit mengsel is ondoorzichtig: elektromagnetische straling (fotonen), bijvoorbeeld zichtbaar licht, kan zich hierdoor niet vrij bewegen. Na het tijdstip van recombinatie werd het heelal dus doorzichtig. Omdat fotonen met een eindige snelheid reizen (de lichtsnelheid), kijken we automatisch terug in de tijd als we sterrenkundige waarnemingen doen. Dit betekent dat we het moment van recombinatie kunnen zien: voor ons lijkt het alsof alle fotonen die in het vroege heelal voor het tijdstip van recombinatie geproduceerd zijn op dat moment uitgezonden werden (net zoals al het licht van de zon voor ons vanaf het zonoppervlak lijkt te komen). We zien dus als het ware het hete, gloeiende vroege heelal. Deze straling wordt de kosmische achtergrondstraling genoemd. Vanwege de uitdijing van het heelal is de golflengte van deze straling uitgerekt, zodat het geen zichtbaar licht meer is met een temperatuur van een paar duizend graden, maar microgolfstraling met een temperatuur van slechts drie graden boven het absolute nulpunt. Het waarnemen van deze straling in 1965 was een belangrijke bevestiging van de Oerknaltheorie.

Behalve deze successen zijn er ook een aantal problemen met de standaard-Oerknaltheorie. Aangezien informatie zich niet sneller kan voortbewegen dan met de lichtsnelheid, is er op ieder moment een bepaalde grens (horizon genaamd) van waarbuiten informatie ons nog niet bereikt kan hebben. Het blijkt dat de verhouding tussen horizon en grootte van het heelal op vroegere tijdstippen kleiner was. Dit betekent dat punten die in twee tegenovergestelde richtingen net binnen onze horizon liggen nooit informatie hebben kun-

nen uitwisselen (niet causaal verbonden zijn). Aan de andere kant zien we dat het heelal er op de grootste schaal in alle richtingen hetzelfde uitziet (isotroop is) en de vraag is dan hoe dat zo gekomen is zonder enige vorm van informatie-uitwisseling. Bovendien lijkt de gelijkmatige (homogene) verdeling van materie in het heelal moeilijk te rijmen met de 'wilde' Oerknal. Om deze en een aantal andere problemen binnen de standaard-Oerknaltheorie op te lossen is het concept van inflatie ontwikkeld, dat gezien moet worden als een uitbreiding van de standaardtheorie. Inflatie is een zeer korte periode van extreem snelle expansie van het heel vroege heelal, een minieme fractie van een seconde na de Oerknal zelf. De inflatie zorgt ervoor dat onze horizon veel groter is dan uit de standaard-Oerknaltheorie volgt, met als gevolg dat het waarneembare gedeelte van het heelal wel degelijk causaal verbonden is (voor een grafische vorm van deze uitleg zie figuur 1.2). Bovendien zorgt de extreem snelle uitdijing tijdens inflatie ervoor dat mogelijke ongelijkmatigheden in het heelal zeer sterk verdund worden, wat de huidige homogeniteit verklaart.

De vraag is nu natuurlijk hoe zo'n periode van inflatie in een fysisch model beschreven kan worden. Het model dat daarvoor ontwikkeld is vereist het bestaan van een speciaal soort materie: scalaire bosonen, beschreven door een scalair veld. Evenals objecten uit het dagelijks leven heeft ook een scalair veld potentiële en kinetische energie. Voor een scalair veld geldt echter dat, indien de kinetische energie te verwaarlozen is ten opzichte van de potentiële energie, de scalaire materie een negatieve druk veroorzaakt. Het is deze negatieve druk die leidt tot de snelle expansie van het heelal. Dit klinkt misschien wat wonderlijk aangezien men mechanisch gezien juist bij positieve druk aan expansie denkt. Dan gaat het echter om drukverschillen en die spelen hier geen rol, omdat de druk min of meer hetzelfde is in het hele heelal. Het gaat hier om effecten volgens de algemene relativiteitstheorie: net als een positieve energiedichtheid creëert een positieve druk een aantrekkend zwaartekrachtsveld en daarom is het juist een negatieve druk die tot expansie leidt. Om ervoor te zorgen dat de kinetische energie te verwaarlozen is, moet de potentiaal van het scalaire veld vrij vlak zijn. Hoe vlakker de potentiaal, des te minder snel het veld 'eraf rolt' en dus des te minder kinetische (bewegings)energie het heeft. Vandaar dat de condities op de potentiaal *slow-roll* condities (condities voor het langzaam rollen) genoemd worden.

De verschillende hoge-energie-theorieën die momenteel als mogelijke benadering van de werkelijkheid gezien worden, bevatten inderdaad zo'n scalair veld. Sterker nog, de meeste bevatten heel veel verschillende scalaire velden die op ingewikkelde manieren gekoppeld kunnen zijn. Daarom is het van groot belang om te onderzoeken hoe inflatie werkt in een dergelijke, meer algemene situatie. In hoofdstuk 3 behandelen we hoe de standaard-inflatietheorie voor één scalair veld uitgebreid kan worden naar het algemene geval met meerdere velden. Zo generaliseren we het slow-roll mechanisme en introduceren we een basis in de veldruimte, die o.a. nodig is om de verschillende velden van elkaar te onderscheiden.

Naast de isotropie en homogeniteit van het heelal op de grootste schaal zijn er natuurlijk allerlei inhomogeniteiten op kleinere schaal: sterrenstelsels en clusters van sterrenstelsels. De vraag die nu opkomt is de volgende: als inflatie ervoor zorgt dat alle inhomogeniteiten 'weggeblazen' worden, waar komen dan deze structuren in ons huidige heelal vandaan? Gelukkig biedt inflatie ook hier een oplossing. Kleine kwantumfluctuaties, die altijd aanwezig zijn, worden door inflatie opgeblazen tot macroscopische dichtheidsfluctuaties. Deze groeien dan vervolgens door zwaartekrachtsaantrekking uit tot de grote structuren die we nu in ons heelal waarnemen. Dit laatste gebeurt overigens pas relatief laat in de evolutie van het heelal; ten tijde van recombinatie zijn de fluctuaties nog miniem (ongeveer hon-

derdduizend keer zo klein als de gemiddelde achtergrondwaarde), zoals we kunnen zien in de achtergrondstraling. Een dichtheidsfluctuatie correspondeert namelijk met een temperatuursfluctuatie in de fotonverdeling. Het feit dat we deze fluctuaties kunnen waarnemen is erg belangrijk voor inflatie: de waargenomen grootte ervan is direct gerelateerd aan bepaalde combinaties van parameters van het inflatiemodel. Op hun beurt zijn deze weer gerelateerd aan parameters in de onderliggende hoge-energie-theorie. Anders gezegd, waarnemingen van de achtergrondstraling bieden een van de weinige mogelijkheden om experimentele informatie te verkrijgen over theorieën bij extreem hoge energieën, die ver buiten het bereik van deeltjesversnellers op aarde liggen. Daarvoor moet men natuurlijk wel de theorie goed begrijpen over de relatie tussen deze temperatuursfluctuaties en de inflatie-grootheden. Het hoofdonderwerp van dit proefschrift is de ontwikkeling en uitwerking van een formalisme voor de beschrijving hiervan in het algemene geval van meerdere scalaire velden. Hoofdstuk 4 behandelt de fluctuaties tijdens de inflatieperiode en hoofdstuk 5 houdt zich bezig met wat er in de periode tussen inflatie en recombinatie gebeurt met de fluctuaties.

Normaal gesproken middelen de oscillerende kwantumfluctuaties uit en zijn ze van geen belang op macroscopisch, klassiek niveau. Maar door de extreme expansie tijdens inflatie gebeurt er iets bijzonders: de golflengtes van de verschillende perturbatiemodi worden uitgerekt totdat ze groter zijn dan de horizon.[1] Zodra dit gebeurt verliest de perturbatiemodus zijn kwantumkarakter en wordt effectief een klassieke perturbatie, die niet meer uitmiddelt. (Heel grof en onnauwkeurig gezegd kan de ene kant van de perturbatie de andere kant niet meer 'zien'; ze 'vergeten' dat ze deel uitmaken van een uitmiddelende fluctuatie en ze stoppen met oscilleren.) De nauwkeurige bestudering van deze overgang voor het algemene geval met meerdere velden maakt een belangrijk deel uit van hoofdstuk 4. Bij inflatie spelen twee soorten fluctuaties een rol: scalaire (energiedichtheid/druk) en tensorperturbaties (gravitatiegolven). De eerste zijn het belangrijkst. Zolang de perturbaties buiten de horizon blijven, blijft hun amplitude vrijwel constant (onder bepaalde voorwaarden, waarop uitgebreid wordt ingegaan in hoofdstuk 5). Omdat na inflatie de horizon harder groeit dan de golflengtes van de perturbatiemodi (tegenovergesteld dus aan wat er tijdens inflatie gebeurt), komen de verschillende modi achter elkaar weer binnen de horizon, in de omgekeerde volgorde als waarin ze er tijdens de inflatie uitgingen. Voor inflatie zijn observationeel gezien vooral die modi van belang die tijdens de recombinatie nog buiten de horizon waren (zodat we in de achtergrondstraling de oorspronkelijke inflatieperturbaties zien zonder beïnvloeding door latere processen), maar die nu wel binnen de horizon zijn gekomen (anders kunnen we ze überhaupt niet zien).

Het belangrijkste gevolg van de aanwezigheid van meerdere velden tijdens inflatie is de beïnvloeding van de scalaire perturbaties. Scalaire perturbaties kunnen in twee soorten verdeeld worden: adiabatische (waarbij geen energie uitgewisseld wordt tussen de verschillende componenten) en *isocurvature* fluctuaties (die de ruimtelijke kromming constant houden). Deze leiden o.a. tot verschillende effecten in de achtergrondstraling. Voor inflatiemodellen met één veld zijn er slechts adiabatische scalaire perturbaties; het is de aanwezigheid van meerdere velden die *isocurvature* perturbaties mogelijk maakt. In het

[1] Eigenlijk zou in deze alinea het woord 'Hubble-lengte' gebruikt moeten worden in plaats van horizon, omdat er hier twee verschillende definities van horizon door elkaar gebruikt worden (zie sectie 2.1 voor details). De Hubble-lengte is een natuurlijke lengtemaat in het heelal, die verkregen wordt door de expansietijdschaal te vermenigvuldigen met de lichtsnelheid. Het is precies dit lengtebegrip dat overal in deze alinea bedoeld wordt, maar het gebruik van het woord 'horizon' in deze situatie is dusdanig ingeburgerd geraakt dat wij ons er hier ook aan bezondigen.

algemeen zijn er ook correlaties tussen deze twee soorten. In hoofdstuk 5 leiden we een aantal resultaten voor de *isocurvature* fluctuaties af, o.a. een conditie die aangeeft in welke gevallen ze onbelangrijk zijn. Wat hier nog ontbreekt en verder onderzoek vereist is een nauwkeuriger behandeling van deze fluctuaties vlak na het einde van de inflatie. Minstens zo belangrijk echter is het feit dat de aanwezigheid van meerdere velden ook de adiabatische perturbaties beïnvloedt. Met onze basis in de veldruimte zijn slechts twee veldcomponenten van belang hiervoor, onafhankelijk van het eigenlijke aantal velden. Dit effect wordt uitgebreid bestudeerd in de verschillende voorbeelden in hoofdstuk 6. In het bijzonder wordt ook stil gestaan bij de effecten van een niet-triviale veldruimte. We zien dat de meer-veld-termen voor maar liefst de helft van het totale resultaat kunnen zorgen en dus zeer belangrijk kunnen zijn. Verder vinden we door numerieke controle dat onze analytische, slow-roll-benaderde uitdrukkingen zeer goed overeenkomen met de exacte resultaten. Tenslotte leiden we een relatie tussen de scalaire en tensorperturbaties af waarmee, als de tensorperturbaties waargenomen kunnen worden, direct uit de observaties kan worden afgeleid of meer-veld-effecten van belang zijn.

Mijn toekomstverwachtingen wat betreft het verkrijgen van observationele informatie over inflatiemodellen zijn gematigd optimistisch. De nieuwe satellietmissies MAP (vanaf het eind van dit jaar) en vooral Planck (vanaf 2007) zullen de nauwkeurigheid van de waarnemingen van de achtergrondstraling sterk verbeteren. Zoals hierboven is gezegd kan dan expliciet worden bepaald of meer-veld-effecten van belang zijn (aangenomen dat de tensorperturbaties groot genoeg zijn om te kunnen worden waargenomen). De verschillende observationele grootheden bieden verder de mogelijkheid om een aantal inflatieparameters te bepalen. Aan de andere kant is het zeer wel mogelijk om veel meer vrije parameters in een inflatiemodel te hebben dan er observationele grootheden zijn, vooral in het algemene geval met meerdere velden en een niet-triviale veldruimte. In dat geval is het niet mogelijk om het model precies vast te leggen en moet er door de hoge-energietheoretici op grond van andere overwegingen bepaald worden welke types inflatiemodellen realistisch zijn. In ieder geval zullen de komende jaren erg interessant zijn voor de (inflatie-)kosmologie vanwege de overvloed aan nieuwe waarnemingen.

Dankwoord

Verschillende mensen hebben op directe of indirecte wijze bijgedragen aan de totstandkoming van dit proefschrift. In de eerste plaats bedank ik mijn promotor, Gerard 't Hooft, voor de mij geboden mogelijkheid een promotieonderzoek in de kosmologie te verrichten. Hij gaf mij de vrijheid om heel zelfstandig te werken. Het grootste deel van dit proefschrift is gebaseerd op onderzoek dat ik samen met Stefan Groot Nibbelink heb gedaan. Hoewel ons onderzoek tegenslagen heeft gekend, is het ons steeds gelukt om verder te gaan. Stefans vele ideeën en de boeiende discussies, mede aangewakkerd door onze verschillende gezichtspunten, waren daarvoor van groot belang. Ik heb veel van onze samenwerking geleerd.

Hoewel mijn onderzoeksrichting mij enigszins afzonderde van de andere theoretici, hebben collega's van het Spinoza Instituut / ITF in Utrecht en van het Nikhef en het ITFA in Amsterdam toch voor een stimulerende omgeving gezorgd, zowel op wetenschappelijk terrein als ook algemener. In het bijzonder bedank ik mijn kamergenoten Sebas, Marcel, Michiel en Giovanni en de secretaresses Leonie, Biene, Natasja, Geertje en Wilma. Met Jan Smit heb ik verschillende plezierige en nuttige discussies over kosmologische onderwerpen gehad.

I thank John Barrow and the other members of the Astronomy Centre and Particle Physics & Cosmology Group of Sussex University, UK, for their hospitality during my stay. Thanks to them my general knowledge of cosmology and of supersymmetry improved considerably. My housemates (Alan and Altaf) and the group of the M.Sc. room (James, Jem, Joy, Nick, Rachel and Toufik) made my stay in Brighton a very pleasant experience. It is great that we have managed to keep in touch!

For scientific development conferences and schools are essential. I am glad I had the opportunity to visit several, among which Les Houches, Cascais and Rovaniemi stand out. Apart from their scientific importance, schools are also good places to get to know your colleagues and make friends. In particular I am happy that my friendship with Masha has survived our separation after Les Houches.

Naast alle wetenschappelijke arbeid is het niet alleen prettig maar zelfs noodzakelijk om zo nu en dan ook lichamelijk bezig te zijn. Ik dank mijn squashpartners (Erik V. en Marcel), tennispartners (Erik M., Charlene, Femke en Freya), tafeltennispartners (Eugène en Thom) en teamgenoten bij volleybalvereniging Protos dat ze over mijn lichamelijke gezondheid gewaakt hebben.

Ook de gezelligheid en interesse van andere vrienden en van familie zijn belangrijk voor me geweest tijdens de afgelopen periode, ook al had ik lang niet altijd zoveel tijd voor hen als ik had gewild. Ik noem in het bijzonder Erik, Michiel en mijn huisgenoten Eugène en Remko. We hebben samen op Zevenwouden een misschien wat vreemde, maar wel gezellige en computerrijke tijd gehad!

Een heel speciale plaats is er voor mijn ouders, die mij door hun eigen levenshouding gestimuleerd hebben het wetenschappelijke pad in te slaan en zonder wier interesse, steun en liefde gedurende mijn hele leven ik nu niet dit punt bereikt zou hebben. Mijn vader dank ik bovendien voor het doorlezen van mijn proefschrift en de nuttige suggesties, voornamelijk wat betreft het Engels. Aan hen draag ik dit proefschrift op.

Bartjan van Tent,
juni 2002.

Curriculum vitae

Bartjan van Tent was born in Amersfoort, the Netherlands, on March 27, 1974. He followed secondary education at the Johan van Oldenbarnevelt Gymnasium in Amersfoort, and passed his finals in 1992. In the same year he started the studies of physics and astronomy at Utrecht University, the Netherlands, and he passed the propaedeutic examination (cum laude) for both branches of study in 1993. During his studies he followed many optional courses on various subjects and wrote computer software for the Westerbork Synthesis Radio Telescope. After writing a thesis on inflationary cosmology under supervision of prof.dr. G. 't Hooft and dr. P. Hoyng, he took his Master's degree ('doctoraalexamen') with the distinction cum laude in both theoretical physics and theoretical astronomy in 1997.

At the end of that year he started his doctoral research in the field of theoretical high-energy physics at the Institute for Theoretical Physics / Spinoza Institute of Utrecht University under the supervision of prof.dr. G. 't Hooft, the results of which are presented in this thesis. During this period he attended several national and international workshops, schools and conferences, and presented results there as well as during seminars at various institutes. He also visited the Astronomy Centre and Particle Physics & Cosmology Group of Sussex University at Brighton, UK, for four months in 1998. Both during his undergraduate and his doctoral studies he organized, supervised and assisted at several exercise classes for undergraduate students. He is the recipient of the 2001 Fenia Berz Award, awarded by the Institute of Physics in the UK.